IN SITU SOURCE CHARACTERISATION OF DENSE NON-AQUEOUS PHASE LIQUIDS (DNAPLs) IN A FRACTURED ROCK ENVIRONMENT

Vierah Hulley

Submitted in accordance with the requirements for the Doctor of Philosophy degree in the Faculty of Natural Sciences and Agriculture, Department of Geohydrology at the University of the Free State, Bloemfontein, South Africa

June 2013

Promoter: Professor K.T. Witthüser

ACKNOWLEDGEMENTS

This thesis is the result of continued support of several people to whom I want to express my gratitude.

Without the funding and faith of the Investigation Site owners this study would never have resulted. Thank you for this wonderful opportunity and for trusting me to undertake and manage this study. The Investigation Site personnel added a vast amount to the understanding of historical site processes and subsequently to the identification of potential release areas.

My gratitude is also extended to Dr. Smit who allowed me the freedom to pursue this research.

I will be eternally indebted to the following Consultants who assisted in collecting field data, preparing of conference papers and on treating me as part of the team: Joe Fiacco, Paul Aucamp, Liam Smith, Ryno Weitz. This has been quite a ride!

To my promoter, Prof. Kai Witthüser, thank you for your patience with my erratic submissions and long periods of silence. Thank you also for the advice on improving this thesis.

I had the absolute pleasure of working with Prof. van Heerden and Dr Botes from the UFS Metagenomic Platform. Thank you for your enthusiasm on the findings from the site.

The last few months have been particularly challenging for me. I would not have survived had it not been for my amazing support system in Houston: Anja, Karen and Raakhi; your generosity and friendship overwhelms me.

Finally, to the most significant people in my life; my wonderful and supporting husband Francois and my adorable daughter, Lara – you are my inspiration, my motivation and my hope. This is for you.

Table of Contents

List of Figures

List of Tables

List of Appendices

(available electronically)

CHAPTER 1

1 INTRODUCTION

1.1 Background and Motivation

The combination of water scarcity and the reliance of communities on groundwater have led to stricter regulations within South Africa to protect and preserve groundwater from anthropogenic degradation. The management and protection of water resources (including groundwater) is legislated through the National Water Act (Republic of South Africa, 1998).

Of the contaminants inventoried in South Africa, DNAPLs represented over 60% of the priority pollutants (Usher *et al.*, 2004). DNAPLs (such as chlorinated hydrocarbons) also make up the most frequently detected contaminants in aquifers in the United States of America (USA). A study undertaken by the United States Environmental Protection Agency (United States Environmental Protection Agency, 1990) found that synthetic organic compounds were found in 17-28% of their public drinking water treatment facilities where groundwater is used as the water source. A more recent study undertaken by the United States Geological Survey (USGS) found that 20% of water samples from aquifers sampled contained volatile organic carbons (Zogorski *et al.*, 2006).

The acronym “DNAPL” was first coined in the United States of America during litigation proceedings in New York State in the late 1970’s - early 1980’s and referred to a black, immiscible liquid that was heavier than water (Pankow and Cherry, 1996). Chemicals falling within this category include halogenated and non-halogenated hydrocarbons (for e.g. chlorinated hydrocarbons, etc.), pesticides, polychlorinated biphenyl mixtures (PCBs), phthalate compounds, substituted aromatic compounds (for e.g. nitrotoluenes, nitrobenzenes, benzyl chlorides, chloroanilines, etc.), mercury, creosotes and coal tars. DNAPLs are normally not released into the environment as a pure or single component chemical, but are often released as spent solvents that contain a fair fraction of other organic compounds. The effect of these components can potentially add to the problem of characterisation and remediation of DNAPL-impacted areas by influencing the properties of the DNAPL (Interstate Technology and Regulatory Council , 2000).

The properties of DNAPLs allow them to have numerous beneficial uses in processes such as degreasing equipment and treating wood. The use of these compounds is not restricted to heavy industry but they are also commonly used in workshops, dry-cleaners and photography workshops located all over South Africa. The potential of contamination of water resources from these chemicals is therefore ubiquitous. Consequently, a comprehensive understanding of the relationship between form/phases, geo-mechanisms, toxicity, degradation and exposure pathways of these priority pollutants is important as it directly affects the effectiveness of remedial solutions. Despite the low solubility of these compounds in water, components of the DNAPLs are soluble enough to present risks to human health and the environment. There are two (2) prevalent exposure pathways of these chemicals to human beings; *viz.* through ingestion of contaminated groundwater, and/or inhalation of toxic vapours (Cheremisinoff, 1990).

In recent years, a number of site-specific investigations and remediation efforts have shown that DNAPL encountered in fractured bedrock poses a particular problem in locating and removing (for e.g. United States Environmental Protection Agency, 2004). Fractured bedrock is the prevalent geo-contaminant setting in the South African scenario. Conventional methods of using the pump-and-treat technology alone has shown to be only partially successful in removing some of the contaminants from the DNAPL source zones (Mackay and Cherry, 1989; MacDonald and Kavanaugh, 1994). This lack of success can be partially attributed to the uncertainty associated with incomplete source zone characterisation.

1.2 Objectives of Thesis

This research was initiated due to the lack of adequate source zone characterisation of DNAPLs within fractured bedrock. The United States Environmental Protection Agency (2003); and the Strategic Environmental Research and Development Program and Environmental Security Technology Certification Program (SERDP and ESTCP, 2001; 2006) prioritised the following as the highest research needs related to DNAPLs:

- The assessment of source zone treatment
- Source zone delineation and characterisation
- Diagnostic tools to evaluate remediation performance.

The Investigation Site (see Chapter 3) presents an ideal opportunity to test source zone characterisation methodologies of a DNAPL-impacted site on a mega-scale.

Additionally, the benefits to industry cannot be undermined. Failure of remediation technologies as a direct result of poor source zone characterisation is not uncommon. However, these have paramount cost implications for site owners.

The objectives of this thesis are as follows:

- Determine the architecture of DNAPLs in a fractured (heterogeneous) system.

- Evaluate the effectiveness of source zone characterisation and delineation using multiple characterisation tools in a fractured system. This is a particularly unexplored process internationally. Focussed studies have been on sites with porous media due to the difficulty in locating source zones in fractured rock aquifers (National Research Council, 2004).

- Demonstrate the effectiveness of utilising the Triad Approach to site characterisation in a fractured system as compared to a conventional site characterisation process. This process will be innovative for characterisation in South Africa.

- Evaluate and document the process to be followed for a complex site with multiple contaminants and source zones within a fractured rock environment.

- Develop criteria to allow Site Owners to optimise data collection that can inform decision-making.

1.3 Structure of Thesis

This thesis is divided into five (5) chapters. Chapter 1 provides the background, motivation and objectives of this thesis.

Chapter 2 describes previous work undertaken by other authors to determine the influence of DNAPL and media properties on the fate, transport and transformation of DNAPLs in the subsurface. Chapter 2 also provides a literature review of site characterisation tools investigated by previous authors and work done to date in attempting to define the optimum level of characterisation required at a site.

Chapter 3 is a synthesis of the background to the Investigation Site and the evaluation of traditional and novel methods and approaches used in this research to characterise the DNAPL source zones. The results of the research are presented.

Chapter 4 documents a qualitative process model to improve source zone characterisation efficiencies in the South African context.

Chapter 5 presents the conclusions of this research and contains recommendations for future work.

The Appendices to this research are provided electronically at the back of the document.

CHAPTER 2

2 LITERATURE REVIEW

Due to the prevalent use of DNAPLs (particularly halogenated hydrocarbons or solvents) during the 20th Century, groundwater contamination from these chemicals has become commonplace in industrialised regions of countries (for e.g. Cohen and Mercer, 1993; United States Environmental Protection Agency, 1993; Usher *et al.*, 2004; Moran, 2006; etc.). This chapter presents a description of the uses and attributes of DNAPLs that allows them to be beneficial while at the same time having toxic and costly ramifications to detect and remediate in the subsurface. This chapter also explores the properties of DNAPLs and their associated behaviour in geo-contaminants settings, with an emphasis on fractured rock environments; the prevalent geo-contaminant setting in the South African scenario.

2.1 Introduction to DNAPLs

DNAPLs are chemicals (organic and inorganic) or groups of chemicals displaying the following properties:

- fluid density greater than 1.01 g/cm^3,
- solubility less than 2% (or 20000 mg/l),
- vapour pressure less than 40 kPa (300 torr) (Pankow and Cherry, 1996).

Huling and Weaver (1991) and Cohen and Mercer (1993) identify over 70 DNAPLs that have been commonly used in a wide variety of applications ranging from product feedstocks to end products. The types of DNAPLs most commonly encountered at contaminated sites are chlorinated hydrocarbons (such as trichloroethane, tetrachloroethane, trichloroethene etc), followed by PCBs, coal tars and creosote (Kerndorff *et al.*, 1992; Cohen and Mercer, 1993; United States Environmental Protection Agency, 1993; Usher *et al.*, 2004). A detailed description of the major groups of DNAPLs is provided in Cohen and Mercer (1993). DNAPLs typically enter the subsurface as a result of activities related to the disposal, storage, usage, transportation and handling of these chemicals.

Chlorinated hydrocarbon DNAPLs such as trichloroethene (TCE or trichloroethylene), tetrachloroethene (PCE or perchloroethene) and trichloroethane (TCA) are used in aerospace and electronics industries, dry cleaning, metal cleansing and degreasing,

the manufacture of pharmaceuticals, pesticide formulation and wood manufacturing (Cohen and Mercer, 1993; Halogenated Solvents Industry Alliance, 2004). Chlorinated solvents are also encountered in everyday household consumer products such as drain/oven/pipe cleaners, household degreasers, pesticides, shoe polishes and deodorizers (United States Environmental Protection Agency, 1980).

DNAPL that is composed of two or more chemical compounds are referred to as multi-component DNAPL or a mixed DNAPL. This is the common scenario at chemical waste landfills, lagoons, chemical waste handling and reprocessing sites and other industrial facilities where various organic chemicals were released into the environment and where DNAPL mixtures are present (Cohen and Mercer, 1993). It is not unusual to find that chlorinated solvents represent a significant portion of mixed DNAPL sites. A mixed or multi-component DNAPL often displays different physical and chemical properties compared to a single component DNAPL (such as tetrachloroethene or PCE at a dry cleaning site). The Investigation Site (Chapter 3) represents the ideal case study of a mixed DNAPL site consisting predominantly of chlorinated solvents or chlorinated hydrocarbon DNAPLs.

Production of DNAPLs began in the 19th Century with coal tars being produced at manufactured gas plants (MGPs) in Europe and the USA. Chlorinated solvents were first produced in Germany in the 1800's and in the USA early in the 20th Century. The rise in industrial activity after World War II saw a corresponding increase in use of DNAPLs, particularly the chlorinated solvents whose properties had tremendous industrial value. Pankow and Cherry (1996) record that from 1940-1980, approximately 2 billion pounds (approximately 907 000 tons) of chlorinated solvents was being produced in the USA alone. Figure 2-1 shows the production of selected DNAPLs in the USA within the period 1920-1998.

Despite the wide production and use of DNAPLs since the 19th Century, the significance of these chemicals as soil and groundwater pollutants was only realised in the 1970's (Schwille, 1988). Rivett *et al.* (1990) and Kueper *et al.* (2003) state the following reasons for this late awareness:

- The general lack of understanding of the significance of groundwater as a supply of potable water;
- The lack of suitable analytical equipment and methodologies for testing these compounds in low enough detection limits. Even with the advent of suitable analytical methods for the detection of DNAPL since the mid-1950's; the lack of knowledge of

these chemicals as groundwater contaminants allowed scientists to concentrate their efforts on other known contaminants such as alkyl benzene sulphonate (ABS) detergents and aldrin;

- The practices of disposing of DNAPL wastes directly onto the ground and into shallow soil systems;
- The extreme difficulty of suspecting and detecting the presence of DNAPL in groundwater due to their lack of any noticeable taste and odour and of their higher densities relative to water.

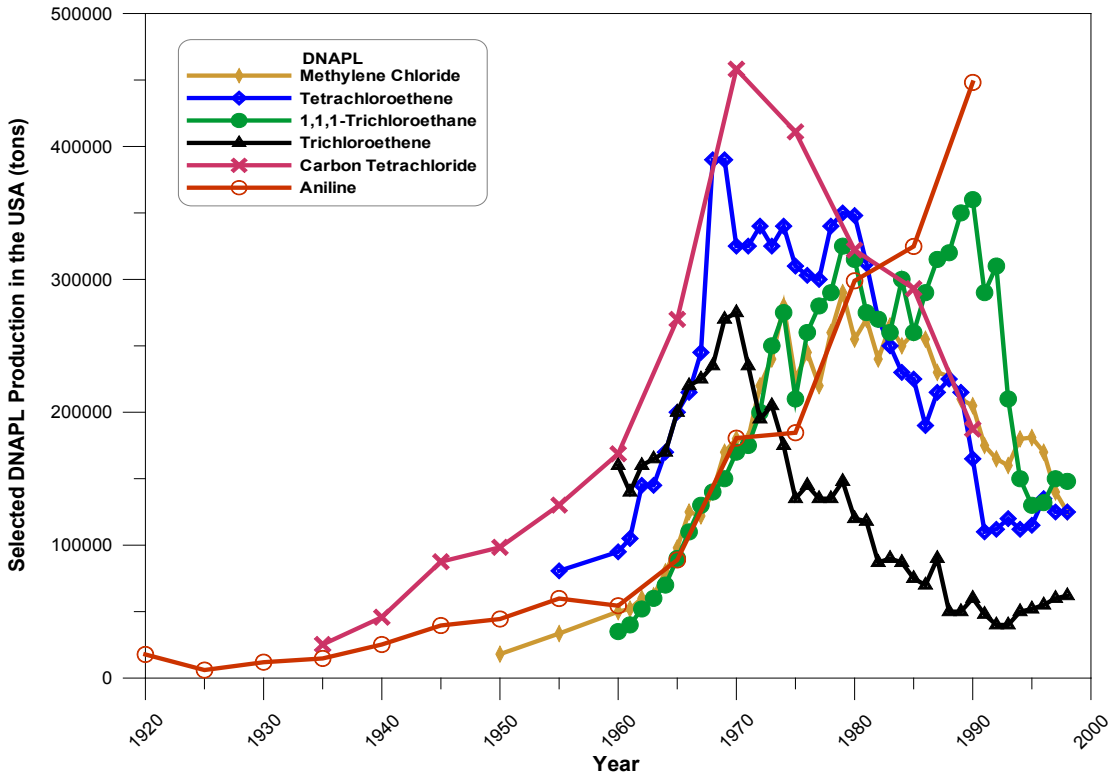

Figure 2-1: Selected DNAPL production in the USA from 1920-1998 (modified from Cohen and Mercer, 1993; and Moran, 2006)

While production of most chlorinated solvents have dropped to levels similar to that of the mid-20th Century (Figure 2-1) as a result of human health and environmental concerns (Pankow and Cherry, 1996), the extensive and widespread use of these chemicals continue to be problematic due to their pervasive and non-conventional behaviour in the subsurface and their continued use as chemicals of choice by users. Doherty (2000) notes the use of PCE as the preferred solvent of approximately 85-90% of approximately 30 000 dry cleaners and launderers in the USA.

Knowledge of detecting DNAPLs as well as the understanding of the fate and transport of DNAPLs in the various geo-contaminant settings has evolved over the last half century (Pankow and Cherry, 1996 and Sale *et al.* 2008). The dominant theories and practices pertaining to DNAPLs that have evolved are shown in Figure 2-2.

2.1.1 DNAPL properties and behaviour in the subsurface

DNAPLs can migrate in the subsurface as volatiles in soil gas, dissolved in groundwater and as a mobile separate "free" phase. According to the United States Environmental Protection Agency (1992), the major factors that control DNAPL migration in the subsurface include:

- The volume of DNAPL released
- The area of infiltration at the DNAPL entry point to the subsurface
- The duration of release
- Properties of the DNAPL such as density, viscosity and interfacial tension
- Properties of the soil/aquifer media such as pore size and permeability
- General stratigraphy such as the location and topography of low permeability units
- Micro-stratigraphic features such as root holes, small fractures and slickensides found in low permeability layers (silt/clay layers).

The various properties affecting the migration of DNAPL in the subsurface is explored at length in Mercer and Cohen (1990), Fetter (1999), Cohen and Mercer (1993), Gebrekristos (2007), etc. The influence of the properties of the DNAPL in its movement in the subsurface and the influence that the changes in aquifer properties have on this migration are briefly described in Section 2.1.1.1. Section 2.1.1.2 focuses on the influence of a fractured rock setting has on the movement of the DNAPL as this is the primary geo-contaminant setting of the Investigation Site (Chapter 3).

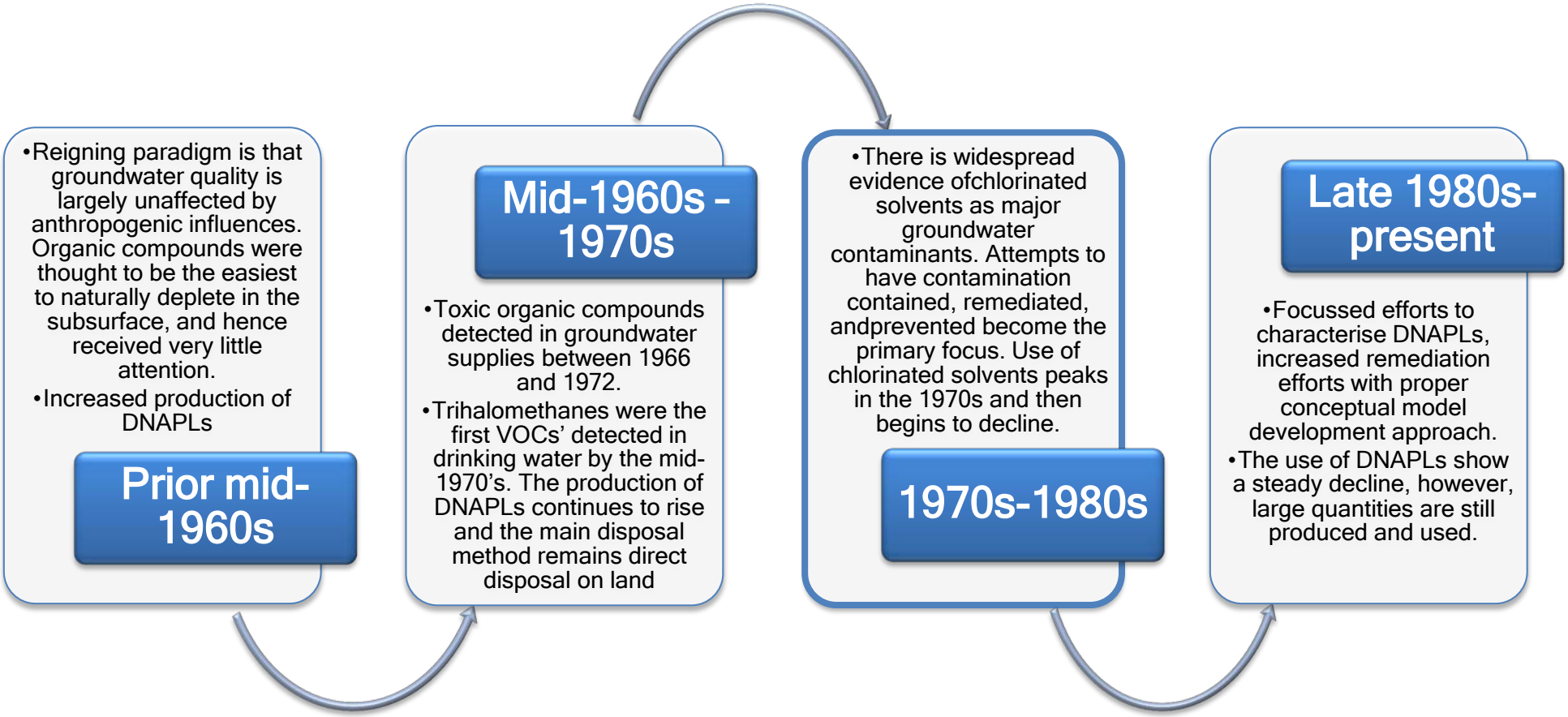

Figure 2-2: Evolution in the knowledge and understanding of DNAPLs as a primary groundwater contaminant (modified from Pankow and Cherry, 1996; Sale *et al.*, 2008)

2.1.1.1 DNAPL migration in the subsurface and the significance of heterogeneity

DNAPLs enter the subsurface through release via spills, leaks or direct disposal onto the ground surface. According to Poulsen and Kueper (1992), once the DNAPL has entered the subsurface, the interaction between the following forces determines the principle flow direction of the DNAPL:

- Gravity (also referred to as buoyancy or hydrostatic pressure): plays an important role in DNAPL migration in the first few meters of instantaneous release.
- Capillary pressure: resists the migration of non-wetting DNAPL from larger to smaller pore openings in water-saturated porous media. Capillary pressure and geological structures such as bedding planes and fractures are the predominant variables that determine DNAPL migration in the subsurface.
- Hydrodynamic pressure (also referred to as hydraulic or viscous force): can either promote or resist DNAPL migration. The effect of hydrodynamic pressure on DNAPL migration increases with decreased gravitational pressure, decreased capillary pressure and increased hydraulic gradient (Cohen and Mercer, 1993).

Capillary pressure is determined by the difference in fluid pressure between the wetting and non-wetting fluid. While wettability is measured or defined by the contact angle, this definition is complicated by the fact that the contact angle is hysteretic, displaying different values which are dependent on whether a fluid is advancing or receding over a surface (Adamson and Gast, 1997; Hiemenz and Rajagopalan, 1997). There are recorded cases of environmental systems where DNAPL is not the non-wetting phase such as the Hill Air Force Base in the USA where the system is partially oil-wetting (Jackson and Dwarakanath, 1999). Experiments undertaken by Mohammad and Kibbey (2005) to test the effects of dissolution on the contact angle indicate that wettability is subject to temporal change should the dissolution reduce the contact angle between the DNAPL and the medium surface. The scenario where the DNAPL has dissolved and the contact angle with the media surface has approached zero may have an effect on remediation times (Mohammad and Kibbey, 2005).

This relationship between a water-NAPL system with water being the wetting phase is described mathematically in the equation below:

$$\mathbf{P_c} = \Delta\mathbf{P} = \mathbf{P_{nw}} - \mathbf{P_w} \quad \textbf{Equation 2-1}$$

Where:

P_c = Capillary pressure

P_{nw} = the pressure of the non-wetting fluid (DNAPL)

P_w = the pressure of the wetting fluid (water) (Cohen and Mercer, 1993; Pankow and Cherry, 1996). The quantification of the capillary pressure function is an empirical relationship between capillary pressure and saturation, S (Thomas, 1982) in the form:

$$\mathbf{P_c = \Delta P = f(S)} \quad \textbf{Equation 2-2}$$

For media with a range in pore sizes, the capillary behaviour of the media is a function of the media saturation. This relationship, shown in Figure 2-3, is dependent on the flow dynamics (Hassanizadeh *et al.*, 2002). The capillary pressure – saturation relationship is hysteric. The curve is double-legged with one leg valid during the drying cycle (i.e. drainage) and the other leg valid during the wetting cycle (imbibition). A higher degree of non-wetting saturation can only be achieved with higher capillary pressure.

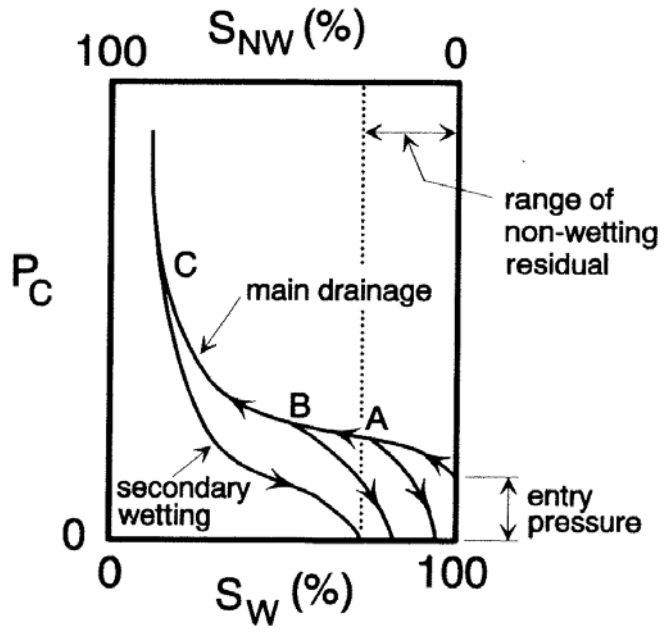

Figure 2-3: Capillary pressure-saturation curve for porous media illustrating the relationship between initial saturation along main drainage (points A, B, C) and residual saturation along secondary wetting (from Kueper *et al.*, 1993)

S_w = wetting phase saturation, S_{NW} = non-wetting phase saturation

The relationship between capillary pressure and interfacial tension, contact angle and pore size is described by the following Laplace equation:

$$\mathbf{P_c = (2\sigma \cos \phi)/r} \quad \textbf{Equation 2-3}$$

Where:

σ = interfacial tension between NAPL and water (N/m)

ϕ = contact angle. In a water-wet system ϕ is < 70°, while in a DNAPL-wet system ϕ is >110°
r = pore throat radius (m) (Mercer and Cohen, 1990; Cohen and Mercer, 1993).

Capillary pressure increases with high interfacial tension, a small pore throat radius and small contact angle. Interfacial tension is the most important physicochemical property controlling multiphase flow in the subsurface. Interfacial tension allows non-wetting DNAPLs to form globules in water and water-saturated media (Cohen and Mercer, 1993).

At the stage when sufficient pressure is produced in the DNAPL to overcome the combined capillary pressure and water pressure, infiltration of the DNAPL into the porous medium will occur. The pathway taken by the DNAPL is determined by the pore throat size distribution (Poulsen and Kueper, 1992). In experimental work undertaken by Harrold *et al*. (2003) on United Kingdom (UK) soil types and shallow aquifer materials it has been shown that under strongly water-wetting conditions, small changes in the interfacial tension can have major effects on the DNAPL head required to overcome the medium's capillary pressure.

The pressure at which a DNAPL will invade a media continuously once the threshold value has been reached is referred to as the entry pressure. For most media the entry pressure corresponds to a water saturation of 0.8 – 0.95 (Pankow and Cherry, 1996). Recent studies (for e.g. Gooddy *et al*., 2002) have demonstrated that experimental entry pressure measurements are lower than those predicted by capillary pressure theory. This implies that infiltration of DNAPL into the media is more likely than has previously been thought.

Relative permeability is a function of phase saturation and the most common manner of expressing this relationship for homogenous porous media are the X – curve and the Corey curve (Diomampo *et al*., 2002). The X - curve describes relative permeability as a linear function of saturation while the Corey curve relates relative permeability to the irreducible or residual liquid and gas saturation. The relative permeability - saturation relations for wetting and non-wetting phases are hysteric (Figure 2- 4). The relative permeability - saturation relationships quantify the relative permeability of the porous medium to a particular fluid phase at different fluid saturation levels.

Two-phase flow through fractures (either smooth or rough-walled) can be modelled by a porous medium approach (Diomampo *et al.*, 2002). In this approach fractures are treated as two-dimensional porous media and a pore spaced occupied by one phase is not available for flow for another phase. In this case flow is governed by Darcy's Law and phase interference is represented by the relative permeability variable.

Three-phase or multiphase relative permeabilities are required to describe the simultaneous movement of NAPL, water and air at a point (Cohen and Mercer, 1993). Chang *et al.* (2009) examines the relationship between relative permeability, saturation and capillary pressure in multiphase flow systems. The study found that the degree of connectivity of micro channels occupied by the wetting phase fluid could influence the relative permeability.

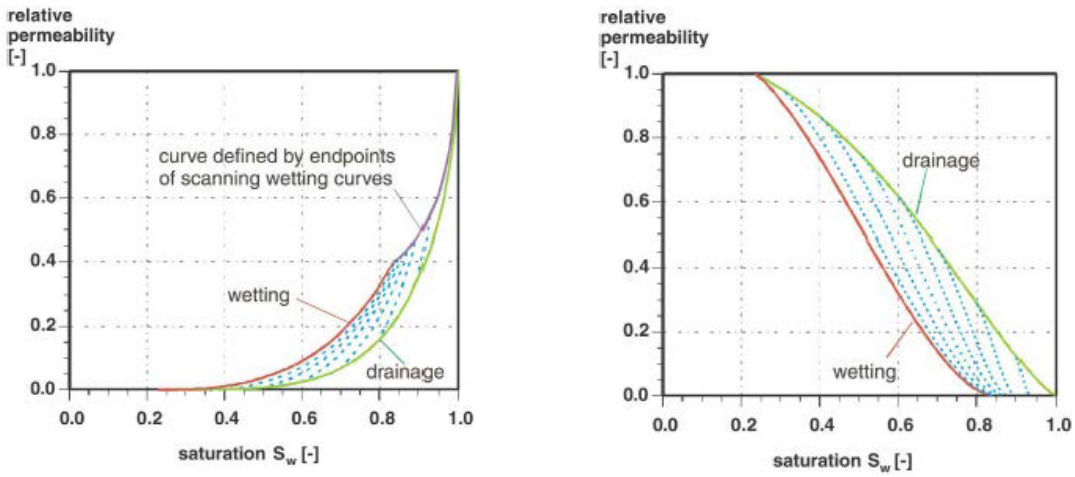

Figure 2- 4: Relative permeability – saturation curves for wetting phase (a) and non-wetting phase (b) (from Vogler *et al.*, 2001)

When a DNAPL enters the subsurface it can partition into the different phases. As the DNAPL sinks through the unsaturated zone, a portion is trapped in the porous media at residual saturation (S_r) due to interfacial tensions and dead-end pores. Residual DNAPL forms discrete blobs or ganglia (Figure 2-5). The distribution of the residual DNAPL is not uniform or easily predictable in the subsurface due to minute variations in the media pore size distributions. According to Cohen and Mercer (1993) a non-wetting fluid is discontinuous at residual saturation, while the wetting fluid is not. Factors affecting wettability include DNAPL and aqueous phase composition, the presence or absence of organic matter, mineralogy, saturation history, aqueous pH (Dawson and Ilangasekasre, 1999; Barranco *et al.*, 1997; Barranco and Dawson,

1999) and dissolution (Mohammad and Kibbey, 2005). Changes in wettability may play a significant role in affecting capillary pressure, relative permeability, residual saturation and the fluid displacement potential (Barranco *et al.*, 1997).

In the unsaturated zone, NAPL spreads as a film (Wilson *et al.*, 1990; Cary *et al.*, 1989) between the water and gas phases given a positive spreading coefficient (∑). Halogenated solvents typically have negative spreading coefficients and hence will not spread in the unsaturated zone as a result of the internal cohesion (Wilson *et al.*, 1990). Residual saturation values in the unsaturated zone range from 0.10 to 0.20.

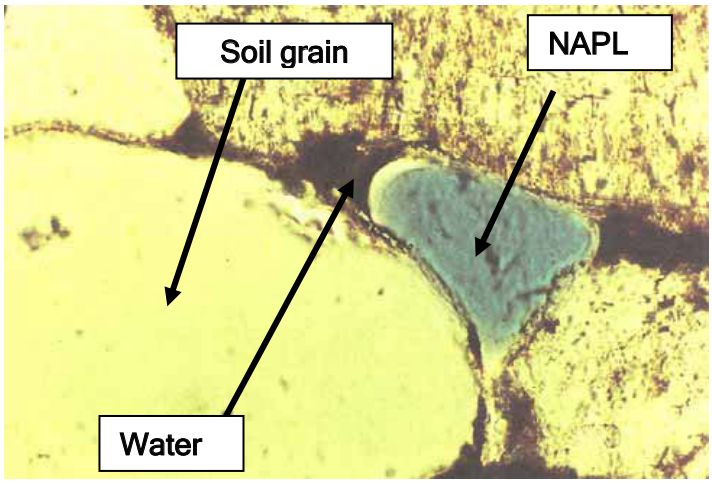

Figure 2-5: NAPL in the pore space of a granular porous media (from Wilson *et al.*, 1990)

In the saturated zone, residual saturation values are larger than those of the unsaturated zone for the following reasons (In Cohen and Mercer, 1993 from Anderson, 1988):

- The fluid density ratio (NAPL:air vs NAPL:water above and below the water table, respectively);
- The NAPL is the non-wetting fluid in most saturated media and is hence trapped in the larger pores;
- NAPL is the wetting fluid (with respect to air) in the unsaturated zone and tends to spread into adjacent pores and leaves a lower residual content behind.

Lenhard *et al.* (2004) found that NAPL in small pores in the unsaturated zone can be considered immobile because:

- the pore dimensions are small
- there are no continuous passages through the channels to conduct the NAPL
- NAPL adjacent to water films that are adsorbed to solid particles do not contribute to NAPL advection, especially if the water film is thin

The formation of residual NAPL through imbibitions in the unsaturated zone is illustrated in Figure 2-6.

Residual saturation values in the saturated zone range from 0.10 to 0.50. The mechanisms that facilitate the trapping of residual NAPL in the saturated zone are documented by Chatzis *et al.* (1983) and Wilson *et al.* (1990) and include the snap-off mechanism and the bypassing mechanism. Snap-off occurs in cases where there is a high aspect ratio between the pore body and the pore throat. This results in single droplets or blobs or residual NAPL. Bypassing occurs when the wetting fluid flow disconnects the non-wetting fluid. This causes ganglia to be trapped in clusters of large pores surrounded by smaller pores. As a result of the snap-off and bypass mechanisms, residual saturation increases with increasing pore aspect ratios and pore size heterogeneity and with decreasing porosity (Chatzis *et al.*, 1983; Powers, *et al.*, 1992).

Residual DNAPL is immobile under normal subsurface conditions (assuming that the equilibrium conditions holding the residual phase DNAPL are unchanged). However, residual DNAPL plays a significant role as long-term sources of contaminants for continued dissolution of contaminants into water and air in adjacent pores.

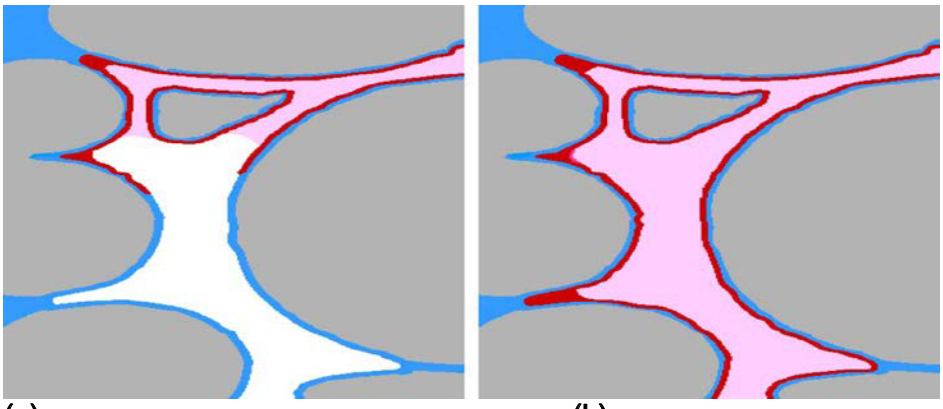

(a) (b)

Figure 2-6: Depiction of NAPL imbibition in the pore spaces. (a) shows small pores and pore wedges filled with NAPL before the larger pore bodies are filled. After these smaller spaces are filled, the NAPL is assumed to be immobile (red). (b) depicts the pore system is NAPL-filled with the mobile (free) NAPL shown as pink. Water is blue and solid particles are grey (from Lenhard *et al.*, 2004)

Residual DNAPL is exposed to air allowing for volatilisation across air-DNAPL interfaces; and to water allowing for dissolution into infiltrating water across DNAPL-water interfaces in the unsaturated zone. Dissolved components in soil moisture become available for partitioning across air-water interfaces. A mathematical model

for the prediction of residual phase NAPL in the air-NAPL-water phase was developed by Lenhard *et al*. (2004). According to Kueper *et al*. (2003), the absence of chlorinated solvents such as TCE and PCE (DNAPL phase) in the unsaturated zone is not conclusive in determining whether a past release occurred at a site or whether the release failed to reach the water table. The absence of the DNAPL phase could be a result of vaporisation processes which can deplete residual chlorinated solvents within a few years in warm and dry climates. The presence of vapour, adsorbed or aqueous phases however remains. Hughes *et al*. (1990) and Jellali *et al.* (2001) show through field experiments using TCE that shallow groundwater contamination can form through vapour transport through advection in the unsaturated zone and dissolution into groundwater. Jellali *et al*. (2001) also show experimentally that mass transport of DNAPL in the unsaturated zone is also affected by mass transfer from groundwater to the unsaturated zone through volatilisation of dissolved components. DNAPL with a higher Henry's Law Constant display higher volatilisation.

When in contact with the capillary fringe, DNAPLs will tend to migrate laterally (Schwille, 1988). At this point the DNAPL will accumulate until gravitational forces at the base of the mass exceed the threshold entry pressure of the underlying saturated zone. The entry pressure for the DNAPL is relative to the pore size. DNAPLs tend to migrate into the largest pores first (Kueper *et al*., 1989; Kueper and McWhorter, 1991). Once the threshold entry pressure is exceeded, the DNAPL will displace the water and continue migrating under capillary and gravitational forces. Zhang and Smith (2002) show that the fingering process in a homogenous porous media can be divided into two stages: the DNAPL finger initiation stage and the finger elongation stage. They also show that fingering of a small amount of DNAPL in homogenous, porous media will penetrate to a much larger depth than previously predicted using classic flow equations, consequently overestimating the average DNAPL content while underestimating the depth of DNAPL penetration.

If the DNAPL encounters a bowl-shaped stratigraphic trap it may be immobilized as a reservoir of continuous immiscible fluid. If no stratigraphic traps are present, the DNAPL will migrate according to the slope of the capillary barrier layer, which might be a different direction from that of the hydraulic gradient (Cohen and Mercer, 1993). DNAPL in unconsolidated media can also pool or mound above fine-grained horizons such as silt and clay units (Kueper *et al*., 1993; Feenstra *et al*., 1996). The maximum pool height is inversely proportional to the permeability of the capillary barrier unit (Durnford *et al*., 1997; Kueper *et al*., 2003). However, in most instances preferential

pathways such as fractures, root holes etc. are present within these low permeability units which allow for the migration of DNAPL (Kueper and McWhorter, 1991; O'Hara *et al.*, 2000; Parker *et al.*, 2004). The architecture of DNAPL in the saturated zone depends on the heterogeneity of the stratigraphic units (Illangasekare *et al.*, 1995) and can exist as pools, disconnected globules and ganglia, or immobilised in stratigraphic traps and residual saturation (Figure 2-7). Irrespective of whether the DNAPL is mobile or immobile in the saturated zone, it can still dissolve and persistently contaminate groundwater. The sparsely distributed ganglia and pools of DNAPL make it very difficult to find (Pankow and Cherry, 1996; Parker *et al.*, 2003). Stratigraphic or geological heterogeneity also has a huge bearing on the mechanisms by which contaminants are stored and released from the source zone to downgradient plumes.

DNAPL will dissolve over time within a hydraulically transmissive layer. Initially, the chemical gradient will be sustained via transport of the dissolved DNAPL constituent away from the source zone. This process occurs through the following mechanisms:

- Transverse diffusion into the groundwater and subsequent horizontal advection along the top of the source
- Advective transport through the source
- Matrix diffusion into low permeability zones

The DNAPL constituents are stored as dissolved phase in water and as a sorbed phase on or in solids in these low permeability zones. Sorption acts as a sink that accelerates DNAPL dissolution. The aqueous phase or dissolved phased plume is typically the most mobile form of DNAPL contamination and most investigation efforts are often focussed on determining the likely risks of the migrating phase on identified receptors.

DNAPLs are only slightly soluble in water. This implies that they persist as long-term sources of contaminants. Most sites consist of complex or mixed contaminants. In these cases, the properties of an individual component in the mixture vary from those of the pure component. The term "effective solubility" is used to describe the solubility of a particular component in a complex mixture. As dissolution proceeds, the composition of the NAPL changes (Mackay *et al.*, 1991). For example Melber *et al.* (2004) document that as the dissolution of creosote proceeds; the more soluble components will be rapidly lost. This causes the mole fraction (and hence the effective solubilities) of the other constituents to increase. The properties of a mixture are determined by the properties of its pure components and their concentrations in

the mixture. Hence, chemicals of interest behave ideally in the matrix containing them. Under these conditions, the concentration of a chemical in the aqueous phase is proportional to the mole fraction of the chemical in the phase corresponding to Raoult's Law. The following expression can be used to predict the concentrations of a chemical in a complex mixture in the aqueous phase (Schwarzenbach *et al.*, 1993):

$$C_w = x_0 S \quad \text{Equation 2-4}$$

Where:

C_w = chemical's concentration in the aqueous phase (mol/L) in equilibrium with the organic phase or the effective solubility

X_0 = mole fraction of the chemical in the NAPL phase

S = aqueous solubility of the pure liquid chemical (mol/L)

The mole fraction can be calculated using the following equation:

$$x_0 = {MF_x MW_0}/{MW_x} \quad \text{Equation 2-5}$$

Where:

MF_x = mass fraction of the selected organic compound in the mixture

MW_0 = average molecular weight of the mixture

MW_x = molecular weight of the selected compound

The octanol-water partition coefficient (K_{ow}) is used to describe the degree to which an organic substance will preferentially dissolve in water or an organic solvent. The larger the octanol-water partition coefficient, the larger the tendency of the organic substance to dissolve in octanol rather than in water and will hence be less mobile in the environment (Fetter, 1999).

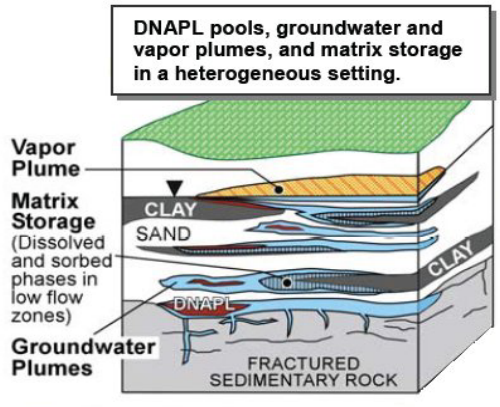

Figure 2-7: Simplified illustration of the existence of different phases of DNAPL within a heterogeneous setting (from Sale et al., 2008)

Matrix diffusion is the process whereby contaminants move into low permeability layers. Matrix porosities of clayey deposits range from 30-70% and between 5-25% for sedimentary deposits (Freeze and Cherry, 1979). Matrix diffusion into low permeability layers can sustain dissolved plumes in transmissive zones after the DNAPL source zone is depleted (Sudicky *et al.*, 1985; Parker *et al.*, 1994; Parker *et al.*, 1997; Liu and Ball, 2002; Chapman and Parker 2005; Air Force Center for Engineering and the Environment, 2007) It can also attenuate the rate at which a plume advances in fractured rock and can result in delayed breakthrough curves (Kueper and Davies, 2009), commonly referred to as "pulses" (Figure 2-8).

The storage of contaminants through matrix diffusion and the consequent back diffusion of these chemicals into transmissive zones is illustrated in Figure 2-9. Four primary factors control the DNAPL mass stored within the low permeability zone:

- the duration of DNAPL present at the interface between the transmissive and the low permeability zones;
- the solubility of the DNAPL constituents;
- The amount of adsorption to solids;
- The rates of biotic and abiotic degradation of contaminants in the low permeability zone (Air Force Center for Engineering and the Environment, 2007).

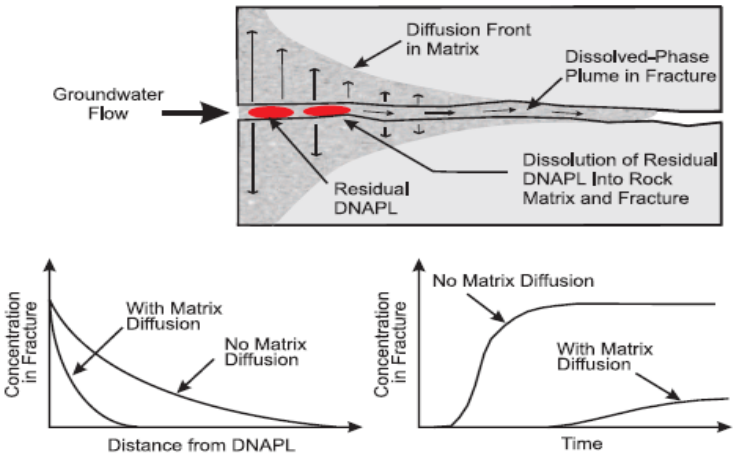

Figure 2-8: Illustration of matrix diffusion of dissolved phase contaminants adjacent to DNAPL source and along length of plume in a fracture. Matrix diffusion can attenuate the rate of plume advance in fractured rock (concentration vs distance plot), and can result in delayed breakthrough curves (concentration vs time figure) (from Kueper and Davies, 2009)

The total chemical mass in a DNAPL source zone consists of the following constituents: DNAPL, dissolved constituents, vaporised constituents (gas phase) and sorped phased (Cohen and Mercer, 1993).

Immediately after a spill or release, free phase DNAPL will be the largest component of the contaminant mass in the source zone. Over time, the DNAPLs dissolve and develop an aqueous phase plume. Mass is also transferred into vapour and sorbed phases. During the late stage, little or no DNAPL will remain and the plumes are sustained via release of contaminant mass through back diffusion from low permeability zones. The mass stored in the aqueous phase and the sorbed phase is referred to as "non-DNAPL source mass" (Air Force Center for Engineering and the Environment, 2007). The evolution of a DNAPL (chlorinated solvent) release is illustrated in Figure 2-10.

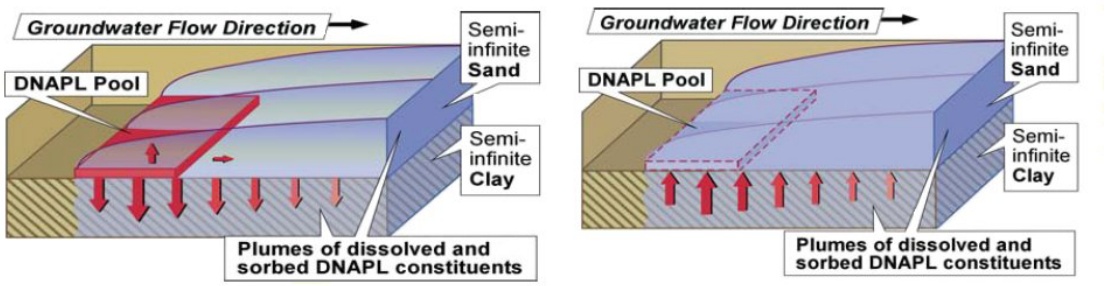

Diffusion of contaminants into a low permeability zone beneath a DNAPL pool and the downgradient plume (arrows depict the movement of dissolved DNAPL)

Diffusion of contaminants out of a low permeability zone after complete DNAPL dissolution (arrows depict the movement of dissolved DNAPL)

Figure 2-9: Significance of matrix diffusion (from Sale *et al.*, 2008)

According to Sale *et al.* (2008) the key factors that control the rate which a release ages include:

- The amount of DNAPL release;
- The solubility of the constituent of DNAPL;
- The rate of groundwater flow; and
- The architecture of transmissive and low permeability zones.

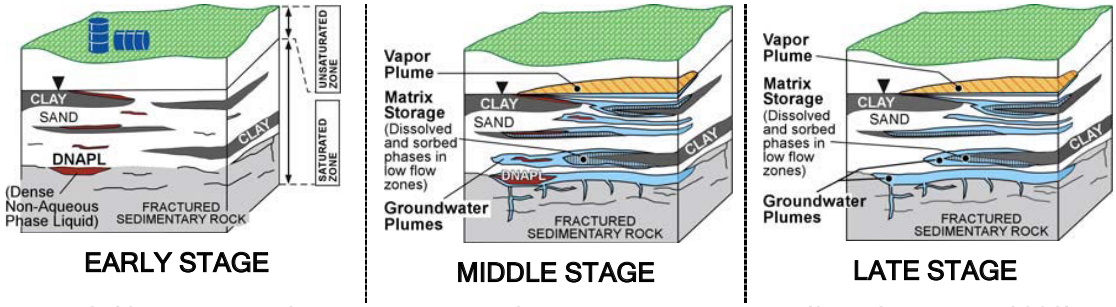

Figure 2-10: Evolution of a DNAPL release from early to late stages (from Sale *et al.*, 2008)

2.1.1.2 DNAPL migration in fractured and dual porosity media

Fracture networks are ubiquitous and dominate the hydrogeological setting of South Africa, having been formed by the deformation of rocks and soils through processes such as tectonic forces, subsurface subsidence or thermal expansion. Groundwater flow through a fracture network is strongly influenced by the geometry of fractures. Fracture flow is flow through a dual porosity system which includes the porous matrix and the fracture network. The degree of interconnection between the matrix and the fracture network defines the character of the flow domain and is a function of bulk hydraulic conductivity which is a function of the fracture network distribution, the matrix hydraulic conductivity, the fracture orientation, connectivity and apertures.

In unsaturated fractured rock, the hydraulic conductivity of a fracture decreases with aperture size (Wang and Narashiman, 1985; Martinez *et al.*, 1992) as a result of capillary forces draining the largest pores in the unsaturated zone first and transforming them into flow barriers. In saturated fractured rock, hydraulic conductivity of a fracture increases with the fracture's aperture. The cubic law (Snow, 1965) describes laminar flow in fracture between two smooth parallel plates and the hydraulic conductivity of the fracture is proportional to the square of the fracture aperture. In natural formations where the fracture aperture is variable and not constant, the cubic law is not valid. Variable apertures result in flow being channelled into preferential flow paths along zones with the largest interconnected apertures (for e.g. Tsang *et al.*, 1991; Murphy and Thomson, 1993; Birkholzer and Tsang, 1997; Ge, 1997; Oron and Berkowitz, 1998; O'Hara *et al.*, 2000).

DNAPL can enter fractures in the unsaturated zone and in the saturated zone (Kueper *et al.*, 2003). Residual DNAPL and DNAPL pools will form in fractured bedrock.

The fracture entry pressure is directly proportional to the interfacial tension and inversely proportional to fracture aperture; resulting in preferential DNAPL migration through the larger aperture fractures of a fracture network. According to Kueper and McWhorter (1991), the critical aperture controlling NAPL flow through a variable aperture is the aperture corresponding to the entry pressure. Steele and Lerner (2001) state that the critical aperture corresponds to the smallest aperture constriction where NAPL first forms a fully connected pathway across a variable aperture network. If static equilibrium is assumed, the capillary pressure immediately above the fracture can be expressed as the height of the pooled DNAPL (Kueper and McWhorter, 1991). Figure 2-11 depicts a fractured network where the vertical extent of migration has been stopped due to the narrowing of the fracture aperture at point 'A'. In this case the capillary pressure at the top of the DNAPL pool is zero. According to Kueper and McWhorter (1991) and Kueper *et al*. (2003), only those fractures that have entry pressure less than the capillary pressure of the DNAPL-water system are invaded. Under hydrostatic conditions, progressively smaller aperture fractures with depth can be invaded. The relationship between the vertical height of the DNAPL pool (H) and the fracture aperture at point 'A' is given by the following equation:

$$\mathbf{H} = \frac{2\sigma \cos \phi}{(\rho_N - \rho_W)ge} \quad \textbf{Equation 2-6}$$

Where:

H = vertical height of pooled DNAPL

σ = DNAPL-water interfacial tension

Φ = contact angle

ρ_N = DNAPL density

ρ_W = groundwater density

g = acceleration due to gravity

e = fracture aperture

A plot of the fractured aquifer required to stop vertical migration versus depth for a range of DNAPLs is shown in Figure 2-12. The graph shows that for the same height of the different DNAPL compositions, the decrease in aperture size for a corresponding chlorinated solvent must be very quick with depth compared to the same pool height of coal tar DNAPL. According to Kueper *et al*. (2003), vertical migration to considerable depths at sites with chlorinated solvent DNAPLs might have stopped by the time the site is investigated due to the very high densities and low viscosities. Larger pool heights, lower viscosities and higher densities allow for quicker penetration of the bedrock fractures (Pankow and Cherry, 1996).

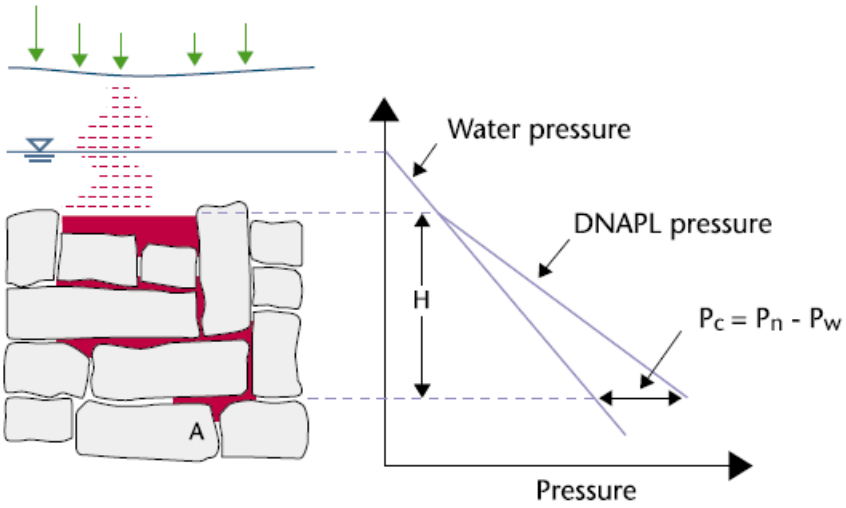

Figure 2-11: Pooling of DNAPL in a fractured network. If hydrostatic equilibrium is assumed, then the capillary pressure increases linearly with depth (from Kueper *et al.*, 2003)

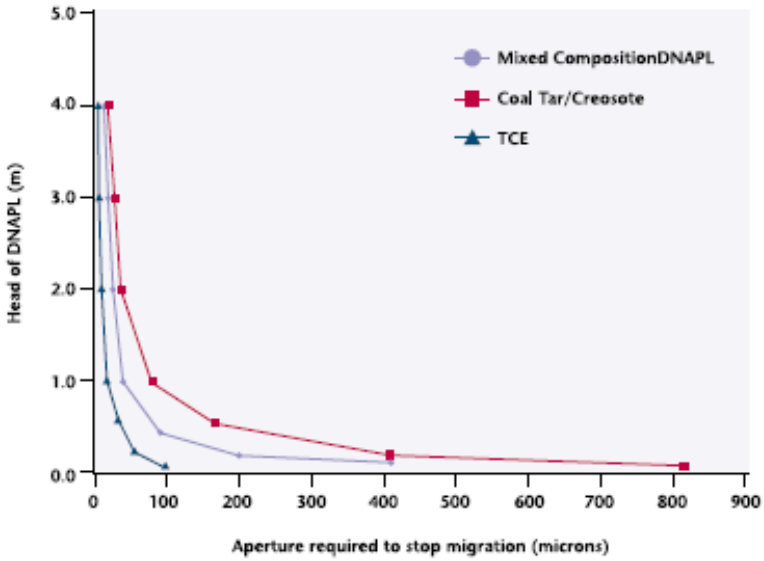

Figure 2-12: Fracture aperture required to stop DNAPL migration versus the height of the accumulated DNAPL (from Kueper *et al.*, 2003)

Other factors that influence the migration of DNAPL include:

- Interfacial tension - A system with a low interfacial tension will show higher vertical movement through a low permeability unit as compared to a higher interfacial tension system (Figure 2-13)

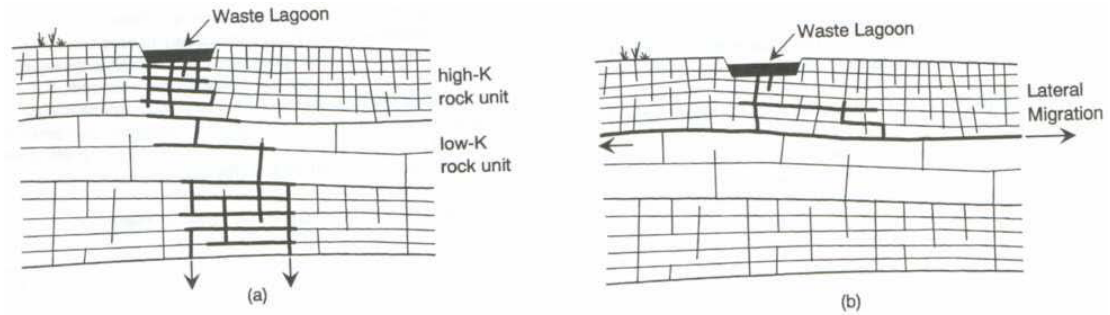

Figure 2-13: Illustration of differing migration pathways for a low interfacial tension system (a) versus a high interfacial tension system (b) (from Pankow and Cherry, 1996)

- Fracture density, orientation and connectivity – DNAPLs migrate through the pathways of least capillary resistance. Hence, the fracture orientation and connectivity will influence the direction in which the DNAPL migrates as compared to the hydraulic gradient. Significant fracture density and interconnectivity in a confining layer such as clay can allow for vertical migration of DNAPL as well as leakage of dissolved contaminants (Harrison *et al.*, 1992). Small scale heterogeneities can influence flow paths of the DNAPL, requiring adequate fracture characterisation (Dennis *et al.*, 2010).

In aquifer systems with dual porosity where the matrix porosity is high, matrix diffusion (see Section 2.1.1.2.) plays an important role. Dissolved contaminants are subject to diffusion out of and into the rock matrix. According to the United States Environmental Protection Agency (2001) and Parker (2007), discrete fracture pathways (as compared to the total fracture network) play a significant role in hydrogeological investigations in fractured rock. As only some subsets of open fractures will have active groundwater flow, the challenge in application of characterisation technologies is to locate the significant fractures and apply these technologies so that they take measurements that are representative of *in situ* conditions. The location of the DNAPL plume is hydraulically downgradient of the DNAPL source zone. Depending on the biogeochemistry environment and the processes involved, the chemical composition of the plume may be different from the DNAPL in the source zone. According to the National Research Council (2004) groundwater plumes tend to have larger spatial extent and are more continuous when compared to the contaminant mass distribution within source zones. As a result of the architecture of DNAPL source zones, irregular and stratified plumes are created.

2.1.2 Transformation of DNAPLs

Three processes affect solute contaminant transport:

- Physical processes (dispersion, diffusion, dilution and volatilisation);
- Geochemical processes (sorption, abiotic reactions); and
- Biotic processes (biodegradation).

According to the United States Environmental Protection Agency (1998) the DNAPL form does not easily attenuate and it is therefore important to determine whether the site has DNAPL in order to account for this during remediation planning and implementation. The dominant attenuation processes at DNAPL contaminated sites are shown in Table 2-1.

DNAPLs can undergo non-destructive attenuation through processes such as dilution, dispersion, diffusion, sorption and volatilisation. These processes can reduce the contaminant concentrations in groundwater and in the case of volatilisation can also reduce contaminant mass. However, these processes rarely have an effect on the contaminant toxicity or mass. The mass and composition of DNAPLs can be affected through destructive attenuation mechanisms. These are discussed in more detail in the following sections.

2.1.2.1 Transformation processes of halogenated DNAPLs

Halogenated DNAPLs (such as chlorinated hydrocarbons/solvents) are the most common types of DNAPLs found at industrial sites. The Investigation Site (Chapter 3) contains chlorinated hydrocarbons as the predominant contaminants of concern; hence this section will focus on the transformation processes that affect these compounds.

Biotic and abiotic processes lead to the transformation of these compounds in the subsurface. Biotic transformations can lead to more toxic daughter or intermediate products (such as cis-1,2-dichloroethene and vinyl chloride) and can further complicate characterisation (Cheremisinoff, 1990). Recently a large amount of focus has been paid to destructive attenuation mechanisms as a remediation technology (for e.g. United States Environmental Protection Agency, 1999; National Research Council , 2000; Newell and Aziz, 2004; Pretorius, 2007; Usher *et al.*, 2008) and to the applications of molecular biological tools (Stroo *et al.*, 2006). It was previously thought (Robertson and Alexander, 1996) that biotransformation close to a

chlorinated solvent source was unlikely due to the high toxicity of the DNAPL contaminant concentrations. Several authors have however reported microbial activity at concentrations at or near the aqueous solubility of PCE (for e.g. Yang and McCarty, 2000; Cope and Hughes, 2001). According to laboratory studies undertaken by Yang and McCarty (2002) and Cope and Hughes (2001), microbial activity can increase DNAPL dissolution by a factor of 5 or more.

Biotic transformations are typically faster than abiotic transformations; provided that there is sufficient substrate, nutrients and a microbial population that can facilitate the transformation (Vogel *et al.*, 1987). The most common abiotic reactions are hydrolysis and dehydrohalogenation. While most abiotic reactions are slow; they can still be significant relative to groundwater movement rates. Intermediates formed during abiotic transformation tend to accumulate and commonly require biotic processes to stimulate the abiotic reactions (Wiedemeier *et al.*, 1999). The transformation process affecting halogenated DNAPLs can be divided into two categories: (i) reactions that require external electron transfer (oxidation reactions such as epoxidation and reduction reactions such as coupling); and (ii) reactions that do not (substitution reactions such as hydrolysis and dehydrohalogenations). The definitions of the various types of transformations are provided in Table 2-2.

If the primary transformation pathway for halogenated DNAPL contaminated groundwater is a physical process such as volatilisation, then the Henry Law's Constant would be the determining factor of the evolution of the groundwater composition (Cho *et al.*, 2004). An example of the transformation of groundwater impacted with 1,1,1-Tricholoroethane (1,1,1-TCA), 1,1-Dichloroethane (1,1-DCA) and 1,1-Dichloroethene (1,1-DCE) is provided in Figure 2-14. This figure illustrates that if the physical process (sorption and volatilisation) are the primary transformation process occurring in mixed chlorinated solvents impacted groundwater, then the groundwater will become increasingly enriched in 1,1,1-TCA. However, with the same starting composition, the groundwater becomes enriched with 1,1-DCA under biotic transformation processes or 1,1-DCE under abiotic transformation process as shown in Figure 2-15 (Vogel and McCarty, 1987; Cho *et al.*, 2004).

Table 2-1: Dominant attenuation mechanisms for DNAPL groups (In Pretorius, 2007 from Carey *et al.*, 2000)

DNAPL Group	Example	Non-Destructive attenuation mechanisms					Destructive attenuation mechanisms				
		Sorption	Dispersion	Diffusion	Volatilisation	Aerobic degradation (Contaminant as electron donor)	Anaerobic degradation (contaminant as electron acceptor)	Reductive dehalogenation	Fermentation	Co-metabolism	Oxidation/reduction
Chlorinated Solvents	PCE, TCE, TCA	×	×	×	×	×	×	××		×	×
	DCM, VC, DCE	×	×	×	×	××	×	×	×	×	
Creosote	Phenols and phenolics		×	×	×	××	××		×	×	
Pesticides	Chlorinated pesticides, organophosphate	×	×	×		×	×	×		×	

Where:

× = of primary importance

×× = of secondary importance

Table 2-2: Biotic and abiotic transformation reaction definitions (modified from Vogel *et al.*, 1987)

Reaction Term	Definition
Coupling	A reaction in which two alkyl groups or aryl groups connect together E.g. $2CCl_4 + 2e^- \rightarrow CCl_3CCl_3 + 2Cl^-$
Dehydrohalogenation	Elimination of HX to form an alkene E.g. $CCl_3CCl_3 \rightarrow CCl_2CH_2 + HCl$
Dihalo-elimination	Reductive elimination of two halide substituents to an alkene E.g. $CCl_3CCl_3 + 2e^- \rightarrow CCl_2CH_2 + 2Cl^-$
Epoxidation	Reaction in which an epoxide is generated E.g. $CHClCl_2 + H_2O \rightarrow CHClOCCl_2 + 2H^+ + 2e^-$
Hydrogenolysis	A reduction reaction in which a carbon-hydrogen bond is broken and hydrogen replaces halogen substituent E.g. $CCl_4 + H + 2e^- \rightarrow CHCl_3 + Cl^-$
Hydroxylation	Addition of a hydroxyl group E.g. $CH_3CHCl_2 + H_2O \rightarrow CH_3CCCl_2OH + 2H^+ + 2e^-$
Solvolysis	Reaction in which the solvent serves as the nucleophile (i.e. a reacting species providing an electron pair) E.g. $CH_3CH_2CH_2Br + H_2O \rightarrow CH_3CH_2CH_2OH + HBr$

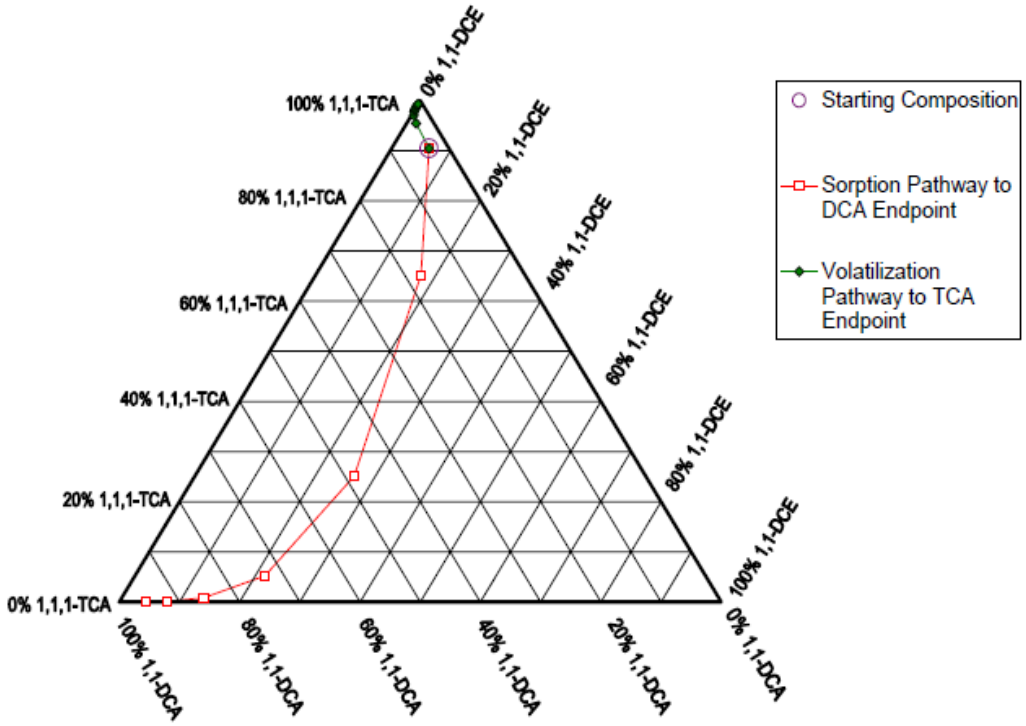

Figure 2-14: Sorption and volatilisation transformation pathways (from Cho *et al.*, 2004)

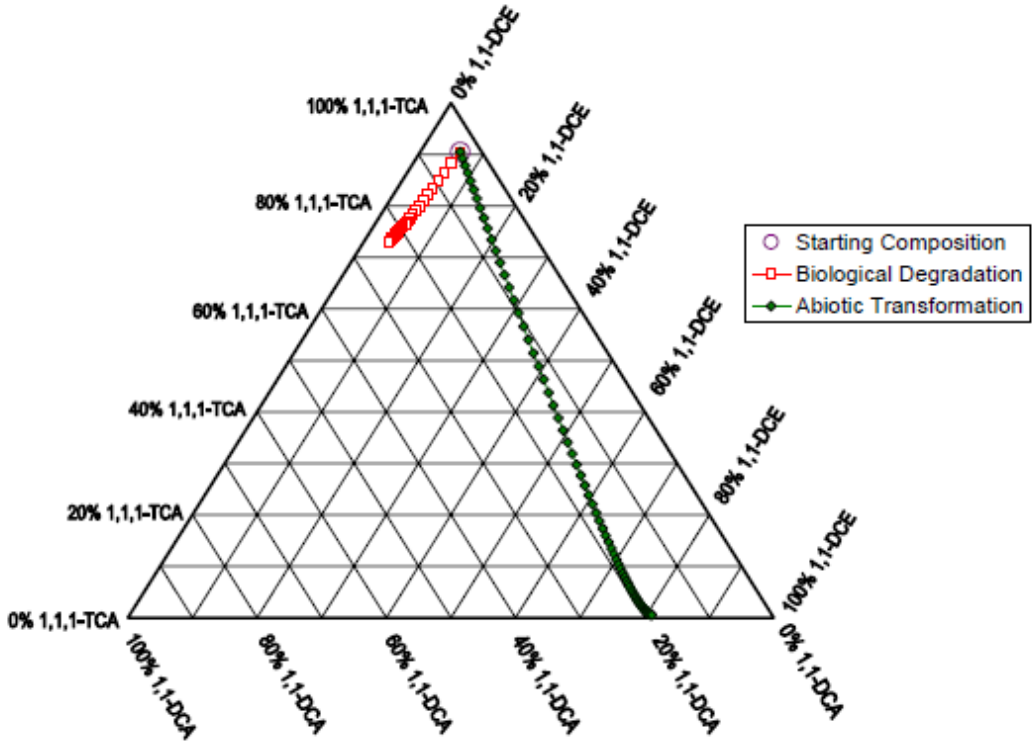

Figure 2-15: Biotic and abiotic transformation pathways (from Cho *et al.*, 2004)

Recent developments in the use of compound specific isotope analysis (for e.g. Hunkeler *et al.*, 2005; Liang *et al.*, 2007) has allowed for distinguishing abiotic from biotic transformations. Compound specific isotope analysis (CSIA) is increasingly becoming a useful tool to assess *in situ* biodegradation and biodegradation pathways of chlorinated solvents. The theory and application of CSIA is described in more detail below (Section 2.1.2.2).

Degradation pathways for chlorinated ethanes and ethenes via reductive dechlorination, dichloroelimination and dehydrohalogenation are shown in Figure 2-16. Under reducing or anoxic conditions, chlorinated ethenes and ethanes can be sequentially dechlorinated by microorganisms (Ballapragada *et al.*, 1997; de Best *et al.*, 1997; de Best *et al.*, 1999; Adamson and Parkin, 2001; Major *et al.*, 2002; Hunkeler *et al.*, 2005). Phylogenetic groups of bacteria that are capable of metabolic reductive dechlorination for chlorinated ethenes *include Dehalobacter, Sulfurospirillum*, *Desulfuromonas*, *Desulfitobacterium*, *Clostridium* and *Dehalococcoides*. A limitation is that not all organisms can allow the complete dechlorination to ethene, causing the subsurface accumulation of toxic intermediates such as dichloroethene and vinyl chloride. The most promising phylogentic group of bacteria in the reductive dechlorination of chlorinated ethenes has been identified to be *Dehalococcoides* (He *et al.*, 2003). According to McCarty (1997) reductive dechlorination of tetrachloroethene (PCE) to TCE only occurs under methanogenic conditions and will not occur in nitrate-reducing zones. Stiber *et al.*, (1999) propose a Bayesian Belief Network (BBN) framework for the reductive dechlorination of TCE (Figure 2-17). A BBN is a graphical probabilistic technique. BBNs are useful for the modelling of causative networks. Various authors have observed the reductive dechlorination of PCE, TCE and carbon tetrachloride (CCl_4) under anaerobic conditions to less-chlorinated products (de Best *et al.*, 1999; Adamson and Parkin, 2001; Major *et al.*, 2002); however, the rate of dechlorination and the transformation products vary widely (Middeldorp *et al.*, 1999; Istok *et al.*, 2007). Push pull tests have been undertaken in order to measure the i*n situ* rates of reductive dechlorination of chlorinated ethenes using injected reactive tracers such as trichlorofluoroethene (TCFE) as a reactive tracer for trichloroethene (TCE) and cis-dichlorofluoroethene (DCFE) for cis-DCE (Hageman *et al.*, 2001; Ennis *et al.*, 2005; Field *et al.*, 2005; Istok *et al.*, 2007; Taylor *et al.*, 2007). These reactive tracers have similar chemical structures and reactivity to the targeted contaminants and are commonly referred to as “surrogates”. Other parameters that can be measured to determine whether biotic

degradation is occurring include: redox potential, dissolved oxygen, iron (II), methane, pH, sulphate, nitrate and chloride.

1,1,2-Trichloroethane and 1,2-dichloroethane may also be transformed by dichloroelimination (a biotic process) to vinyl chloride and ethane respectively (Belay and Daniels, 1987; Chen *et al.*, 1996; Klecka *et al.*, 1998). Dehydrohalogenation is an abiotic transformation process which leads to the formation of TCE from 1,1,2,2-tetrachloroethane, dichloroethane from 1,1,2-trichloroethane and vinyl chloride from 1,2-dichloroethane (Jeffers *et al.*, 1989; Pagan *et al.*, 1998).

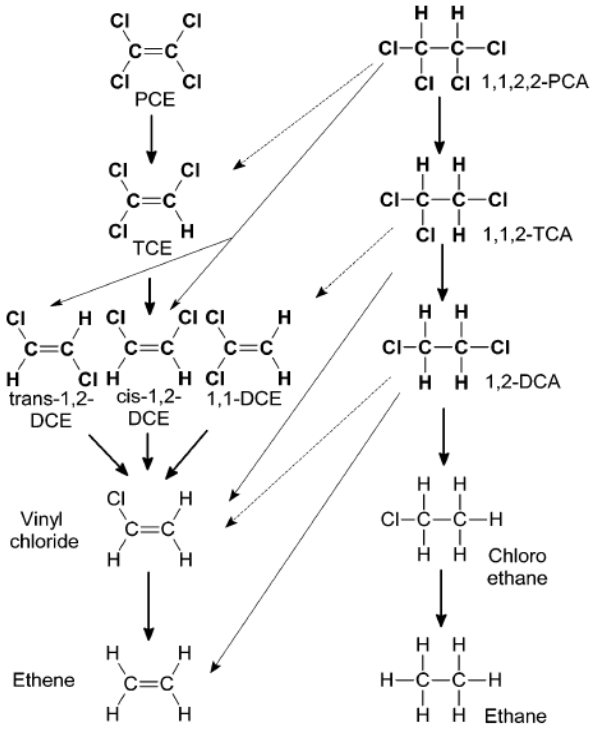

Figure 2-16: Degradation pathways of chlorinated ethenes and ethanes. Bold arrows, reductive dechlorination; fine arrows, dichloroelimination; dashed arrows, dehydrohalogenation (from Hunkeler *et al.*, 2005)

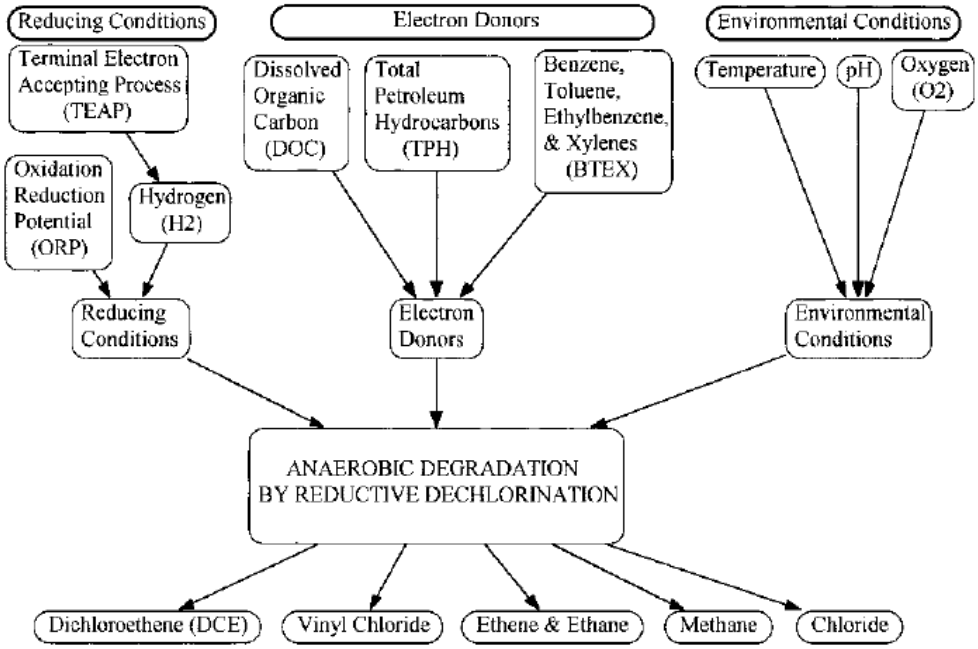

Figure 2-17: Bayesian Belief Network for the reductive dechlorination of TCE in groundwater (from Stiber *et al.*, 1999)

2.1.2.2 Compound specific isotope analysis (CSIA)

The last two decades have seen a proliferation in the use of isotopes in solving hydrogeochemical problems (Bottcher *et al.*, 1990; Clark and Fritz, 1997; International Atomic Energy Agency, 2002). Stable isotopes that are useful in environmental studies include hydrogen, carbon, nitrogen, oxygen, sulphur and chlorine. Stable isotopes can be subdivided into the light stable isotopes such as ^{13}C, ^{2}H, ^{37}Cl and the radiogenic stable isotopes that are produced by the decay of radioactive elements with long half-lives such as ^{87}Sr which is produced from the decay of ^{87}Rb. The deviation of the stable isotope value of the sample from the international standard (V-PDB for carbon, V-SMOW for hydrogen and the standard abundance of the heavier chlorine isotope (^{37}Cl) is referred to as 24.47% of total chlorine) will be either negative or positive. A negative value means that the sample is depleted in its heavy isotope content while a positive delta indicates that the sample is enriched in its heavy isotope content (Clark and Fritz, 1997).

Isotope ratios can change due to biological and chemical processes which cause isotope fractionation. Stable isotope fractionation is the term used to refer to the change in stable isotope ratios. Slater *et al.* (1999), Wang and Huang (2003), Mancini *et al.* (2003), Kopinke *et al.* (2005) show that changes in isotope ratio resulting from processes such as volatilisation, dispersion and sorption are significantly smaller

(<2‰) due to these processes being isotopically conservative when compared to the changes in isotope ratio as a result of biodegradation (>2‰). Large fractionations (>10‰) are associated with biotic and abiotic degradation as compared to dissolution and volatilisation (Slater *et al.*, 1998). During these processes, molecules containing the lighter isotopes exclusively (for e.g. ^{12}C, ^{1}H, ^{35}Cl) will react more rapidly when compared to molecules containing the heavier isotope (for e.g. ^{13}C, ^{2}H, ^{37}Cl), due to the lighter isotopes having weaker bonds. As the reaction continues there is a shift in the ratio of the lighter isotope to the heavier isotope. The extent to which isotope fractionation occurs during the process of producing the organic compounds induces an isotope composition fingerprint that can provide evidence for the identification of sources, types of transformation reactions and sinks of organic compounds (Meckenstock *et al.*, 2004).

Stable isotope fractionation can be expressed as the stable isotope fractionation factor (α). This expression is described below:

$$\alpha = R_a/R_b = \left(1000 + \delta^h E_a\right)/\left(1000 + \delta^h E_b\right) \quad \text{Equation 2-7}$$

Where:

^{h}E= heavy isotope of a given element E

R = stable isotope ratio of the compound; and

the subscripts a and b may represent a compound at time zero (t_0) and at a later point (t) in a reaction; or a compound in a source zone, versus a down gradient well (Hunkeler *et al.*, 2008).

Stable isotope fractionation during biotic and abiotic degradation can also be (and commonly is) quantitatively described using the Raleigh equation, originally developed for homogenous batch systems (Clark and Fritz, 1997):

$$R = R_0 f^{(\alpha-1)} \quad \text{Equation 2-8}$$

Where:

R_0 is the initial isotope value of the compound

f is the ratio (C/C_0) of the compound at time t and zero.

In flow-through studies the application of the Raleigh equation leads to an underestimation of the amount of biodegradation due to physical and chemical heterogeneities (Kopinke *et al.,* 2005). The Raleigh equation can be rearranged to form the following expression:

$$f = e^{\left(\delta^h E_{groundwater} - \delta^h E_{source}\right)/\varepsilon} \quad \text{Equation 2-9}$$

The relationship between the change in isotopic composition and contaminant reduction is expressed as the isotopic enrichment factor (ε) and is defined as:

$$\boldsymbol{\varepsilon = (\alpha - 1) \times 1000} \quad \text{Equation 2-10}$$

The larger the fractionation during the reaction, the more negative is the corresponding value of epsilon (ε) (Hunkeler *et al.*, 2008). Loglinear regression of the stable isotope ratio versus decreasing concentration results in a straight line. The slope of this line denotes ε.

Depending on the underlying reaction mechanism, isotope fractionation occurs according to a kinetic isotope effect (KIE_E) for the element (E) at the reacting bond(s). Hence, isotope enrichment factors are characteristic for a given degradation pathway. The differing energy of activation between the ground state of the isotopic reactants versus their transition states are as a result of the different KIEs (Melander and Saunders, 1980). This is because the different KIEs reflect the different reaction rates of bonds containing light and heavy isotopes or the distinction in their frequency of vibrational energy; i.e.

$$\boldsymbol{KIE_E = {}^{l}k \big/ {}_{h}k} \quad \text{Equation 2-11}$$

Where:
l is the light isotope and
h is the heavy isotope.
KIEs are large if bonds are broken or formed in the rate limiting step, the nature of the bond broken and the reaction mechanism.

Isotope enrichment factors are calculated assuming the observed isotope fractionation in the bulk organic compound is a result of intermolecular isotopic competition between molecules containing exclusively n isotopically light atoms of element E. While the bulk ε values are used to assess the fractionation of entire molecules, it is not suitable to comparing isotope effects and reaction mechanisms among different compounds. For this type of comparison, the KIEs at the reacting bond are necessary (Elsner *et al.*, 2005). Isotope enrichment factors can be converted into apparent kinetic isotope effects (AKIE) by calculating the isotope enrichment factors at the reactive position of the molecule ($\varepsilon_{\text{reactive position}}$):

$$\boldsymbol{\ln\left(\frac{\delta^{h}E_0 + {}^{n}/_{x}.\Delta\delta^{h}E + 1000}{\delta^{h}E_0 + 1000}\right) = \frac{\varepsilon_{\text{reactive position}}}{1000}.\ln\left(\frac{C}{C_0}\right)} \quad \text{Equation 2-12}$$

The reactive position is the position in the molecule where the heavy isotope is located and where the initial enzymatic bond transformation takes place (Cook, 1991; Melander and Saunders, 1980). The AKIE is often lower than the KIE and can be calculated with the following equation (Elsner *et al.*, 2005):

$$\mathbf{AKIE} \approx \frac{1}{1+\frac{n\varepsilon}{1000}} \quad \textbf{Equation 2-13}$$

Recent years have seen an increase in the use of compound specific isotope analysis (CSIA) that have been used to quantify biodegradation of several organic compounds such as MTBE, BTEXs, chlorinated solvents and PAHs (Sturchio *et al.*, 1998; Meckenstock *et al.*, 1999; Hunkeler *et al.*, 1999; Hunkeler *et al.*, 2002; Griebler *et al.*, 2004; Meckenstock *et al.*, 2004; Elsner *et al.*, 2005; Fischer *et al.*, 2008).

The uses of CSIA include the determination of:

- which contaminants are being degraded;
- the extent of biodegradation;
- geochemical processes that are involved (for e.g. aerobic, sulphate reducing, etc.);
- contaminant degradation pathways;
- first order biodegradation rates; and
- contaminant mass loss.

Comparison of the site-specific ε against published values can provide information on the type of reaction and organism involved at the site. The isotope enrichment factor can be used to determine the progress of degradation at sampling time t (Hunkeler *et al.*, 2005).

Until recently CSIA analysis of chlorinated hydrocarbons has been limited to the use of C isotopes. However, chlorine and hydrogen isotopes are being increasingly used (for e.g. by Shouakar-Stash *et al.*, 2003; Abe *et al.*, 2009). Dual or two-dimensional isotope approaches are useful:

- in rationalising the variations observed in the enrichment factors
- to identify reaction mechanisms of organic contaminants
- to quantify the relative contribution of two reaction pathways
- to distinguish between variations between commercial products and
- to distinguish between different sources at the same field site (Hunkeler *et al.*, 2001; Mancini *et al.*, 2003; Sturchio *et al.*, 2007). The dual isotope approach

works on the premise that through measurement of isotope ratios for two elements of a compound simultaneously (for e.g. $\delta^{13}C$ and $\delta^{2}H$ or $\delta^{13}C$ and $\delta^{37}Cl$) the observed correlations between isotope fractionation are characteristic of the reaction mechanism. According to Abe *et al.* (2009), such a correlation is independent of contaminant concentrations.

Available literature values for $\delta^{13}C$ values for PCE and TCE from different manufacturers are provided in Table 2-3.

Table 2-3: Published $\delta^{13}C$ values for TCE and PCE from various manufacturers

Compound	Results from Shouakar-Stash *et al.* (2003)			Results from van Wamerdam *et al.* (1995)			Results from Beneteau *et al.* (1999)		
	n	Mean $\delta^{13}C_{VPDB}$ ‰	STDEV 1σ	*n*	Mean $\delta^{13}C_{VPDB}$ ‰	STDEV 1σ	*n*	Mean $\delta^{13}C_{VPDB}$ ‰	STDEV 1σ
TCE DOW 92	7	-31.57	0.01	2	-31.9	0.05	-	-	-
TCE DOW 95	4	-29.33	0.1	-	-	-	3	-29.84	0.07
TCE PPG 93	4	-27.37	0.09	2	-27.8	0.01	-	-	-
TCE PPG 95	4	-31.12	0.06	-	-	-	3	-31.68	0.01
TCE ICI 93	4	-31.01	0.09	3	-31.32	0.03	-	-	-
TCE StanChem 93	3	-29.19	0.14	-	-	-	-	-	-
PCE DOW				3	-23.19	0.1			
PCE ICI				4	-37.2	0.03			
PCE PPG				2	-33.84	0.03			
PCE Vulcan				3	-24.1	0.04			

2.2 DNAPL Site Characterisation

2.2.1 Site characterisation and the significance of the conceptual site model (CSM)

Site characterisation is an important process of gaining insight into the nature, extent, complexities and risks associated with the contamination at a particular site. The site characterisation process is undertaken as a scientific, iterative, phased approach (Kiersch, 1958; Cohen and Mercer, 1993; Soesilo and Wilson, 1997; Sara, 2003; Gebrekristos, 2007; Hulley, 2009). Site characterisations often begin on a regional scale or far-field and then progressively become localised or near-field (Figure 2-18). The early phases of site characterisation utilises intrusive, non-intrusive and laboratory investigations to develop a conceptual site model (CSM) which provide a holistic overview of the site complexities, the source areas, the pathways of contamination and the receptors (Sara, 2003; United States Environmental Protection Agency, 2003). The CSM is revised as the investigation progresses and becomes an important and dynamic planning tool.

Generic DNAPL conceptual site models have been developed for various geological settings (Huling and Weaver, 1991; Kueper *et al.*, 2003; Pretorius, 2007). DNAPL CSM are utilised to assess:

- Site characterisation properties and site-specific data;
- The potential for separate phase DNAPL migration;
- The potential for vapour transport of DNAPL chemicals;
- The potential for dissolution and transport of DNAPL chemicals;
- The distribution of chemicals in the subsurface;
- Cross-contamination risks associated with characterisation and remedial activities;
- Planning of detailed site characterisation activities;
- Planning of remediation activities;
- Consideration of alternative remediation activities.

Non-intrusive investigations such as reconnaissance site visits and surface geophysics add important information to the investigation when combined with the intrusive investigations (MacDougall *et al.*, 2002). Non-intrusive investigations are often rapid and cost-effective and provide a guide for where drilling and direct sampling (intrusive investigation) should occur (MacDougall *et al.*, 2002).

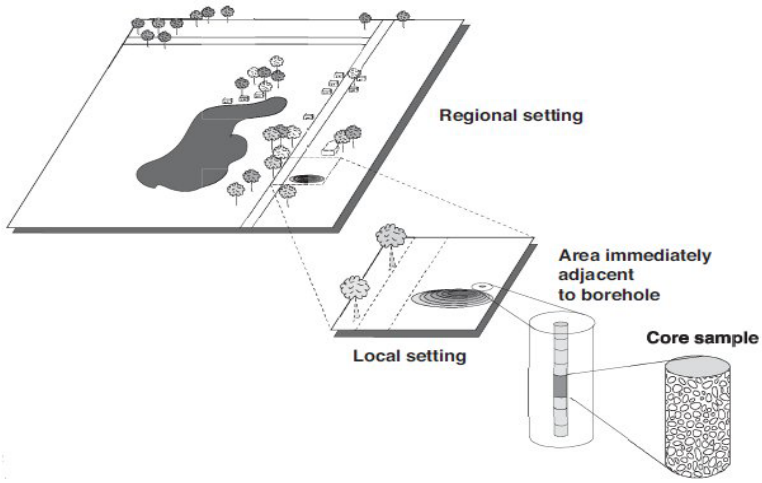

Figure 2-18: Transition from regional to site-specific data during the progression of the site characterisation (from Sara, 2003)

The last decade has seen a paradigm shift from the traditional site characterisation approach to a more dynamic approach or the Triad approach (Interstate Technology and Regulatory Council, 2003). According to Interstate Technology and Regulatory Council (2003) the central principle of the Triad approach is the management of decision uncertainty. Decision uncertainty during a site investigation is managed through the development of an accurate conceptual site model. Data uncertainty during the process is minimized though the use of various tools to address data gaps during the relevant phases of the investigation. The sources of data uncertainty (which subsequently may lead to decision uncertainty) as well as the tools that can be applied to minimise error or uncertainty are further elaborated on by the Interstate Technology and Regulatory Council (2003).

The Triad approach was developed as an initiative by the United States Department of Energy in an effort to make site investigations and site remediation more cost effective (Burton *et al.*, 1993). The Triad approach is three pronged and incorporates:

- Systematic project planning: A coordinated effort is made to identify and manage factors and issues that may contribute to uncertainty and decision errors. Cost effective strategies to manage the factors and variables are developed. Systematic planning is also used to identify decision end-points and to estimate acceptable levels of uncertainty for the decisions that are required for the site.
- Dynamic work plan strategies: These types of strategies use real-time decision-making in the field to limit the number of mobilisations back to the field to fill data gaps or take remediation actions. A dynamic work plan strategy is where

decisions are made and the work plans guide sampling and analysis are adjusted in response to data generated while the field crew is still on site.

- Real-time measurement technologies: Real-time measurements are those that are produced within a rapid time-frame so that real-time decision-making and maturation of the CSM can occur in real-time. Rapid-time measurement technologies include *in situ* detection techniques, on-site analytical tools, mapping data in real-time, rapid sampling platforms and rapid turn-around from a laboratory.

The Triad approach has both advantages and disadvantages (Table 2-4) and the best results are obtained by combining traditional approaches with the Triad approaches in order to manage uncertainty, realise long term cost savings and effectively characterise and remediate a site. A combination of these methodologies and techniques are applied to the Investigation Site.

Table 2-4: Advantages and disadvantages of the Triad approach (Interstate Technology and Regulatory Council, 2003)

Advantages	Disadvantages
Better investigation quality	Higher up-front costs
Faster investigations, restoration and redevelopment	Change in approach to data quality
Lower life-cycle costs	Lack of tools to manage decision uncertainty
Improved stakeholder communication	Greater need for training about Triad
More effective clean-ups	Negative bias towards field-generated data

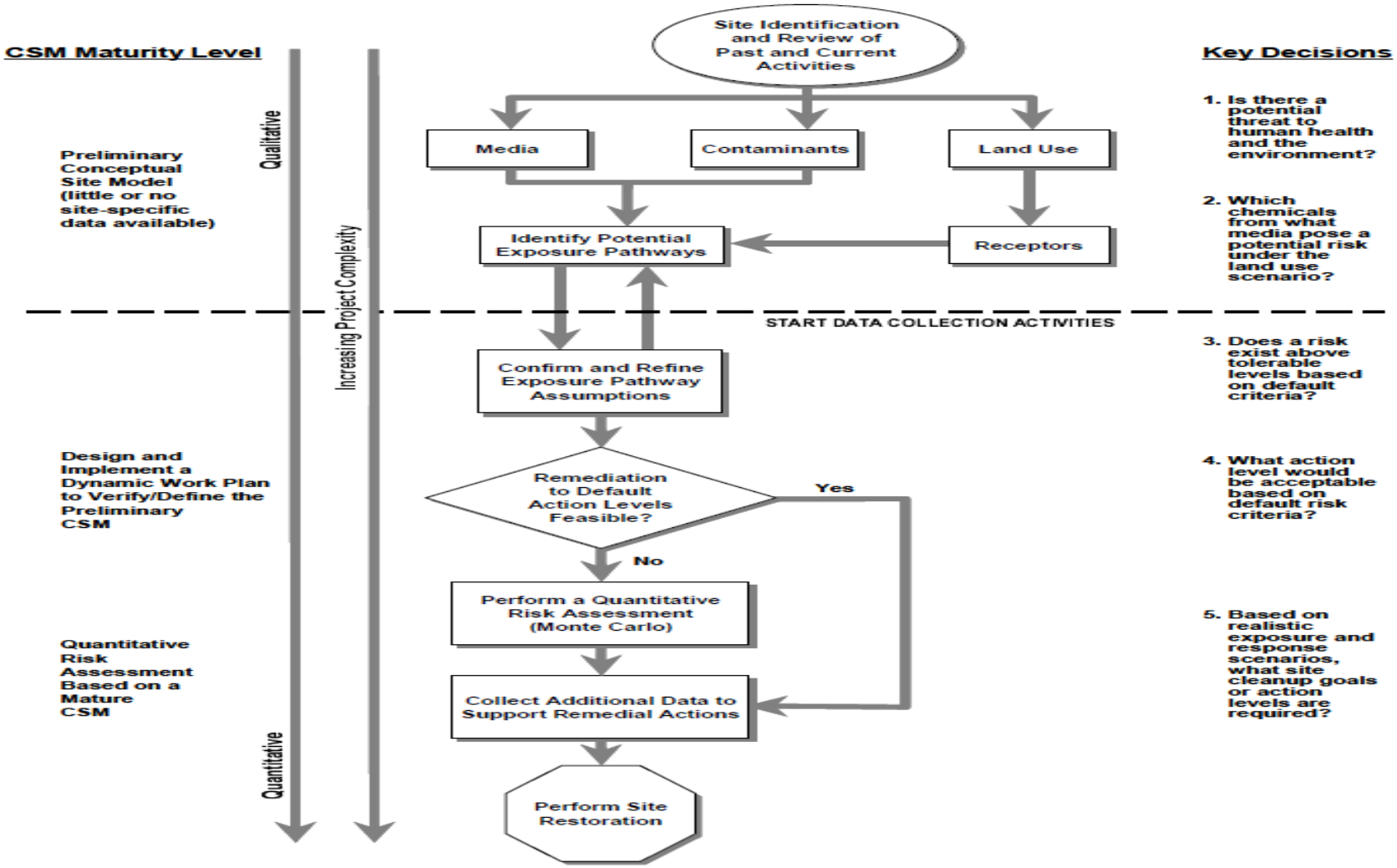

Figure 2-19: Life cycle of the CSM (from United States Environmental Protection Agency, 2003)

2.2.2 DNAPL source zone characterisation in complex geo-contaminant settings

2.2.2.1 General

A successful and cost-effective remediation strategy is dependent on how well the source areas are characterised. This is particularly pertinent for DNAPL-contaminated sites. DNAPL physicochemical properties (refer to Section 2.1.1.) make them difficult to characterise. The site characterisation process is often compounded through the presence of mixed DNAPLs and complex geological and hydrogeological settings.

The DNAPL source zones together with geological heterogeneities play an important role in dissolution kinetics and plume geometry. DNAPLs source zones can sustain contaminant plumes over long distances and long periods of time. A hypothetical DNAPL source zone is depicted in Figure 2-20. In reality source zones have more heterogeneity than that shown below with DNAPL occurring in lenses and ganglia as compared to pooling of DNAPL.

Subsurface conditions are generally heterogeneous, often complex and arise from a range of different geophysical and geochemical processes. The heterogeneities produced by varying degrees of fracturing, compaction and cavity formation within the different geological settings provides a challenge for making broad or generalised statements regarding the source zone characteristics and the efficacy of remediation technologies (National Research Council, 2004).

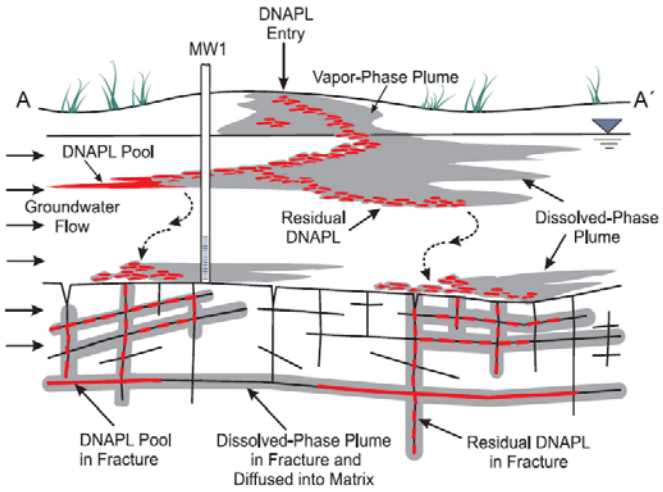

Figure 2-20: Hypothetical DNAPL source zone (from Kueper and Davies, 2009)

Five general geo-contaminant settings are shown in Figure 2-21, which broadly illustrate differing conditions. Spatial variations in permeability and porosity (Figure 2-22) differentiate the five settings (National Research Council, 2004). The setting encountered at the Investigation Site includes a combination of Type IV and Type V settings (i.e fractured media with varying matrix porosity). This is typical of one of the major aquifer systems in South Africa where the dominant groundwater flow occurs in fractured and dual porosity systems such as the Karoo Supergroup (Woodford and Chevallier, 2002) and Table Mountain Group. The Karoo Supergroup is the dominant geology type at the Investigation Site (Chapter 3). According to Woodford and Chevallier (2002) the fractures within the Karoo Supergroup are commonly sub-horizontal ($<50^0$) in attitude. The Karoo Supergroup is intercepted by numerous dolerite dykes, sills and plugs that cut through the sedimentary rocks. The dolerite rocks are generally fine or medium grained. However, they also coincide with faults and are fractured (Botha *et al.*, 1998), making them unreliable as DNAPL barriers. According to Woodford and Chevallier (2002), the fractures occasionally extend several tens of meters from the dolerite intrusions into the Karoo Supergroup country rock.

As the Type IV and V geo-contaminant settings are encountered at the Investigation Site, the following paragraphs elaborate on the variations and characteristics of these settings.

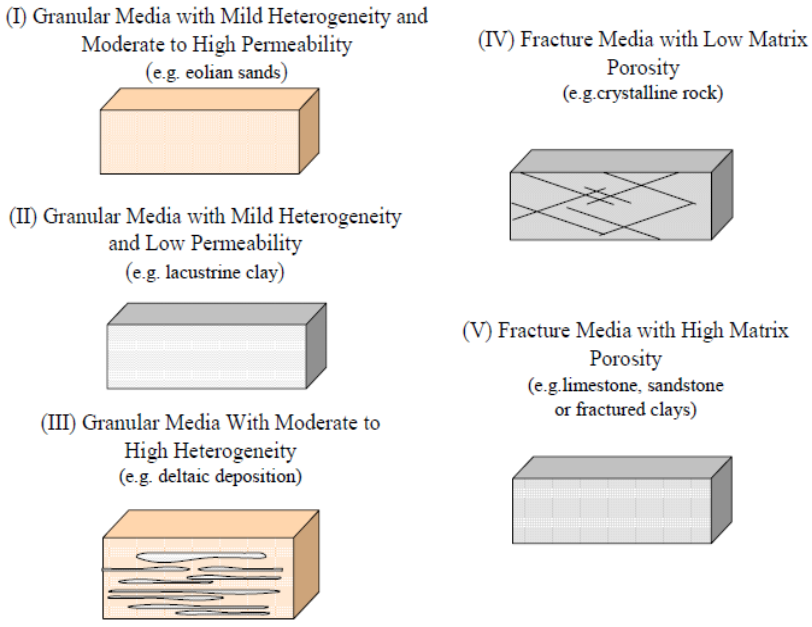

Figure 2-21: Geo-contaminant settings (from Air Force Center for Engineering and the Environment, 2007)

In Type IV settings the primary transmissive feature is secondary permeability resulting from fractures. Little or no void space exists in the matrix that typically has a very low permeability of less than $10^{-17}m^2$ ($K < 10^{-10}$ m/s. The bulk permeability of the media is however dependant on the fracture network (including the frequency, aperture size and degree of interconnectivity). The bulk permeability of Type IV settings media is considered to range from 10^{-15} - 10^{-11} m^2 ($K = 10^{-8}$ - 10^{-4} m/s). In Type IV settings, advection is limited to fractures. Due to the low matrix porosity, little mass is stored in low permeability zone. In this scenario, the primary source is DNAPL. Over time, the DNAPL is depleted from the more transmissive fractures and are dominated by DNAPL in dead-end fractures. According to Parker *et al.*, 1997, a common feature of the Type IV setting is large plume dimensions due to high contaminant migration velocity. The primary challenge in a Type IV setting is the complexity of the fracture network.

In a Type V setting the bulk permeability of the media ranges from 10^{-16} - 10^{-13} m2 ($K = 10^{-9}$ - 10^{-6} m/s), while the permeability in the rock matrix is less than 10^{-17} m^2 ($K < 10^{-10}$ m/s). Typically the porosity of the fractures is <1% compared to the total unit volume of the rock mass. In a Type V setting the porosity of the rock matrix ranges from 1-40%. The low permeability zones in Type V settings initially attenuate the DNAPL constituents that partition into groundwater through diffusion from the fractures into the rock matrix. When the DNAPL is depleted (late stage in plume evolution), reverse diffusion from the rock matrix sustains dissolved phase concentrations in groundwater flowing in fractures. In scenarios where the matrix has a large sorptive capacity, the low permeability zones will act as a contaminant sink and accelerate the rate of DNAPL depletion.

The National Research Council (2004) lists the following as critical information that are crucial for source zone characterisation:

- Understanding the source presence and nature;
- Characterising hydrogeology;
- Determining source zone geometry, distribution, migration and dissolution rate in the subsurface; and
- Understanding the biogeochemistry.

Site specific heterogeneities do not allow the source characterisation methodology to be duplicated in their entirety from one site to the other. However, depending on the

site conditions a number of characterisation methods can be used to provide information about the source zone.

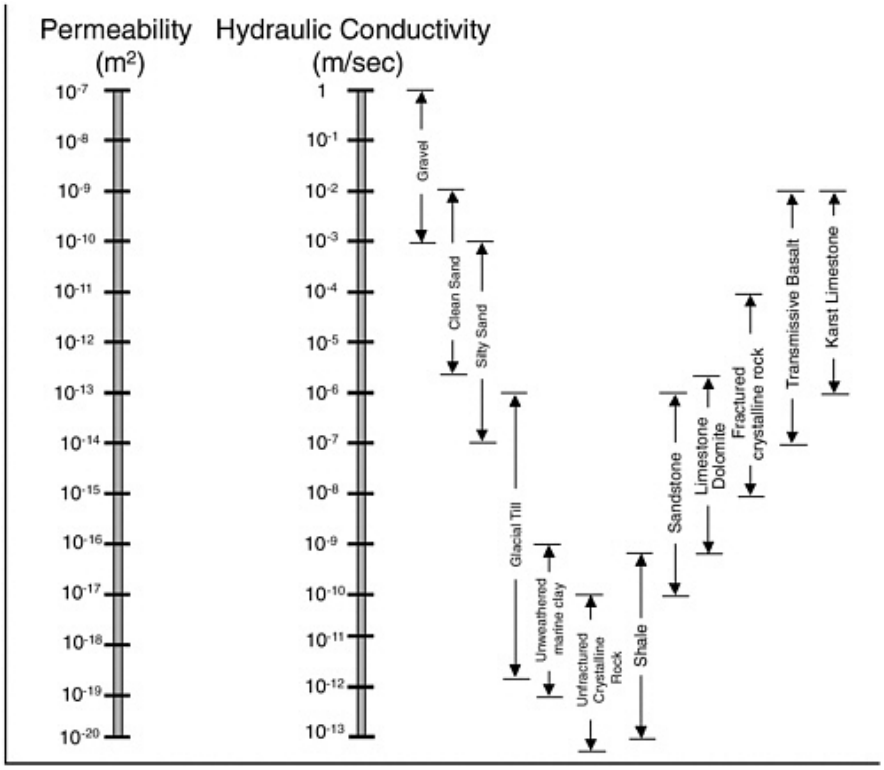

Figure 2-22: Variations in permeability and hydraulic conductivity for different geological media (from National Research Council, 2004)

Table 2-5 shows some characterisation methods that can be used to address the crucial points listed above. Also shown is the potential of the methods to provide information about the source zone. The complexities of undertaking DNAPL site characterisations are largely overcome by using the "Toolbox Approach" prescribed by previous authors (Kueper *et al.*, 2003; Fiacco *et al.*, 2005; Gebrekristos, 2007; Pretorius, 2007; Gebrekristos *et al.*, 2008; Hulley *et al.*, 2008) who utilize a variety of non-intrusive and intrusive approaches to adequately characterise a DNAPL-contaminated site. When combined with the Triad approach the Toolbox approach can allow for successful DNAPL site characterisation and remediation. Kram *et al.* (2001), United States Environmental Protection Agency (2003), Griffin and Watson, (2002), Kueper and Davies (2009) amongst others provide information on the various available and emerging source delineation and site characterisation tools.

Table 2-5: Characterisation methods and their potential for providing information about the source zone (from National Research Council, 2004)

Method/Tool	Source Material	Hydrogeology	Source zone delineation	Biogeochemistry
Historical Data	Maybe	Maybe	Maybe	No
Regional geology	No	Yes	No	Maybe
Geophysical tools	No	Yes	No	No
Direct push	Maybe	Yes	Yes	Yes
Core analysis	Maybe	Yes	Maybe	Yes
Downhole methods	Maybe	Yes	No	No
Piezometers	No	Yes	No	No
Pump tests	No	Yes	No	No
Groundwater analysis	Maybe	No	Maybe	Yes
Solid (matrix) characterisation	No	No	No	Yes
Microbial analysis	No	No	No	Yes
Soil vapour analysis	Maybe	No	Maybe	No
DNAPL analysis	Yes	No	No	No
Partitioning tracer tests	No	Maybe	Yes	No
Ribbon NAPL samplers	Yes	No	Yes	No
Dyes	Maybe	No	Maybe	No

* Methods highlighted above were applied to characterise the source material, hydrogeology, source zone and biogeochemistry at the Investigation Site (Chapter 3)

2.2.2.2 Characterisation and delineation of DNAPL source zones

The objectives for DNAPL source zone delineation varies from site to site and may include one of more the following:

- To ensure that the flow paths and quality of groundwater downgradient of the source zone are monitored for the presence of dissolved phase contaminants to assess the protection of current and potential receptors.

- To facilitate the proper design of containment systems involving groundwater extraction and/or physical barriers.
- To facilitate implementation of DNAPL mass removal technologies.
- To establish boundaries for institutional controls (Kueper and Davies, 2009).

According to Kueper and Davies (2009) it is not feasible to determine the exact location and extent of individual DNAPL migration pathways within the source zone. Uncertainty in delineating the spatial extent of the source zone is derived through taking a finite number of local scale measurements at discrete locations. They recommend the delineation of "Confirmed/Probable" as well as "Potential" DNAPL source zone. Overestimation of the size of Confirmed/Probable source zone could overstate the costs for technology application and may result in a particular technology being prematurely screened out. In contrast to this, underestimation of the size of the Confirmed/Probable source zone could lead to underestimation of costs and the poor performance or the chosen technology.

As with conventional site characterisation processes, the characterisation of DNAPL source zones is an iterative process requiring multiple lines of evidence. Figure 2-23 shows the line of evidence that can be used to assess the presence of DNAPL at a site. These include direct and indirect methods. Table 2-6 provides the degree of uncertainty of the presence of source zone(s) based on various events. At sites where a DNAPL cannot be isolated from the source zones, indirect methods are used to infer the presence of DNAPL. Such methods include the measuring of high dissolved or vapour contaminant concentrations relative to saturated aqueous or vapour concentrations; or the measurement of high concentrations of the contaminant in soil cores. According to Mackay *et al*. (1991) and Cohen and Mercer (1993); aqueous concentrations greater than 1% of DNAPL solubility is indicative of the presence of DNAPL. In a field experiment undertaken by Broholm *et al.* (1999), the dissolved-phase plume measured from the DNAPL source was greater than 10% of the effective solubility of the DNAPL components across the lateral and vertical extent of the source zone.

The United States Environmental Protection Agency (1992) state that concentrations of DNAPL-related chemicals in soils greater than 10 000 mg/kg are indicative of DNAPL presence. The National Research Council (2004) proposes a cautionary approach when inferring the presence of DNAPL as a result of the heterogeneous distribution of DNAPL in the subsurface. They state that short of collecting actual chemical samples from a DNAPL sample, the nature of the source

material in terms of key physical and chemical parameters may not be fully understood. According to Kueper and Davies (2009) the two primary lines of evidence that a DNAPL source zone exists includes visual observation of a DNAPL sample retrieved from a monitoring well and/or if you have chemical concentrations in soil exceeding the value corresponding to a threshold DNAPL saturation. Other converging secondary lines of evidence can be used to determine the presence of DNAPL in the subsurface (Figure 2-23). These include:

- Chemical concentrations in soil exceeding the value corresponding to equilibrium partitioning relationships. These threshold chemical concentrations can be calculated using the following equation:

$$\mathbf{C_i^T = \frac{C_i}{\rho_b}(K_d \rho_b + \theta_w + K_H \theta_a)} \quad \textbf{Equation 2-14}$$

Where:

C_i^T = soil concentration (mg/kg) threshold for component i (calculated). C_i^T represents the maximum amount of contaminant i that can be present in a porous media sample in the sorbed, aqueous and vapour phases with a DNAPL phase present.

C_i = effective solubility (mg/l) of component i (calculated)

ρ_b = dry bulk density (kg/l) (site specific measurement)

K_d = soil-water partition coefficient (l/kg) (calculated using $K_d=K_{oc}f_{oc}$, where K_{oc} is the organic carbon-water partition coefficient (l/kg) and f_{oc} is the fraction organic carbon present in the soil)

θ_w = air-filled porosity (no unit) (site specific measurement).

K_H = Henry's Law constant

θ_a = air-filled porosity (site specific measurement)

The above calculation for the threshold chemical concentration can be applied below the water table by setting $\theta_a = 0$.

- Site Use/Site History can be ascertained by methods such as employee interviews, company purchase and sale records, aerial photographs and building plans. Former lagoons, underground tanks, floor drains and leach fields are sometimes coincident with the location of DNAPL source areas.
- The location of vapour-phase plume may be coincident with the current or former presence of DNAPL in the unsaturated zone. Mapping of the vapour-phase plume is usually useful in deciding where to collect additional data. Active and passive techniques can be used. This line of evidence is not applicable to DNAPLs that lack significant vapour pressures such as coal tars and creosotes.
- Hydrophobic dyes such as Oil Red O® partitions into the DNAPL imparting a red colour to the organic liquid. Hydrophobic dye techniques include a shake test in which soil or water is placed into a jar/bag with a small amount of dye, and down-

hole samplers that force a dye impregnated absorbent ribbon against the borehole wall. Only pooled DNAPL can migrate towards the ribbon sampler and hence false negatives does not preclude the presence of residual DNAPL in the adjacent formation.

- Evaluating groundwater quality data:
    - Sampled groundwater showing greater than 1% of effective solubility of DNAPL (see Equation 2-6 for the calculation of effective solubility) indicate that the sampled groundwater may have come into contact with DNAPL. The distance to the possible DNAPL locations cannot be determined from the magnitude of the concentration alone. Sampled groundwater concentrations downgradient of a DNAPL source zone can be significantly less than the effective solubility because of hydrodynamic dispersion, wellbore dilution, non-optimal monitoring well placement and degradation processes.
    - The presence of a persistent plume extending from suspected release locations in the downgradient direction is evidence of a continuing source. If significant back diffusion is occurring in the subsurface, the plume may persist even if the DNAPL has been depleted. This line of evidence is therefore most applicable to high permeability settings.
    - The presence of contaminated groundwater in locations that are not downgradient of known or suspected sources may be evidence of DNAPL presence hydraulically upgradient of the monitoring point.
    - Abrupt reversals of groundwater contaminant concentration levels with depth or increasing concentrations with depth can be associated with DNAPL presence. Concentration trends can be best detected using small interval sampling techniques.
    - Groundwater downgradient of a multi-component DNAPL may exhibit a temporal decline in the concentrations of the higher effective solubility compounds and a stable or increasing trend in time of the lower effective solubility compounds. Compound specific biodegradation may result in certain compounds decreasing and others (such as low molecular weight daughter products) increasing within the plume.
    - Detection of highly sorbing and low solubility compounds which have low mobility in groundwater may be associated with a nearby DNAPL source. This line of evidence can be useful in delineating the extent of the DNAPL in the downgradient direction.

- Other methods that are considered a line of evidence for DNAPL includes the use of partitioning interwell tracer tests (PITTs), which involves the injection and withdrawal of a tracer that has the ability to partition into the DNAPL. PITTs are typically employed after some level of source zone characterisation has been completed. The use of measurement probes such as the membrane interface probe or the hydrosparge probe with direct push techniques is becoming popular. Most of these devices provide a relative measure of the total concentration.

Table 2-6: The degree of uncertainty regarding the presence of a source zone at a site based on the occurrence of various events (National Research Council, 2004)

Event	DNAPL Source
Known or probable historical release of DNAPL	High certainty
Process or waste practice suggests probable DNAPL release	High certainty
DNAPL visually detected in subsurface, monitoring wells, etc.	High certainty
Chemical analyses indicate DNAPL presence (≥ saturation)	High certainty
DNAPL chemicals used in appreciable quantities at site	Likely; some uncertainty
Chemical analysis suggests possible source zone	Likely, some uncertainty

According to Sale *et al*. (2008) the reasons why source delineation investigations miss a portion (s) of the source include:

- The use of limited datasets with insufficient resolution
- The heterogeneous distribution of DNAPL and the other phases
- Not being able to gain information regarding the distribution of the DNAPL, the sorbed phase, vapour phase and the mass stored in low permeability zones. This arises from the heavy reliance on groundwater data obtained from boreholes with long screen intervals in transmissive zones
- The failure to investigate low permeability zones at older sites
- Hastily implementing a source zone remediation system without adequate site characterisation
- Difficulties in resolving where the source ends and the plume begin.

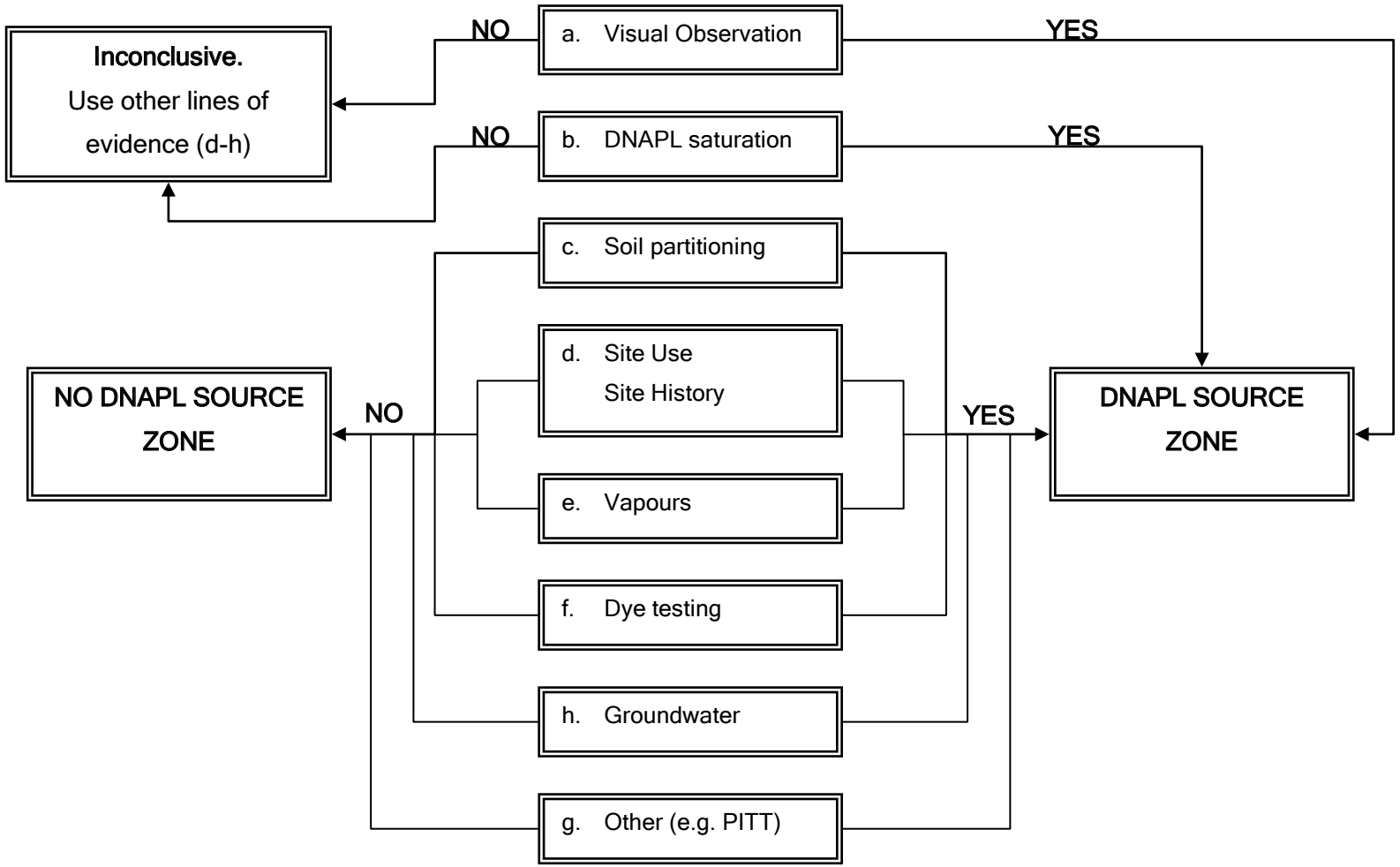

Figure 2-23: Lines of evidence to assess DNAPL presence (modified from Kueper and Davies, 2009)

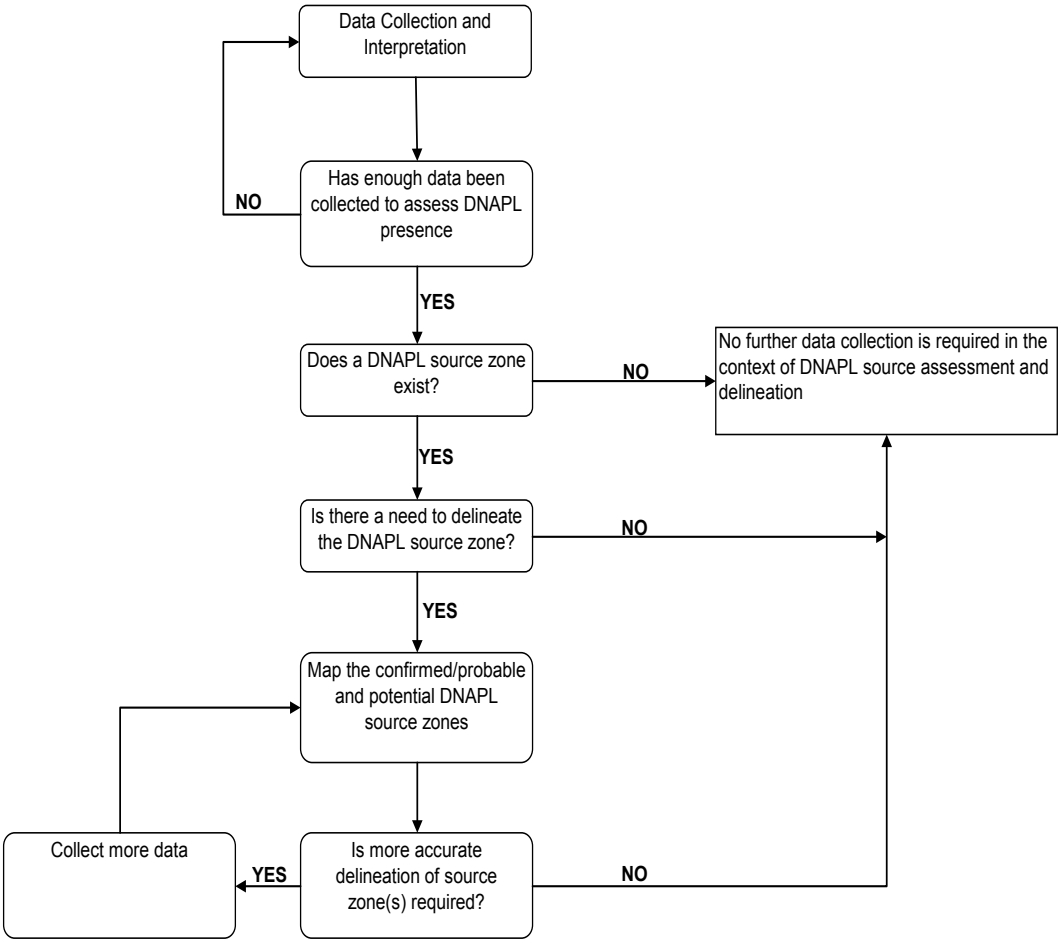

Figure 2-24: Flowchart depicting iterative data collection process used in refining the DNAPL source zone boundaries (modified from Kueper and Davies, 2009)

2.3 Defining the Level of Characterisation Required and Cost Implications

The goal of a site characterisation is to define the nature and extent of the contamination. While in most cases this is achieved concurrently, a distinction can be made between these two goals (SERDP and ESTCP, 2006).

The level of site characterisation required at a site is dependent on the following criteria:

- The complexity of the site conditions (for e.g. the types of contaminants and their characteristics and distribution, the hydrogeological setting, the biogeochemical setting of the subsurface);

- The clean-up targets or goals (this is dependent on factors such as the regulatory drivers, the pathways and receptors, community pressure).

The Strategic Environmental Research and Development Program and Environmental Security Technology Certification Program (SERDP and ESTCP, 2006) recommend the use of high resolution sampling of cores in order to determine the location and distribution of DNAPL contaminants in great detail as the mass distribution is typically controlled by small-scale features. High resolution core sampling is hence essential to determine the nature or style of contaminant mass distribution within source zones. In some cases minor heterogeneities can result in extremely complex migration pathways and localized entrapment of DNAPL.

The sampling scale in this case is a function of the geological setting and the age and type of the contaminant. However, high resolution sampling and analysis is costly if the sampling scale is large. Site screening tools should therefore be an integral part of the characterisation method and should aim to reduce the uncertainty associated with source zones and facilitate the use of more rigorous delineation methodologies.

Kram *et al*. (2002) use three unit model scenarios with predetermined parameters and compare these to selected site characterization techniques and approaches. Costs for three (3) different model scenarios were determined based on pre-defined assumptions and the application of different characterisation techniques. Each unit model scenario consisted of approximately 22 250 m3, with identical depths to groundwater, depth of resolution and volume of DNAPL released. Each unit model scenario consisted of different soil types. According to Kram *et al*. (2002) the most cost-effective technique is the FLUTe^{TM} approach with the most expensive technique being the PITT.

Miansney and McBratney (2002) defined efficiency of different methods used in predicting water retention and hydraulic conductivity of soil samples in terms of effort, cost or value of information. The study found that due to large spatial variations of soil hydraulic properties, the use of cheaper qualitative and semi-quantitative methodologies are more efficient than the use of costlier methods with higher levels of precision. The value of the use of less expensive, qualitative methodologies in contaminated land management is further elaborated by a guideline document produced by Barnes (2009). The use of these tools (termed “rapid measurement tools” in the document) is presented within the framework of risk management for

contaminated sites in conjunction with the use of laboratory-based analysis (quantitative methodologies).

3 DNAPL SOURCE ZONE CHARACTERISATION IN A FRACTURED SYSTEM

The mid-twentieth century saw an increasing number of chemical industries being developed in South Africa; largely as a result of sanctions against the country and increasing national demand. The Investigation Site was one of the earliest chemical facilities in the country. As the site is confidential, information related to site ownership, locality etc. are excluded from this thesis.

The site is a large industrial complex, consisting of several production facilities and covering an area of approximately 400 ha. It is located within a heavy industrial zone and is proximal to residential areas, agricultural lands, open municipal land and underground mining and other chemical production facilities (Figure 3-1).

This chapter provides background into the Investigation Site and evaluates traditional and novel technologies for adequate source zone characterisation in a fractured system.

3.1 Background to the Investigation Site

The production of chemicals is a highly integrated process involving a combination of steps:

- Receiving of raw products via road, rail and/or pipeline
- Storage of the raw products in warehouses and/or tank farms (underground and/or above ground tanks)
- Transport of the raw materials as input into the process
- Blending of raw materials
- Transport of product via pipes, road for storage on-site
- Temporary storage of waste products on-site
- Treatment and disposal of effluent and solid waste (hazardous, non-hazardous/inert)
- Transport of product via pipes, road or rail off-site.

During operations, chemicals can enter the subsurface as a result of poor housekeeping (such as uncontained spills during loading/off-loading), through

seepage from disposed wastes in lagoons and waste sites and via leaking storage tanks.

Manufacturing operations at the Investigation Site began in the mid-1960's and included the bulk chemical production of a wide range of chemical products consisting of polyvinyl chloride, peroxides, carbon fluorocarbon, 1,2-dichloroethane, polyethylene, tetrachloroethene, carbon tetrachloride, cyanide, carbon fluorocarbons and chlorine. Production facilities built in the mid-1960s that handled and manufactured DNAPLs were decommissioned and demolished in the late-1990s (Table 3-1). The on-site disposal of chemicals also ceased with increased awareness of the risks associated with the inappropriate disposal of chemicals and with stricter environmental controls. A new production facility where vinyl chloride and 1,2-DCA are stored and handled as part of the manufacturing process was built in the late-1990s to updated international standards. Figure 3-2 shows the facilities that are or were associated with the production, storage and disposal of DNAPLs at the Investigation Site. These facilities can be considered potential source areas, based on the processes that were or are occurring at the site.

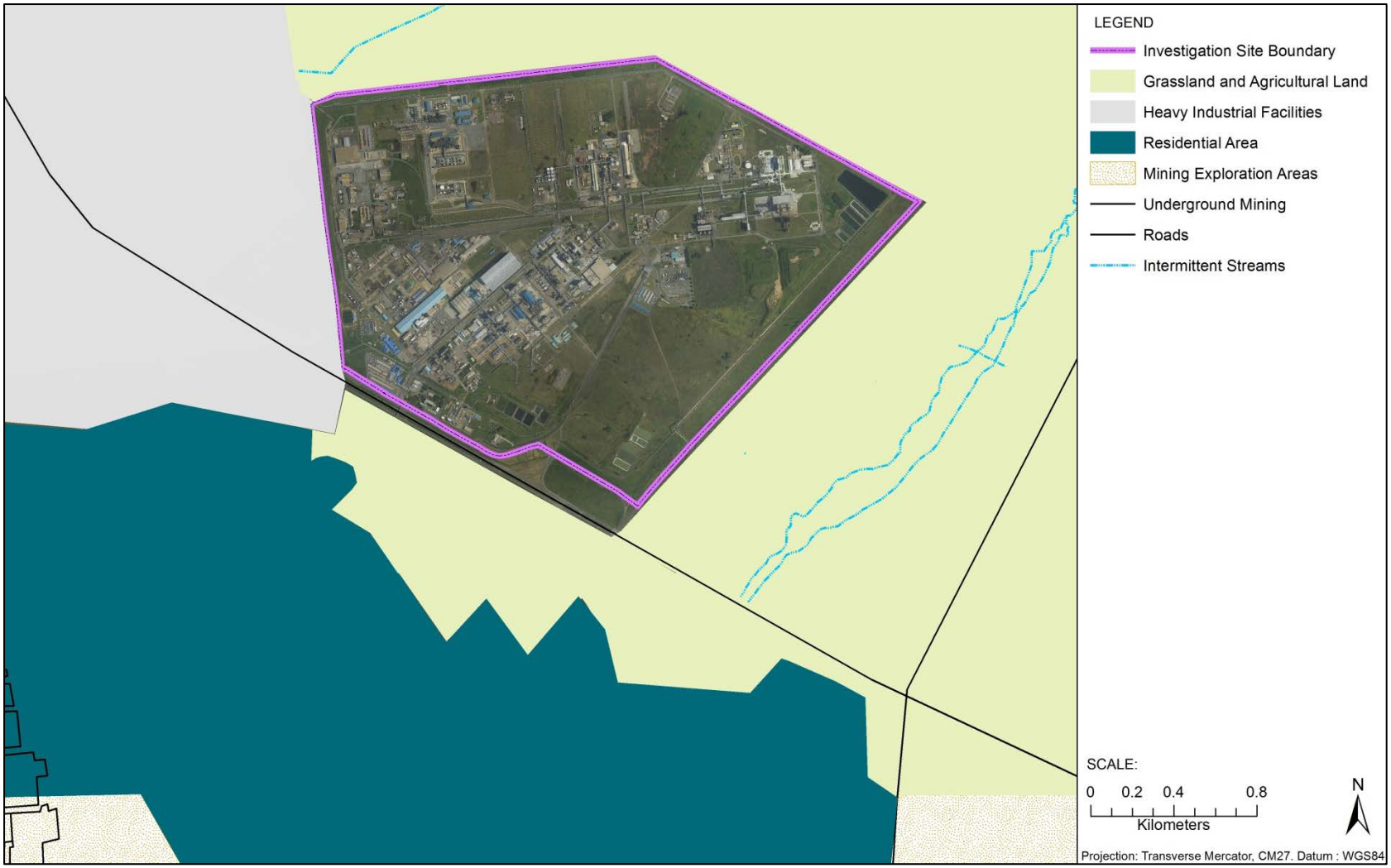

Figure 3-1: Land use surrounding the Investigation Site

Figure 3-2: Potential source areas at the Investigation Site

Table 3-1: Facilities at the Investigation Site that are/were associated with production, handling and/or disposal of DNAPLs

Map Legend (Figure 3-2)	Plant Production/function	Area (ha)	Duration of Operations	Probable DNAPL of Concern
Historical DNAPL production and handling facility 1	Activated carbon with mercuric chloride used to produce acetaldehyde and vinyl chloride	3.5	1966-1996	Mercury; 1,2-DCA; coal tar residue; vinyl chloride
Historical DNAPL production and handling facility 2	Carbon tetrachloride, PCE, 1,2-DCA, TCE, Arcton 11/12, Frezone 22 and HCl, chloride Storage of 1,2-DCA	7.5	1967- 1996 1967-1998	PCE; CCl_4; chloroform; TCE; 1,2-DCA; 1,1,2,2-TetCA; vinyl chloride; 1,1,2-TCA, mercury 1,2-DCA
Redundant hazardous waste site 1	Redundant disposal site	8	1966-1978	Mercury; 1,2-DCA; coal tar residue; PCE; CCl_4; TCE; vinyl chloride
Redundant hazardous waste site 2	Redundant disposal site	5	1978-2004	Mercury; 1,2-DCA; coal tar residue; PCE; CCl_4; TCE; vinyl chloride
Effluent Dams	Storage of storm water and effluent on southern section of site	4	1966-current	Mercury; 1,2-DCA; coal tar residue; PCE; TCE; CCl_4
Operational plant using DNAPL	1,2-DCA manufactured and used to produce other chemicals	13	1996-current	1,2-DCA; vinyl chloride

3.2 Methodologies Used to Investigate the Site

The Investigation Site has been under characterisation by different Consulting Companies since the early 1990's. Groundwater monitoring reports showed the presence of dissolved phase and free phase DNAPL. Additionally, assessments at facilities that used mercury (Table 3-1) indicated the presence of elemental mercury (H^0) in soil and building rubble within the footprint of the demolished facilities. The long history of various studies and monitoring at the site has allowed for a vast amount of historical information to be available. Staff members who began work at these facilities in the 1970's and whom are still employed at the site were interviewed. The author gathered the following information from these employees during interviews:

- Samples from the storage tanks containing 1,2-DCA were obtained by opening the valves for approximately 5 minutes and allowing the product to drain into the ground (the storage area has no secondary containment) prior to sampling. This occurred at least once every day during the history of these tanks being used for the storage of 1,2-DCA (1967-1998).
- Disposal of off-specification material in the basements or pump houses of the production facilities was common practice.
- The waste sites were unlined.

The traditional approach in determining the extent of the DNAPL contamination on site relied heavily on gathering information through the drilling of boreholes below potential source areas. As a result approximately 40 borehole pairs up to a maximum depth of 40 metres below ground level were drilled in the 1990s. At the time very little was understood regarding the fate and transport of DNAPLs (Figure 2-2) and much less was understood on the significance of geology on the fate and transport of DNAPLs in bedrock.

A site-specific conceptual site model (CSM) is developed as an outcome of this study through source zone characterisation. The methodologies used in the characterisation process are an integration of traditional and novel approaches. For the purposes of this investigation, traditional site characterisation approaches are defined as following the following criteria:

- Having a fixed work plan
- Samples for analysis are sent to a fixed laboratory
- Field methods that are employed are quantitative

- High level of uncertainty which can be reduced sequentially over an extended period of time through repeated mobilisations to site
- Well placement is based on available knowledge on the potential release areas or source zones.

In comparison, novel source zone characterisation approaches may have aspects of traditional approaches (such as confirmatory sampling using a fixed laboratory), but also include dynamic work plans and the use of rapid measurement tools and *in situ* methodologies to reduce uncertainty within a shorter time frame.

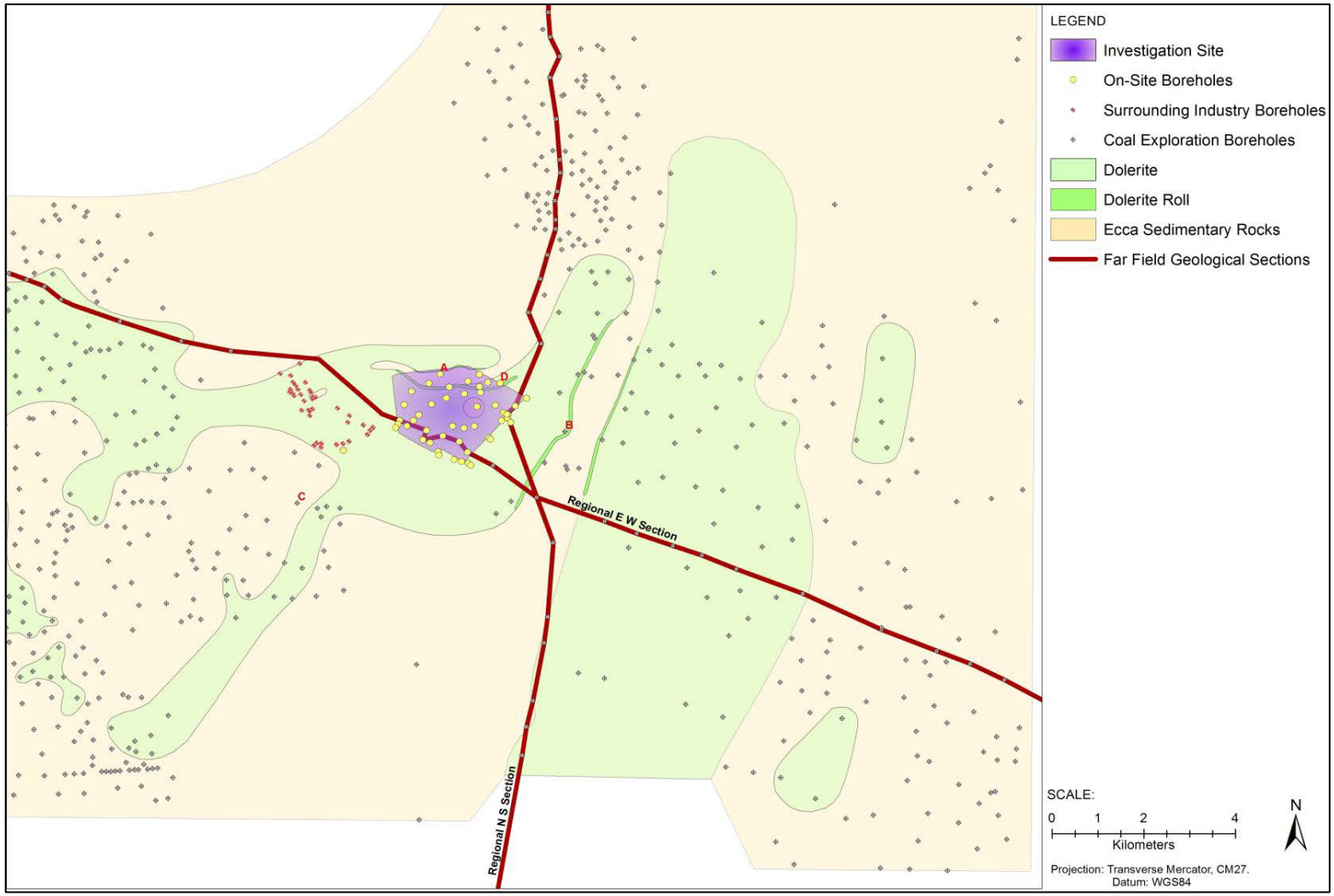

Figure 3-3: Available historical near-field and far-field borehole information (modified from Hulley *et al.*, 2008)

Figure 3-4: Historical evidence of DNAPL contamination in the subsurface at the Investigation Site (modified from SRK Consulting, 1995; SRK Consulting, 2001; ERM, 2008)

3.2.1 Collation and review of historical information and the identification of information gaps

A significant amount of geological and geohydrological information was available from the Investigation Site, neighbouring industrial facilities and mines at the commencement of this research. The data included information on the geology of the area. Approximately 2000 coal exploration boreholes had been advanced in a 10 km radius from the site providing an extensive database with existing information. Additional information was collated from the following sources:

- Previous reports prepared by Consultants for the mines and industries
- 1:50 000 topographical sheets,
- 1:250 000 hydrogeologcial maps obtained from the Department of Water Affairs and the National Groundwater Database data on groundwater wells in the region
- 1:250000 regional geological maps published by the Council for Geoscience.

A far-to-near field approach was adopted to evaluate the available data. The reason for this was to first evaluate regional geological controls that could affect the migration of DNAPL. When working at DNAPL sites, drilling within sources without understanding the exact dimensions of the source areas can lead to cross-contamination of aquifers or the mobilisation of the contamination. The boreholes with available geological information (existing historical datasets) are shown in Figure 3-3.

The following were identified as information gaps that required further investigation:

- Obtain near-field (site-specific) geological and hydrogeological information in order to:
    - Determine the local geology underlying the Investigation Site;
    - Establish the depth of overburden and the weathering profile;
    - Establish the depth and configuration of intrusive dolerite sills into the Karoo Ecca Sequence;
    - Define the nature and depth of the pre-Karoo basement rock
    - Define the nature of the fracture network
    - Understand the types of aquifers at the Site and the interrelationship between the aquifers;
    - Determine the aquifer parameters
- Characterisation of the source zone through the delineation of the sources or release areas and determining the source material characteristics

- Biogeochemical characterisation of the plume.

Careful planning of all activities associated with the characterisation preceded any work being undertaken. This involved the development (by the author) of the project execution and communication plans for internal and external stakeholders. The Consultants developed the Safety, Health and Environmental plans which included emergency preparedness plans, personnel occupational health monitoring requirements, task work procedures and risk assessments and a DNAPL contingency plan should DNAPL be encountered during drilling.

3.2.2 Source zone characterisation

Source zones contaminated with elemental mercury (Figure 3-4) were investigated extensively by Consultants using test pits and Draeger™ tube analysis and will not be elaborated on further in this research. This section will focus on characterising source zones consisting of organic DNAPLs.

DNAPL source zones were delineated through the application of the following approaches:

- Rapid, cost-effective methods to confirm release zones and the presence of DNAPL
- Rapid, cost-intensive methods to confirm the presence of free phase DNAPL in the weathered aquifer.

In the context of this study the “weathered zone” includes the overburden and weathered portion of the dolerite or Karoo Ecca sediments located within the upper portion of the site, while the “fractured rock” refers to the unweathered portion of the stratigraphy. The subdivision is made on the basis of the different technologies used to characterise the source zones. The term “fractures” used in the context of this study includes planar structural features or discontinuities such as joints, cracks, fractures and bedding planes. Hence, the weathered zone in this context is also “fractured” based on the large amount of jointing identified at its base. The tasks and tools associated with source zones characterisation in the weathered and fractured zones are shown below (Figure 3-5).

3.2.2.1 Weathered source zone characterisation

Confirmation of source zones in the unsaturated zone was done through a semi-quantitative method. The GORE Module (also known as the GORESORBER™ Module) was used to collect chlorinated hydrocarbon vapour concentrations in the unsaturated zone. The GORESORBER™ modules consist of several engineered granular adsorbent materials that are encased in a chemically inert, hydrophobic, micro-porous GORE-TEX™ membrane. Modules were placed approximately 100 meters apart in a grid that covered known, probable and potential source areas. The sampling event was undertaken during winter in order to prevent false negatives due to the effect of temporal variability effects on gas partitioning (Washington, 1996; McHugh *et al.*, 2007). Subsurface borings were to an approximate depth of 500 to 800 mm below ground level (bgl) advanced using a handheld hammer drill or a 35 mm diameter hand auger, depending on subsurface geological conditions. Each hole was sealed with inert materials to minimize vapour exchange with the atmosphere, and allowed to equilibrate with subsurface vapours for a period of approximately twelve to fourteen days. The unique serial number, sample locality and date were recorded on site. Once removed, the modules were couriered to W.L. Gore Associates, Inc. (Gore) in the USA for laboratory analysis of chlorinated hydrocarbons using US EPA Method 8260 and the gas chromatograph/mass spectroscopy (GC/MS) technique. The target compounds analyzed during the passive soil gas survey are summarized in Table 3-2.

The only successful geophysical technique that was employed within the boundaries of the Investigation Site was the ABEM LUND (2-D) Resistivity Imaging System[1]. The purpose of the geophysical surveys was to:

- Map the bedrock sub outcrop surface including the depth of the overburden and the weathering. The bottom of weathering could be stratigraphical lows where DNAPL could collect.
- Define the geological units including the depth and configuration of the units.
- Identify preferential groundwater migration pathways.

[1]Controlled Source Array Magneto Telluric (CSAMT, Stratagem EH4 system by Geometrics Inc.) surveys were undertaken outside the site boundary to confirm the depth to basement. CMSAT surveys were restricted to outside the site due to interferences from the facilities on-site. Drums containing chlorinated solvents were suspected of being buried in a redundant production area, based on information provided during interviews with site Employees. Ground penetrating radar (GPR) was used in order to try and isolate this source. No useful results were obtained.

- Identify potential contaminant plumes.

Electrode spacing within source zones was reduced from 10 to 5 meters. Resolution depths varied between 20 m bgl to 70 m bgl. The location of the 2-D resistivity surveys are shown in Figure 3-7. Typically, these traverses should be undertaken with a grid configuration with traverses along parallel lines in order to maximize data coverage. However, due to the large amount of surface and sub-surface infrastructure at the site this was not possible.

Drilling in the weathered zone was undertaken using an ATV 600 C roto-sonic drilling equipment for soil core retrieval. This is the first application of a roto-sonic drill rig for an environmental investigation in South Africa. Sonic drilling is a soil penetration technique that applies the principles of Binghams' findings on the fluidization of porous materials (Bingham, 1916) in combination with the law of inertia. This technique was applied to the site as it allows for the fast retrieval of core without the use of any fluids[2], hence enabling the tracking of seepage zones. The soil cores retrieved from each boring were screened for the presence of chlorinated hydrocarbons using the MiniRAE 3000 PID on 0.25 m intervals. Where high PID readings (> 150 ppm) indicated the possible presence of DNAPL, field shake tests using the hydrophobic dye Oil Red O® was employed to verify the presence of DNAPL (Figure 3-6).

An on-site field laboratory was set up and managed by the Consultants. The purpose of this laboratory was to ensure that samples were analysed in real-time in order to facilitate rapid decision-making regarding the delineation of release areas. The laboratory consisted of two gas chromatographs that were dedicated to analysing samples generated from the sonic drilling. Gas chromatography is widely accepted as a primary analytical tool for site characterisation due to its capability to separate, detect and quantify target analytes in a complex mixture of thermally stable organic compounds. The gas chromatographs were operated by trained and experienced laboratory technicians.

[2] Attempts with direct-push equipment (Geo-probe) failed at the site as a result of the high subsurface clay content.

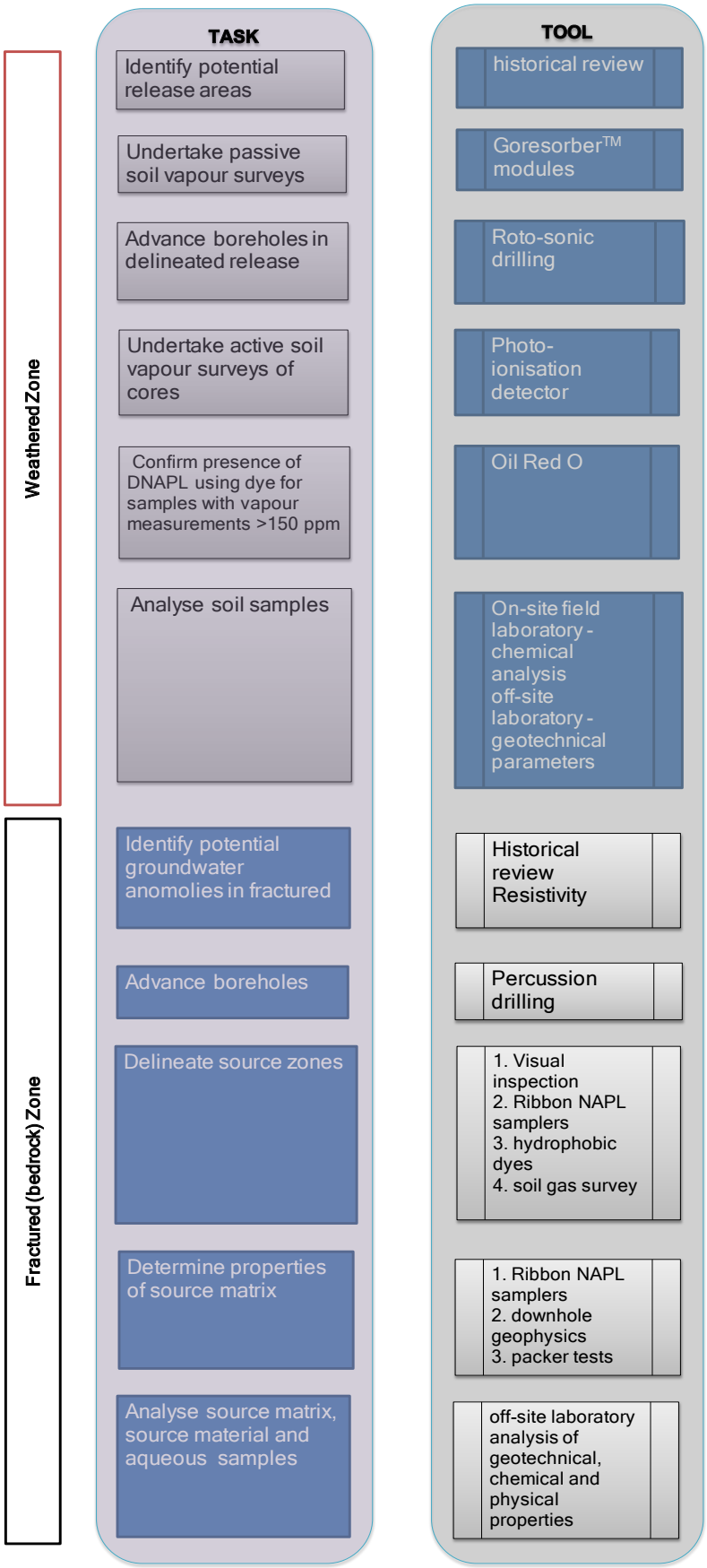

Figure 3-5: Tasks and tools/methods for source zone characterisation at the Investigation Site

Table 3-2: Target compounds for the passive soil gas survey

Compound	Method Detection Limit (µg)
Total petroleum hydrocarbons	
Total petroleum hydrocarbons	0.01
Chlorinated Ethenes	
Tetrachloroethene	0.01
Trichloroethene	0.01
1,1-dichloroethene	0.03
cis-1,2-dichloroethene	0.01
trans-1,2-dichloroethene	0.03
vinyl chloride	0.23
Chlorinated ethanes	
1,1-dichloroethane	0.01
1,1,1-trichloroethane	0.01
1,2-dichloroethane	0.01
1,1,2-trichloroethane	0.01
1,1,1,2-tetrachloroethane	0.01
1,1,2,2-tetrachloroethane	0.01
Chlorinated methanes	
Chloroform	0.01
carbon tetrachloride	0.01
Chlorinated benzenes	
chlorobenzene	0.01
1,4-dichlorobenzene	0.01
1,3-dichlorobenzene	0.01
1,2-dichlorobenzene	0.01

Figure 3-6: Oil Red O® staining of residual DNAPL in soil boring 177

Figure 3-7: 2-D Lund surface geophysical traverses (Results from ERM, 2008; ERM, 2012)

Soil samples taken at 0.25 to 0.5 m intervals were submitted under chain of custody QA/QC procedures to the field laboratory. The methanol was extracted using a combination of shake and centrifugal techniques. Samples were analysed by EPA SW846 Method 8620 (gas chromatograph/mass spectrometer, GC/MS) for the same VOCs analysed as part of the passive soil vapour survey (Table 3-2). The laboratory quality control system adhered to the requirements specified in EPA SW846 Method 8620 and included daily QC checks, GC/MS run logs, laboratory control samples, matrix spike/matrix spike duplicate samples, continuing calibration verification and blank samples. Sample results were submitted electronically as electronic tables (Excel spreadsheets) and electronic data deliverables.

The results obtained from the analysis of the samples from the weathered zone were treated statistically using Monte Carlo simulations to determine their threshold concentrations (based on Equation 2-16). The constants used in the simulations are provided in Table 3-3. The randomizing factors for dry soil bulk density, water-filled porosity, air-filled porosity and fraction of organic content were based on the site specific results obtained.

Solid models for the chlorinated hydrocarbons were developed using RockWorks15. Frequency distribution histograms were generated for each compound as well as for the sum of groups of compounds. Based on this, data was filtered to exclude the maximum concentration outliers. The data was modelled using the built-in software inverse distance anisotropic algorithm. High fidelity smoothing was applied to the solid models.

Soil samples taken from sonic-drilled boreholes (EDC 2S, BH 221 and BH 61) were sent to Soil Lab (Pty) Ltd in Pretoria (South Africa) for the following analyses:

- particle size (grain size distribution)
- permeability tests
- organic content
- porosity tests
- dry density, and
- moisture content.

Grain size distribution tests were taken at intervals of 0.5 m for BH 221 and BH 61, and at visible lithological changes for EDC 1S. The lithological parameters analysed for the soil samples is provided in Table 3-4.

.

Table 3-3: Constant values used for the Monte Carlo simulations to determine soil concentration threshold values

Chlorinated hydrocarbon DNAPL	Solubility (mg/l)	Reference	Henry's Law Constant (unit less)	Reference	Organic carbon-water partition coefficient (L/Kg)	Reference
PCE	206	Horvath *et al.*, 1999	0.72363	Gossett, 1987	94.94	Meylan *et al.*, 1992
TCE	1280	Horvath *et al.*, 1999	0.402698	Leighton and Calo, 1981	60.7	Meylan *et al.*, 1992
1,1-DCE	2420	Horvath *et al.*, 1999	1.067048	Gossett, 1987	31.82	Sabljic *et al.*, 1995
Cis-1,2-DCE	6410	Horvath *et al.*, 1999	0.166803	Gossett, 1987	39.6	
Trans-1,2-DCE	4520	Horvath *et al.*, 1999	0.16683	Gossett, 1987	39.6	
VC	8800	Horvath *et al.*, 1999	1.13655	Gossett, 1987	21.73	
1,1,2,2-TetCa	2830	Horvath *et al.*, 1999	0.015004	Leighton and Calo, 1981	94.94	Meylan *et al.*, 1992
1,1,1-TCA	1290	Horvath *et al.*, 1999	0.703189	Gossett, 1987	43.89	Meylan *et al.*, 1992
1,1,2-TCA	4590	Horvath *et al.*, 1999	0.033688	Leighton and Calo, 1981	60.7	Meylan *et al.*, 1992
1,1-DCA	5040	Horvath *et al.*, 1999	0.229763	Gossett, 1987	31.82	
1,2-DCA	8600	Horvath *et al.*, 1999	0.048242	Leighton and Calo, 1981	39.6	Meylan *et al.*, 1992
CCl_4	793	Horvath, 1982	1.128373	Leighton and Calo, 1981	43.89	Meylan *et al.*, 1992
$CHCl_3$	7950	Mackay *et al.*, 1980	0.150041	Gossett, 1987	31.82	Meylan *et al.*, 1992

3.2.2.2 Fractured (bedrock) source zone characterisation:

Potential source zones in the fractured bedrock were identified based on the presence of free phase DNAPL found at the site during previous investigations, through anomalies identified through geophysical surveys (see Section 3.2.) and by drilling directly within inferred release areas (for example, within the footprint of the historical plants) determined through the soil vapour investigations and the results from testing of soils in the overburden and weathered zones.

Rotary percussion drilling was planned to commence in the release areas and to then work on an outward on a grid system dependent on whether DNAPL is intercepted on not. This method was not possible. Site clearance (as part of the site safety requirements) for drilling was undertaken on a per borehole basis and the drill rig was moved across the site depending on where permission was granted. The primary release area/source zone was targeted from drilling from the most likely point of direct release to the ground to outward to delineate the lateral extent. Drilling targeted the different fractured bedrock stratigraphic zones in order to delineate the vertical extent of the DNAPL.

Rotary percussion boreholes were advanced within source zones to depths of between 6 m and 85 m bgl. VOC headspace screening of recovered drill chips were undertaken at 1 m intervals using a MiniRAE 3000™ PID equipped with an 11.7 eV lamp. Recovered cores were also tested using Oil Red O®. Drilling was permanently stopped when free phase DNAPL was intercepted or other lines of evidence (such as high PID readings, strong odours, positive Oil Red O®) indicated the probable presence of DNAPL in the borehole. The final depths of bedrock boreholes drilled are provided in Appendix A. A bottom loaded bailer was immediately lowered to the base of each bedrock borehole to determine the presence/absence of DNAPL on completion of the hole. Drilled boreholes were inspected daily using the bail-down test thereafter to check whether any DNAPL had mobilised into the borehole from an intercepted fracture.

The presence of residual DNAPL in the fractured bedrock was identified using ribbon NAPL samplers (Flexible Liner Underground Technologies Ltd, FLUTe™ membrane system). This marks the first use of ribbon NAPL samplers in South Africa. These samplers allows for depth discrete mapping of residual DNAPL within the fractured

zone. The FLUTe^{TM}s were also used to develop vertical transmissivity profiles by measuring the descent velocity with depth

Bedrock samples were sent to the Centre for Applied Geosciences (ZAG) at Tübingen University in Germany for laboratory analyses of the following parameters:

- Matrix porosity using a helium porosimeter test
- Dry bulk density
- Rock density
- Matrix permeability using a permeameter test, and
- Fraction of solid-phase organic carbon (f_{OC}) using EPA method 410.4 / SM 5220D.

The lithological parameters analysed for the bedrock samples is provided in Table 3-4.

Free phase DNAPL samples retrieved from the source zones were submitted to laboratories in the USA (Alpha Laboratory and Stone Environmental Laboratory) to determine the chemical composition. Samples were also submitted to the SABS in Pretoria and Tufts University in the USA for analysis of density, viscosity, interfacial tension and water content. The following methodologies were employed by Tufts University in order to determine the physical properties:

- Samples were centrifuged in 40 mL centrifuge tubes using a Beckman

Coulter Centrifuge to separate the NAPL from any aqueous phase and/or fines that may be present in the samples

- The samples were centrifuged at 1500 rpm for 10 min. Samples were allowed to equilibrate in a constant temperature room (22 ± 0.1^0 C) for a minimum of 24 hours before performing analysis
- Density measurements were done using 10 mL pycnometer (nominal size).
- Water content measurements were done with a DL38 Karl Fisher Titrator.
- Interfacial tension measurements were done using drop shape analysis (IT Concept Tracker) using the pendant drop technique.
- Viscosity measurements were done over a range for shear rates (5-100 s^{-1}), using an AR-G2 Rheometer with a stainless steel concentric cylinder geometry.

Source zones in bedrock were also inferred through the evaluation of the effective solubility of the chlorinated hydrocarbons detected in the groundwater sampled at these wells, adapted from the method in Kueper and Davies (2009).

Table 3-4: Lithological parameters measured at selected soil and bedrock cores

Borehole Number	Depth (m bgl)	Lithology	Analysed for
BH 221	3.0-3.3	Weathered sandstone	Organic content
BH 221	4.3-4.5	Residual sandstone	Moisture content, dry density, coefficient of permeability, organic content
BH 221	6.0-6.20	Residual sandstone	Moisture content, dry density, coefficient of permeability, organic content
BH 221	9.0-9.2	Weathered mudstone	Moisture content, dry density, coefficient of permeability, organic content
EDC 2S	0.55	Residual dolerite	Moisture content, dry density, coefficient of permeability, organic content, porosity
BH 61	2.0-2.15	Residual dolerite	Moisture content, dry density, coefficient of permeability, organic content, porosity
BH 61	2.8-3.0	Residual dolerite	Moisture content, dry density, coefficient of permeability, organic content
BH 61	3.3-3.45	Residual dolerite	Moisture content, dry density, coefficient of permeability, organic content
CAP 1	12-12.5	Weathered dolerite	Matrix porosity using a helium porosimeter, Dry bulk density, Rock density, Matrix permeability using a permeameter, Fraction of solid-phase organic carbon (f_{oc})
CAP 1	22-22.5	Unweathered dolerite	Matrix porosity using a helium porosimeter, Dry bulk density, Rock density, Matrix permeability using a permeameter, Fraction of solid-phase organic carbon (f_{oc})
SWD 1	20-20.5	Unweathered dolerite	Matrix porosity using a helium porosimeter, Dry bulk density, Rock density, Matrix permeability using a permeameter, Fraction of solid-phase organic carbon (f_{oc})
SWD 1	35-35.5	Unweathered sandstone	Matrix porosity using a helium porosimeter, Dry bulk density, Rock density, Matrix permeability using a permeameter, Fraction of solid-phase organic carbon (f_{oc})
SWD 1	76-76.5	Unweathered andesitic lava	Matrix porosity using a helium porosimeter, Dry bulk density, Rock density, Matrix permeability using a permeameter, Fraction of solid-phase organic carbon (f_{oc})

3.2.3 Near-field geological and hydrogeological characterisation

Geological and hydrogeological fieldwork was undertaken with the Consultants contracted to do the work and under supervision of the author. Drilling was undertaken in a phased approach with the initial drilling of a limited number of core holes (6) and percussion boreholes (9) on-site in order to refine the preliminary conceptual model that was based on historical data. Once the source zones in the weathered aquifer was delineated, additional diamond drilled core holes (13) and percussion drilled holes (103) were advanced into the bedrock.

The geology of the site was investigated by:

- Using existing databases of construction logs
- Using a core drill rig to advance boreholes to the basement.

The factors that determined the locality of the core holes included:

- 2-D resistivity anomalies (for e.g. low resistivity zones) which could suggest the presence of a transmissive fracture zones or groundwater with elevated specific conductivity (for e.g. contaminated groundwater)
- Logistical considerations.

Diamond core drill runs were at 3 m lengths. Hydrophobic dye (Oil Red O®) was sprinkled onto the recovered core to determine whether DNAPL was present. Additionally, fractures and joint sets within the core were screened for VOCs using a handheld MiniRAE 3000™ PID equipped with an 11.7 eV lamp. Where the PID readings exceeded 50 ppm and/or a positive dye test was recorded, the borehole was advanced by up to 3 m to create a sump to allow for DNAPL collection. Drilling was then stopped.

All core holes were logged and the logs are provided in Appendix A. Core Logging included geotechnical, structural and lithostratigraphic parameters:

- Core recovery – amount of core recovered (measured in the core box) as a percentage of length drilled as determined by the driller (core run length). A significant loss of core is usually the result of core destruction by the drill bit (grinding) in poor, weak or soft ground conditions. A minor core loss or gain is usually a function of slightly more or less core collected in the core barrel measured against the length drilled (core run length);
- RQD (Rock Quality Designation) – the collective sum of pieces of core greater than 100mm length per core run length expressed as a percentage (%). A low

RQD reflects broken core usually due to the presence of jointing, fractures and other structural discontinuities; and

- Joint or fracture frequency – a measure of the number of all joints and fractures including open and closed (sealed joints) per core run length expressed as number of joints per meter.
- Joint or fracture discontinuity
- Geology:
    - Stratigraphic code (provided in Appendix A)
    - Rock type – main description of rock type i.e. sandstone, shale, lava, dolerite
    - Grain size of main rock type:
        - very coarse - >6mm i.e. conglomerate;
        - coarse – 2 to 6mm i.e. grit;
        - medium– 0.6 to 2m i.e. sandstone, dolerite, lava;
        - fine - 0.2 to 0.6mm i.e. siltstone, lava; and
        - very fine - <0.2mm i.e. shale, clay.
    - General weathering of the rock type:
        - extreme weathering;
        - very weathered;
        - moderately weathered ;
        - slightly weathered; and
        - unweathered.
    - Colour of main rock type;
    - Hardness of main rock type:
        - very hard– extremely difficult to break;
        - hard – difficult to break;
        - moderate – can be broken with hammer;
        - soft – can be scratched with a knife; and
        - very soft – easily crumbles or deforms.
    - Bedding dip – bedding / core angle of a sedimentary rock i.e. 0-5 is 0° to 5° from the horizontal – a flat or sub-horizontal bedding;
    - True width – a measure of the true thickness of the geological unit.

Rock coring is significantly slower (approximately 1m/hour) than air percussion methods and is therefore more costly.

Borehole geophysical methods, such as electrical resistivity or natural gamma logs, provide continuous stratigraphic column information relevant to a specific location or

station. The purpose of the borehole geophysical logging at the Investigation Site was to:

- Collect fracture orientation data to enhance the regional geologic conceptual model;
- Identify potential transmissive fractures/fracture zones; and
- Collect proxy geology data for comparison with the detailed geologic logs to determine if borehole geophysical logging can be used as a more cost effective means of interpreting geologic conditions.

The following borehole geophysical logging tools (the probe system is denoted in parenthesis) were used to log diamond core boreholes advanced at the site:

- Acoustic Televiewer (ATV) – acoustic imaging of the borehole that is interpreted to identify the depth, orientation and aperture of bedrock fractures. This tool can only be used in the presence of water.
- Fluid Temperature (FT4/GTC3) – measures groundwater temperature within a borehole; inflections in the groundwater temperature profile may be attributable to groundwater entering or leaving the borehole via transmissive bedrock fractures.
- Fluid Conductivity (FT4) - measures groundwater specific conductivity within a borehole; inflections in the groundwater conductivity profile may be attributable to groundwater entering or leaving the borehole via transmissive bedrock fractures.
- Caliper (GTC3) – provides a continuous measurement of the borehole diameter. Enlargements in borehole diameter may represent bedrock fractures, fractured zones, weathered zones, or zones of softer rock.
- Natural gamma (GTC3) – measures natural gamma activity due to the presence of minerals containing radioactive elements such as potassium, which can be used to interpret geologic stratigraphy (e.g., in sedimentary sequences, shales contain potassium-bearing clay minerals such as illite or montmorillonite whereas sandstones contain relatively few clay minerals).
- Self Potential (RR2) – measures self-potential anomalies that are typically attributed to the presence of graphite, high concentrations of base metal sulphides such as pyrite), or fluid flow in porous media.
- Resistivity (RR2) – measures the electrical resistivity of the rock, which is dependent on the mineral content (e.g., metal sulphide or oxide minerals are highly conductive whereas other minerals are typically weakly conductive), water content, and/or water quality. Given that the majority of minerals are poor conductors, low resistivity anomalies typically represent zones of increased porosity, fracturing, or groundwater conductivity.

• Dual density (DD6) – measures the density of geologic formations, which can serve as a proxy for rock type, by lowering a gamma source into a borehole and measuring the gamma rays arriving at dual detectors placed at fixed distances from the gamma source.

"Fracture pick" analysis was undertaken by Reeves Wireline Services on the diamond drill core holes using the acoustic televiewer data. In this method, the planar structures (fractures, joints, bedding places) present in the sidewall of the borehole are identified. The planar structures are classified as one of the following:

- Visible layering including bedding
- Major fractures
- Intermediate fractures
- Minor fractures; and
- Open fractures

Rotary percussion drilled boreholes were used to determine the hydrogeological regime at the site.

Ten (10) In-Situ Inc. Level Troll 700™ data-logging pressure transducers were installed in existing boreholes around the site by the Consultants (ERM, 2005) in order to collect dynamic groundwater elevation data. This was to support detailed evaluation of horizontal and vertical hydraulic gradients as well as seasonal variations in hydraulic gradients. On average each borehole was monitored over a two year period. The rainfall at the site was also monitored over this period.

The hydraulic conductivity for aquifers was determined by two methods viz, packer testing and through the insertion of ribbon NAPL samplers in some boreholes.

A straddle packer system was used to isolate each geological unit and pressure tests were conducted on selected boreholes to evaluate the hydraulic parameters of each interval. The tests were carried out using leak-proof upper and lower packers in order to isolate specific lengths of the borehole. The spacing of the packers was approximately 1.50 meters. The tests consisted of pumping water into the isolated zone at three different pressures: a, b and c in the following sequence:

1st: 10 minutes at low pressure……a

2nd: 10 minutes at medium pressure……b

3rd: 10 minutes at high pressure……c

4th: 10 minutes at medium pressure……b

5th: 10 minutes at low pressure……a

The flow of water into the isolated zone was measured by means of a flow meter for each of the pressure stage periods. The duration of the pressure test for each interval was recorded. The starting pressure for each interval was 50 kPa and this was increased by 50 kPa increments. The permeability (*K*) of each discrete test interval was estimated using the relationship between the flow rate and the applied hydraulic pressure using the following equation:

$$\mathbf{K} = \frac{\mathbf{Q}\ln(\mathbf{R}/\mathbf{r})}{2\pi \mathbf{P_i} \mathbf{L}} \quad \textbf{Equation 3-1}$$

Where:

r = radius of borehole

R = assumed radius of influence

L = length of the test interval

Q = flow rate

P_i = net injection pressure

Drawdown tests were conducted on selected boreholes by removing water at a constant rate of 1.2 L/minute over a period of 1 hour, using a peristaltic pump. Ribbon NAPL samplers were only installed in boreholes with water level difference before and after the drawdown tests was < 1.5 m^3. This was based on the assumption that the borehole intersected sufficient transmissive fractures for installation of the ribbon NAPL samplers. The transmissivity measurements are taken by recording the liner position with time, the tension on the liner and the excess head driving the liner.

All the newly-drilled wells were gauged by the Consultants using a Solinst™ electronic dip-meter/interface probe.

The location of all investigation boreholes (weathered and fractured zones) are shown in Figure 3-8.

Shallow piezometers (up to 7 m bgl) drilled along the boundary of the intermittent streams were gauged to determine whether these streams were gaining or losing

[3] This assumption was based on failed attempts at installing ribbon NAPL samplers in low transmissivity boreholes.

streams. The piezometers were designed so that the screened sections were set below one m bgl to the base of each hole. A plain riser was installed to rise approximately 500 mm above ground level. Each piezometer was equipped with 63 mm uPVC screen and solid casing. A 2-5 mm silica gravel pack was installed across the screened interval and a bentonite seal was installed within 0.1 m of ground level in order to minimise the potential for ingress of surface water. All piezometers were capped.

3.2.4 Hydrogeochemical and biogeochemical characterisation

A low-flow peristaltic pump was used to retrieve groundwater samples. The field sampling procedure is illustrated by means of a flow diagram (Figure 3-9). The low-flow pump was installed within the screen zones. The position of the pump varied depending on whether or not the screen depth was known. Groundwater was pumped at flow rates of 0.1-3 L/minute (depending on the volume of water in the well). The field parameters (Temperature, pH and electrical conductivity) were monitored using an overflowing bucket system until the parameters stabilize. The overflow bucket system consisted of field probes that were placed within a jug. This was allowed to overflow into a bucket, ensuring recycling of water within a jug. The volume of water purged depended on how quickly the field parameters stabilized. In order to determine the sampling set-up, the well volume at each well was first calculated, and thereafter a pump was selected.

Retrieved groundwater samples were analysed for chlorinated hydrocarbons. Additionally, selected samples were analysed for toxicity, an empirical measure of biodegradability of samples, compound specific isotope analyses and microbial analysis (focus on PCE degradation). The wells purged during the additional sample collection were also measured for dissolved oxygen and redox potential. Samples collected for compound specific isotope analysis (CSIA) were sent to the University of Waterloo (37-Cl isotope analysis) and Microseeps (13-C isotope analysis), where the ratio of stable isotopes were determined using an Isotope Ratio Mass Spectrometer (IRMS). The method for sample collection and preservation for CSIA as described by Hunkeler *et al.*, 2008 was used.

The sampled boreholes were analysed for toxicity by measuring the percentage inhibition using a Hach Eclox luminometer. Toxicity screening was undertaken on site and was a rapid inexpensive methodology to provide an overview of the site

toxicological profile. The field kit luminometer contains *Vibrio fischeri* luminescent bacteria. Individual samples were placed in the luminometer and the amount of light made by the bacteria after exposure to the sample is compared to the amount of light made by the bacteria after exposure to a control. The control used was 2% NaCl solution.

The biochemical oxygen demand (BOD) determination is an empirical test which determines the relative oxygen requirements of wastewaters, effluents and polluted waters under aerobic conditions. The test measures the molecular oxygen utilised for the biochemical biodegradation of organic material (carbonaceous demand) during a specific period of time. Chemical oxygen demand (COD) is used to indirectly measure the amount of organic compounds in water. The Chemical oxygen demand (COD) test uses a strong chemical oxidant in an acid solution and heat to oxidize organic carbon to CO_2 and H_2O (Boyles, 1997). The biodegradability index of a sample can be determined from the BOD/COD ratio. The following applies:
BOD/COD > 0.4.....biodegradable
0.2<BOD/COD<0.4.....medium biodegradable
BOD/COD< 0.2.....non-biodegradable/very little biodegradability.

Samples for mibcrobial analysis were collected in sterilized glass bottles. The analyses were undertaken at the University of the Free State Metagenomics Platform under the supervision of Professor E. Van Heerden. The purpose of the analysis was to detect the presence of genomic DNA. Water samples were filtered through a 0.22µl polyethersulfone filter and demonic DNA was extracted from each filter using FastDNA SPIN for Soil Extraction (MP Biomedicals) kit. The DNA extracts were visualised on a 1% agarose minigel with ethidium bromide and UV-illumination after electrophoresis in TAE buffer (90 V for 1 hour). DNA concentration and purity were assessed using a Nano Drop spectrophotometer 3300 fluorospectrometer.

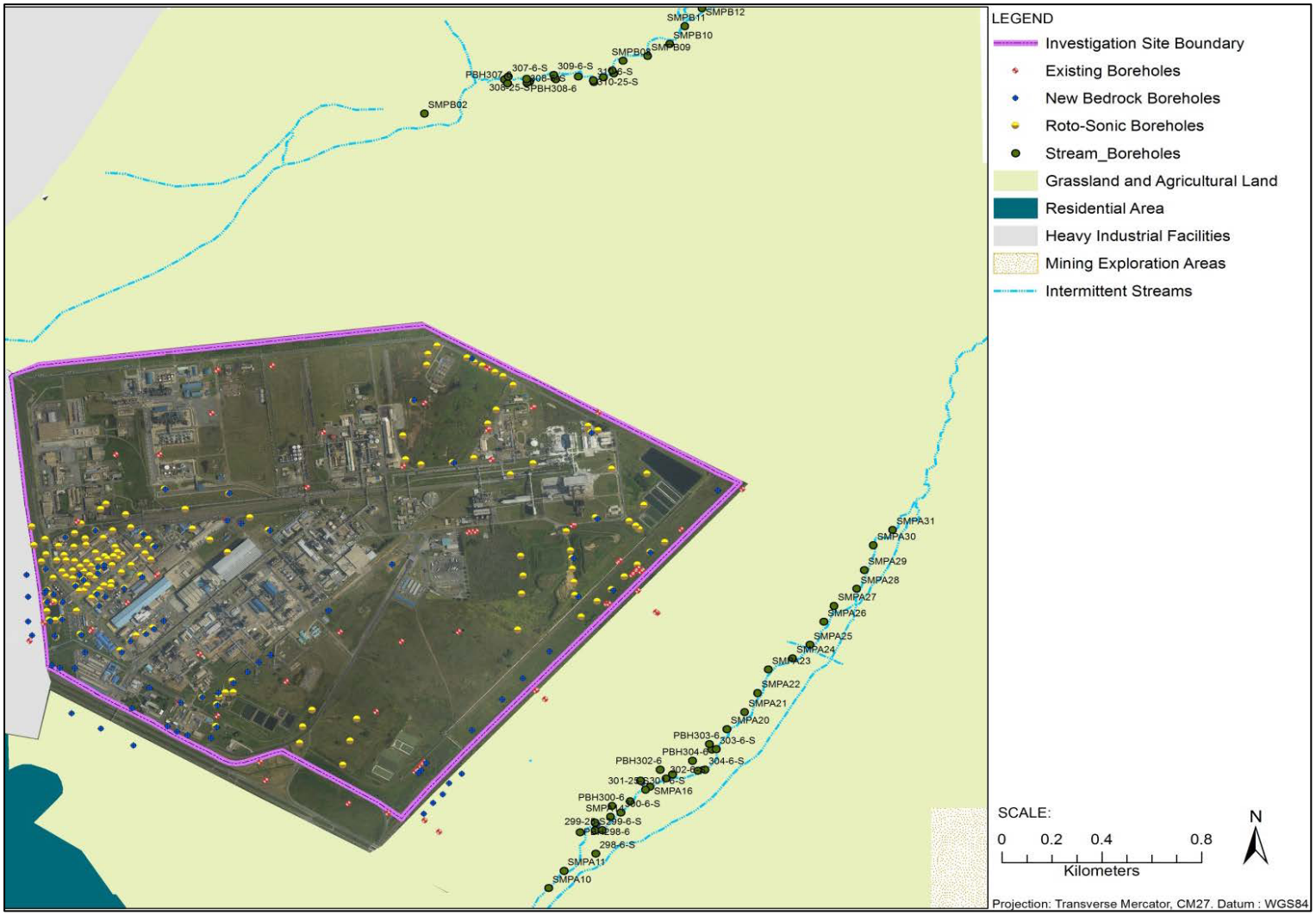

Figure 3-8: Location of all boreholes drilled at the Investigation Site (results from SRK Consulting, 1995; SRK Consulting, 2001, ERM, 2005; ERM, 2012)

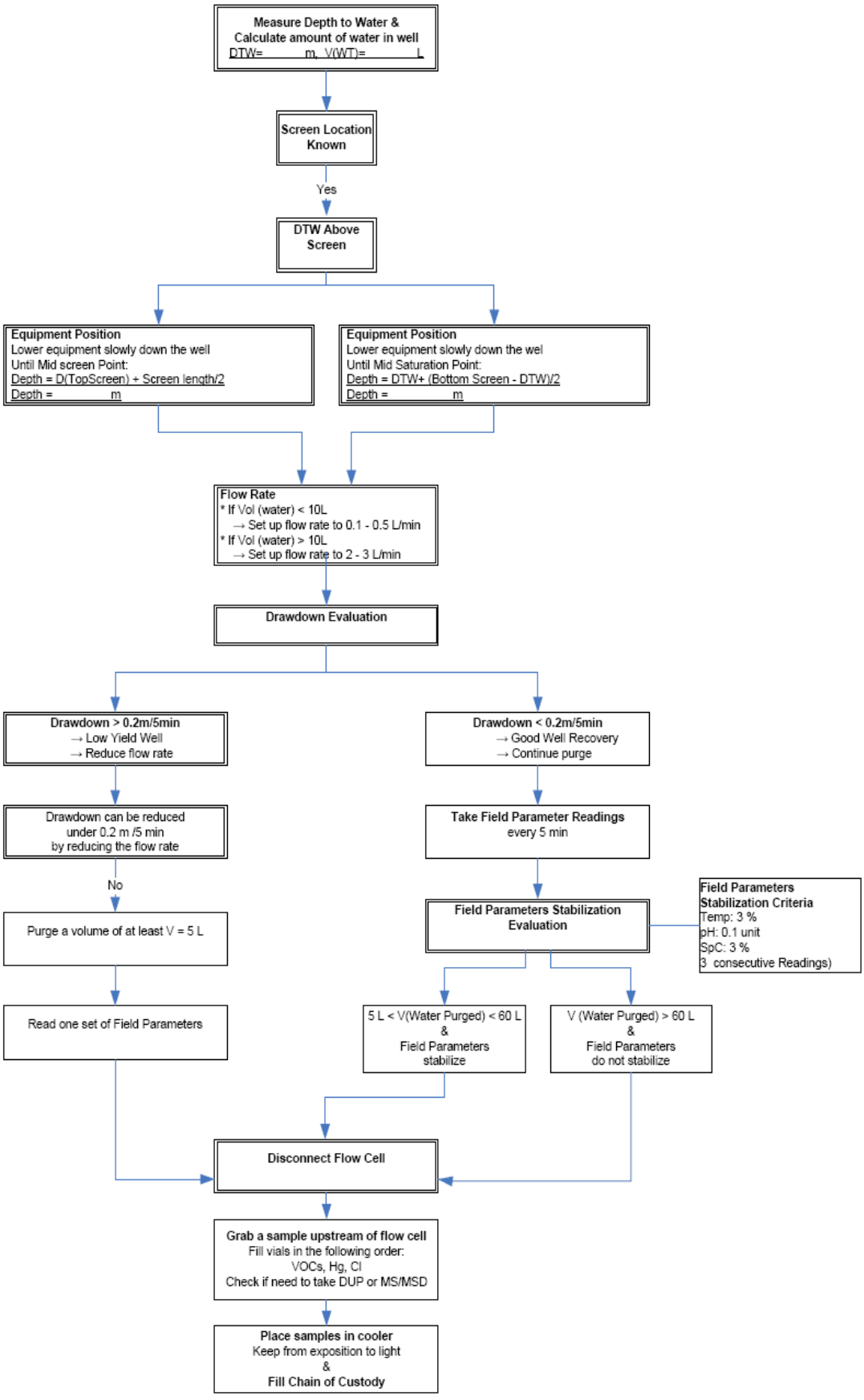

Figure 3-9: Flow diagram for groundwater sampling at the Investigation Site (from ERM, 2008)

3.3 Results

3.3.1 Regional geology

The regional geology of the area is dominated by the following lithologies (Figure 3-10 and Figure 3-11, cross section locations are indicated on Figure 3-3):

- Pre-Karoo basement: The regional pre-Karoo basement is characterised by andesitic lavas of the Pretoria Group Hekpoort formation, various quartzite marker units of the Witwatersrand Group (i.e. Orange Grove and Turffontein quartzites), the Black Reef quartzite and the top contact of the Chuniespoort dolomites. The outcrop patterns of the marker horizons show circular deformation around the domal Vredefort impact structure. These folds consist of a steeply dipping overturned syncline, tight anticline and open syncline plunging at 4-8° NW. The basement suboutcrops 5km north and 14km west of the Investigation Site and gently deepens southeastwards under Karoo cover rocks.
- Karoo Supergroup: The Karoo Supergroup is characterized by a gently undulating (elongated domes and basins) mixed succession (in the order of 40m thick) of mudstone, shale, siltstone, sandstone and coal seams (collectively called the Ecca formation), with a basal tillite (Dwyka formation). The undulating features of the succession mimics the surface topography of the underlying pre-Karoo basement, with Karoo sequence domes and basins overlying basement highs and lows, respectively. An overlapping unconformable relationship is evident between the lower units of the Karoo succession against the basement highs with the basal (C1), middle (C2) and occasionally, the top (C3) coal seams pinching out against the basement highs. The coal seams average between 4-6m thick reaching a maximum in basement lows of 10-12m thick.

  The lower mixed succession (lower Ecca formation) contains variable, but often significant, mudstone and shale units which range from less than 1m to greater than 10m thick. The lower succession of the Ecca formation suboutcrops below unconsolidated overburden to the north of the Investigation Site. The upper part of the formation (sandstone dominated) suboutcrops south and west of the Investigation Site.
- Unconsolidated overburden generally varies between 2- 7 meters thick. This increases to 10-18 meters NNE of the Investigation Site and >24 meters in the area of the primary River.
- Regional structures/features:
    - Late Karoo sub-horizontal dolerite sill intrusion, generally between 30-60 m thick is a major geological feature in the region resulting in extensive

areas of dolerite sub outcrop. Sills may change elevation within the Ecca formation along steep linear “roll” structures.

- The main linear structural trends are NNW-SSE and E-W. A NS trend is prevalent in the south of the region. These features are characterized by linear drainage features, faults and airborne magnetic anomalies, the latter often locally confirmed as dolerite dykes in outcrop. The NNW trend is associated with dolerite dyke intrusion with minor faulting and is dominant in the east of the area. The E-W trend is associated with both faulting and/or dolerite dyke intrusion.
- Major dolerite dykes are dominant north of the primary River.
- A possible E-W fault with a down throw of 55m to the north may be present close to the primary River between boreholes NVL0787 and NVL5037
- The depth of weathering is highly variable but generally varies between 2-18 meters in all lithologies with a maximum record showing 35 meters in the shale (Ecca Formation)

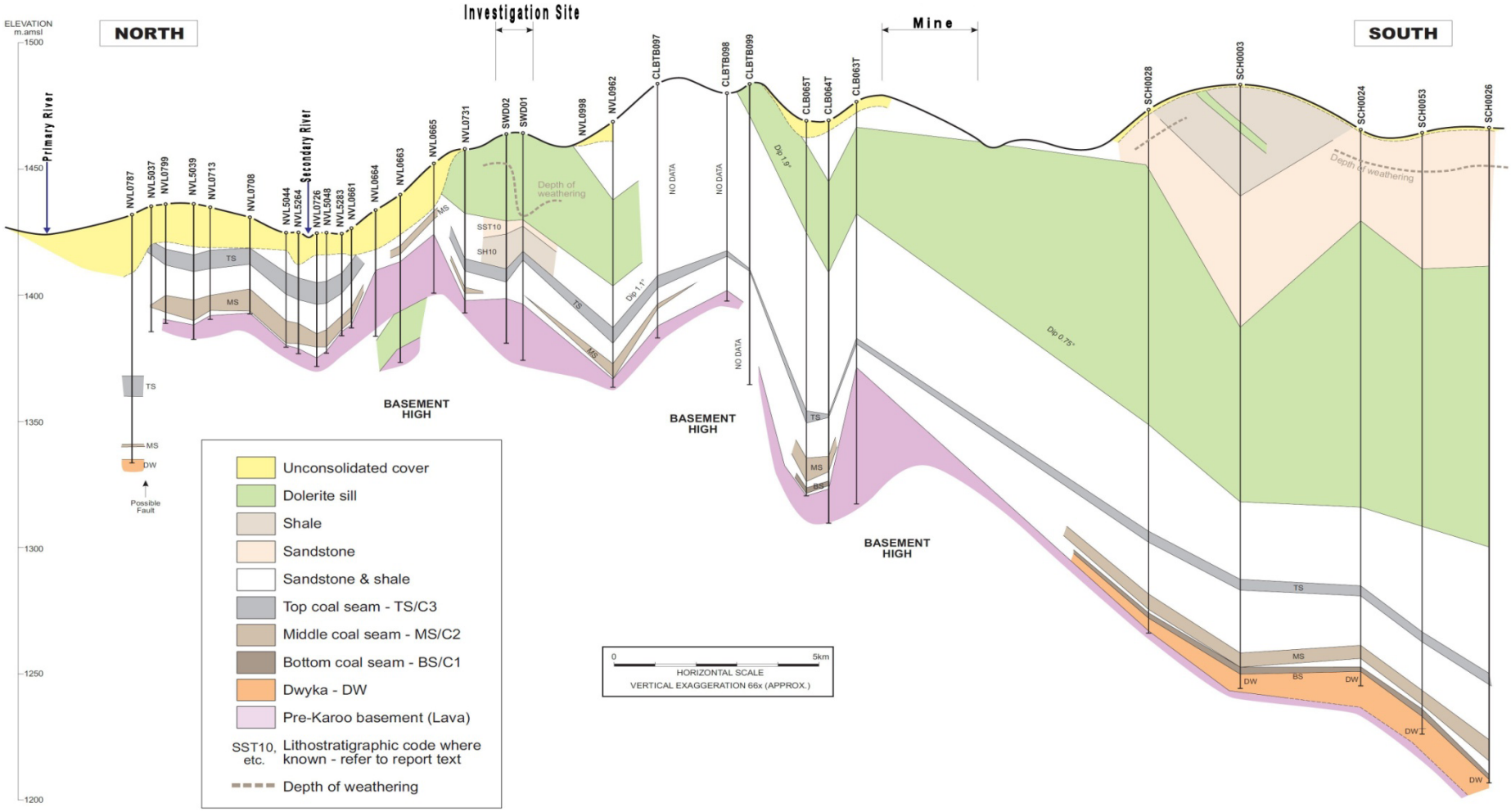

Figure 3-10: North-south trending regional geological cross section (modified from ERM, 2008)

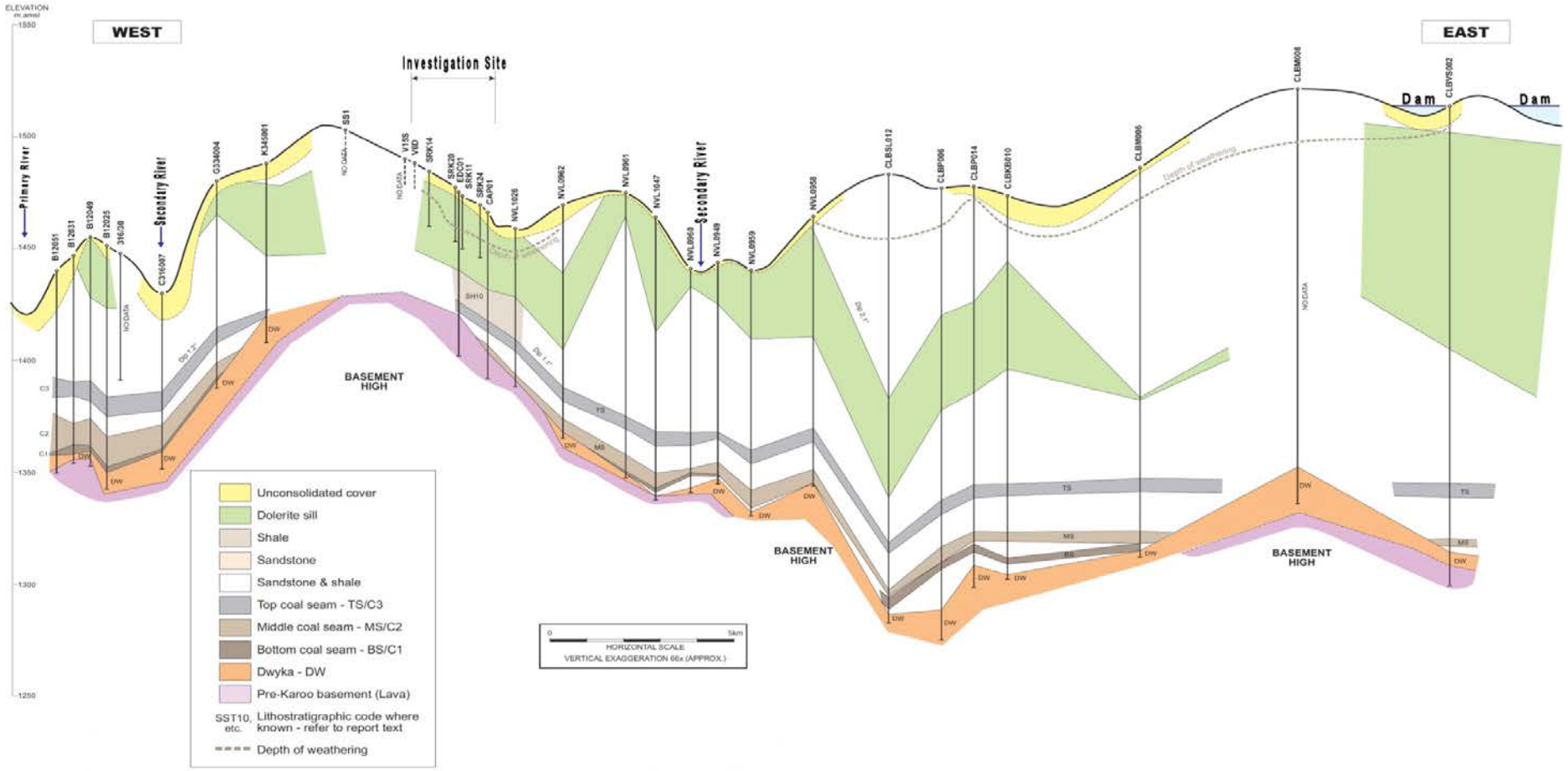

Figure 3-11: East-west trending regional geological cross section (modified from ERM, 2008)

3.3.2 Local geology

In general the local geology underlying the Investigation Site consists of overburden and weathered rocks with high to moderate permeability and bedrock characterised by low permeability. The general site stratigraphy is shown below (modelled using RockWorks15 software, with the Inverse Distance Weighted algorithm). Further details on the lithostratigraphy as well as the structural discontinuities are provided below. Stratigraphic profiles across the source zones are shown in Section 3.3.4.

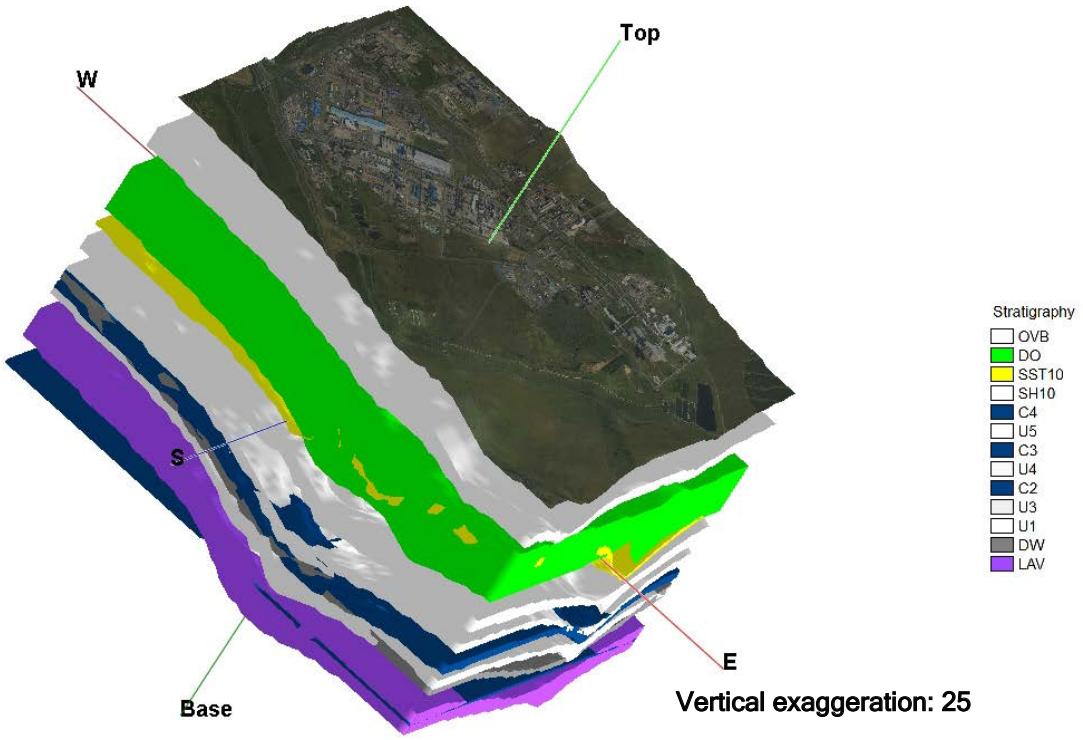

Figure 3-12: Stratigraphic model

The key to the stratigraphic codes shown in the stratigraphic model above are as follows:

OVB: Overburden, unconsolidated material includes aeolian sand, silt and clay

DO: Dolerite intrusions

SST10: Dominantly sandstone unit, subordinate siltstone (massive), shale and mudstone

SH10: Dominantly shale or mudstone unit, subordinate siltstone (banded). Rare thin sandstone and coarse sediment units

C4: Coal unit, C4 or leader seam

U5: Alternating shale, siltstone and sandstone on centimetre / decimetre scale

C3: Coal unit, C3 or Top seam, subordinate clastic sedimentary partings

U4: Alternating shale, siltstone and sandstone on centimetre / decimetre scale
C2: Coal unit, C2 or Middle seam, subordinate clastic sedimentary partings
U3: Alternating shale, siltstone and sandstone on centimetre / decimetre scale
U1: Alternating shale, siltstone and sandstone on centimetre / decimetre scale
DW: Dwyka Tillites
LAV: Pre-Karoo Basement Lava

2-D Lund resistivity methods allowed for discrimination between low and high resistivity sub-surface features. Resistivity profiles are provided in Appendix B. In general, the correlation of geological zones identified through core logging with the resistivity profile data is summarised as follows:

- The high resistivity zones (> 70 Ohm-m) in the geophysical profiles can be correlated with unweathered rock types (i.e. dolerite sill and Pre-Karoo Ventersdorp lava)
- Moderately resistive zones (20-70 Ohm-m) correlate with Karoo Ecca sedimentary rocks (20-50 Ohm-m for sandstone and 10-20 Ohm-m for shale), partly weathered dolerite sill or thinly developed dolerite sill
- Low resistivity zones (5-20 Ohm-m) reflect a variety of different geological features (e.g. overburden, clay-rich residual weathering profiles, possible structural breaks such as faults or large fractures in otherwise competent bedrock), zones of increased groundwater content (preferential groundwater flow paths), or potentially contamination zones.
- Very low resistivity zones (<5 Ohm-m) reflect possible conductive groundwater, overburden, *in situ* clay rich profiles or very weathered Ecca sedimentary rocks (likely to be shale dominant).

The resistivity profiles are generally characterised by horizontal stratification (for e.g. Traverse 102 and 103, Figure 3-13, with very low resistivity at the surface and increasing resistivity with depth reflecting a horizontal sequence of overburden, *in situ* clay, weathered bedrock and bedrock (dolerite sill). The depth to the base of the overburden and *in situ* clay is recognisable due to the resistivity contrast between the two features. However, in areas where the Ecca sedimentary sequence outcrops at surface, this contrast is not easily discernible due to the Ecca sedimentary rocks being reflected as having low resistivity. Within specific resistivity profiles there are marked horizontal variations. In these instances (e.g. Traverse 109, Figure 3-14) zones of high and low resistivity are often separated by a steeply orientated break, reflecting a change in rock type (between dolerite and Ecca sedimentary rocks).

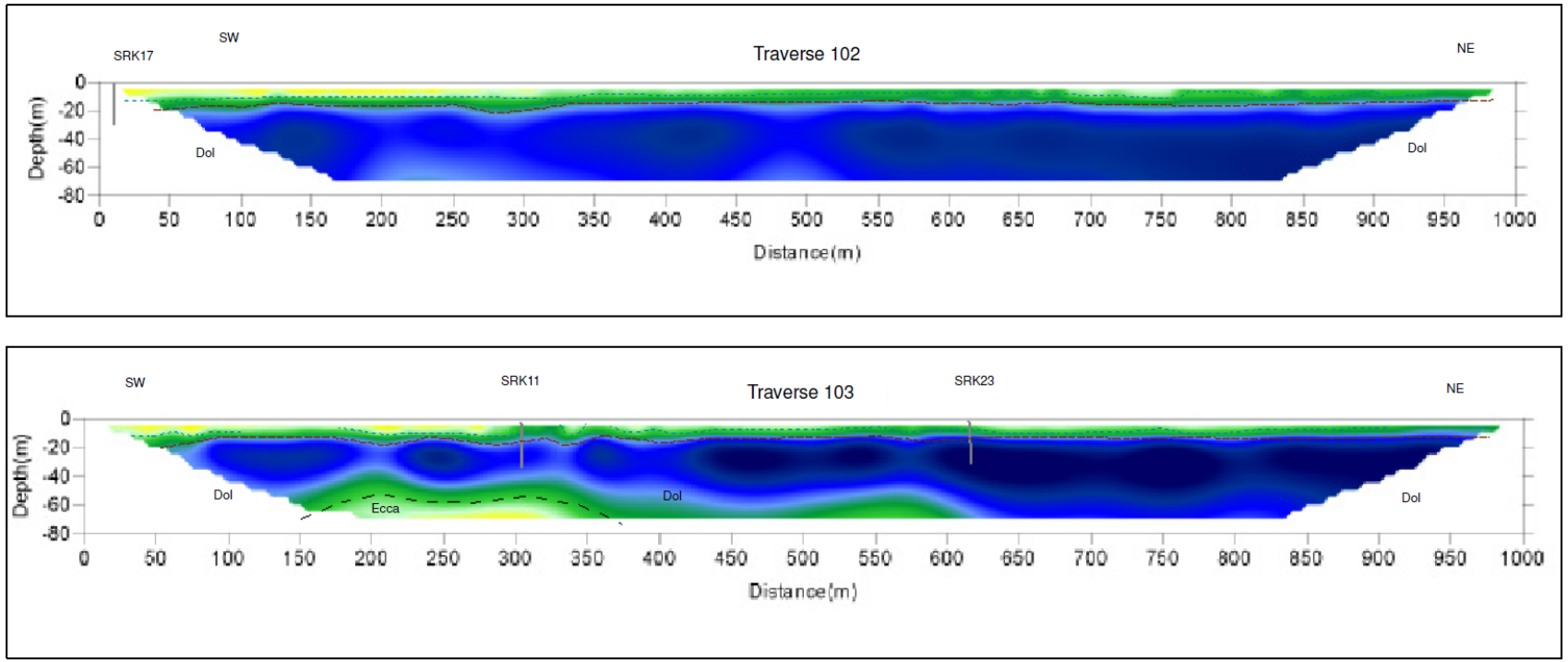

Figure 3-13: 2-D resistivity profiles of Traverses 102 and 103

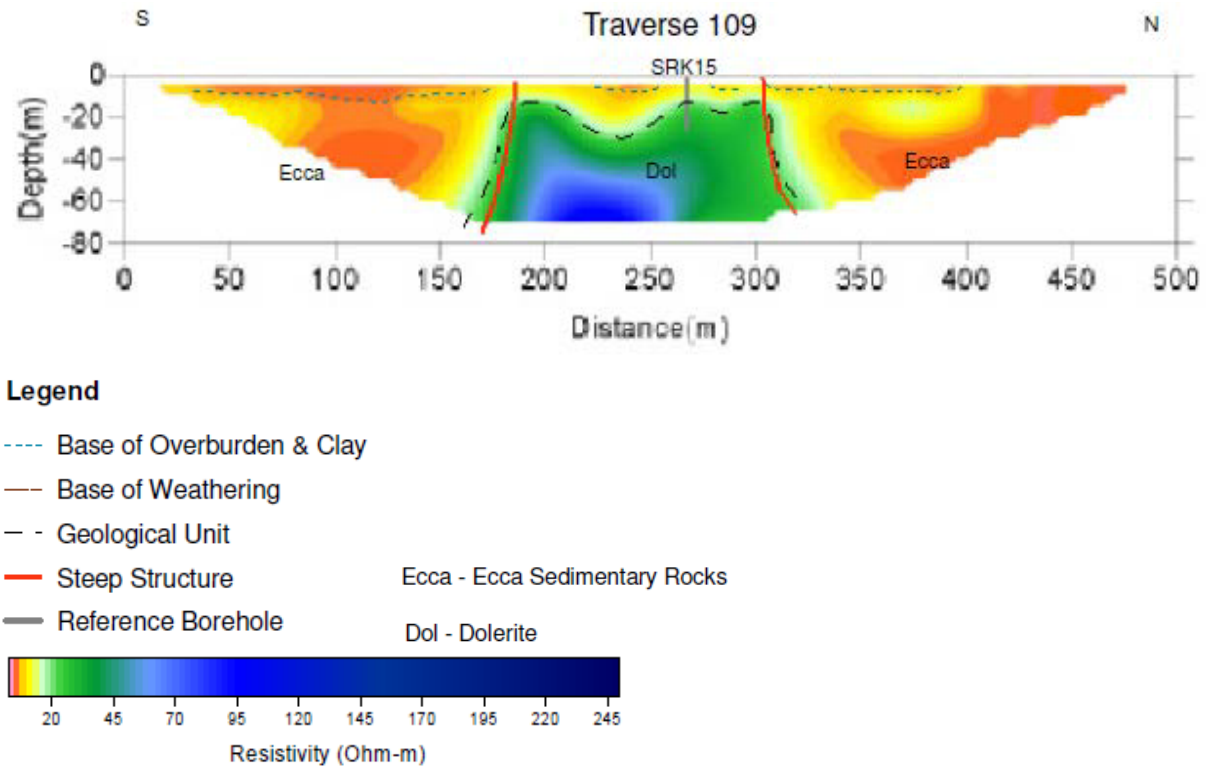

Figure 3-14: 2-D resistivity profile of Traverse 109

From the core and borehole logs for the site (Appendix A) it was possible to distinguish between the upper sand dominated soil, fill and transported material and underlying in-situ clay dominated weathered bedrock. The former is classified as overburden and the latter is part of the weathered bedrock profile. The overburden consists of sandy transported material up to a depth of approximately 6.5 m bgl, thereafter the material becomes predominantly clayey as a result of the weathering of dolerite. Overburden is more developed in the southern portion of the site boundary and adjacent to the intermittent stream to the south.

A sandy and silty clay layer, varying up to 8m thick, is present in all boreholes drilled at the site area, except along the northern boundary. It mostly represents an *in situ* extreme weathering of dolerite and Ecca shale/siltstone. A typical profile of the weathered zone at the Investigation Site is shown below (Figure 3-15). Weathered Ecca sedimentary formation (consisting of residual sandstone or residual mudstone/shale) underlies the colluvium. The colluvium or the weathered Ecca sedimentary formations overlies weathered dolerite. Particle size distribution analysis determined from the analysis of Borehole EDC2 indicates a decrease of clay content with depth and a corresponding increase in gravel content with depth (Figure 3-16). This marks the transition from clayey residual dolerite or Ecca sedimentary rocks to highly weathered bedrock dolerite (Figure 3-17). The weathering in the dolerite varies

laterally and vertically across the site. Zones of deep (>35 m) and shallow (<15 m) lie adjacent to each other. Elongated pockets of deeper weathering show a primarily NW-SW with a second subordinate N-S trend which tend to coincide with synclinal and anticlinal flexure axes in the underlying dolerite and Ecca sedimentary rocks. The surface weathering base slopes to the SE across the site with a gradient of 0.0125 (0.718°). An isopach map showing the base of weathering elevation (or the upper contact of bedrock) at the Investigation Site is shown in Figure 3-18.

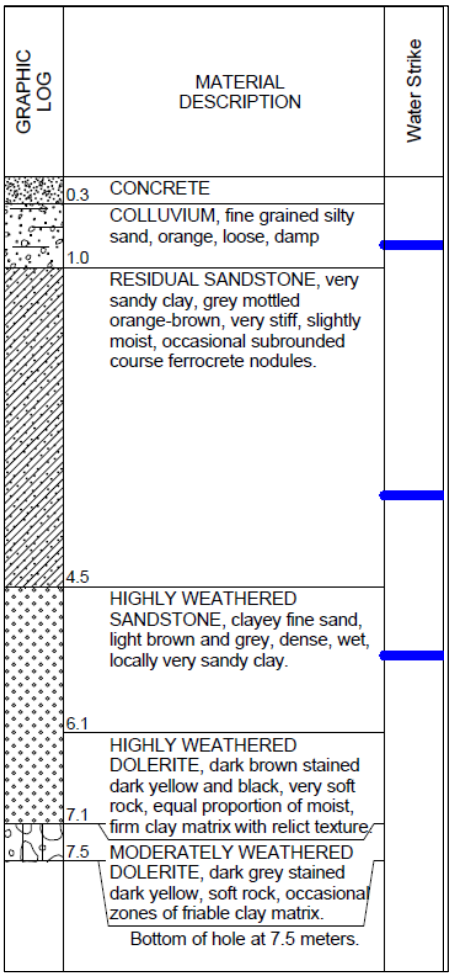

Figure 3-15: Typical weathered zone profile at the site

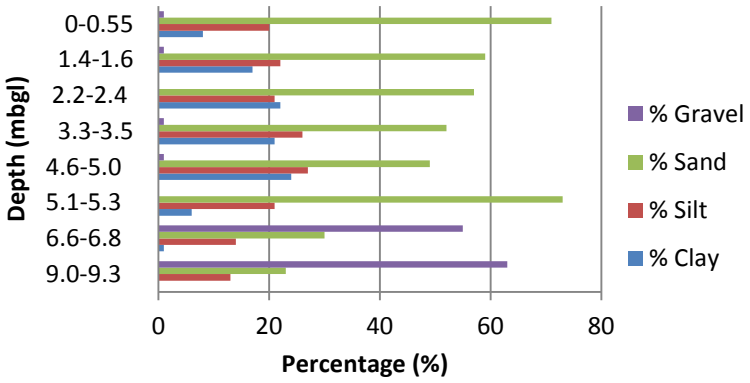

Figure 3-16: Particle size distribution of borehole EDC2S

Figure 3-17: Picture taken of roto-sonic core (EDC2S) showing the transition from residual clay dolerite to highly weathered dolerite

The geotechnical properties of the weathered or residual lithologies are shown in Table 3-5. The fraction of organic carbon in this zone is higher than that observed for the bedrock. Residual and weathered Ecca sedimentary rocks have lower permeability (classified as very low permeability; Lambe and Whitman, 1969) than that observed for weathered and residual dolerite (classified as medium permeability; Lambe and Whitman, 1969). Soil permeability analysis of the residual and weathered Ecca sedimentary and dolerite samples show variations in permeabilities. The residual Ecca sedimentary samples exhibited permeability values ranging from 2.5 x 10^{-6} m/d to 5 x 10^{-6} m/d, while the weathered dolerite samples exhibited permeability values ranging from 2.6 x 10^{-6} m/d to 2.1 x 10^{-3} m/d.

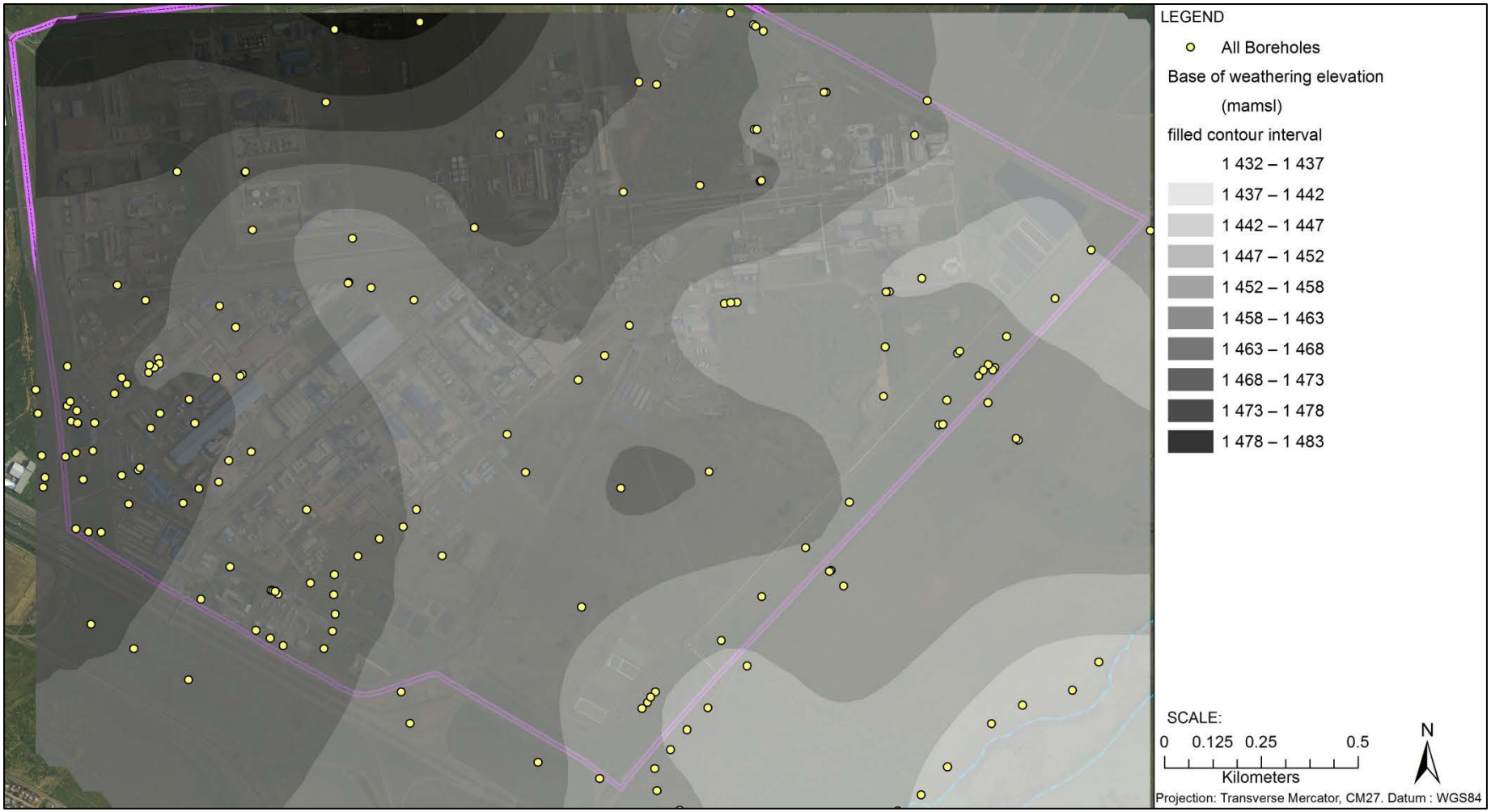

Figure 3-18: Base of weathering elevation

Bedrock characteristics are determined through logging of holes during diamond core drilling as well as through downhole geophysical analysis in selected core holes. The effectiveness of the downhole geophysical tools used has been differentiated by those that showed the best responses for the varying lithological units and geological features (Table 3-5). The responses observed using natural gamma, the acoustic televiewer, density probe, calliper, and resistivity probe corresponded closely to the geological/core logs. The following planar structures were identified using the "fracture pick" analysis on the diamond drill core holes using the acoustic televiewer data:

- Visible layering including bedding
- Major fractures
- Intermediate fractures
- Minor fractures
- Open fractures.

A summary of the fracture pick analysis is provided in Table 3-6. Fractures within the bedrock are most developed in weathered zones. In general, sub-horizontal (i.e $<30^0$) fractures or bedding planes dominate over moderate (i.e. 30^0 - 60^0) to steeply (i.e. 60^0 – 90^0) dipping fractures/bedding planes.

Table 3-5: Effectiveness of the borehole geophsyical tools used at the Investigation Site

Borehole Geophysical Tool	Effective
Natural Gamma (GRTH)	Yes
Self potential (SP)	No
Acoustic Televiewer (TIMM and AMPM)	Yes
Density (DENB and DENL)	Yes
Resistivity (FE1 and FE2)	Yes
Fluid Temperature (TEMP)	No
Calliper (CATH)	Yes
Fluid Conductivity (CONN)	No

A core retrieved through diamond core drilling is shown in Figure 3-19 and shows the general bedrock succession underlying the Investigation Site.

Table 3-6: Summary of fracture pick analysis on selected core holes

	SWD1	SWD02	MLR01	CAP01	ASH01
Dolerite Sill	Depth: 0-32.88 m bgl · Upper weathered zone (to 11.5 m bgl) - intense ENE to ESE dipping sub-horizontal fractures · Central part of sill (11.5-26.0 m bgl) – a few minor sub-horizontal fractures and 3 major NE dipping sub-horizontal fractures (14-17 m bgl) · Lower part of sill (subsurface weathered basal contact zone) (26.0-32.88 m bgl) – very intense ENE to ESE dipping sub-horizontal minor fractures and a SSE dipping (27.25 m bgl) and NW dipping (29.75 m bgl) steep major fractures	Depth: 0-33.59 m bgl · Moderately intense multidirectional dipping sub-horizontal fractures in upper part (0-23 m bgl). Open multidirectional sub-horizontal dipping fractures at 9-14.6 m bgl · Central part of sill (23-31.5 m bgl) – a few minor sub-horizontal fractures · Lower part of sill (basal contact zone) (31.5-33.59 m bgl) – very intense easterly dipping sub-horizontal minor to intermediate fractures · No steep dipping fractures recorded	Depth: 0-22.42 m bgl · Intense multidirectional sub-horizontal to moderate dipping fractures and NW to NE, E and W dipping steep fractures. · Open N, NE and E dipping steep fractures at 14.75-16.0mbgl	Depth: 0-35.51mbgl · Moderately intense multidirectional dipping sub-horizontal fractures in upper part (0-23 m bgl). · Central part of sill (23-30.5 m bgl) – no fractures recorded · Lower part of sill (basal contact zone) (30.5-35.51 m bgl) – very intense multidirectional dipping sub-horizontal minor to intermediate fractures. Open SW moderately dipping fracture at 32.2 m bgl · No steep dipping fractures recorded in dolerite sill	Depth: 23.49-79.64 m bgl · Weathered zone – intense multidirectional sub-horizontal dipping fractures and NE to E and WNW moderate dipping fractures in weathered zone (to 36 m bgl) with 6 open fractures between 27.75-31.75 m bgl (with 1 steep SW dipping fracture) · Central part of sill (36-62 m bgl) – weakly to moderately intense ENE to ESE sub-horizontal to moderate dipping fractures and SW to NW and E to NE steep dipping fractures · Multiple dolerite intrusion zone (64.25-67.27 m bgl) – intense sub-horizontal to steep E dipping fractures present between 62-69 m bgl.

Karoo Ecca Sedimentary Sequence	Depth: 32.88-66.20 m bgl · Dominated by NE to SE dipping sub-horizontal bedding planes with 2 open fractures at 40.5-40.75 m bgl (dipping SE and SW) in a shaly sandstone of the SH10 shale unit · Occasional NW, ENE and SE moderate dipping fractures · C3 coal seam (45.15-47.80 m bgl) – intense NE to SE moderate dipping fractures including 3 open fractures in lower portion of the C3 seam (46.5-47.5 m bgl)	Depth: 33.59-64.42 m bgl · Dominated by E to NE dipping sub-horizontal bedding planes. · No moderate to steep dipping fractures recorded (apart from 1 open fracture – see below) · Open WNW moderate dipping fracture at 46.6 m bgl in shale (SH10 unit) · Open SE dipping sub-horizontal fracture at 49.4 m bgl close to shale (SH10) / C3 coal seam contact · More intense E to NE dipping sub-horizontal bedding planes in lower part of C2 coal seam (55-58 m bgl)	Depth: 22.42-42.00 mbgl · Dominated by S to SW dipping sub-horizontal bedding planes · Moderate to steep NW to NE dipping fractures 27-32 m bgl · U5 grit and sandstone (32.14-33.92 m bgl) – 3 open southerly and NW dipping sub-horizontal fractures	Depth: 35.51-62.87 m bgl · Dominated by NE and SW sub-horizontal to moderate dipping bedding planes / fractures · No steeply dipping fractures recorded · More intense development of sub-horizontal to moderate dipping bedding planes/fractures (46.5-47.5 m bgl) along contact zone between C4 leader seam and shale (SH10) · Open N dipping sub-horizontal fracture/ bedding plane at 46.5 m bgl in shale (SH10) · Open NE moderate dipping fracture at 47.5 m bgl in siltstone/ shale (SH10)	Depth: 0-23.49-76.45 m bgl · No data

Pre-Karoo Ventersdorp Lava	Depth: 66.20-89.08 m bgl · Subsurface weathered zone (66.20-71.0 m bgl) – NE to SSE moderate dipping minor and major fractures including a NE moderate dipping open fracture at 69.5 m bgl · Minor fracturing throughout most of the remainder of the lavas · Narrow intense zone of sub-horizontal to steep multidirectional dipping minor fractures at 81.0-81.5 m bgl corresponding to a subsurface weathered zone in amygdaloidal lavas	Depth: 64.42-81.38 m bgl · Moderately intense multidirectional sub-horizontal to steep dipping fractures throughout the lava unit · Open SW dipping sub-horizontal fractures at 72.4 m bgl and 80.2 m bgl	Depth: 42.00-79.28 m bgl · Upper subsurface weathered zone (42.00-42.57 m bgl) – intense narrow zone of ENE and SW shallow, moderate and steeply dipping minor and major fractures · Sub-horizontal and steep minor fracturing throughout most of the remainder of the lavas with steep major fractures at 48.25 m bgl (NNE dipping), 53.75 m bgl (SSW dipping) and 66.75mbgl · Narrow intense zone of moderate to steep minor fractures at 72.62 m bgl coinciding with contact between upper massive lava and lower amygdaloidal lava	Depth: 62.87-90.38 m bgl · Weak to moderately intense multidirectional sub-horizontal to moderate dipping fractures throughout the lava unit	No data

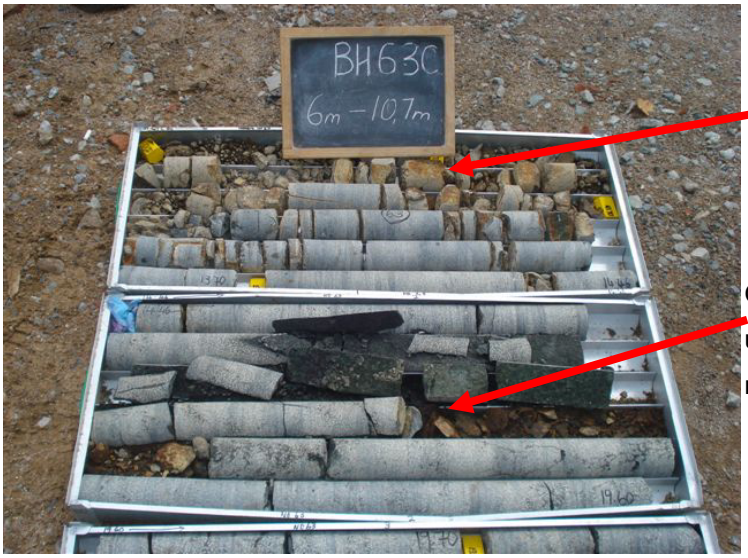

Highly fractured dolerite

Open vertical fracture in unweathered dolerite (~15 mbgl)

Massive dolerite with low fracture frequency (19-30 mbgl)

Dolerite - Ecca Group contact (~32 mbgl)

Karoo Ecca Sandstone

Figure 3-19: Photographic log of core hole BH63C

The dolerite sill has intruded the lower portion of the SST10 sandstone unit (within the Ecca sedimentary sequence) in the Investigation Site area. The elevation of the sill lower (basal) contact has been modelled as an isopach map using GIS software (Figure 3-20). In the site area it generally slopes to the SE with a gradient of 0.0142 (0.81°). However, abrupt changes in elevation of the lower contact indicate the presence of dolerite rolls in the site and ENE, W and SW of the site. The dolerite sill is generally medium grained becoming fine grained within a few metres of the lower contact. The contact is characterised by a very fine grained chilled margin up to 0.5 m thick at depths of 31-34 m bgl. The dolerite displays orthogonal jointing (sub-vertical: 70°-90° and sub-horizontal: 0°-20°). The dip directions are multidirectional in the shallow weathered zone and parallel to the basal contact in the basal contact zone i.e. the fractures dip east within the dolerite sill for most of the Investigation Site. A very high frequency of open weathered joints occurs in the surface weathered zone. A high frequency of partly open to closed joints is present in the lower portion of the sill in a zone up to 7m wide above the lower contact. Joint development in the dolerite sill is likely to be in response to the following events in the structural history of the rock:

- An orthoganol extensional joint system (3 joint sets orientated perpendicular to each other with 2 sub-vertical joints and a sub-horizontal joint orientation) as a consequence of tensional stresses developed during cooling, solidification and contraction in the dolerite sill.
- Extensional joint sets developed in the fold/flexure zones parallel and normal to the flexure axis i.e. NW-SE to NNW-SSE and NE-SW to ENE-WSW.

A NNW-SSE trending dolerite dyke, with evidence of multiple dolerite intrusion at ~ 65.25-66 m bgl, is present below the dolerite sill under a portion of the historical waste sites (Figure 3-20). This feeder zone does not cross-cut through the dolerite sill and is therefore assumed to be a concurrent feeder zone rather than a later dyke. The dolerite dyke has displaced Ecca sedimentary rocks upwards in a local horst structure.

The dominant sedimentary units underlying the site (generally occurring below the dolerite sill), in terms of thickness are fine grained rocks consisting of the SH10 shale unit, U4 mixed shale, siltstone, sandstone unit and Dwyka tillite unit. The sandstone units higher in the succession, i.e.SST10 and SST11 are not significantly developed having been displaced by the intrusion of the dolerite sill. The C3 and C2 coal units and lower units in the succession only occur along the west, south and east periphery

of the site as they are pinched out against the basement palaeo-high under the site. Sub-vertical joints are recognised occasionally in the sandstone and siltstone units. Sub-horizontal joints are not easily recognisable as they are likely to be coincident with bedding and contact planes in the sedimentary sequence. The upper contact of the C3 coal seam has been modelled (Figure 3-21) and illustrates the presence of basins and swells in the Ecca sedimentary sequence which generally reflects the underlying pre-Karoo basement relief. A NW-SE swell axis runs under the site and continues SE of the site. The dip of the sedimentary sequence is radial outwards from the site with dips in the order of 1.20-2.69°.

Unweathered crystalline Ventersdorp andesitic lavas are found at depths ranging from 30 -40 mbgl in the northern portion of the site to 60 – 70 mbgl along the south western and south eastern boundaries of the site. The lavas display alteration, bleaching and quartz veining in the upper portion of the sequence (generally 0 – 10 m thick), immediately below the contact with the Dwyka tillite (Karoo Ecca sedimentary sequence). This is a pre-Karoo paleo-weathering feature. The lavas are fractured and jointed. The joints are closed to partly open and slightly to moderately weathered. Fractures in the lavas are generally moderately (20^0 – 45^0) to steeply dipping (70^0 – 90^0) with chlorite and slickenside surfaces. The basement lavas are characterised by an undulating topography with highs and lows (Figure 3-22) and generally dip 2.23^0 south easterly.

The geotechnical properties of selected rock core samples are provided in Table 3-7. The unweathered dolerite sample contains no measurable amount of organic carbon nor any measurable primary porosity or permeability. The Ecca sandstone sample has trace levels of organic carbon. It has a low primary porosity (3.7%) and very low horizontal and vertical permeabilities. The bedrock core analytical data indicates that groundwater flow and solute transport within the bedrock units are likely dominated by flow within secondary porosity features such as fractures, joints, bedding planes and faults. The Ecca sedimentary sequence has too low values for porosity and permeability to support advective transport within the rock matrix; resulting in very limited diffusion of contaminant mass into the rock matrix.

The results obtained pertaining to fracture characteristics as they relate to the mobility of DNAPL within source zones are discussed in greater detail in Section 3.3.4.2.

Figure 3-20: Dolerite sill lower contact elevation

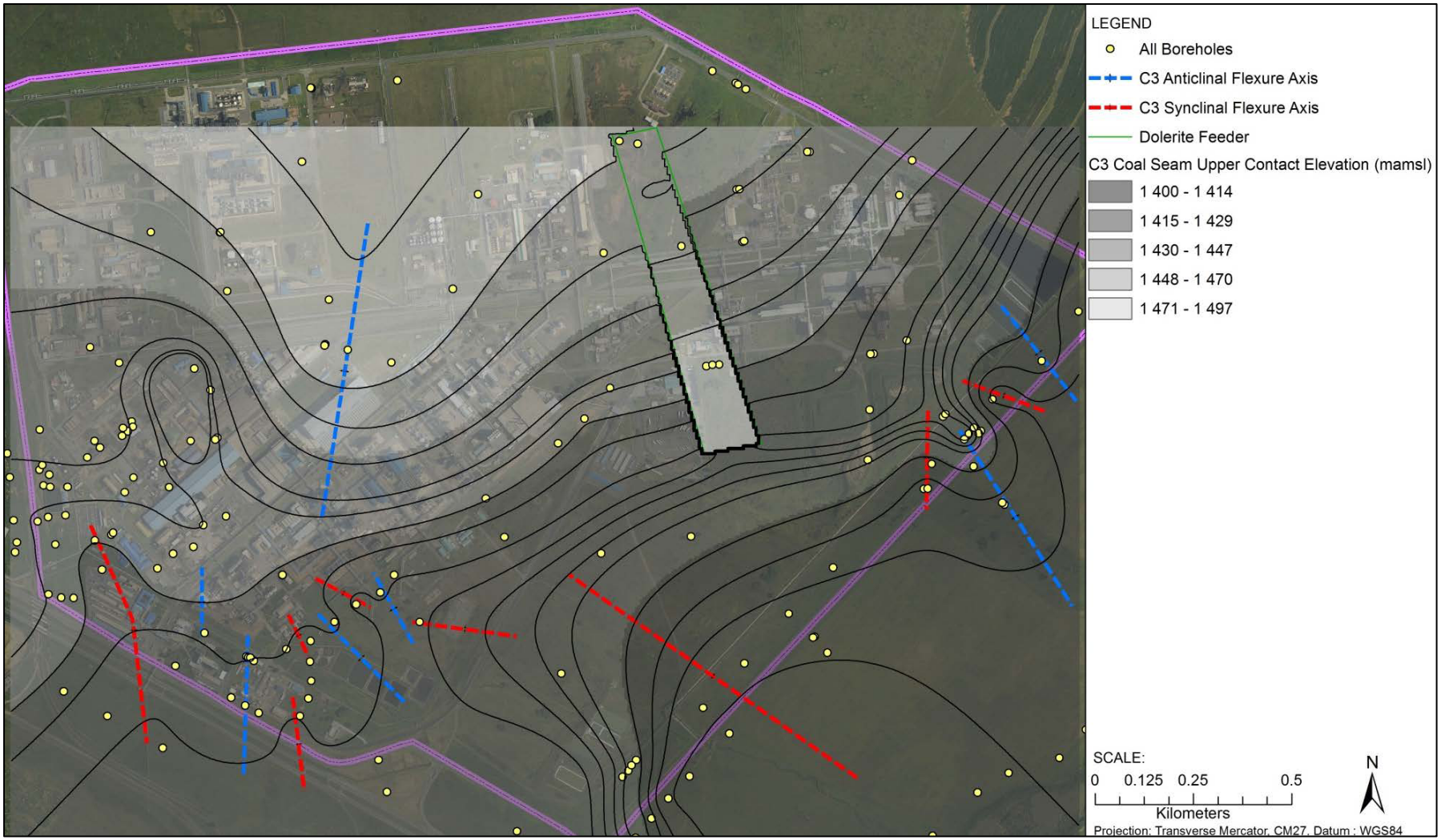

Figure 3-21: C3 coal seam upper contact elevation

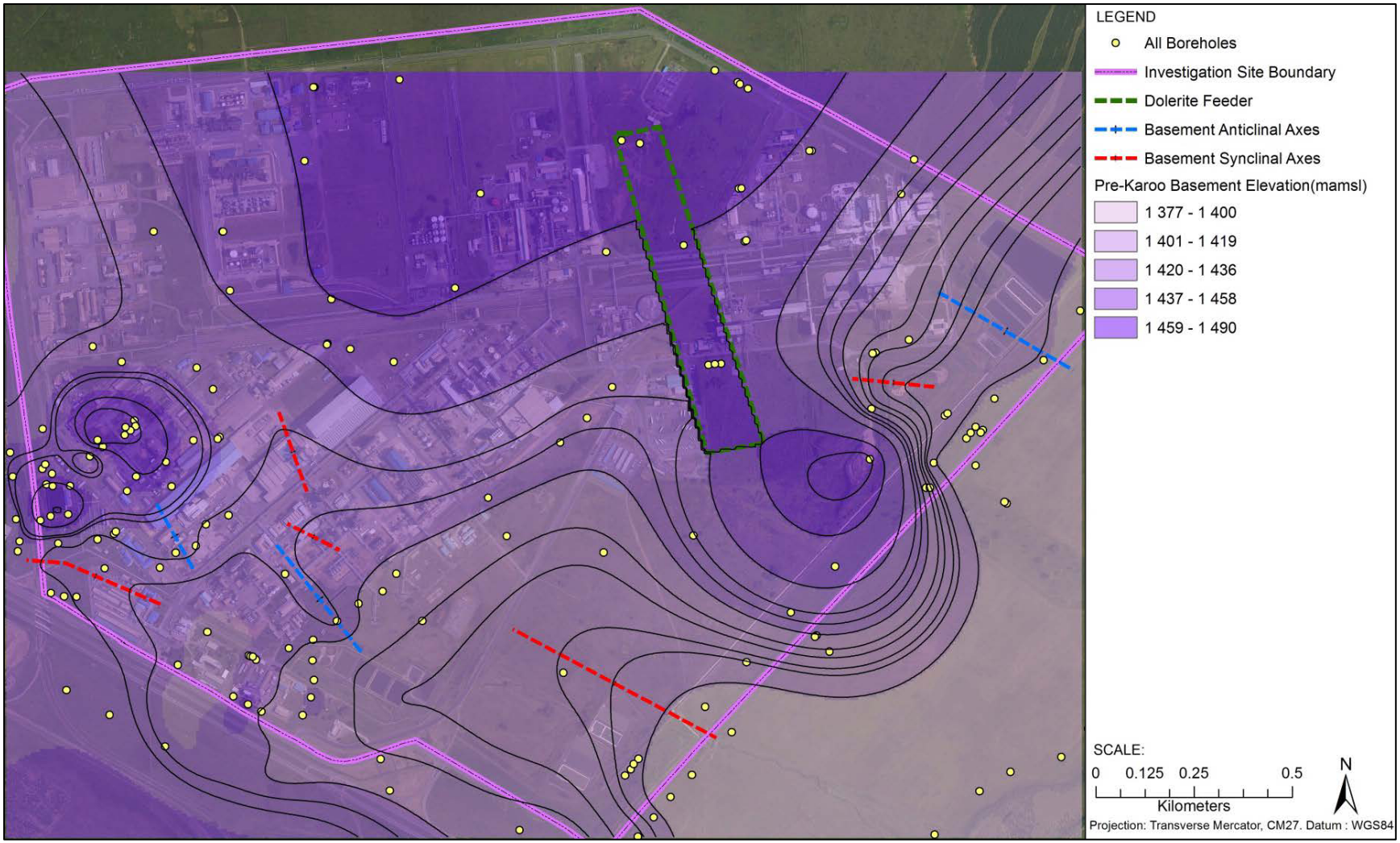

Figure 3-22: Pre-Karoo basement elevation

Table 3-7: Geotechnical results of samples retrieved from soil and bedrock cores

Borehole ID	Depth (mbgl)	Lithology	f_{OC} (%)	Dry bulk density (g/cm^3)	Rock density (g/cm^3)	Porosity (%)	Non - Capillary Pore space (%)	Vertical Permeability (Darcy)	Horizontal Permeability (Darcy)	Moisture Content (%)
BH 221	3.0-3.3	weathered sandstone	0.59	ND	ND	-	-	-	ND	
BH 221	4.3-4.5	residual sandstone	5.44	1.77	ND	-	-	6.02E-06	ND	19.8
BH 221	6.0-6.2	residual sandstone	6	1.647	ND	-	-	3.06E-06	ND	22
BH 221	9.0-9.2	weathered mudstone	9.41	1.548	ND	-	-	3.39E-06	ND	13.5
EDC2	0.55	residual dolerite	ND	1.636	ND	14.7 (Capillary Pore space)	21.9	1.26E-02	ND	10
BH 61	2.0-2.15	residual dolerite	5.3	1.798	ND	6.5(Capillary Pore space)	28.4	2.59E-03	ND	17.6
BH 61	2.8-3.0	residual dolerite	5.61	1.639	ND	-	-	3.21E-06	ND	21.4
BH 61	3.3-3.45	residual dolerite	6.62	1.624	ND	-	-	1.28E-05	ND	23.3
CAP 1	12-12.5	Weathered Dolerite	< 0.05	2.86	2.87	-	-	-	-	ND
CAP 1	22-22.5	Unweathered Dolerite	< 0.05	2.91	2.98	-	-	-	-	ND
SWD 1	20 - 20.5	Unweathered Dolerite	< 0.05	2.93	2.93	-	-	-	-	ND
SWD 1	35 - 35.5	Unweathered Ecca Sandstone	0.05	2.71	2.61	3.7	-	1.12E-02	1.60E-02	ND
SWD 1	76 - 76.5	Unweathered Basement Lava	< 0.05	2.78	2.79	-	-	-	-	ND

Where:

- : no measurable porosity/permeability

ND : not determined

3.3.3 Geohydrology

Multiple water strikes were encountered in the upper 0.5-7.5 meters at the site (Figure 3-15). Groundwater was typically encountered between 0.5 and 1.0 m bgl (Figure 3-23).

Typically, depth to groundwater is a function of surface elevation at the site (Figure 3-24). Pressure transducer data collected at the site indicate a seasonal response to groundwater elevation, with an increase noticed during the wet months and a decrease in groundwater elevation observed during dry months (Figure 3-25). The transducer data also indicates correlated groundwater elevation patterns within the weathered and unweathered portions of the dolerite sill.

Regional topographic data as well as a review of groundwater elevation data indicate the presence of a north-south trending hydrogeological basin divide at the site. Groundwater flows to the northeast in the northern portion of the site and from north west to south east in the southern portion (Figure 3-26). The hydraulic gradient is 0.01 in both flow directions.

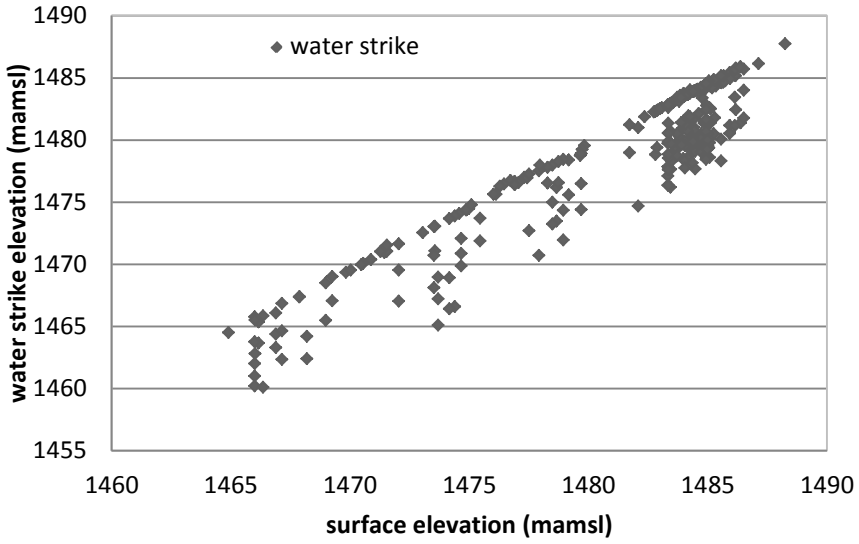

Figure 3-23: Water strike elevation as a function of surface elevation

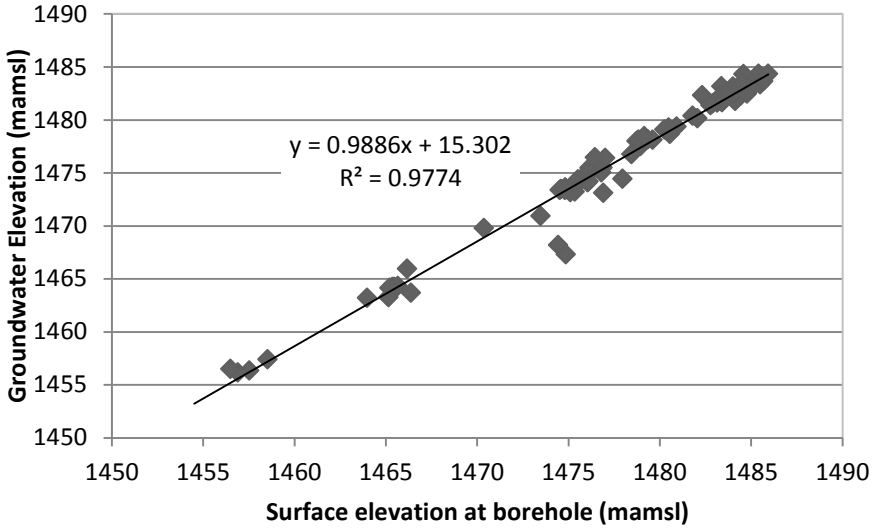

Figure 3-24: Groundwater elevation as a function of surface elevation at borehole

The following hydrostratigraphic units are identified at the site:

- *In situ clay and dolerite hydrostratigrahic unit:* This represents all groundwater present within the surface weathered (clays) and unweathered zone of the dolerite sill. Groundwater flow within the weathered portion is controlled by intragranular flow (controlled significantly through the thickness, spatial extent and continuity of sandy water-bearing units). Groundwater flow within the unweathered portion of the dolerite aquifer is within the fracture networks. Given the higher porosity of the weathered compared to the unweathered zones, groundwater is largely yielded from the weathered portion of the dolerite aquifer. The weathered and unweathered sections act as a single hydrogeologic unit, but the physical flow properties within the aquifer vary depending on the amount of weathering. This is a complex system of unconfined and semi confined units.
- *Karoo Ecca hydrostratigrahic unit:* The Karoo Ecca hydrostratigraphic unit is spatially representative across the far-field and near-field scale, but shows variability in its hydraulic properties. At the site, it is spatially continuous, except where intruded by the dolerite sill. This is a semi-confined unit. Groundwater strikes are commonly observed at the contact zone between the dolerite sill and the Karoo Ecca sedimentary rocks.
- *Pre-Karoo Basement hydrostratigraphic unit*: This hydrostratigraphic unit is represented by the andesitic basement lavas of the Ventersdorp. Static water levels measured for boreholes drilled within this aquifer indicated that it is a semi-confined unit.

Hydraulic conductivity results from packer testing and from ribbon NAPL samplers installation indicate variable hydraulic conductivity values for the dolerite and the Karoo Ecca hydrostratigraphic units (Table 3-8). Hydraulic conductivity results obtained from packer testing represent the bulk hydraulic conductivity for fractures and matrix over the length of the packer. Ribbon NAPL samplers were selectively installed in high transmissivity boreholes (Figure 3-27) and the measurement was depth discrete to regions of high ratios of fractures. Fractures in both the dolerite and the Karoo Ecca hydrostratigraphic units have high conductivities, with the hydraulic conductivity for the fractures within the Karoo Ecca unit ranging between 0.54 – 5.48 m/day and those for the dolerite aquifer ranging between 0.15 – 0.45 m/day. Bulk hydraulic conductivity for the Karoo Ecca hydrostratigraphic unit was calculated to be a maximum of 0.0078 m/day while the bulk hydraulic conductivities for the dolerite aquifer and the pre-Karoo basement aquifer was determined to be <0.0 m/day in all cases using the Packer testing methodology (Table 3-8). Analysis of vertical gradients between the shallow overburden boreholes and the weathered bedrock boreholes and between the weathered bedrock boreholes and competent bedrock boreholes were inconclusive. Vertical gradients across the site were not consistently upward or downward oriented (Figure 3-26). Calculated gradients ranged between 0 – 0.06 meters per meter indicating that vertical groundwater flow is not a significant component of the overall site hydrogeology.

The results from gauging of the intermittent stream boreholes /piezometers (Figure 3-8), taken during the dry season, are provided in Table 3-9. The intermittent streams located to the north as well as to the south of the site show portions where they are losing streams and portions where they are gaining streams. Generally, it appears that groundwater discharges to the intermittent stream located to the north, while surface water recharges groundwater in the intermittent stream located to the south of the site.

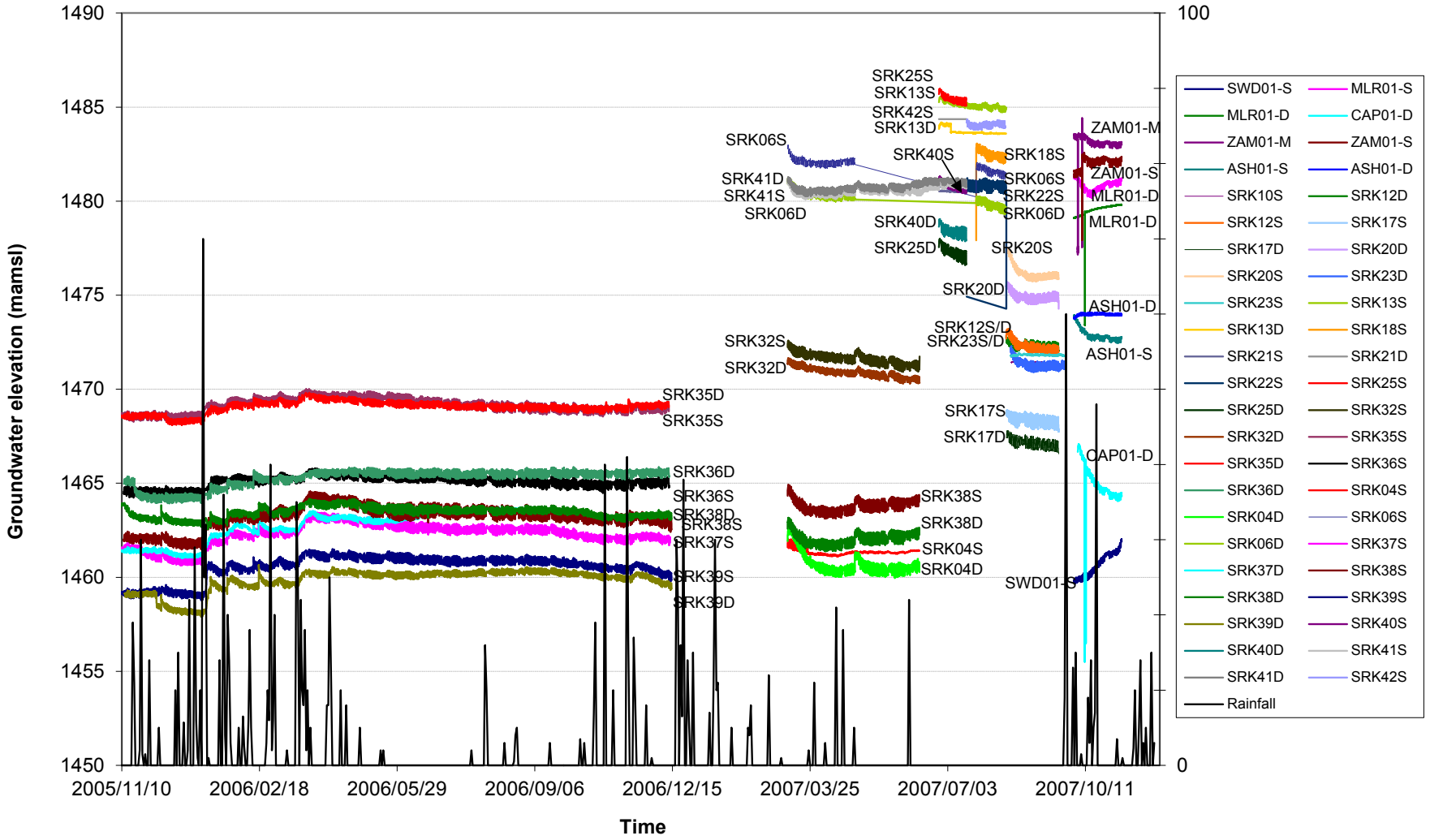

Figure 3-25: Pressure transducer data for selected boreholes at the site (results from ERM, 2008)

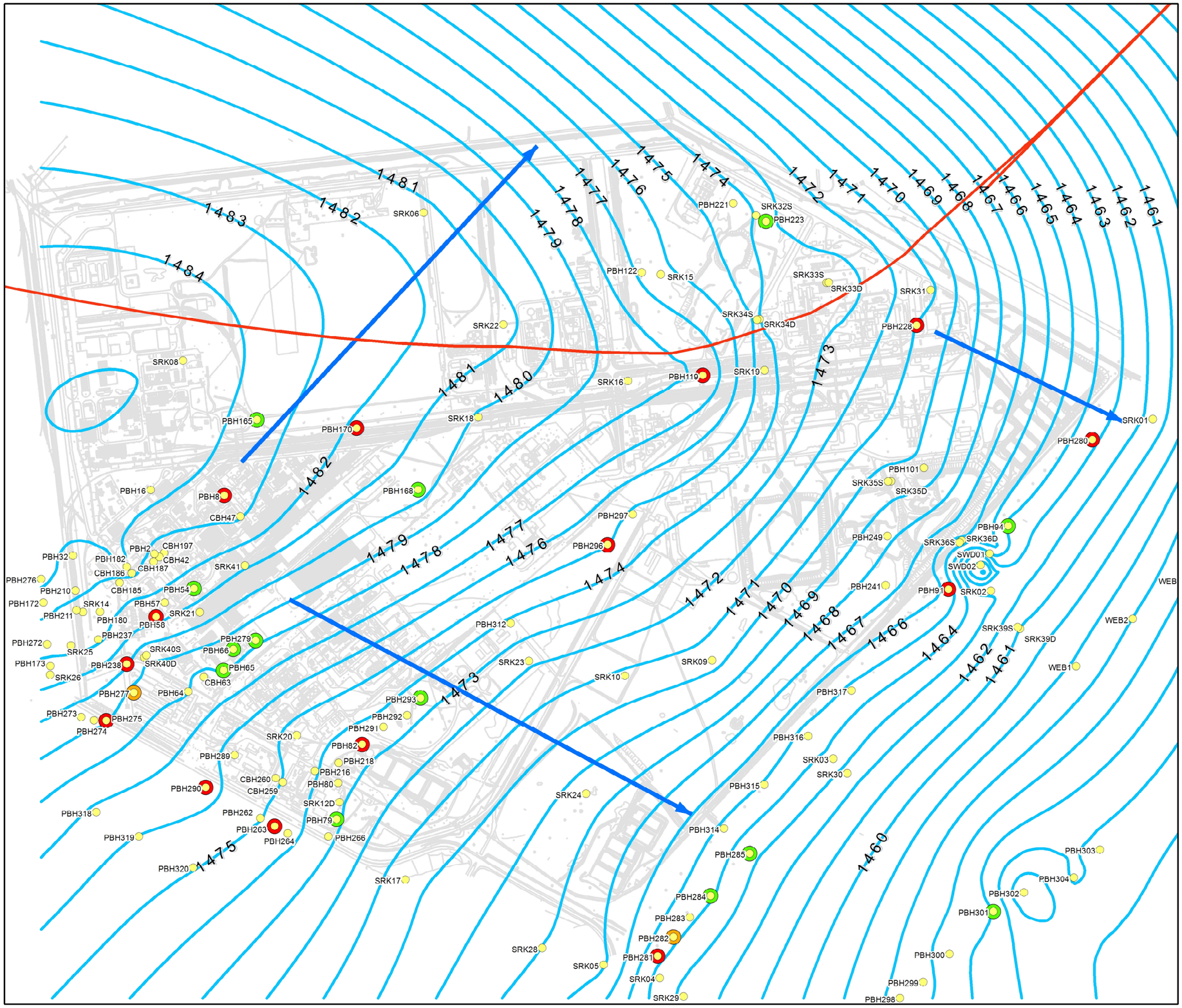

Figure 3-26 : Groundwater flow direction and hydraulic gradient (results from SRK, 2001; ERM, 2008; ERM, 2012)

Figure 3-27: Relative transmissivities of boreholes (results from ERM, 2012)

Table 3-8: Hydraulic conductivity values for the dolerite, Karoo Ecca and pre-Karoo basement aquifers

Borehole ID	Depth zone (m bgl)	Aquifer Type	K (cm/sec)	Methodology to determine K
CBH42	9.14-12.19	dolerite	5.90E-4	Ribbon NAPL sampler
CBH42	12.19-15.24	dolerite	5.21E-4	Ribbon NAPL sampler
PBH221	15.24-18.23	Karoo Ecca	1.48E-3	Ribbon NAPL sampler
PBH222	18.23-21.34	Karoo Ecca	5.67E-4	Ribbon NAPL sampler
PBH223	27.43-30.48	Karoo Ecca	6.34E-3	Ribbon NAPL sampler
PBH228	15.0-18.23	dolerite	1.74E-4	Ribbon NAPL sampler
PBH229	18.23-21.34	dolerite	3.13E-4	Ribbon NAPL sampler
PBH230	21.34-24.48	Karoo Ecca	1.22E-3	Ribbon NAPL sampler
PBH231	24.38-27.43	Karoo Ecca	6.25E-4	Ribbon NAPL sampler
SWD01	10.0-18.0	dolerite	<0.00	packer
SWD01	18.0-25.0	dolerite	<0.00	packer
SWD01	25.0-32.5	dolerite	<0.00	packer
SWD01	32.5-37.0	Karoo Ecca	<0.00	packer
SWD01	37.5-45.0	Karoo Ecca	<0.00	packer
SWD01	45.0-52.0	Karoo Ecca	9.03E-6	packer
SWD01	52.0-59.0	Karoo Ecca	3.01E-6	packer
SWD01	59.0-65.0	Karoo Ecca	<0.00	packer
SWD01	65.0-72.0	Pre-Karoo Basement	<0.00	packer
SWD02	14.0-22.0	dolerite	<0.00	packer
SWD02	22.0-29.0	dolerite	<0.00	packer
SWD02	29.0-33.5	dolerite	<0.00	packer
SWD02	33.5-38.0	Karoo Ecca	<0.00	packer
SWD02	38.0-46.0	Karoo Ecca	<0.00	packer
SWD02	46.0-54.0	Karoo Ecca	<0.00	packer
SWD02	54.0-62.0	Karoo Ecca	<0.00	packer
SWD02	62.0-81.38	Pre-Karoo Basement	<0.00	packer
CAP01	15.0-23.0	dolerite	<0.00	packer
CAP01	23.0-31.0	dolerite	<0.00	packer
CAP01	31.0-39.0	Dolerite/Karoo Ecca Chill margin	<0.00	packer
CAP01	39.0-47.0	Karoo Ecca	1.97E-6	packer
CAP01	47.0-55.0	Karoo Ecca	<0.00	packer
CAP01	55.0-62.0	Karoo Ecca	<0.00	packer
CAP01	62.0-69.0	Pre-Karoo Basement	<0.00	packer
CAP01	69.0-90.38	Pre-Karoo Basement	<0.00	packer

Table 3-9: Groundwater vs surface water elevation for the stream boreholes/piezometers

Borehole ID	Depth to groundwater (m bgl)	Groundwater elevation (mamsl, GW)	Co-located Surface water elevation (mamsl, SW)	Δ (GW-SW)	Losing/Gaining stream
PBH 298-6	1.26	1457.614	1457.786	-0.172	losing
PBH299-6	1.11	1457.407	1458.035	-0.628	losing
PBH299-25	1.11	1457.407	1458.035	-0.628	losing
PBH300-6	1.18	1456.347	1456.780	-0.433	losing
PBH301-6	1.00	1455.893	1456.191	-0.298	losing
PBH301-25	0.74	1456.153	1456.191	-0.038	losing
PBH302-6	4.50	1452.859	1455.958	-3.099	losing
PBH303-6	1.09	1454.710	1454.525	0.185	gaining
PBH304-6	1.26	1455.237	1454.931	0.306	gaining
PBH307-6	1.45	1457.220	1454.024	3.196	gaining
PBH308-6	1.94	1456.308	1453.476	2.832	gaining
PBH308-25	1.71	1456.338	1453.476	2.862	gaining
PBH309-6	1.05	1455.090	1452.798	2.292	gaining
PBH310-6	0.17	1452.900	1451.611	1.289	gaining
PBH310-25	0.23	1453.120	1451.611	1.509	gaining
PBH311-6	1.39	1451.585	1449.880	1.705	gaining
SMPA11	2.00	1456.83	1457.93	-1.101	losing
SMPA13	0.96	1457.99	1458.25	-0.260	losing
SMPA14	0.98	1456.98	1457.19	-0.206	losing
SMPA15	0.96	1456.39	1456.38	0.011	gaining
SMPA16	0.73	1456.00	1455.99	0.006	gaining
SMPA17	1.10	1455.81	1455.85	-0.037	losing
SMPA18	0.86	1455.03	1455.02	0.009	gaining

SMPA19	0.98	1454.65	1454.46	0.189	gaining
SMPA21	1.51	1454.01	1453.94	0.077	gaining
SMPA22	1.27	1453.73	1453.69	0.043	gaining
SMPA23	1.06	1453.37	1453.49	-0.116	losing
SMPA24	1.15	1453.22	1453.33	-0.110	losing
SMPA25	1.14	1452.69	1452.89	-0.195	losing
SMPA26	1.31	1451.97	1452.39	-0.424	losing
SMPA27	1.61	1451.06	1451.19	-0.127	losing
SMPA28	1.27	1450.21	1450.34	-0.131	losing
SMPA29	1.55	1449.94	1450.31	-0.371	losing
SMPA30	1.63	1449.52	1450.02	-0.494	losing
SMPA31	1.29	1448.67	1448.63	0.044	gaining
SMPB03	3.51	1454.56	1454.33	0.230	gaining
SMPB04	3.29	1453.61	1453.60	0.011	gaining
SMPB05	2.54	1453.34	1452.90	0.446	gaining
SMPB06	1.29	1453.21	1451.96	1.250	gaining
SMPB07	1.79	1451.24	1451.33	-0.093	losing
SMPB08	1.48	1450.50	1449.30	1.199	gaining
SMPB09	1.74	1449.13	1448.34	0.791	gaining
SMPB10	1.17	1448.80	1447.71	1.093	gaining
SMPB11	1.39	1447.52	1447.71	-0.188	losing
SMPB12	1.12	1446.65	1447.22	-0.568	losing

3.3.4 DNAPL source zones delineation

Local geological and geohydrological characteristics of the source zone are provided in Sections 3.3.2. and 3.3.3. respectively. This section focusses on identifying the source zone characteristics in terms of release areas, DNAPL distribution in the weathered zone and DNAPL characteristics/architecture in the fractured bedrock zone.

3.3.4.1 Weathered source zone delineation

2-D resistivity anomalies, representing areas of low resistivity (high conductivity) and potentially DNAPL source areas or contaminated groundwater, were identified in the weathered and fractured bedrock zones (Figure 3-28). These areas mark sharp contrasts to the resistivity in the surrounding rocks and cannot be explained through their lithological characteristics. The locations of these anomalies correspond to historical release areas identified through collection of historical data.

Results from the passive soil-gas are provided in Appendix C. Frequency distribution histograms of the grouped chlorinated hydrocarbon DNAPLs are shown in Figure 3-29. All distributions are skewed to the left of the distribution curves. Results indicate that PCE and $CHCl_3$ are the most prevalent chlorinated hydrocarbons, observed in 77% and 62% respectively of the samples analysed (Figure 3-30). TCE and CCl_4 were detected at 25% of sample locations. The isomers 1,1-DCE, cis-1,2-DCE, and trans-1,2-DCE were detected in 7 to 12% of the sample locations. Vinyl chloride was only encountered in 4% of sample locations. The majority of the samples analysed (439 of 460 samples) have chlorinated ethene concentrations ≤ 100 µg (absorbed mass). The remaining sample concentrations (absorbed mass) for chlorinated ethenes ranged between 100 and 800 µg. The result from a single location was high for the chlorinated ethanes, with the rest of the localities (459 out of 460) having concentrations ≤ 100 µg (absorbed mass). Absorbed mass concentrations for chlorinated benzenes and chlorinated methanes were low with 99.9% of the samples showing concentrations of ≤ 100 µg (absorbed mass). The maximum concentration detected for the chlorinated benzenes was 6.51 µg. The concentration of absorbed gaseous mass from one sample location was between 100 and 200 µg for chlorinated methanes.

The spatial variability of the grouped targeted hydrocarbons can be characterised by the calculation of the coefficient of variation (Table 3-10). The coefficient of variation is a normalized measure of variability that is independent of the measurement scale and can thus be used to compare data sets. The chlorinated benzenes and the chlorinated ethanes showed a higher amount of spatial variability than the other grouped hydrocarbons (i.e. TPH, chlorinated ethenes and the chlorinated methanes). Only trace levels of chlorinated benzenes are found at the site.

The spatial distribution, using inverse distance weighting (IDW), of chlorinated ethenes with concentrations greater than 72 µg (absorbed mass) is shown in Figure 3-31. The chlorinated ethenes are predominantly located close to the waste sites and the historical organics plant. In contrast the spatial distribution of the chlorinated ethanes (predominantly consisting of 1,2-DCA), using the inverse distance weighting method (IDW), shows an inferred release point is adjacent to the effluent dams on the southern part of the Investigation Site (Figure 3-32). This anomaly is likely to be a false positive and is attribute to the spills that occurred during the bailing of free phase DNAPL (composition 1,2-DCA and VC) from that locality (EDC 1) in 2007. The spatial distribution of chlorinated methane is shown in Figure 3-33. Chlorinated vapours occur at smaller concentrations of absorbed mass and are found in the historical production and handling facility 1.

The soil-gas vapours of chlorinated hydrocarbon DNAPLs in the unsaturated zone are spatially distributed at the historical production and handling facilities and the redundant hazardous waste sites. Based on the results obtained from the passive soil vapour analysis and the 2-D resistivity anomalies, release areas are inferred at the hazardous waste sites and the historical plant area (Figure 3-34).

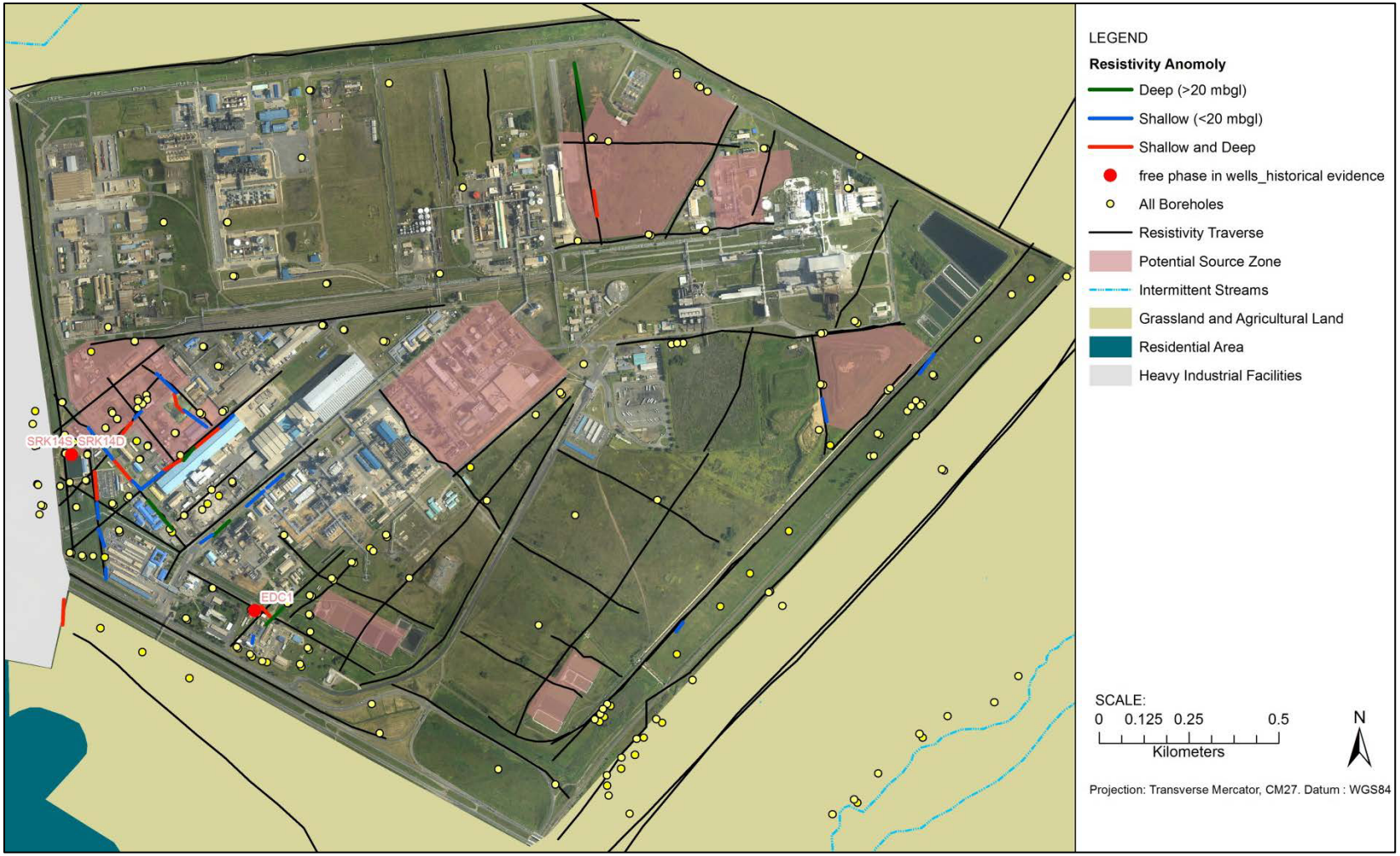

Figure 3-28: 2-D resistivity anomalies detected at the Investigation Site (Results from ERM, 2008; ERM 2012)

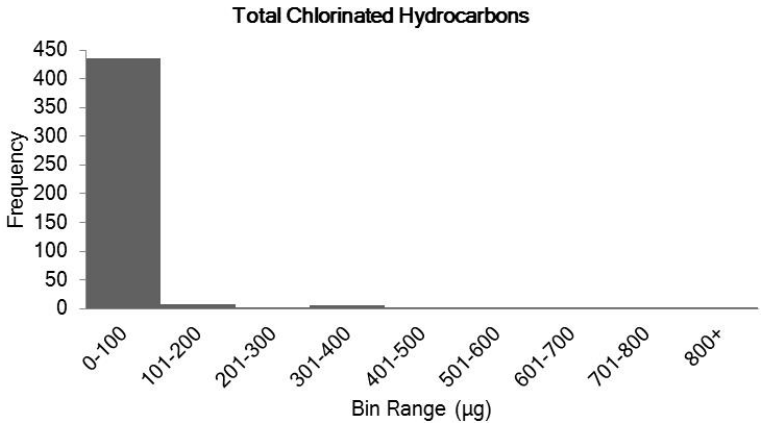
Total Chlorinated Hydrocarbons
Frequency
450
400
350
300
250
200
150
100
50
0
0-100
101-200
201-300
301-400
401-500
501-600
601-700
701-800
800+
Bin Range (µg)

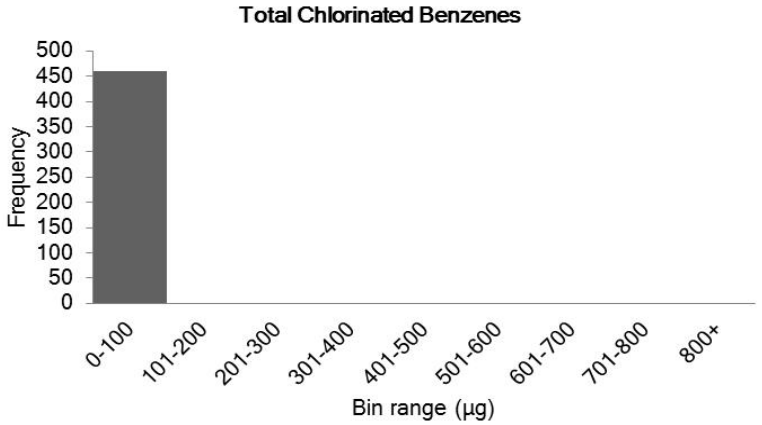
Total Chlorinated Benzenes
Frequency
500
450
400
350
300
250
200
150
100
50
0
0-100
101-200
201-300
301-400
401-500
501-600
601-700
701-800
800+
Bin range (µg)

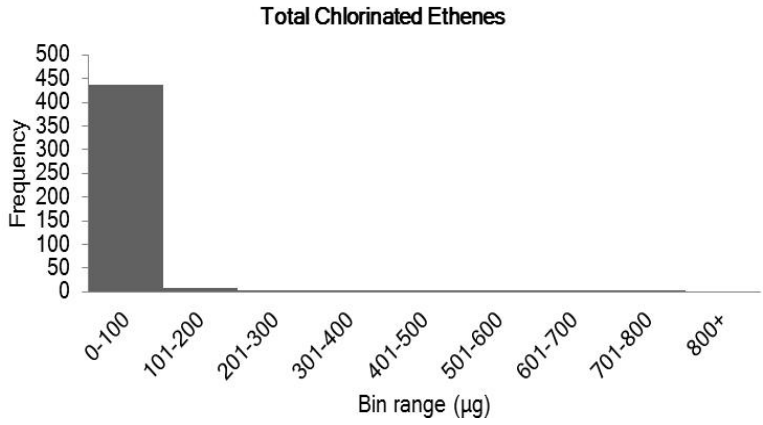
Total Chlorinated Ethenes
Frequency
500
450
400
350
300
250
200
150
100
50
0
0-100
101-200
201-300
301-400
401-500
501-600
601-700
701-800
800+
Bin range (µg)

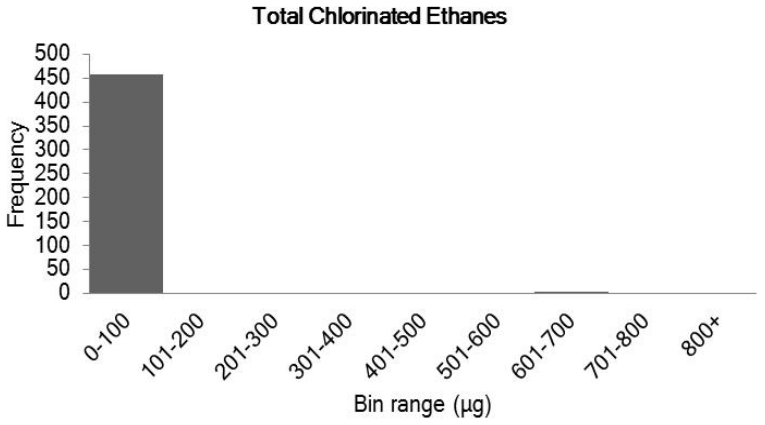
Total Chlorinated Ethanes
Frequency
500
450
400
350
300
250
200
150
100
50
0
0-100
101-200
201-300
301-400
401-500
501-600
601-700
701-800
800+
Bin range (µg)

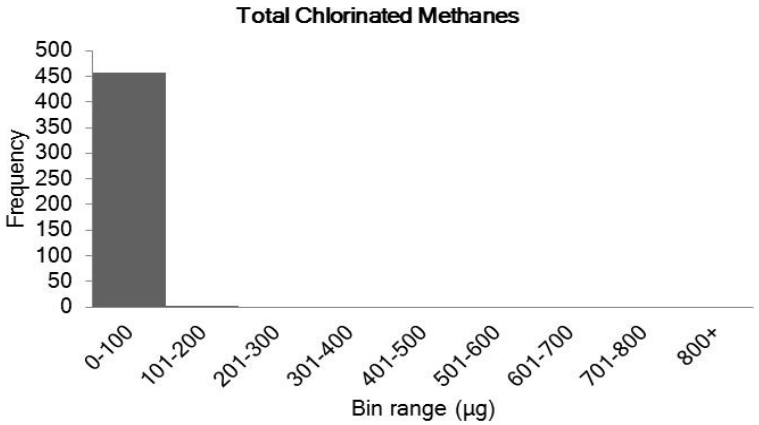

Figure 3-29: Frequency distribution histograms of grouped chlorinated hydrocarbon compounds found at the Investigation Site

Where:
Total chlorinated hydrocarbons = total chlorinated benzenes + total chlorinated ethenes + total chlorinated ethenes + total chlorinated ethanes + total chlorinated methanes
Total Chlorinated Benzenes (ClBENZ) = 1,2-dichlorobenzene + 1,3-dichlorobenzene + 1,4-dichlorobenzene + chlorobenzene
Total Chlorinated Ethenes (ClEthenes) = tetrachlorethene + trichloroethene + cis-1,2-dichloroethene + trans-1,2-dichloroethene + 1,1-dichloroethene + vinyl chloride
Total Chlorinated Ethanes (ClEthanes) =1,1,1-trichloroethane + 1,1,1,2-tetrachloroethane + 1,1,2,2-tetrachloroethane + 1,1,2-trichloroethane + 1,1-dichloroethane +1,2-dichloroethane
Total Chlorinated Methanes (ClMethanes) = carbon tetrachloride + chloroform

Table 3-10: Descriptive statistics for grouped chlorinated hydrocarbon compounds found at the Investigation Site

	ClBENZ	ClEthenes	ClEthanes	ClMethanes
Count	460.00	460.00	460.00	460.00
Minimum (µg)	0.01	0.08	0.05	0.02
Maximum (µg)	6.51	705.17	609.78	119.54
Range (µg)	6.50	705.09	609.73	119.52
Mean (µg)	0.03	17.53	2.01	1.51
Standard Deviation (µg)	0.30	73.96	28.75	8.55
Standard Error	0.01	3.45	1.34	0.40
Coefficient of Variation	12.03	4.22	14.28	5.67
Median (µg)	0.01	0.25	0.06	0.05
Mode (µg)	0.01	0.10	0.06	0.02
Confidence Level (95.0%)	0.03	6.78	2.63	0.78

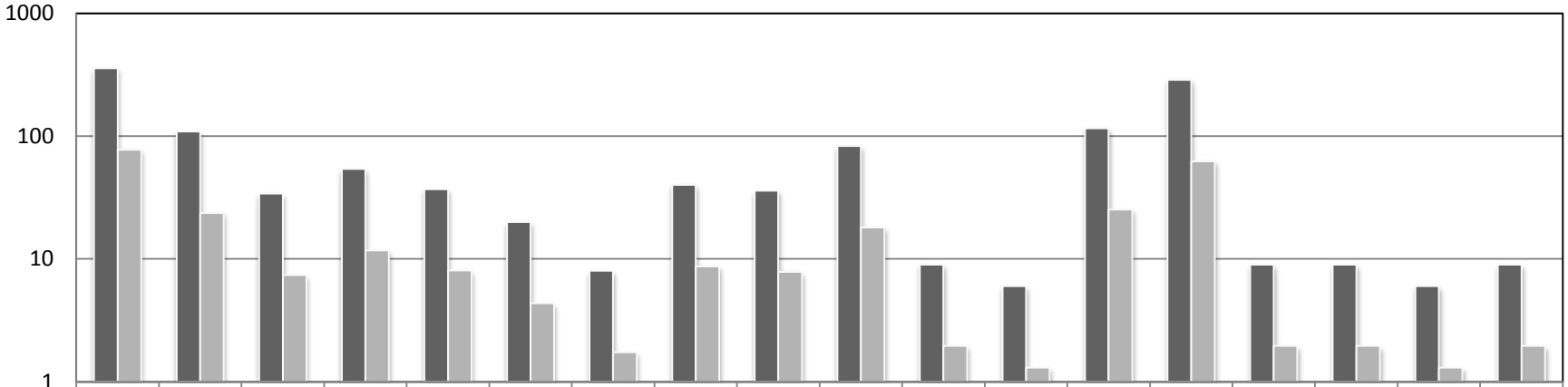

	PCE	TCE	11DCE	c12DCE	t12DCE	VC	111TCA	112TCA	11DCA	12DCA	1112TetCA	1122TetCA	CC14	CHC13	CIBENZ	12DCB	113DCB	14DCB
n	356	109	34	54	37	20	8	40	36	83	9	6	116	287	9	9	6	9
%	77	24	7	12	8	4	2	9	8	18	2	1	25	62	2	2	1	2

Figure 3-30: Target chlorinated hydrocarbon compounds detected during the passive soil gas survey

Where:

n = number of detections,

% = percentage of detections compared to the number of samples

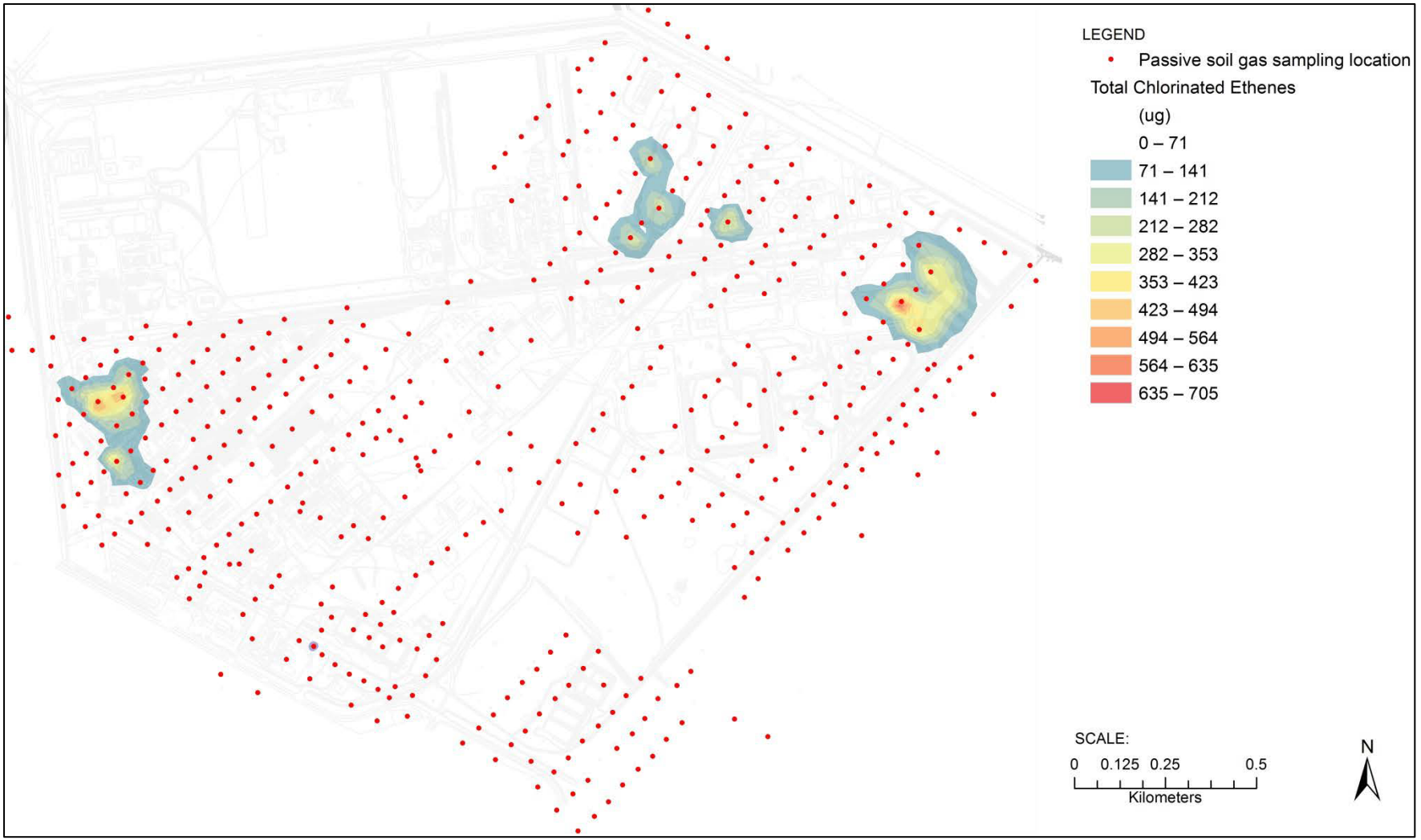

Figure 3-31: Spatial distribution of chlorinated ethene vapours at the Investigation Site (results from ERM, 2010)

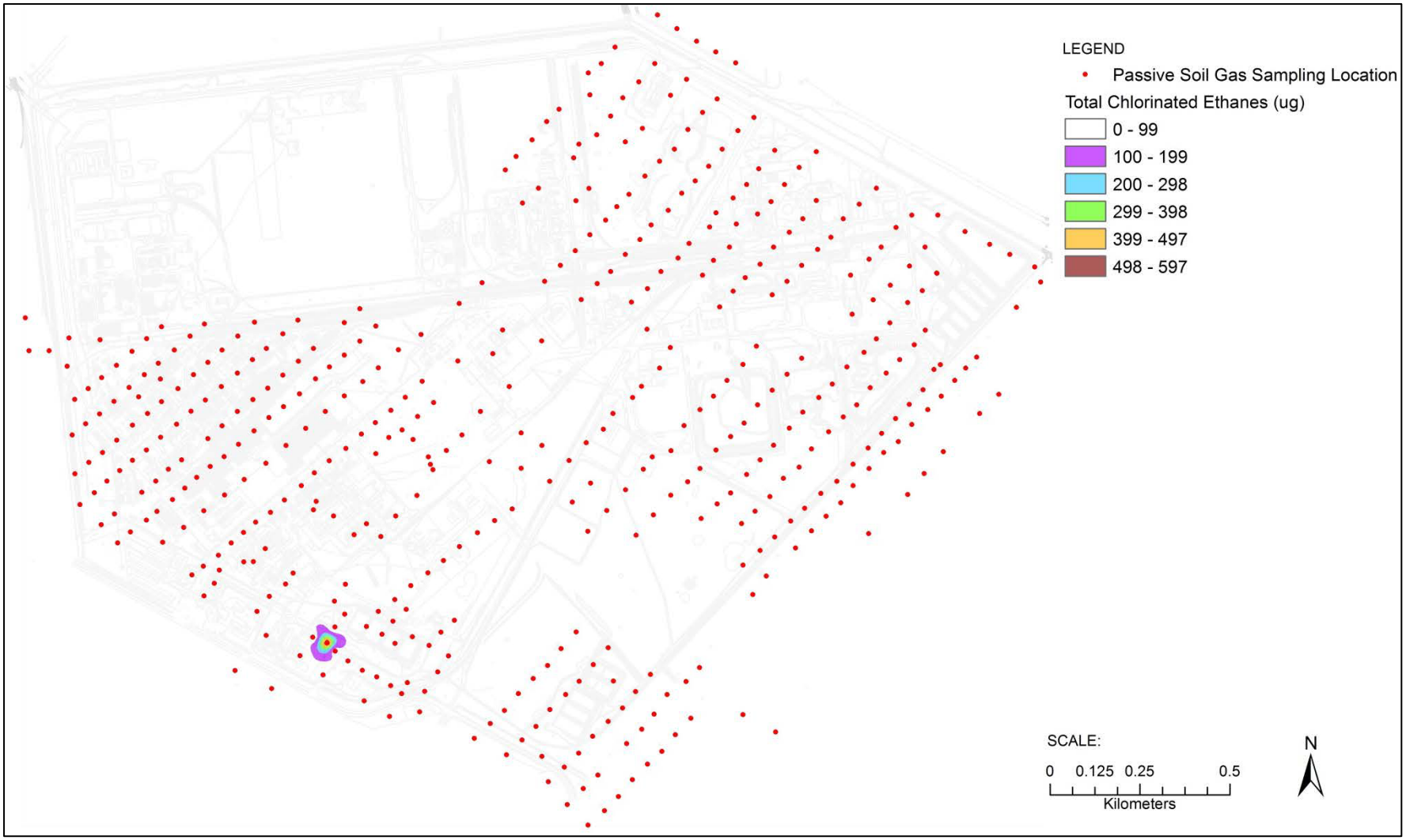

Figure 3-32: Spatial distribution of chlorinated ethane vapours at the Investigation Site (results from ERM, 2010)

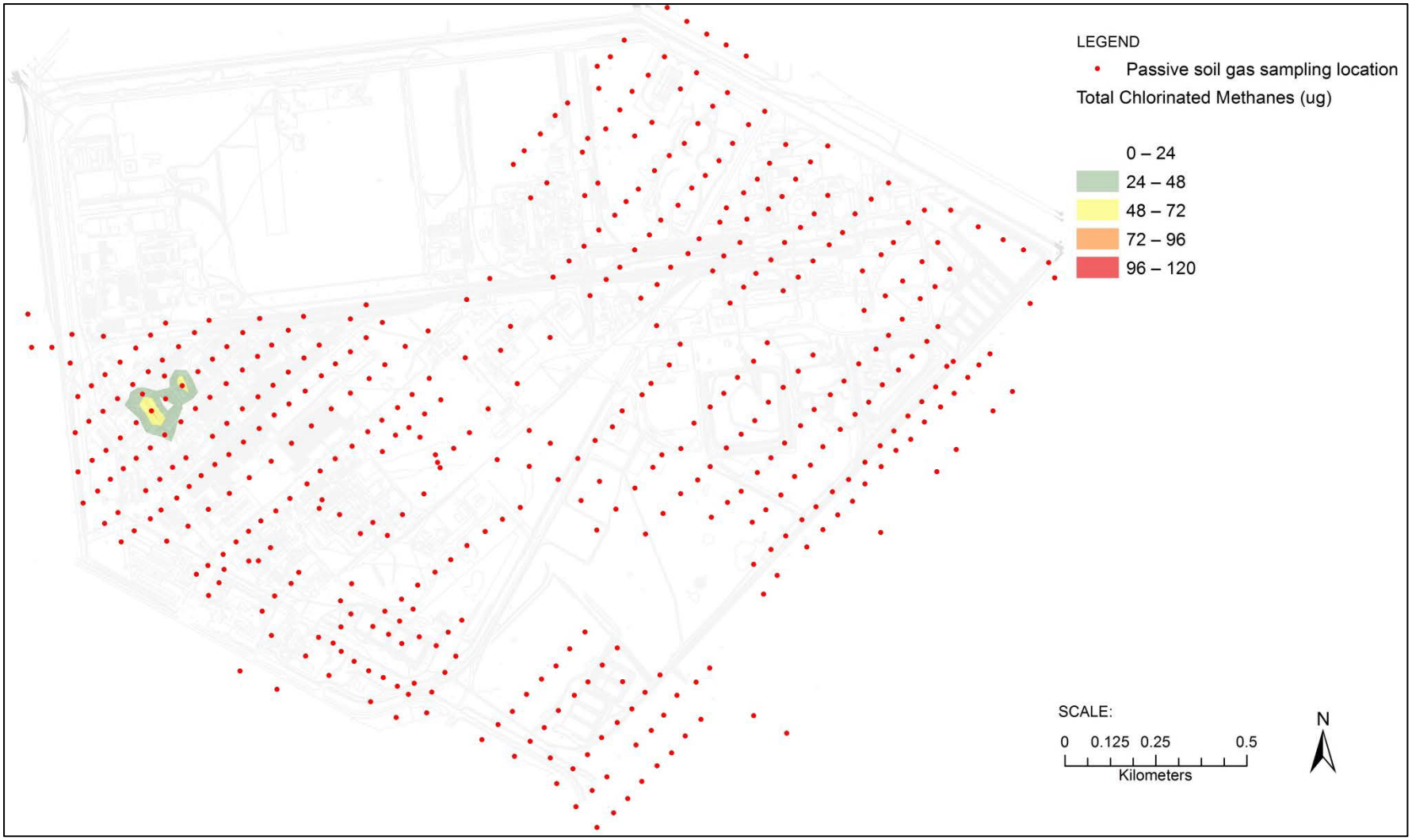

Figure 3-33: Spatial distribution of chlorinated methane vapours at the Investigation Site (results from ERM, 2010)

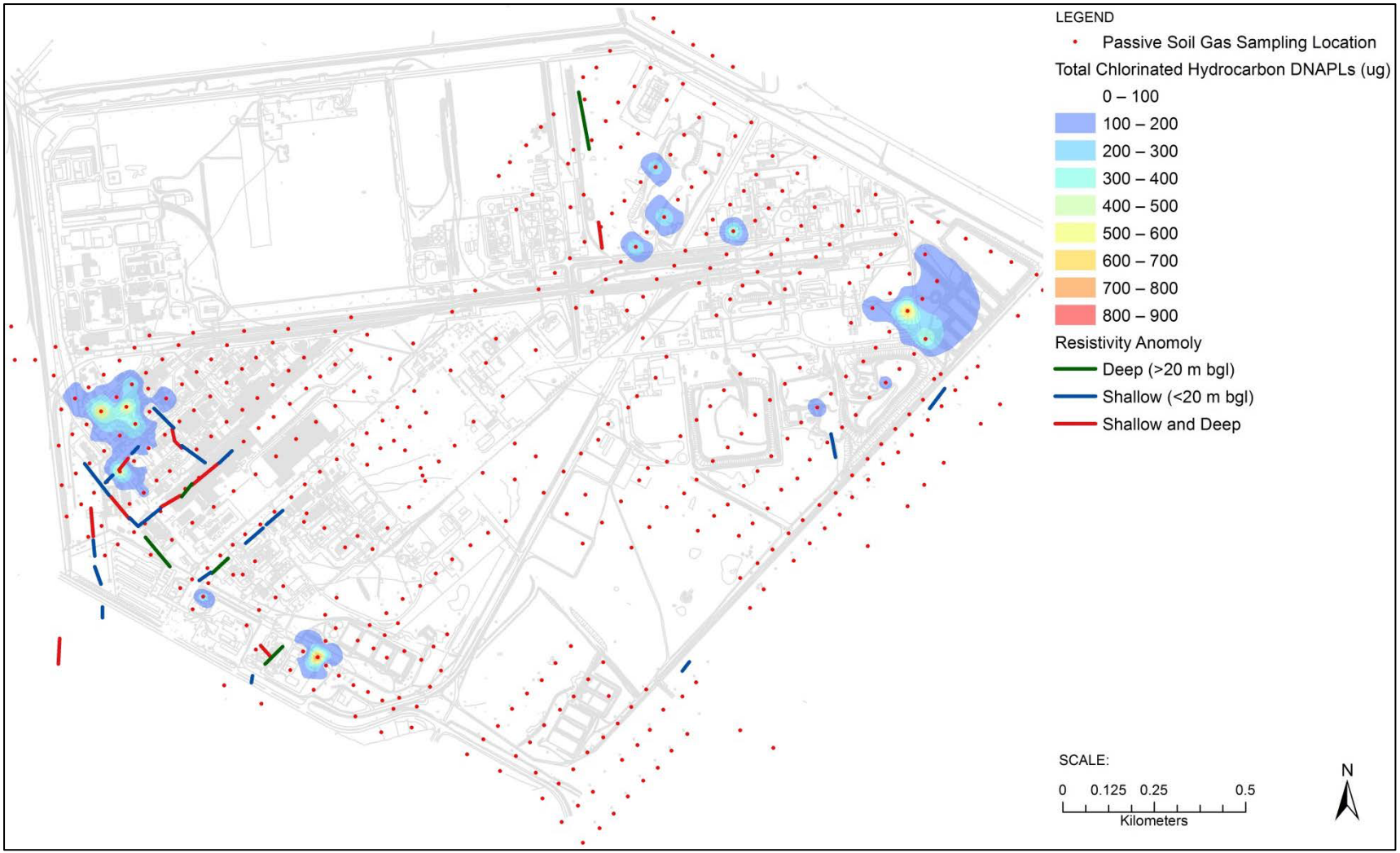

Figure 3-34: Inferred chlorinated hydrocarbon DNAPL release areas (results from ERM, 2010)

Chlorinated hydrocarbon results obtained from the analysis of soil samples are provided in Appendix D. The results obtained indicate large vertical and horizontal heterogeneities. Horizontal spatial distributions of total chlorinated hydrocarbons are shown in Figure 3-35. Chlorinated hydrocarbons are spatially located below their release area (Figure 3-36). The compositions mimic the types of products that were handled at these release areas. It is not possible to distinguish transformation products from parent products from the results obtained as a result of the vast array of chlorinated hydrocarbon raw materials, intermediates and products handled at the site. Maximum total concentrations were detected between 0.5 to 3 m bgl. Figure 3-37 shows the 3-D architecture of the grouped chlorinated hydrocarbon DNAPLs within the weathered zone. 3-D solid models of individual chlorinated hydrocarbon DNAPL compounds are provided in Appendix D. The frequency distribution of the chlorinated hydrocarbon DNAPLs are skew to the left (Appendix D). The solid models maximum concentrations were filtered by excluding outliers. Chlorinated benzenes are not very prevalent in the weathered profile. Chlorinated ethanes and ethenes dominate the total chlorinated hydrocarbon concentrations. Chlorinated ethenes and ethanes are prevalent at the redundant hazardous waste sites as well as at the historical production and handling facilities.

Monte Carlo simulations (Appendix E) were undertaken to determine the soil chlorinated hydrocarbon threshold concentrations. These minimum and maximum concentrations obtained for the predominant chlorinated hydrocarbon DNAPLs are provided in Table 3-11 below. Based on the minimum threshold values, nine boreholes are inferred to contain residual phase DNAPL: BH2, BH39, BH187, BH189, BH190, BH193, BH196, BH197, BH198. Oil Red O® tests were positive for the following sonic holes: BH02 at 0.5 mbgl, BH03 at 0.5 m bgl, BH177 at 0.3 m bgl, BH181 at 0.5 m bgl, BH187 at 3.5 m bgl, BH189 at 0.5 m bgl, BH190 at 0.5 m bgl, BH196 at 0.5 m bgl and BH197 at 0.5 m bgl.

The results indicate that the primary source zone for chlorinated hydrocarbons as free phase and residual DNAPL in soils is located in the shallow soils beneath the redundant production and handling facilities. These high concentrations are related to direct releases to surface over a long period of time.

A sharp decrease in concentrations occurs with distance from the areas of direct release. Very low levels of chlorinated hydrocarbon DNAPL is present at the

redundant waste sites and the southern effluent dams. No free phase DNAPL was visible or can be inferred from the results obtained for these areas.

The DNAPL source zone at the redundant production and handling facilities in the weathered zone is inferred based on the multiple lines of evidence (Figure 3-38).

Table 3-11: Calculated soil chlorinated hydrocarbon concentration threshold minimum and maximum values for the Investigation Site

Chlorinated Hydrocarbon	Minimum C_i^T (mg/kg)	Maximum C_i^T (mg/kg)
Chlorinated Ethenes		
PCE	480	1 600
TCE	1 500	6 000
Cis-1,2-DCE	6 000	19 500
trans-1,2-DCE	4 000	14 000
VC	6 000	16 500
Chlorinated Ethanes		
1,1,1-TCA	1 400	4 500
1,1-DCA	4 000	12 500
1,1-DCA	2 000	6 500
1,1,2-TCA	6 000	21 000
1,2-DCA	8 000	25 500
Chlorinated Methanes		
CCl_4	950	3 000
$CHCl_3$	6 000	19 500
Chlorobenzenes		
1,2-DCB	1 200	4 500
1,3-DCB	400	1 400
1,4-DCB	650	2 500
ClBenz	2 500	9 000

Figure 3-35: Soil total chlorinated hydrocarbons concentrations, spatial distribution and composition at the Investigation Site (results from ERM 2012)

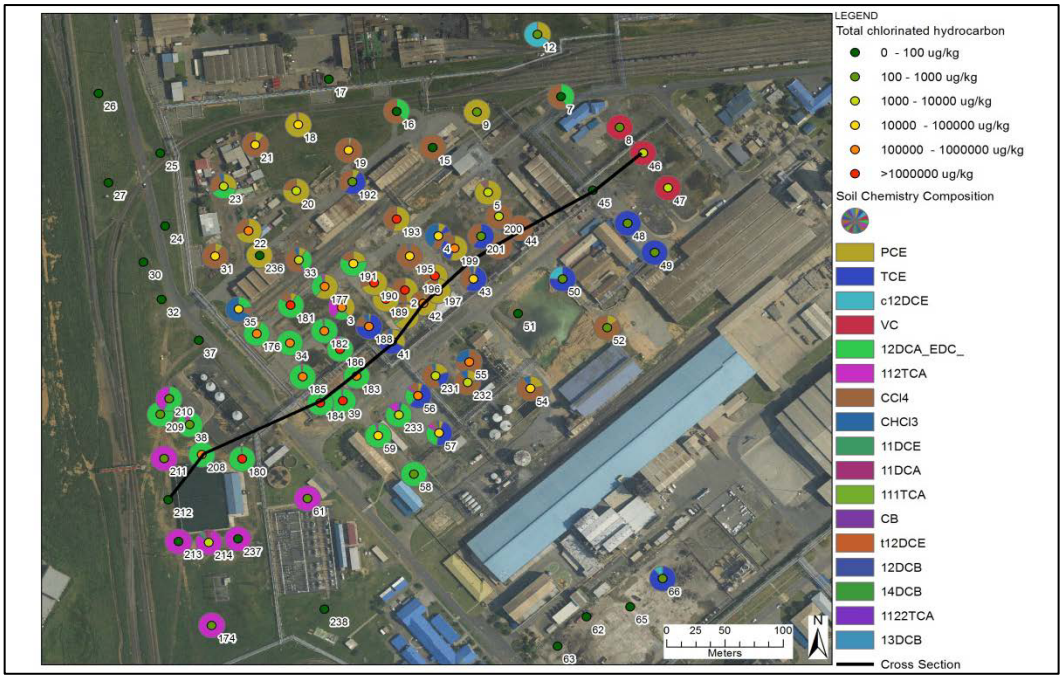

i. 1,2-DCA distribution

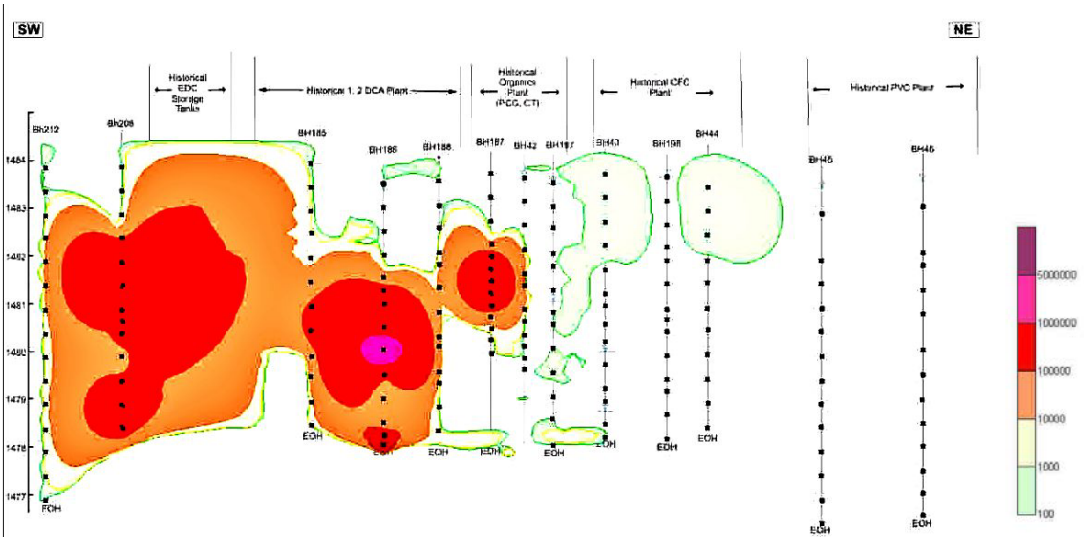

ii. 1,1,2-TCA distribution

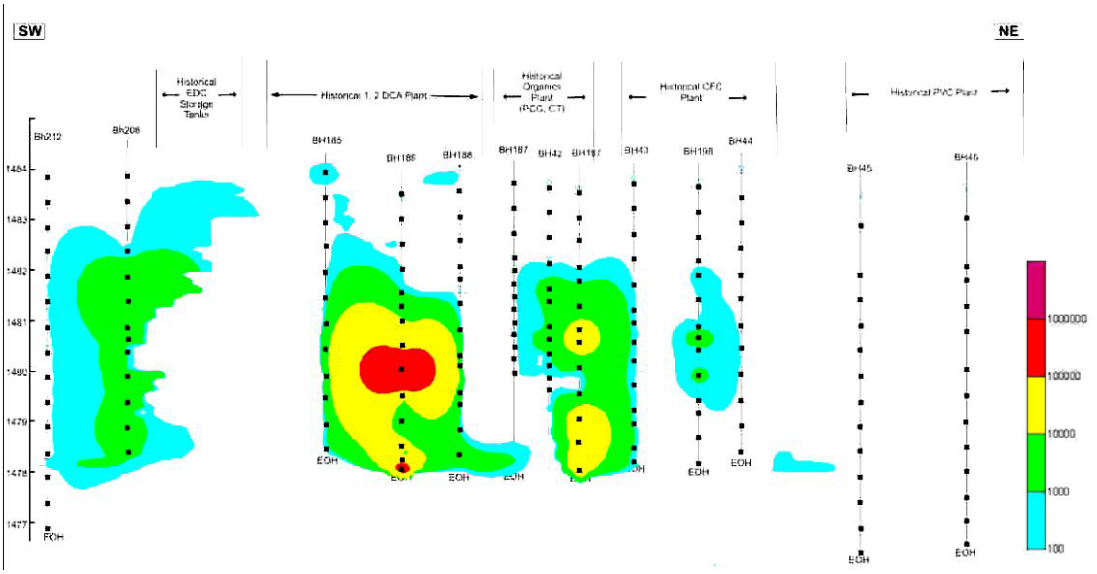

iii. PCE distribution

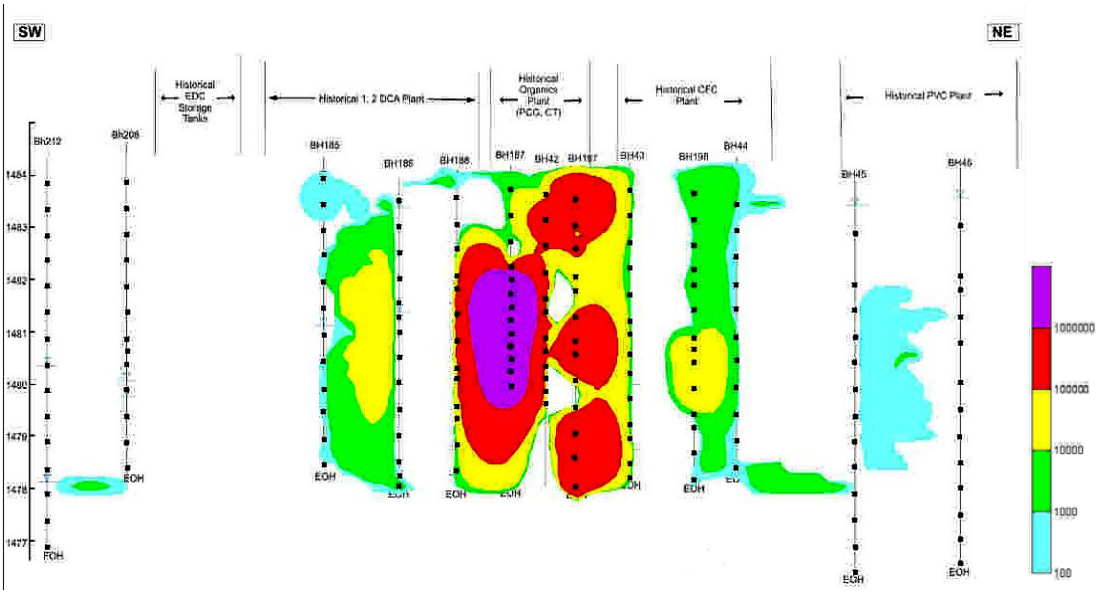

iv. TCE distribution

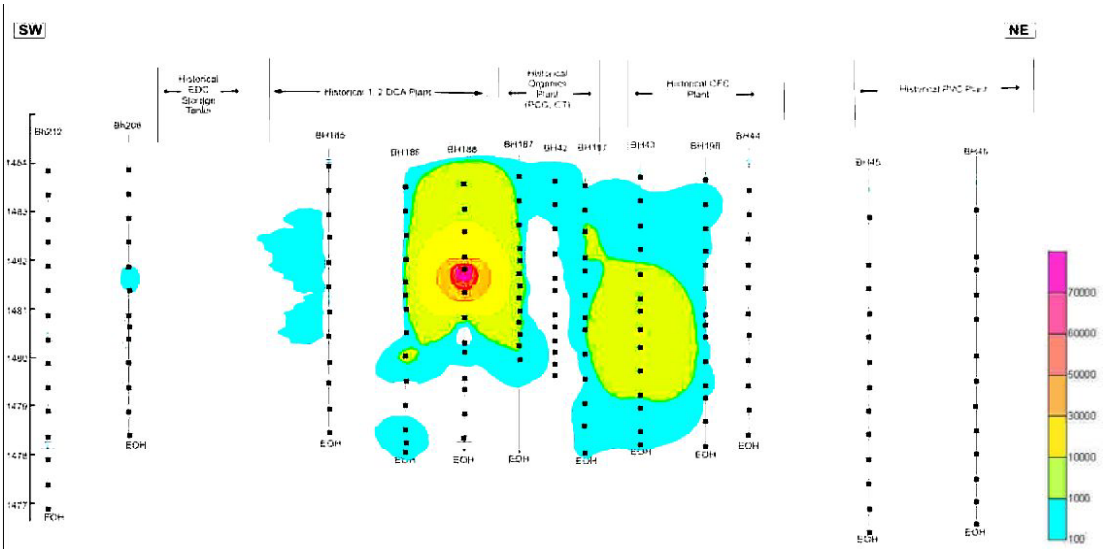

v. $CHCl_3$ Distribution

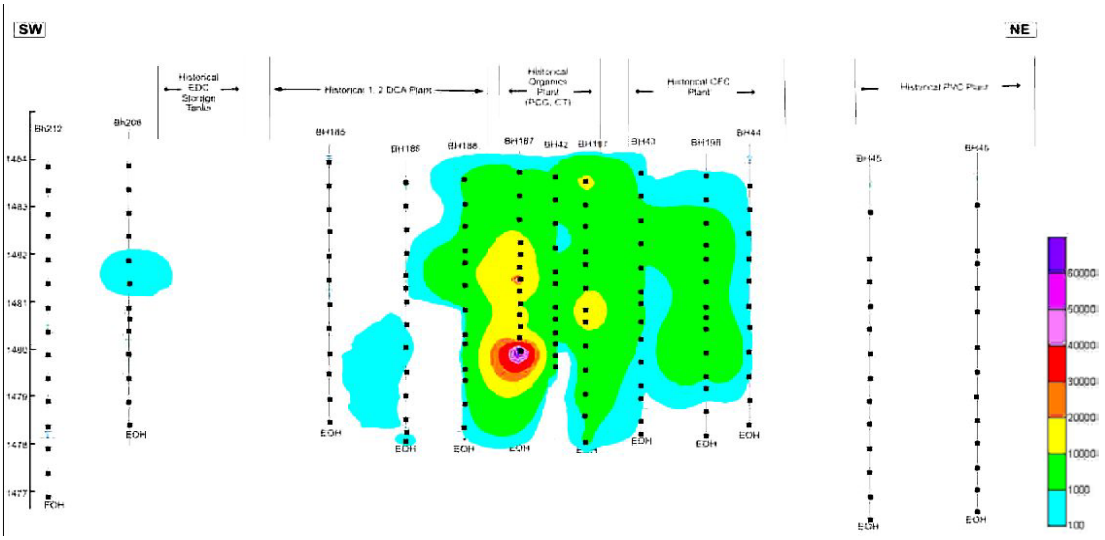

Figure 3-36: Chlorinated hydrocarbons distribution in the soils (in µg/kg) beneath the historical production, storage and handling area 1

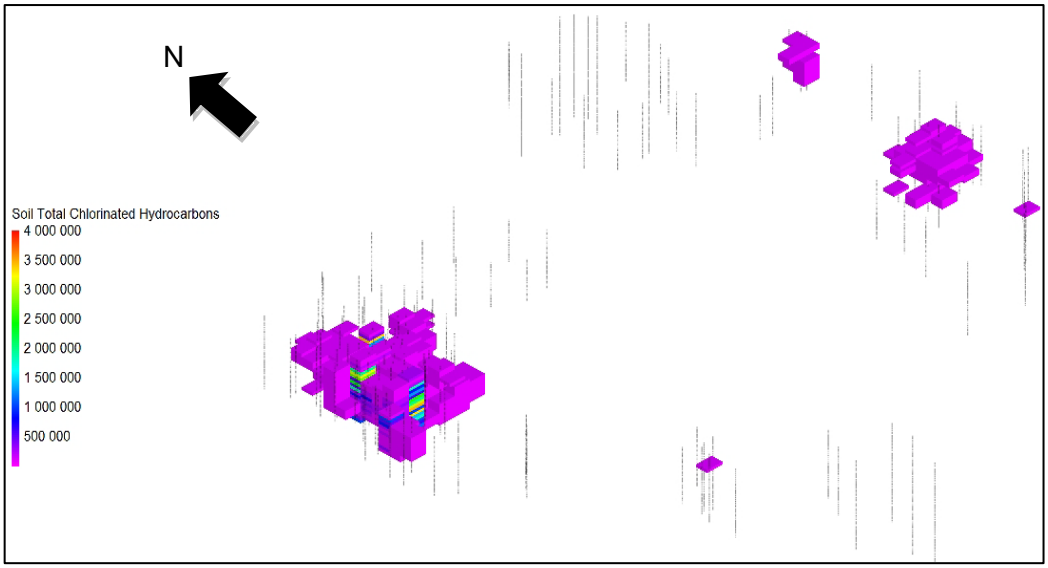
N
Soil Total Chlorinated Hydrocarbons
4 000 000
3 500 000
3 000 000
2 500 000
2 000 000
1 500 000
1 000 000
500 000

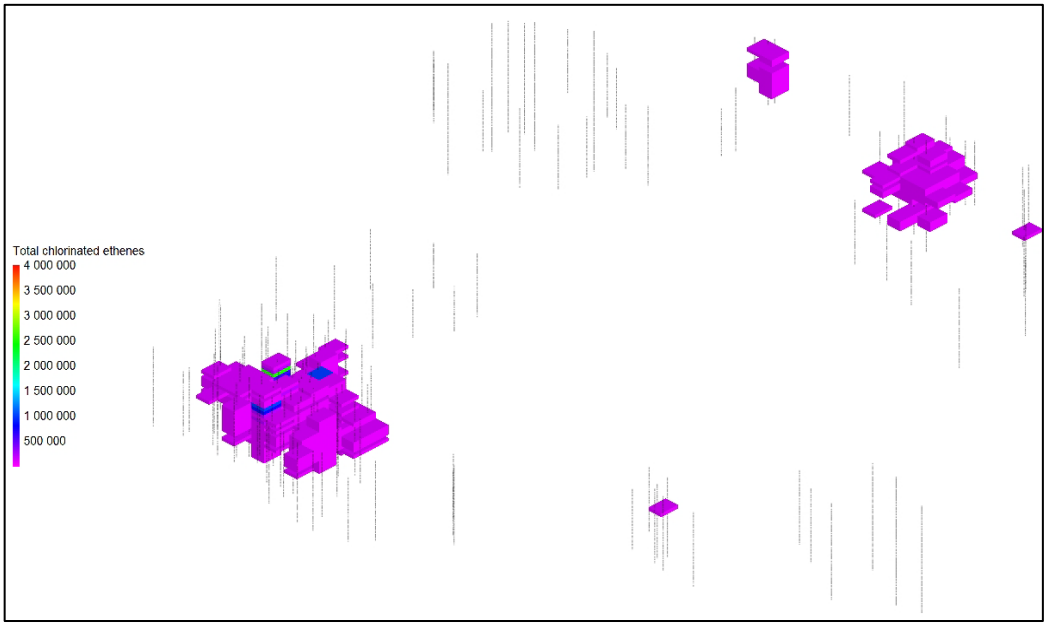
Total chlorinated ethenes
4 000 000
3 500 000
3 000 000
2 500 000
2 000 000
1 500 000
1 000 000
500 000

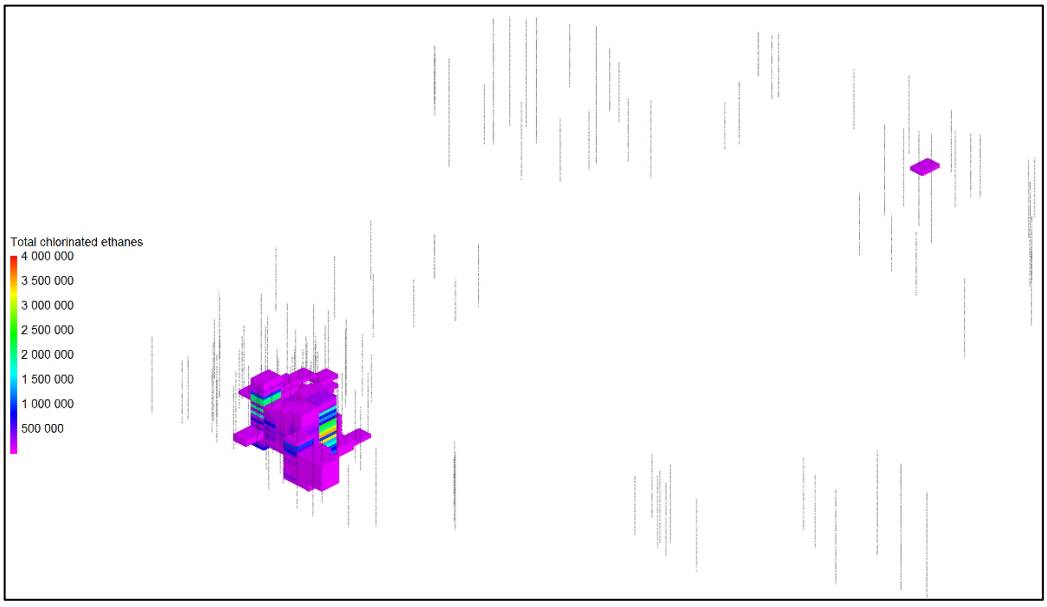
Total chlorinated ethanes
4 000 000
3 500 000
3 000 000
2 500 000
2 000 000
1 500 000
1 000 000
500 000

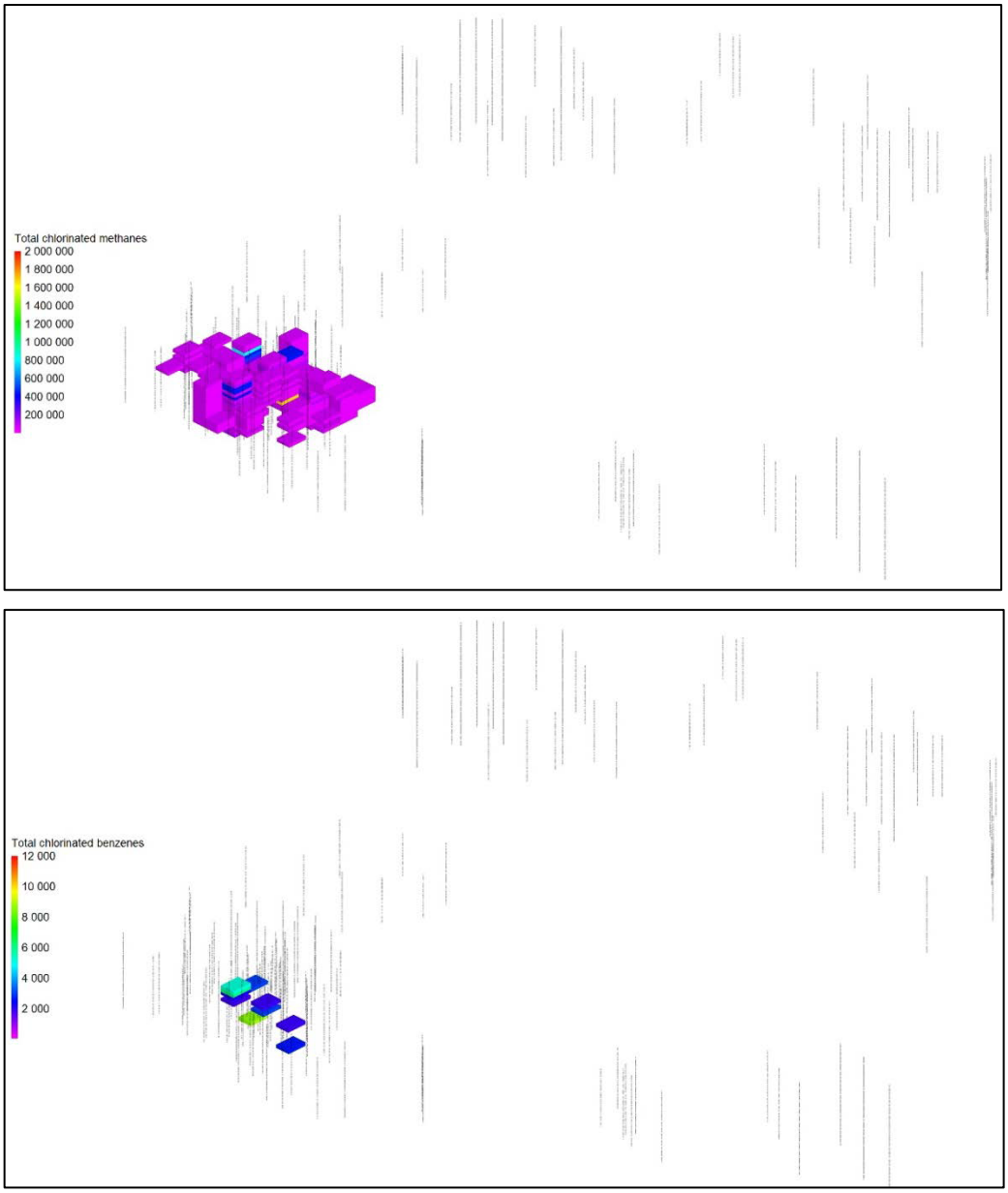

Figure 3-37: 3-D solid models of grouped chlorinated hydrocarbons soil concentrations (µg/kg)

Where:
Total chlorinated hydrocarbons = total chlorinated benzenes + total chlorinated ethenes + total chlorinated ethenes + total chlorinated ethanes + total chlorinated methanes
Total Chlorinated Benzenes (ClBENZ) = 1,2-dichlorobenzene + 1,3-dichlorobenzene + 1,4-dichlorobenzene + chlorobenzene
Total Chlorinated Ethenes (ClEthenes) = tetrachlorethene + trichloroethene + cis-1,2-dichloroethene + trans-1,2-dichloroethene + 1,1-dichloroethene + vinyl chloride
Total Chlorinated Ethanes (ClEthanes) =1,1,1-trichloroethane + 1,1,1,2-tetrachloroethane + 1,1,2,2-tetrachloroethane + 1,1,2-trichloroethane + 1,1-dichloroethane +1,2-dichloroethane
Total Chlorinated Methanes (ClMethanes) = carbon tetrachloride + chloroform

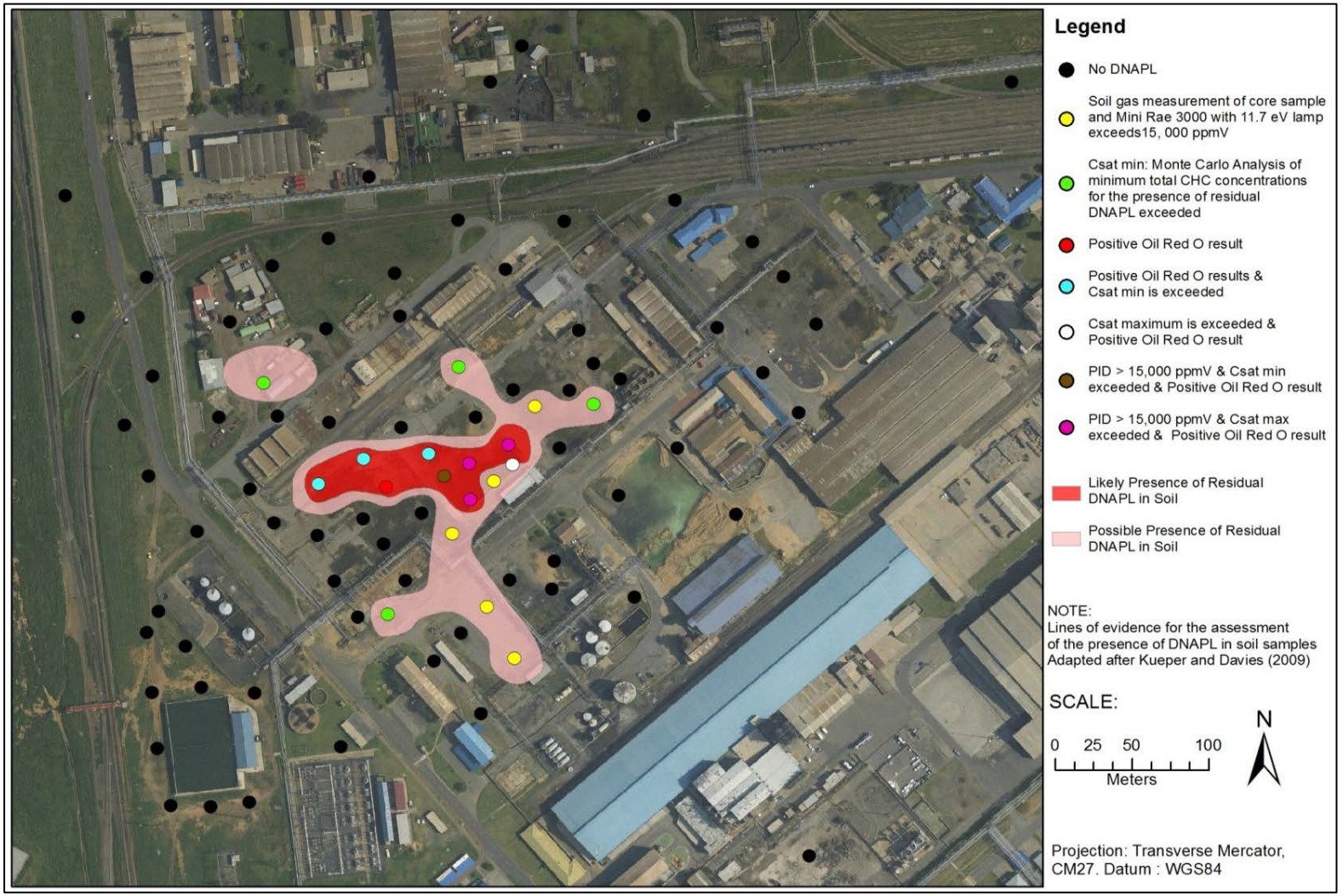

Figure 3-38: Plan view of inferred DNAPL source zones in soil

3.3.4.2 Fractured (bedrock) source zones delineation

3.3.4.2.1 Fracture network characteristics

As mentioned in the section on the site's local geology (Section 3.3.2.), the bedrock underlying the site is characterised by fractured networks. This section focuses on the characteristics of the fractured network as it is a significant factor in the chlorinated hydrocarbon DNAPL migration.

The following tools were useful in characterising the fractures at the site:

- Downhole borehole geophysical logging, particularly using the acoustic televiewer and the results obtained from the fracture pick analysis.
- Detailed core borehole logging
- Ribbon NAPL samplers

Downhole borehole geophysical logging was restricted to core holes drilled outside the source zones. The results obtained were extremely useful in assisting with the understanding of the local geology and the extent of fracturing at the site (Figure 3-39). The probes are however not compatible with use in open holes located within source zones, containing free phase DNAPL. The value of information deduced from detailed core logging was found to be sufficient for the requirement of this study, without the need for further downhole geophysical log profiling in holes with ribbon NAPL samplers installed.

Transmissivity profiling using the ribbon NAPL samplers (FLUTe^{TM}) was useful in determining the location of transmissive fractures.

The dolerite sill is characterised predominantly by steeply dipping, sub-horizontal fractures (Figure 3-40). The stereonet and rose diagram shown below were created using RockWorks15. Core holes drilled within the soils source zones were selected for the analysis. Examination of the stereonet in Figure 3-40 shows an underrepresentation of vertical fractures. This is the result of the drilling orientation as all core holes drilled at the site were vertical.

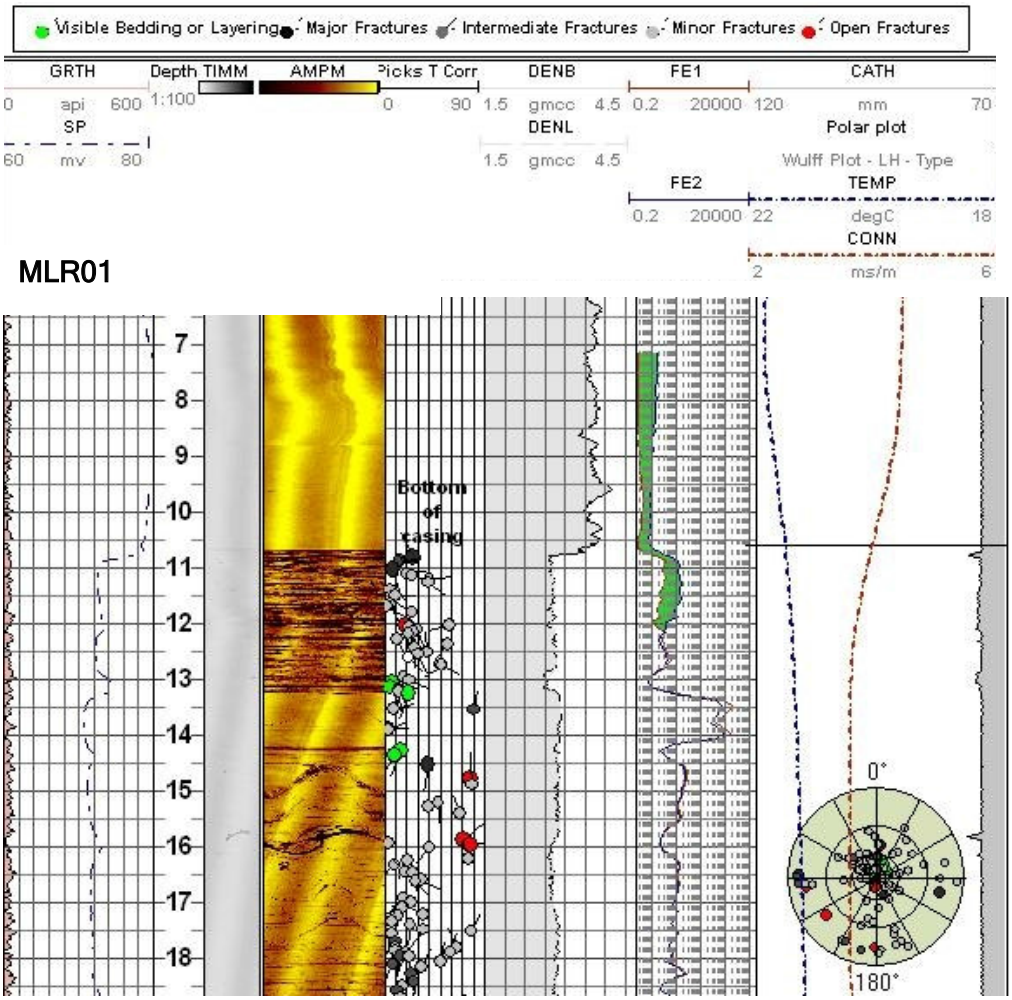

Figure 3-39: Portion of downhole geophysical log for core hole MLR01 showing the large density of fractures

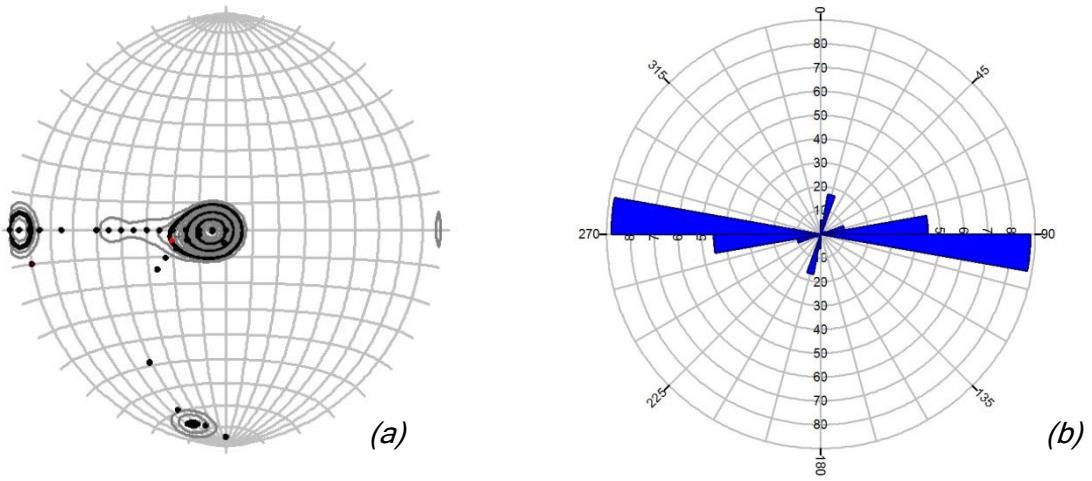

Figure 3-40: (a) Schmidt net (equal area, contoured) stereonet and (b) Rose diagram of fractures within the source zones (uncorrected)

Figure 3-41 provides 3-D strip logs showing fracture orientation of core holes drilled into the historical production and handling area footprint (identified in Section 3.3.4.1 as the primary soil/weathered source zone).

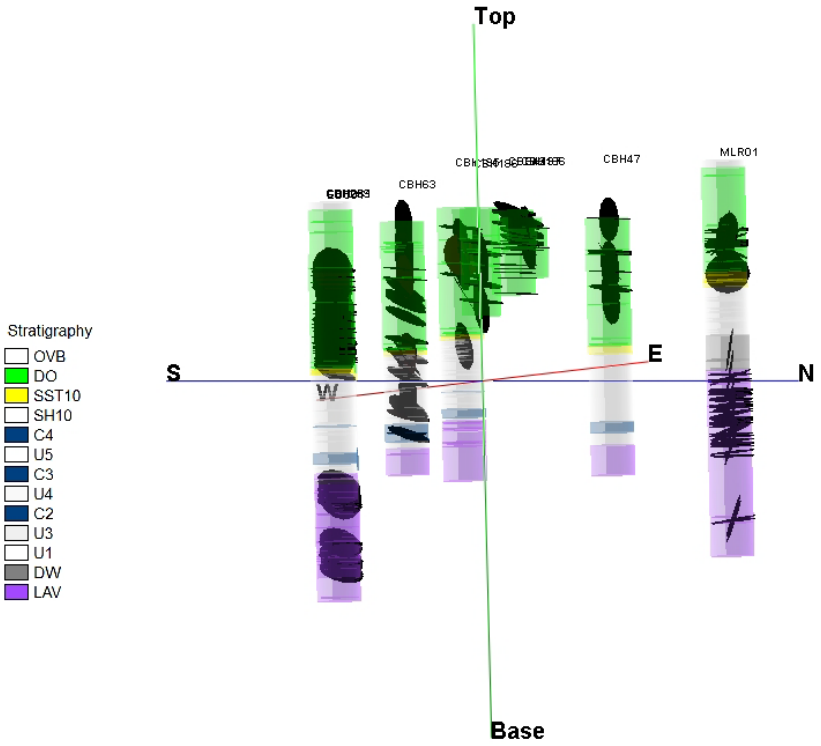

Figure 3-41: 3-D strip logs showing fracture discs of core holes drilled in the historical production and handling facility

The variation in the fracture density per meter with elevation within the source zone is shown in Figure 3-42. While the density of fractures decreases within the unweathered portion of the dolerite sill, it still remains fractured with discrete fracture networks. The Karoo Ecca sedimentary rocks are characterised by sub-horizontal bedding planes. Sub-vertical fractures extend from the dolerite sill, through the low permeability contact zone between the dolerite and the Karoo Ecca sedimentary rocks.

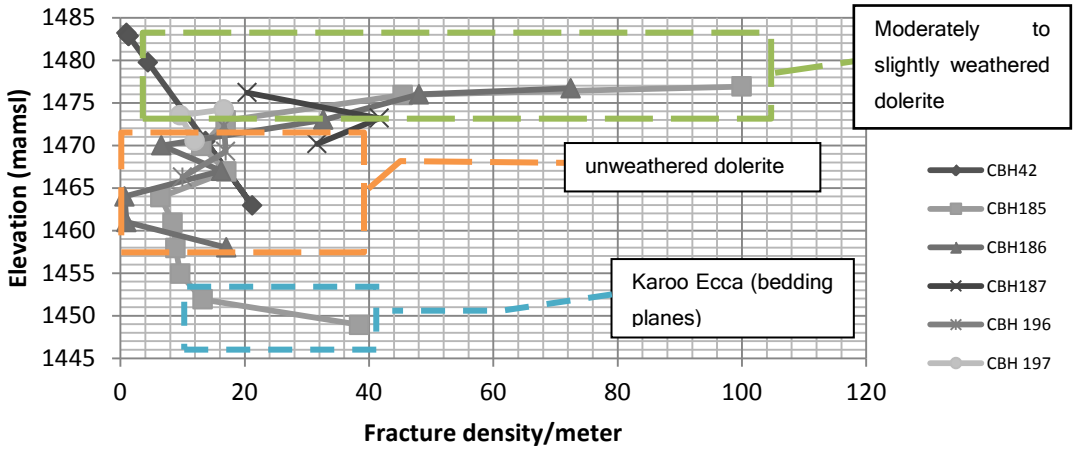

Figure 3-42: Variation of fracture density with elevation at the historical production and handling facility

Figure 3-43 is a plot of the ribbon NAPL sampler descent velocity into PBH221 with depth. A change in the liner velocity occurs when a flow path is sealed. A tranmissive fracture/feature is determined through analysis of the descent velocity of the ribbon NAPL sampler with depth. Descent velocity decreases rapidly with depth of the borehole in the absence of transmissive fractures. An analysis of the data from the other boreholes that were installed with ribbon NAPL samplers shows an apparent lack of small transmissive fractures. This could be caused either by an absence of smaller transmissive fractures or through masking of the presence of other fractures due to the larger intake of groundwater by the highly transmissive fracture.

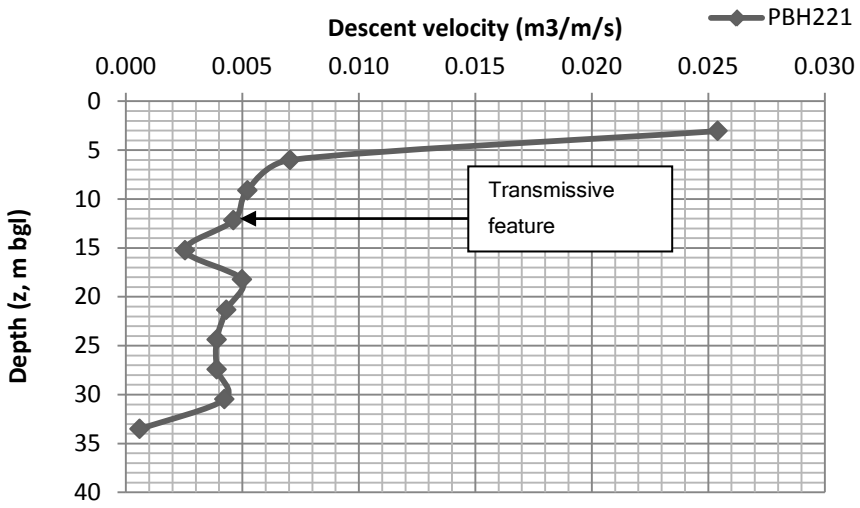

Figure 3-43: Location of transmissive fracture in PBH221

The smallest fracture along a flow path will control groundwater flow through a fracture in a network. The hydraulic aperture (viz. the value assigned to the smallest fracture along a flow path) for CBH42 was calculated using the cubic law (Snow, 1968 as modified by Bear, 1993):

$$\mathbf{2b} = \sqrt[3]{\frac{\mathbf{12\mu T_{fr}}}{\mathbf{\rho g N}}} \quad \textbf{Equation 3-2}$$

Where:

2b = hydraulic aperture

μ = dynamic viscosity of water

ρ = density of water

g = acceleration due to gravity

T_{fr} = fracture transmissivity

N = number of fractures per interval

The average groundwater temperature at the site is approximately 20^0C. Hence values for ρ and μ used were 0.998 g/cm^3 and 1.003 mPa·s (CRC Handbook of Chemistry and Physics, 1986). The values used for *N* and T_{fr} are indicated in Figure 3-44 below.

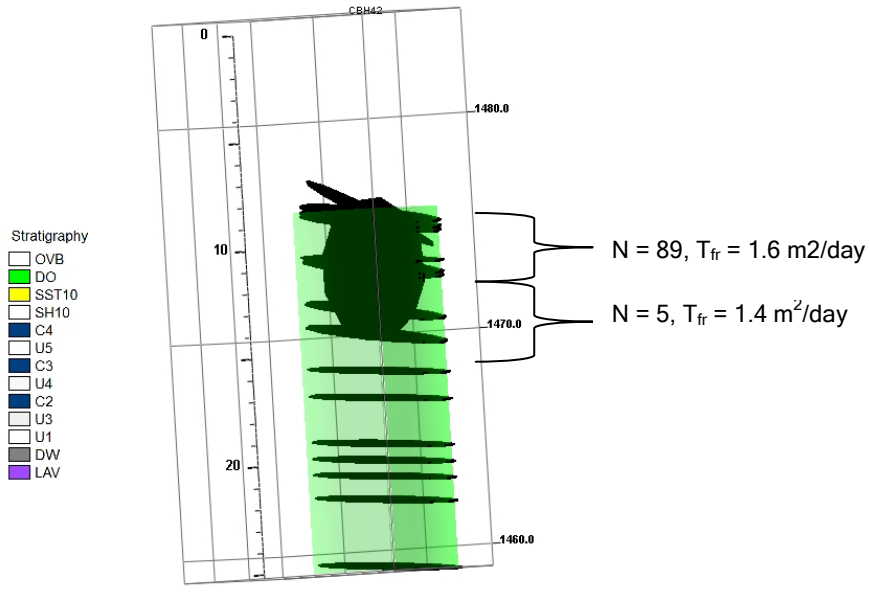

Figure 3-44: 3-D strip log of CBH42 showing the intervals and values used for calculating hydraulic aperture

Hydraulic aperture (2b) for CBH42 is calculated to be 63.5 μm at depths of between 9 - 12 m bgl and 159 μm at depths of between 12 and 15 m bgl.

3.3.4.2.2 DNAPL source delineation

Historical site data indicated evidence through direct observation of pooled chlorinated hydrocarbon DNAPL at two locations at the Investigation Site *viz.* SRK 14 S/D and EDC 01 (Figure 3-4). Neither the transport mechanics nor the transport media could however be discerned through the available information.

Source zone delineation was undertaken through further drilling and sampling, utilising both *in situ* and *ex situ* tools. Residual and pooled DNAPL was found in additional core holes and percussion holes. A summary of the boreholes containing pooled or residual DNAPL and the method of detection is provided in Table 3-12. The location of boreholes positive for pooled or residual DNAPL is provided in Figure 3-48. From this figure it is observed that DNAPL occurrence in the fractured bedrock is associated with the redundant production and handling facilities in the north western part of the site. The southern effluent dams are not considered release areas for free phase DNAPL, but may be associated with the high concentrations of dissolved chlorinated hydrocarbon DNAPL in boreholes.

Three on-site lines of evidence were useful in the detection of pooled DNAPL:

1. Anomalous PID measurements (> 10 ppm) made on the drill chips,
2. Odours emanating from drill chips, and
3. Visual observation of pooled DNAPL through bailer testing of the borehole.

The depth of visual observation of pooled DNAPL ranged from 20 m bgl – 47 m bgl. Pooled DNAPL was intersected at approximately 20 m bgl beneath the historical 1,2-DCA storage tanks, located west of the historical production facilities (Figure 3-48). The pooled DNAPL is associated with the dolerite in this area. Information provided by plant personnel indicate a loss of approximately 5 L/day of 1,2-DCA from these tanks over a 31 year period. This occurred during routine sample collection to test the quality of the product for production purposes. This excludes any additional spills or leaks from these tanks during this period. DNAPL pools in boreholes are found away from the original release point. Distances of up to 850 m are recorded for boreholes showing pooled DNAPL (Figure 3-48). Boreholes with pooled DNAPL showed anomalous PID readings of > 10 ppm.

Apparent thickness of DNAPL was measured in the boreholes over a 1 month period. The change in apparent thickness over time is shown in Figure 3-45. In general, DNAPL flow into the boreholes stabilised after 1 week. DNAPL was only measured in CBH174 after 1 week, indicating the mobilisation of DNAPL along an interconnected

horizontal fracture. DNAPL thickness in the boreholes did not decrease during the measuring period, indicating a large mass of free phase located

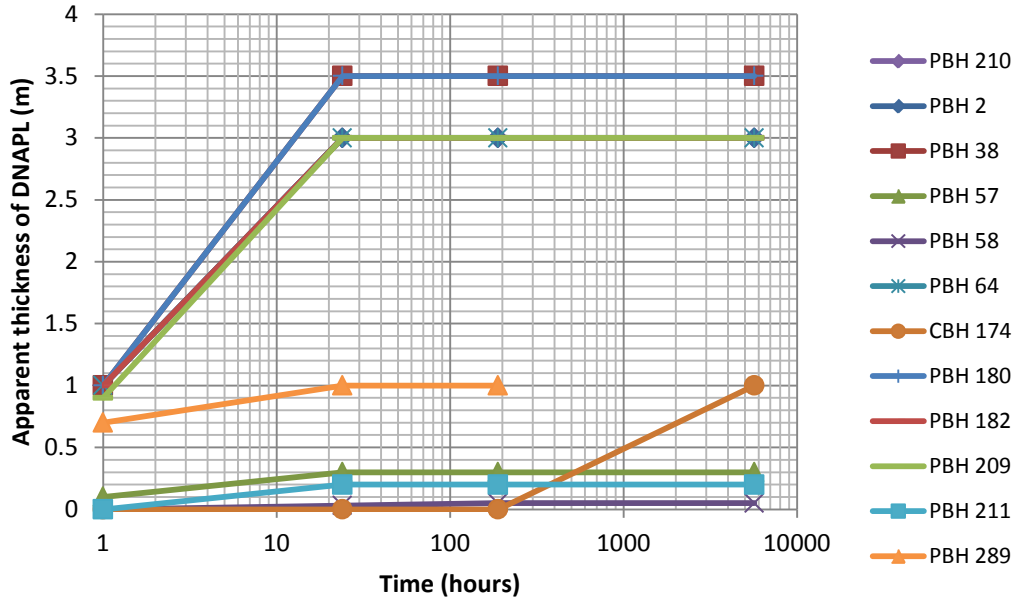

Figure 3-45: Apparent DNAPL thickness measured in boreholes

Ribbon NAPL samplers containing a hydrophobic dye were installed in the boreholes shown in Table 3-13. Residual DNAPL was detected in core hole CBH42 and percussion borehole PBH213 through the use of ribbon NAPL samplers. Both these boreholes are located within the footprint of the historical production and storage facilities. Residual DNAPL thicknesses ranged from 1 to 50 cm in CBH42 and PBH213. From the log of CBH42, it is observed that the location of residual DNAPL is related to the fractures in the upper portion of the dolerite sill (Figure 3-46).

PID measurements taken in CBH42 and PBH213 were < 10 ppm, indicating that the effect of volatilization from the retrieved core or drill bits may produce false negatives in zones where DNAPL (pooled or residual) may be present and can thus not be used as a solitary tool to determine the presence of DNAPL on a site.

Residual DNAPL was also detected in CBH42, CBH186, CBH196 and CBH197 through the use of Oil Red O®. Figure 3-47 is a photograph of the staining observed in core hole CBH42 at a depth of 22.7 m bgl. The ribbon NAPL sampler was installed in this borehole to a depth of 18 m bgl and hence this zone of residual DNAPL was not detected. This is a limitation of the technology in fractured bedrock with low transmissivities.

Bedrock cross sections are provided below (Figure 3-49 -Figure 3-53). The cross sections show the association of anomalous PID measurements and odours in relation to the stratigraphy. Pooling of DNAPL at the site has occurred above the following lithologies: siltstone and mudstone (SST10) of the Karoo Ecca, the contact zone between the dolerite sill and the Karoo Ecca sandstone (SST10); and the carbonaceous shale (SH10).

Table 3-12: Method of detection of residual and pooled DNAPL within boreholes

Borehole ID	Method(s) of detection
EDC01	Visual observation of pooled DNAPL (bailer test), odours
SRK14 S/D	Visual observation of pooled DNAPL (bailer test), odours
CBH42	Residual DNAPL staining on ribbon NAPL liner, Positive result using hydrophobic dye indicating residual DNAPL
PBH213	Residual DNAPL staining on ribbon NAPL liner
PBH2	Visual observation (bailer test) @ 30 m bgl, Anomalous PID measurements, odours
PBH38	Visual observation (bailer test) @ 20 m bgl, Anomalous PID measurements, odours
PBH57	Visual observation (bailer test) @ 45 m bgl, Anomalous PID measurements, odours
CBH174	Visual observations (bail test) @ 30 m bgl
PBH64	Visual observation (bailer test) @ 37 m bgl, Anomalous PID measurements, odours
PBH180	Visual observation (bailer test) @ 20 m bgl, Anomalous PID measurements, odours
PBH182	Visual observation (bailer test) @ 25 m bgl, Anomalous PID measurements, odours
PBH209	Visual observation (bailer test) @ 20 m bgl, Anomalous PID measurements
PBH210	Visual observation (bailer test) @ 20 m bgl, Anomalous PID measurements
PBH211	Visual observation (bailer test) @ 20 m bgl, Anomalous PID measurements
PBH289	Visual observation (bailer test) @ 37 m bgl, Anomalous PID measurements, odours
CBH186	Positive result using hydrophobic dye indicating residual DNAPL
CBH196	Positive result using hydrophobic dye indicating residual DNAPL
BH197	Positive result using hydrophobic dye indicating residual DNAPL

Table 3-13: Summary of maximum depth of ribbon NAPL sampler installation

Borehole ID	Maximum Depth (m bgl) of ribbon NAPL sampler installation
CBH42	18.23
PBH213	24.38
PBH228	32
PBH221	36.58

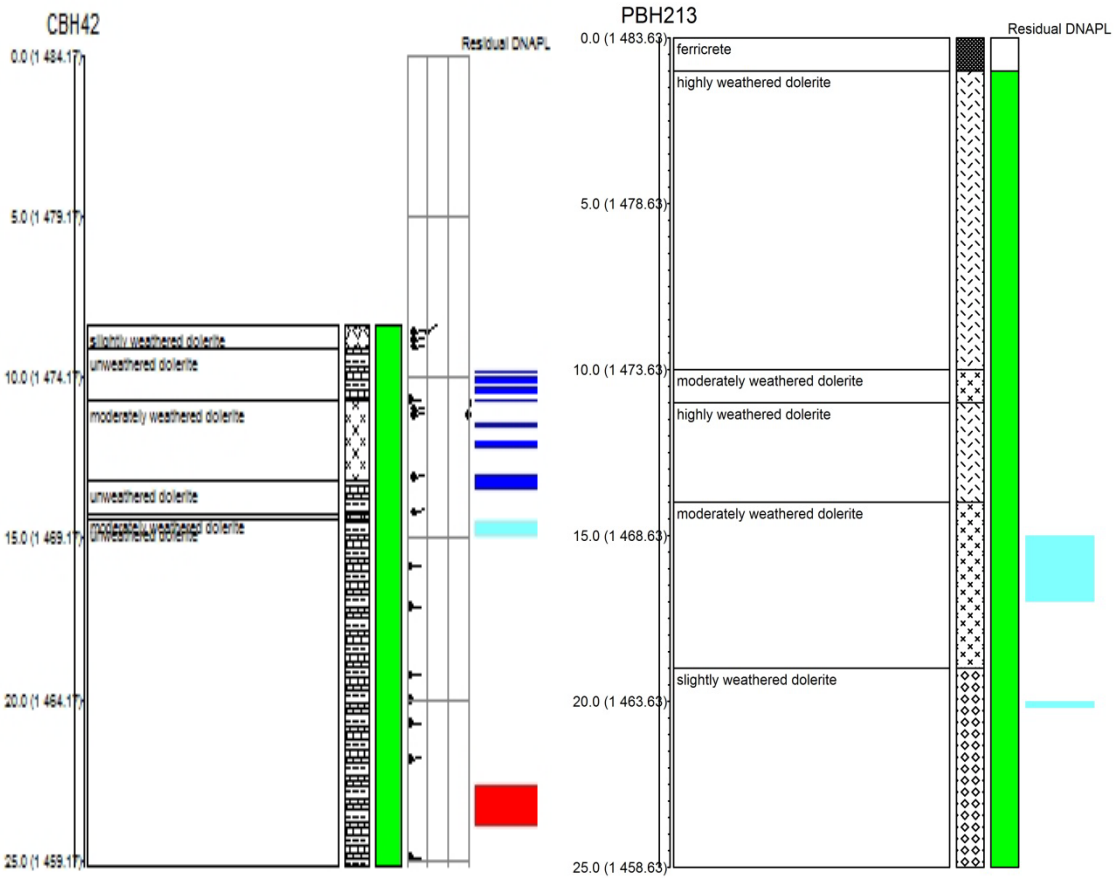

Figure 3-46: Logs of CBH42 and PBH213 showing the location of residual DNAPL (shown in blue as determined through the use of ribbon NAPL samplers and in red as observed using Oil Red O®) in relation to the litho-stratigraphy

Figure 3-47: Oil Red O® staining at 22.7 m bgl in core hole CBH42 indicating the presence of residual DNAPL

In addition to direct observation of DNAPL (described above), chlorinated hydrocarbon DNAPL is also inferred at boreholes where the sum of the mole fractions of the chlorinated hydrocarbon DNAPL in the groundwater sample exceeds 1% of the total effective solubility. The 1% effective solubility threshold is calculated using the following equation:

$$\sum_{i=1}^{n} \frac{C_i^{obs}}{S_i} = \alpha \quad \text{Equation 3-3}$$

Where:

C_i^{obs} = sampled groundwater concentration in mg/l of component i

S_i = single-component solubility of component i

α = cumulative mole fraction of sample

n = number of components in the groundwater sample.

A summary of the results for boreholes where chlorinated hydrocarbon DNAPL can be inferred is provided in Figure 3-48.

The DNAPL aqueous phase plume migration results are discussed further in Section 3.3.5.

DNAPL chemical composition (in mole fraction) for selected samples taken from the site is provided in Table 3-14. The spatial distribution of the sampled boreholes and

their chemical compositions are shown in Figure 3-54. The following observations are made:

- As expected, the DNAPL compositions within the release area mimic the chlorinated hydrocarbon that was produced, stored or handled at the facility.
- The chemical composition of DNAPL found 600 – 800 m down gradient of the above ground storage tanks (boreholes PBH64, PBH289, EDC01 and CBH259) is primarily 1,2-DCA which is the same as the composition of DNAPL pooled below the above ground storage tanks and inferred/pooled at the historical 1,2-DCA production facility. Small percentages of other associated chlorinated hydrocarbons such as 1,1,2-TCA is also found in these boreholes.
- DNAPL with chemical compositions of 1,1-DCA, CCl_4 and $CHCl_3$ are also found downgradient (600 – 800 m) of the original release point.

Neither free phase nor residual phase has migrated further than the site boundary. The length and movement of the dissolved phase plume is discussed in detail in the next section. Movement of the DNAPL has been primarily along the contact zone between the dolerite sill and the Karoo Ecca sedimentary rocks as well as along bedding planes located in the Karoo Ecca sedimentary rocks. However, close inspection of the cross sections (such as cross section G-H) also indicate vertical upward migration. Additionally, based on the observations made above on the free phase DNAPL compositions found in downgradient boreholes it can be inferred that two contiguous DNAPL pools (one originating from the historical 1,2-DCA storage facility and the other from the historical production facilities) have migrated towards the southern boundary of the site.

Physical property results for EDC01, PBH57 and PBH180 are also provided in Table 3-14. A plot of the rheological properties of the site samples is shown in Figure 3-55. The samples display analogous physical properties. As the samples are composed primarily of 1,2-DCA it would have been expected that the rheological properties would be the same. However, as is seen from Figure 3-55, the analysed samples have higher viscosities compared to pure phase 1,2-DCA. PBH57 also displays a higher density value (approximately 5% higher) compared to 1,2-DCA and the other samples analysed (PBH 180 and EDC01). This is attributed to the variances in composition of PBH 57 compared to the other samples.

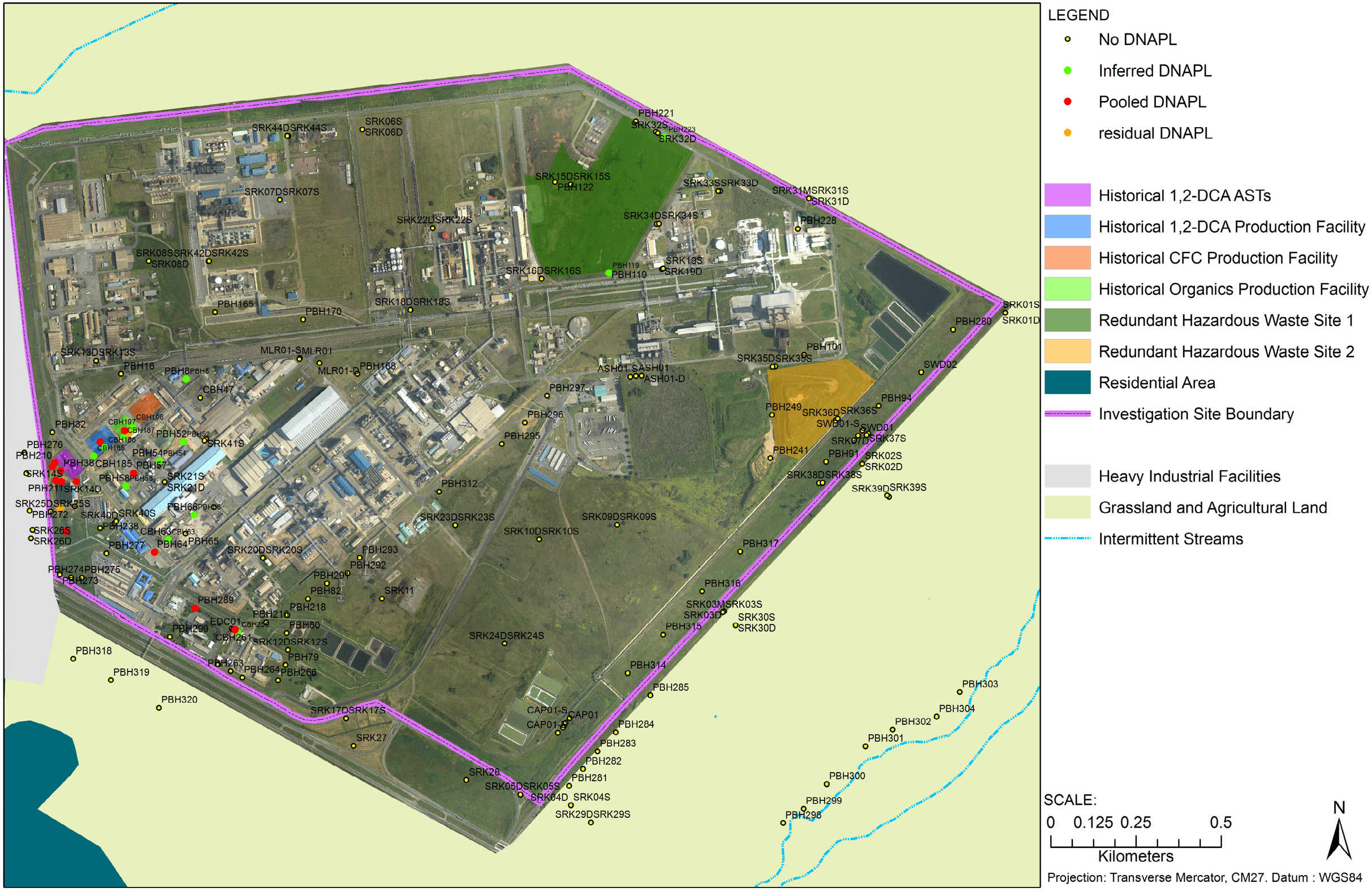

Figure 3- 48: Locations of pooled, residual and inferred DNAPL in the fractured bedrock at the Investigation Site

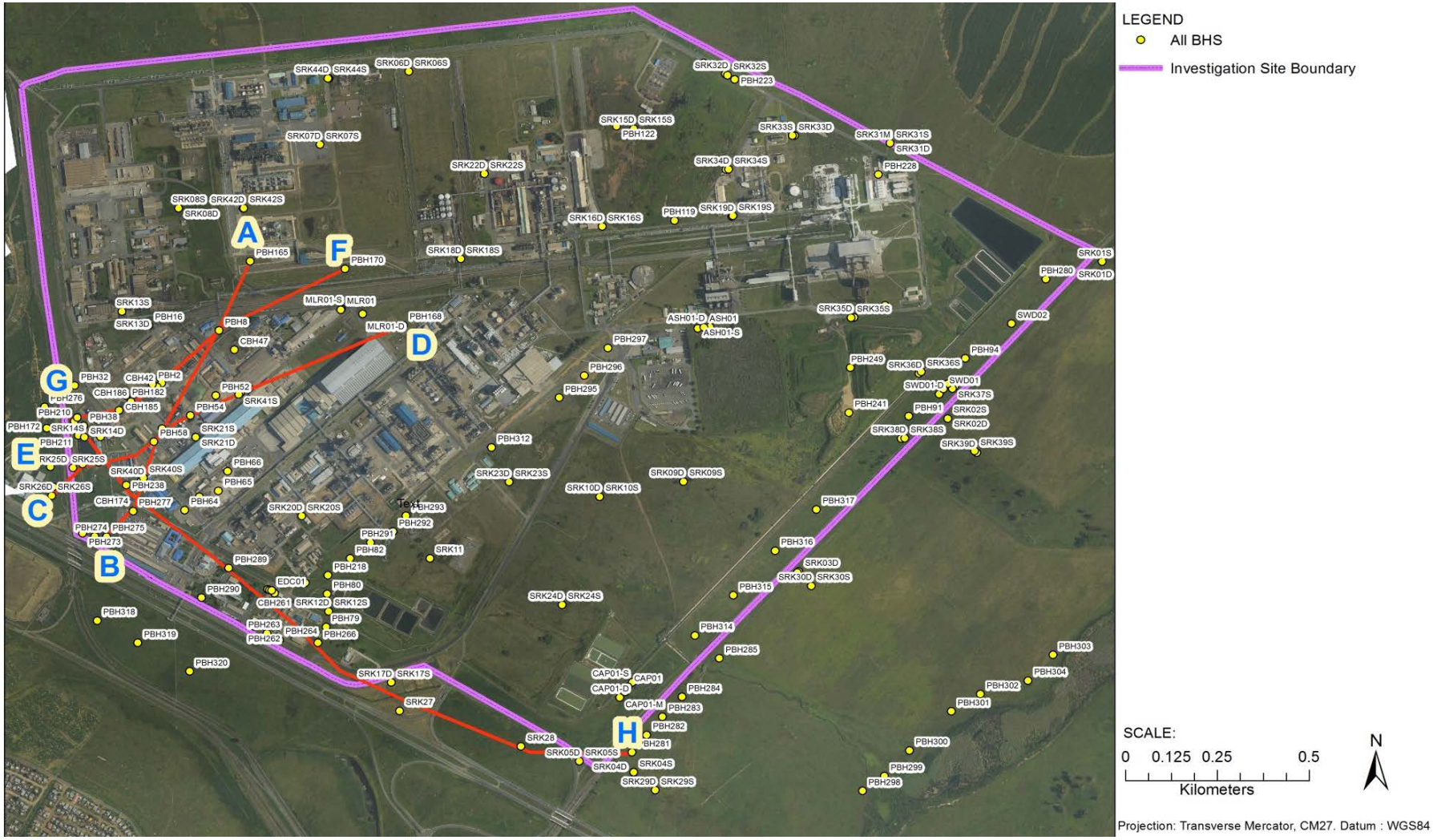

Figure 3-49: Location of bedrock source zone cross sections

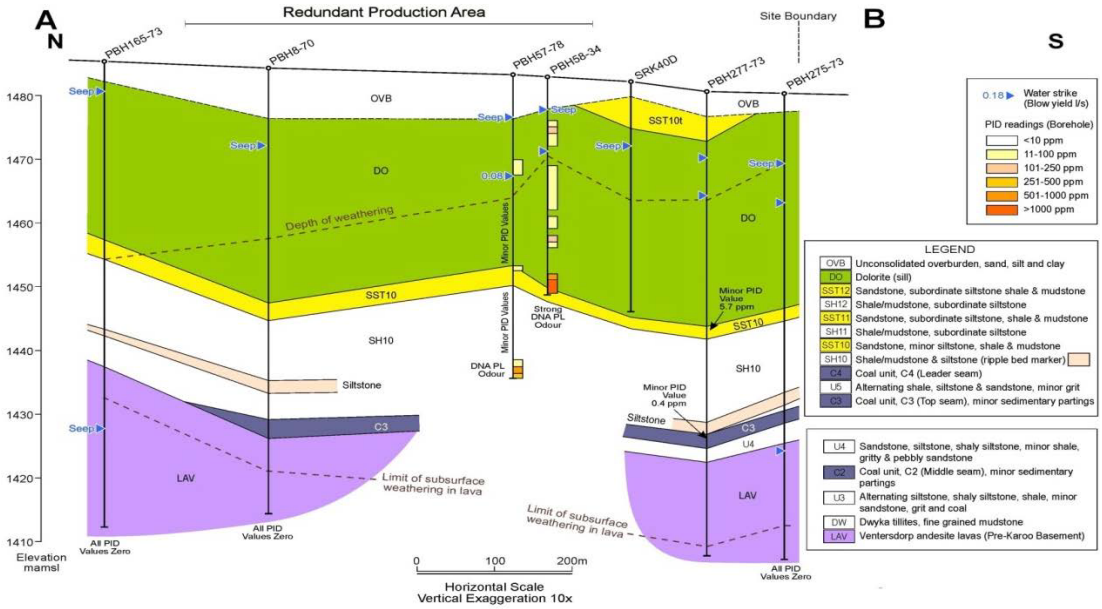

Figure 3-50: Bedrock cross section A-B (modified from ERM, 2012)

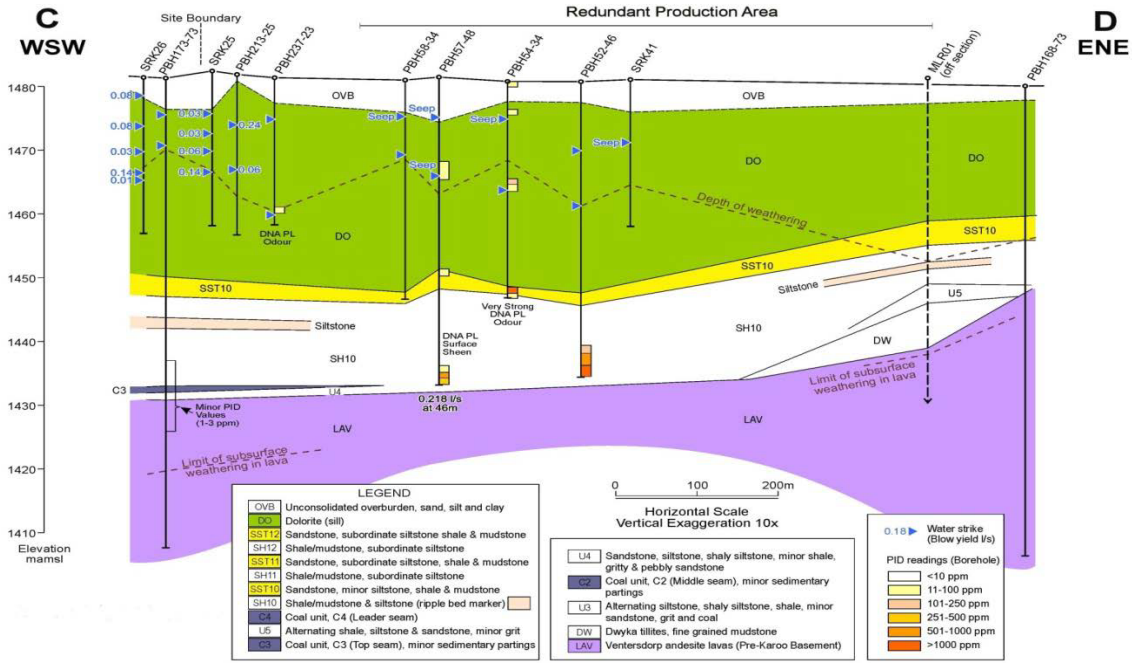

Figure 3-51: Bedrock cross section C-D (modified from ERM, 2012)

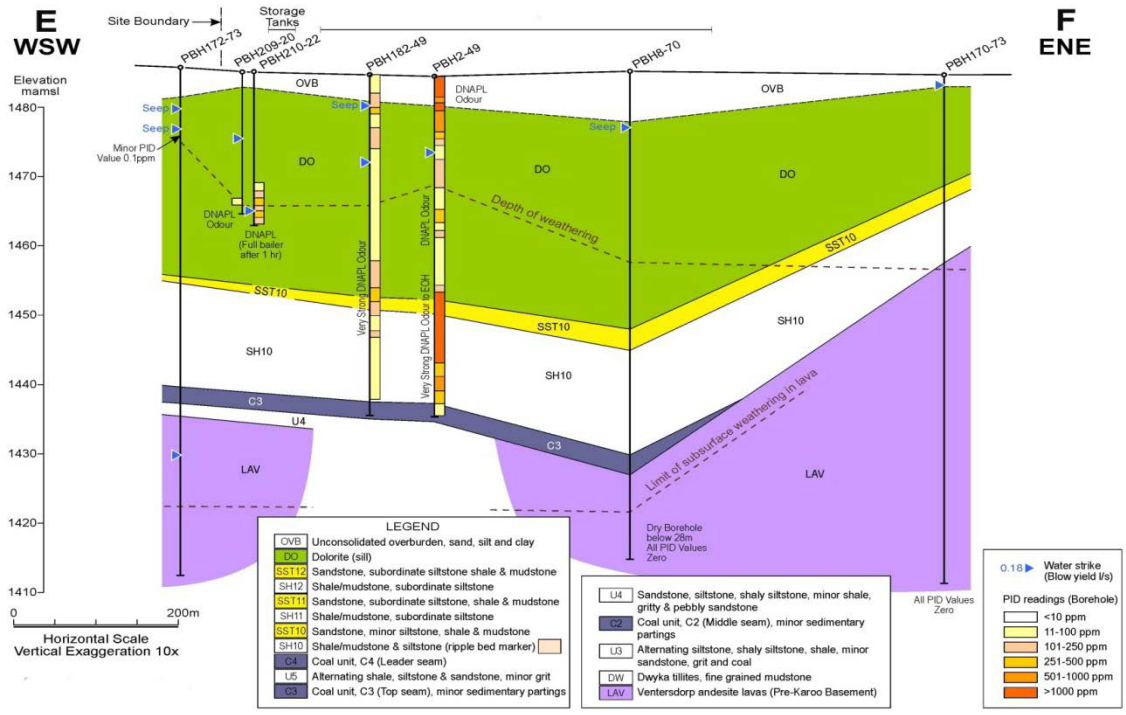

Figure 3-52: Bedrock cross section E-F (modified from ERM, 2012)

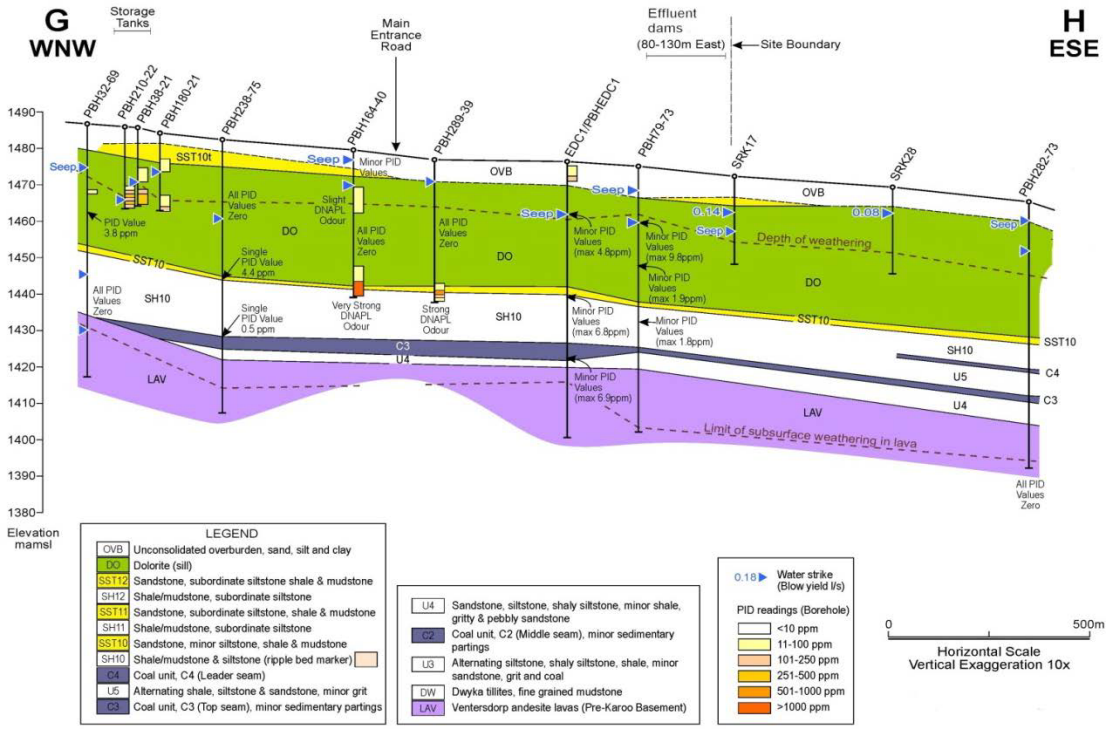

Figure 3-53: Bedrock cross section G-H (modified from ERM, 2012)

Table 3-14: Summary of mole fractions (%) composition of groundwater samples with inferred chlorinated hydrocarbon DNAPL (results from ERM, 2012)

Borehole ID	PCE	TCE	1,1-DCE	Trans 1,2-DCE	VC	1,1,1-TCA	1,1,2-TCA	1,1-DCA	1,2-DCA	CCl_4	$CHCl_3$
PBH52	75.4	0.0	0.0	0.0	0.0	0.0	0.0	0.0	0.0	11.5	13.1
PBH54	15.5	1.6	0.0	0.0	0.0	0.0	0.0	0.0	12.5	8.1	62.3
PBH63	2.7	4.5	0.0	0.0	0.0	0.0	1.8	0.0	41.7	8.9	40.3
PBH223	68.5	0.0	0.0	0.0	0.0	0.0	0.0	0.0	5.2	8.1	18.2
PBH58	0.0	0.0	0.0	0.0	0.0	0.0	2.9	0.0	97.1	0.0	0.0
PBH66	41.9	0.0	0.0	0.0	0.0	0.0	0.0	0.0	1.8	23.4	32.9
PBH8	16.8	0.0	0.0	0.0	0.0	1.6	0.0	0.0	3.8	0.0	77.8
PBH119	38.4	1.0	0.0	3.6	0.0	0.0	0.0	5.1	0.0	45.1	0.0
PBH54	19.7	1.7	0.0	0.0	0.0	0.0	0.0	0.0	0.0	61.9	16.7
CBH63	2.5	0.0	0.0	0.0	0.0	0.0	2.3	1.8	86.2	3.6	3.7
CBH185	0.0	0.0	0.0	0.0	0.0	0.0	0.0	0.0	99.5	0.0	0.0
CBH186	0.0	0.0	2.0	0.0	9.4	0.0	0.0	0.0	87.1	0.6	0.0
CBH187	26.8	0.0	0.0	0.0	0.0	0.0	0.0	0.0	1.7	23.0	48.5
CBH196	27.6	0.0	0.0	0.0	0.0	0.0	0.0	0.0	0.0	2.1	70.2
CBH197	36.7	0.4	0.0	0.0	0.0	0.0	0.0	0.0	0.0	36.6	25.5
CBH259	0.0	0.0	1.5	1.4	0.0	0.0	0.0	0.0	96.3	0.0	0.0

Table 3-15: Physical and chemical properties of pooled DNAPL samples from the Investigation Site

Borehole ID	Physical Properties					Chemical Composition (mole fraction %)							
	Density (g/cm^3)	Water Content (% weight)	Interfacial Tension (mN/m)	Viscosity @ 15^0C (mPa·s)	Viscosity @ 22^0C (mPa·s)	PCE	1,1-DCE	VC	1,1,2-TCA	1,2-DCA	1,1-DCA	CCl_4	$CHCl_3$
EDC01	1.2511	0.1497	22.31	1.03	0.98	0.0	3.5	0.5	3.0	92.2	0.4	0.0	0.2
PBH57	1.3159	0.0875	23.94	1.04	0.95	5.5	0.6	0.4	8.0	77.3	0.6	7.0	0.2
PBH180	1.2582	0.0985	24.10	1.06	0.96	0.0	0.3	0.3	0.6	98.6	0.1	0.0	0.0
PBH2	Not Analysed					13.4	0.1	0.1	0.9	61.1	0.6	20.8	2.8
PBH64						0.4	1.2	0.7	3.3	93.4	0.4	0.0	0.0
PBH182						3.5	0.3	0.2	2.3	89.2	1.7	2.3	0.5
PBH289						0.7	2.5	0.6	2.4	92.8	0.4	0.0	0.5

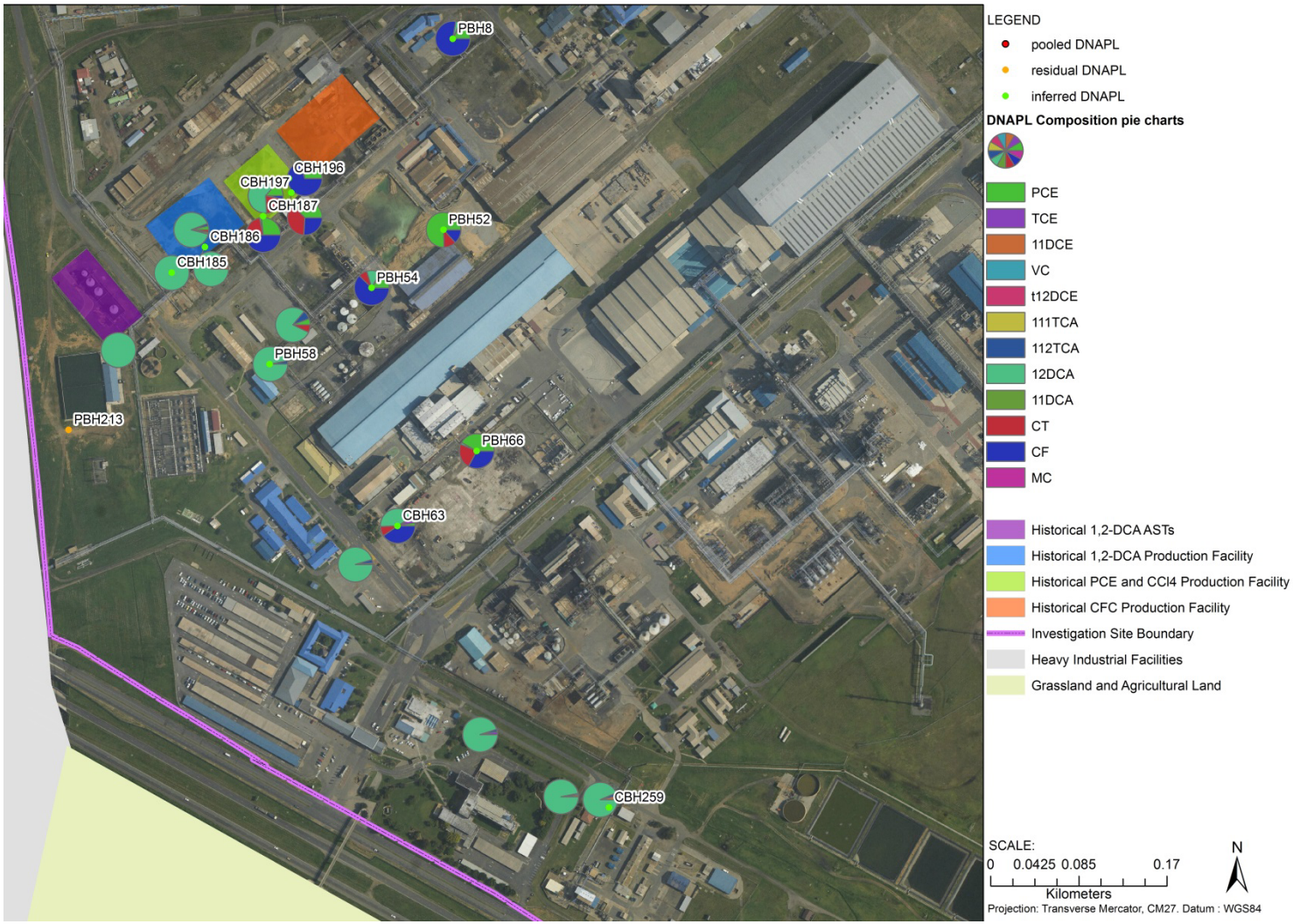

Figure 3-54: DNAPL composition in boreholes (Results from ERM, 2012)

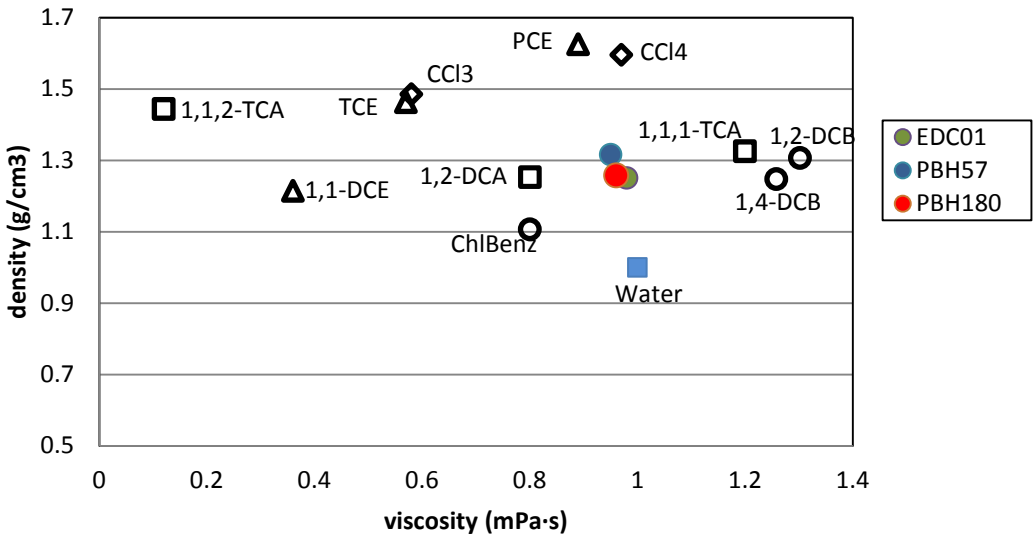

Figure 3-55: Plot of density vs viscosity for samples analysed from the Investigation Site

3.3.5 Hydrogeochemical characteristics

Groundwater chemistry data were subdivided to reflect (1) historical data (and associated trends) and (2) current data (which includes the results obtained from newly drilled boreholes). A comparison is made of the evolving plume with time. Production and storage of chlorinated hydrocarbon ceased at the site in 1998. Groundwater monitoring results are available from 1998 to present. The historical data obtained is sporadic. Groundwater samples were taken from all boreholes (overburden as well as bedrock wells) in 2012 and this provides the most recent development of the chlorinated hydrocarbons plumes.

SRK14S/D is located within the source zone at the historical 1,2-DCA above-ground storage tanks. Figure 3-56 shows the chlorinated ethenes, ethanes and methanes time-series trends. Both piezometers are located in the dolerite aquifer, with the shallow piezometer recording data in the weathered zone and the deep piezometer recording data in the fractured bedrock. As expected, similar trends and concentrations are observed within the weathered and the fractured zone. All graphs show a general decrease in concentrations followed by an increase in July 2009 and a subsequent decrease in concentrations to the present date. The presence of daughter products such as cis-1,2-DCE indicates that biodegradation is occurring at the site.

Figure 3-57 - Figure 3-58 show the changes in the dissolved phase plumes, represented as isoconcentration filled contours, in bedrock over time for the sum of

the chlorinated ethenes and the sum of the chlorinated ethanes respectively. An increased number of boreholes were drilled over the years and this is reflected by the shape of the plumes observed, with better refinement in the interpolation with an increased number of datasets over the years. The 1998 chlorinated ethanes concentration data shows two distinct plumes, one originating from the historical chlorinated hydrocarbons production and handling facilities (located in the north western part of the site); the other plume originating from the redundant hazardous waste site 2 located in eastern part of the site. In 2002, there is a reduction of the plumes sizes. Inspection of the 2012 concentration contours show that two chlorinated ethanes plumes start emerging from the redundant hazardous waste site 1, while the chlorinated ethanes plume from the redundant hazardous waste site 2 is no longer present. The isoconcentration filled contour plots for the chlorinated ethanes show similarities and differences compared to the chlorinated ethenes plots. Four plumes are visible in the 1998 plot, one originating from the historical chlorinated hydrocarbons production and handling facilities/storage tanks (located in the western part of the site); the second plume originating approximately 500 m downgradient of historical production facilities/storage tanks, a third originating from the redundant hazardous waste site 2 located in eastern part of the site; and a fourth originating from the redundant hazardous waste site 1. The chlorinated ethanes plot for 2002 is significantly different. In this case only one plume originating from the historical production facilities/storage tanks is visible. The 2012 chlorinated ethanes plot shows a single continuous plot from the historical production facility/storage tank. The anomalous data obtained for the 2002 chlorinated ethanes plot may be a result of sampling and/or analytical errors.

The total chlorinated hydrocarbons isoconcentration plots are provided in Figure 3-59. As discussed in the previous section, no free-phase DNAPL was evident at the redundant hazardous waste site 2. The groundwater plume originating from this source has likely resulted from residual DNAPL sources. The total chlorinated groundwater plume lengths are shorter than what would be expected for the volume of pooled and residual DNAPL at the site. A number of reasons (or combinations thereof) could be the cause of this. Fracture flow dominates movement of groundwater and contaminant at the site. It is possible that low interconnectivity of fractures together with low transmissivity has led to smaller than expected groundwater plumes.

Figure 3-57 to Figure 3-59 indicate a persistent dissolved phase plume emanating from the source zones. The persistence of the plumes resulting from the redundant hazardous waste sites may be attributed to current releases through the leakages of drums. However, this is not the case in the source zones associated with the historical handling and production facilities. The time required for dissolved and adsorbed contaminants to be flushed from the source zone was calculated assuming unidirectional and steady-state flow conditions which are subject to advection and sorption (dispersion was not considered in this calculation). The following equation was used (modified from Kueper and Davies, 2009) in the calculations:

$$t = \frac{LR_f}{v} \qquad \text{Equation 3-4}$$

Where:

t = the time required for contaminants to migrate through the source zone of length L in the direction of groundwater flow

v = average linear groundwater velocity

L = length of source zone in the direction of the flow

R_f = retardation factor for the contaminant of interest

The average retardation factor for each compound was calculated using Monte Carlo simulations (Appendix F). Results obtained are provided in Table 3-16 and indicate the presence of persistent plumes in the weathered zone.

Table 3-16: Calculated length of time required for the dissolved phase plume to detach from the weathered source zone

Chlorinated Hydrocarbon	Rf (Avg)	L (m)	v (m/yr)	t(yr)
PCE	79	90	0.43	16534.88
TCE	48	90	0.43	10046.51
Cis-1,2-DCE	34	90	0.43	7116.279
Trans-1,2-DCE	33	90	0.43	6906.977
1,1-DCE	26	90	0.43	5441.86
VC	18	90	0.43	3767.442
1,1,1-TCA	35	90	0.43	7325.581
1,1-DCA	25	90	0.43	5232.558
1,1,2,2-TetCA	77	90	0.43	16116.28
1,1,2-TCA	48	90	0.43	10046.51
1,2-DCA	33	90	0.43	6906.977
CCl_4	38	90	0.43	7953.488
$CHCl_3$	27	90	0.43	5651.163

Table 3-17 provides the summary of pore water analysis of samples taken from stream piezometers. Only four (4) piezometers showed detectable trace values of dissolved chlorinated hydrocarbon. Analysis of chlorinated ethenes and methanes were below detection limit in all samples. Trace concentrations of 1,2-DCA was

present in the piezometer samples shown below. The presence of 1,2-DCA in pore water beneath the streams indicates that dissolved phase 1,2-DCA discharges to the southern intermittent stream. This is consistent with the measurement of upward vertical gradients obtained from the piezometer data.

Table 3-17: Pore water results for stream piezometer samples

Piezometer ID	1,2-DCA (µg/L)
SMPA14	2.1
SMPA15	1.5
SMPA16	2.5
SMPA18	0.74

In addition to a hydrophobic liner installed in CBH42, a felt activated carbon technology (FACT) was concurrently installed in the hole in order to test the technology as a method of obtaining depth discrete dissolved phase chlorinated hydrocarbon pore water concentrations. The complete set of results obtained is provided in Appendix G. The results are semi-quantitative and are measured in µg/g of activated carbon. Figure 3-60 shows the comparison of the results obtained from the FACT liner to the locations of DNAPL found using the ribbon NAPL sampler. Two (2) peaks in concentrations are seen in the graph of concentration vs depth, which correspond to the locations of the transmissive fractures identified through installation of the ribbon NAPL sampler.

The biogeochemical characteristics of the free phase DNAPL and the aqueous phase DNAPL are provided in the next chapter. Plots of time-series graphs of the compounds in the PCE and 1,1,2,-TetCa sequential biodegradation sequence along transacts was inconclusive. Generally, all compounds have high concentrations in the source zone with no distinct patterns. Concentrations of daughter products outside the source zone are negligible. An additional complication is that a vast number of compounds where used or produced (either as final product or as intermediates) at the site. This makes it extremely difficult to determine any sequential patterns using concentration data alone.

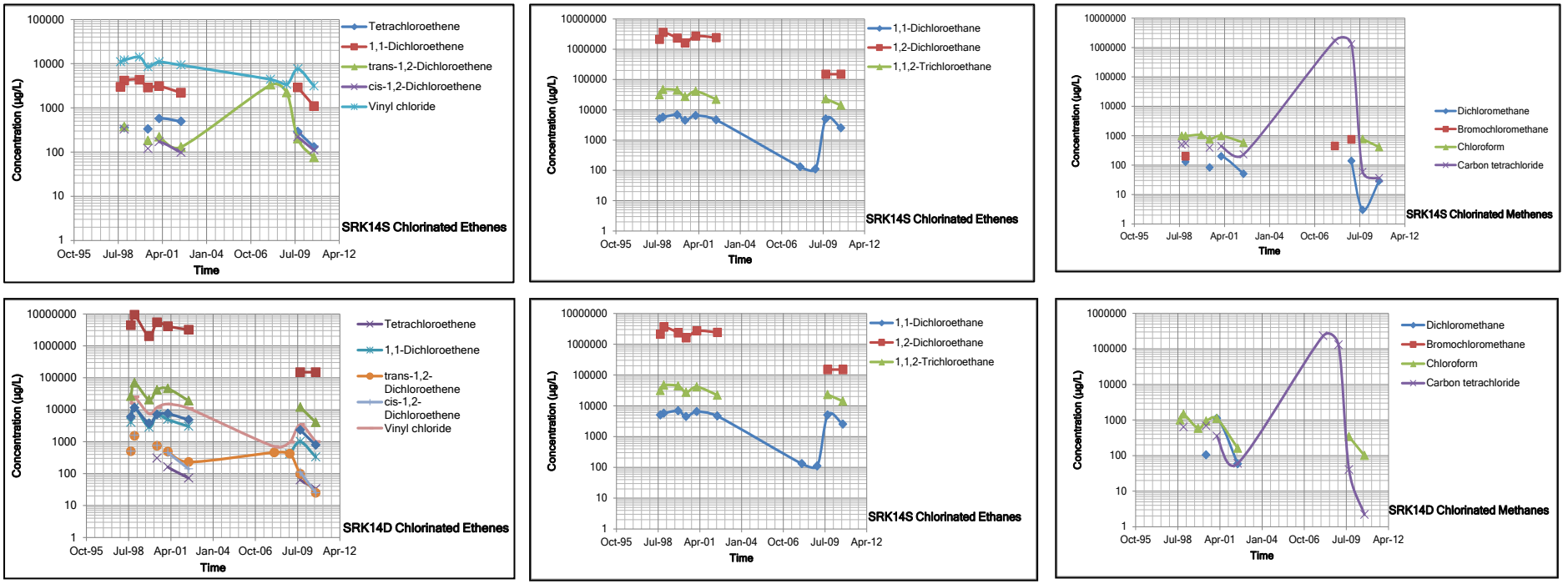

Figure 3-56: Variation in chlorinated ethenes, ethanes and methanes concentrations in SRK14S/D

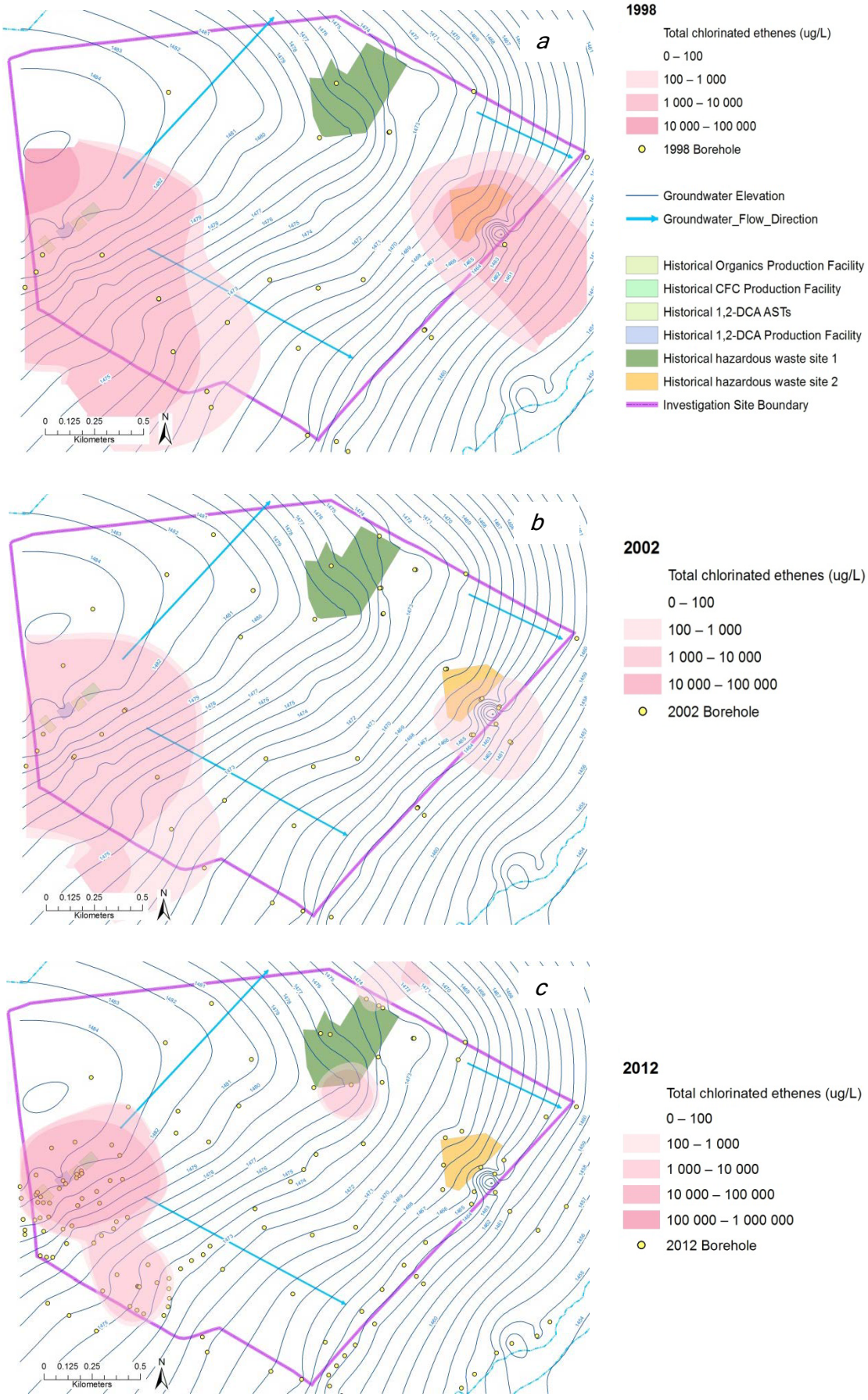

Figure 3-57: Total chlorinated ethenes plume (a) 1998, (b) 2002 and (c) 2012

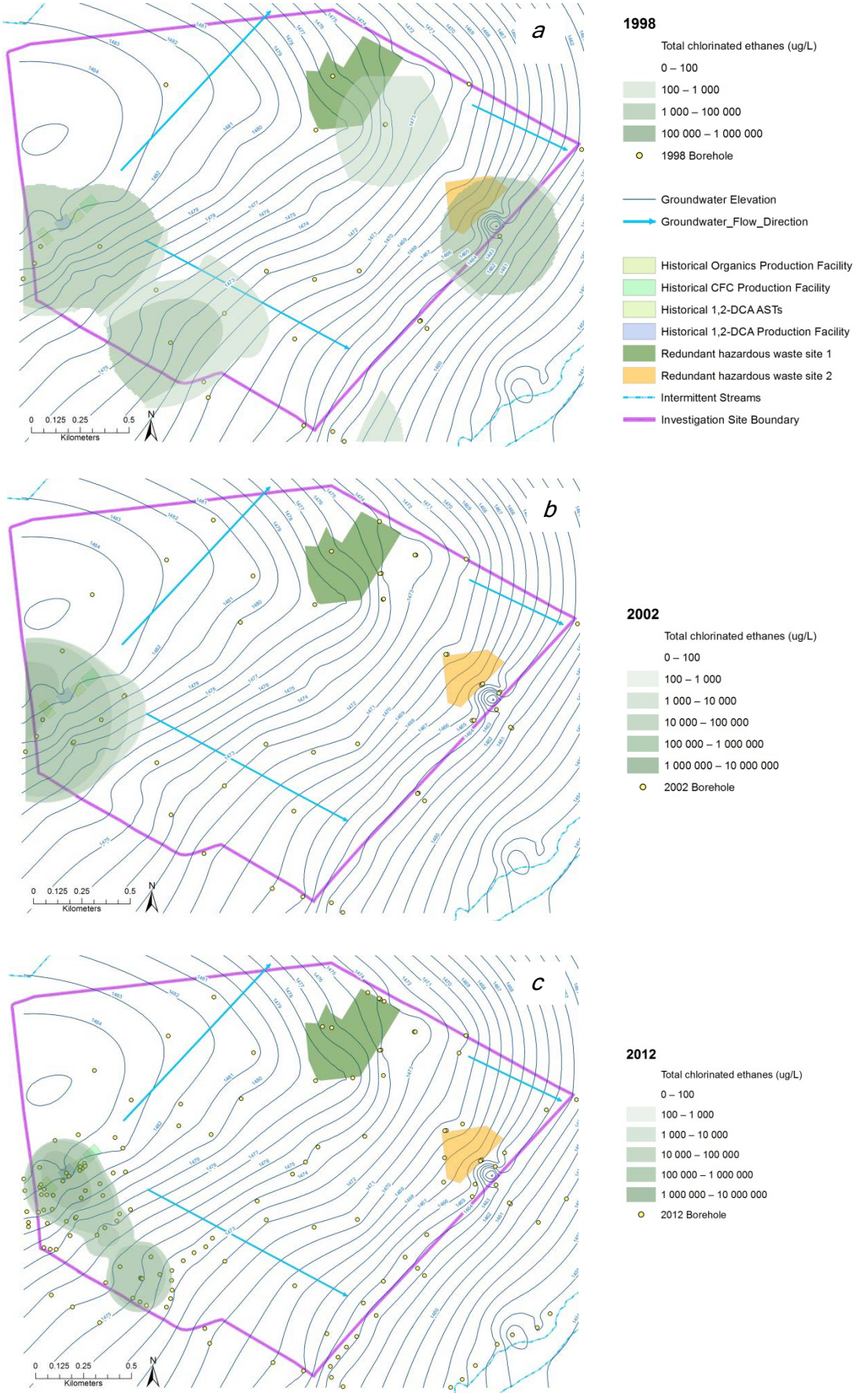

Figure 3-58: Total chlorinated ethanes plume (a) 1998, (b) 2002 and (c) 2012

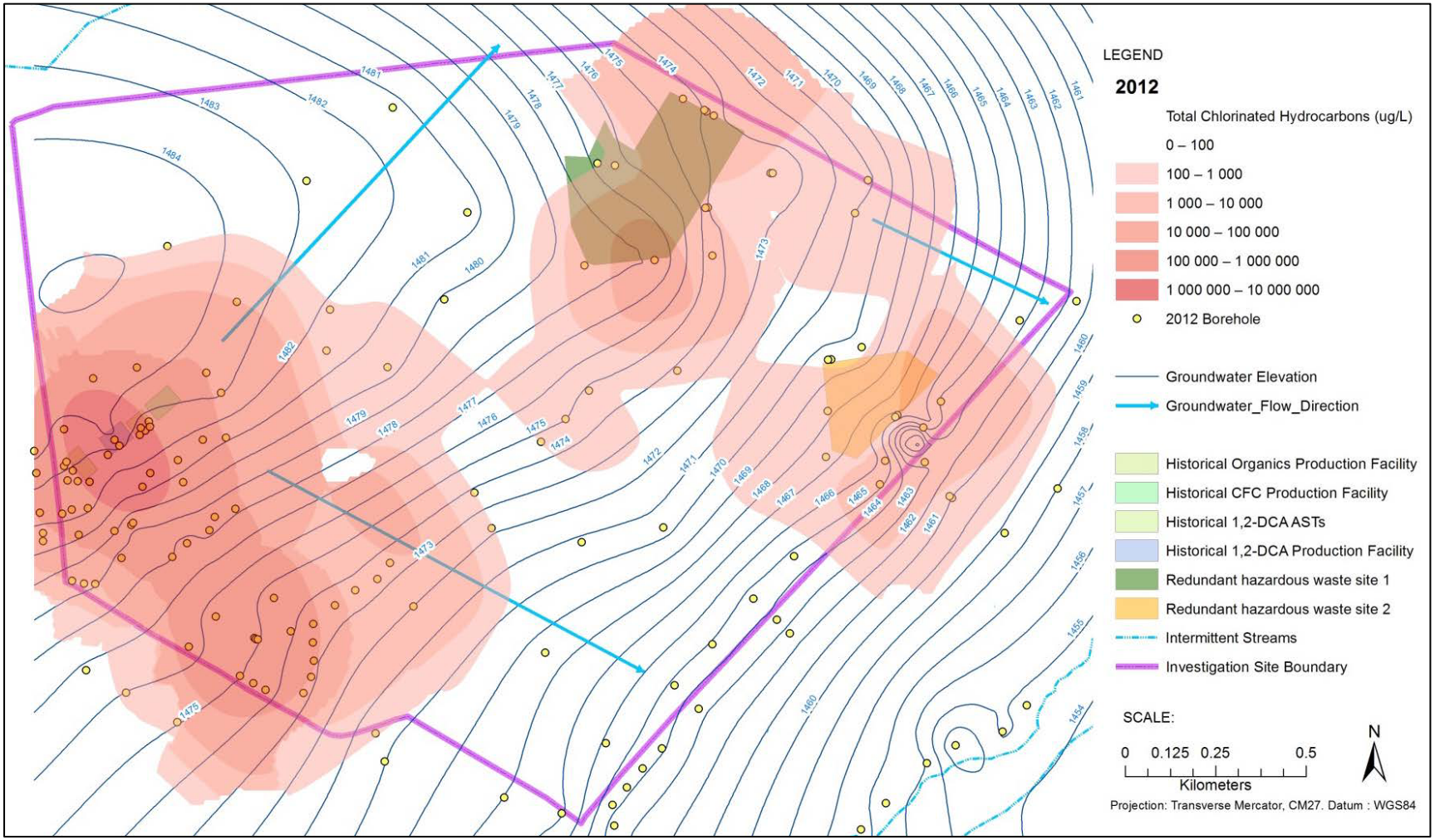

Figure 3-59: Total chlorinated hydrocarbon DNAPLs isoconcentrations filled contours plot (boreholes located in unweathered dolerite)

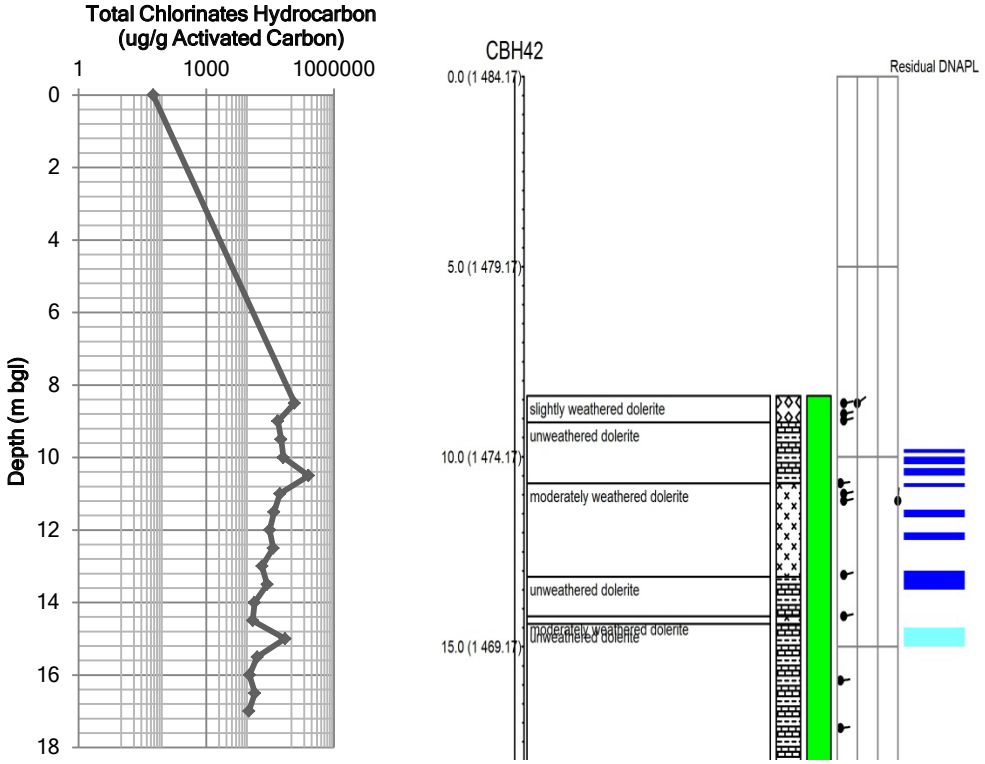

Figure 3-60: Semi-quantitative depth discrete total dissolved hydrocarbon concentrations

3.3.6 Biogeochemical characteristics

3.3.6.1 Biodegradability of chlorinated solvent DNAPL

The modelled results for the individual components of the DNAPL samples (Table 3-15) using EpiWeb v4.0.BioWIN are provided in Appendix H. The results indicate that the DNAPL at the site is not readily biodegradable.

3.3.6.2 Toxicity profile of the groundwater downgradient of source zones

The BOD, COD and DO results for groundwater samples from selected boreholes at the site are provided in Table 3-18. The biodegradability indices of the selected boreholes (located downgradient of potential source zones) indicate that in general biodegradation is not likely to occur at the site. The BOD:COD ratio for CAP01S indicate that there is potential for biodegradation at this sample point. This borehole is located outside of any DNAPL source zones or plumes.

Table 3-18: Chemical oxygen demand, biological oxygen demand and dissolved oxygen results

Borehole ID	COD (mg/L)	BOD (mg/L)	BOD:COD	Biodegradability Index Descriptor	DO (mg/L)
SRK02S	159	15	0.09	Not biodegradable	0.1
SRK02D	15	5	0.33	May be biodegradable	0.1
MLR01S	68	10	0.14	Not biodegradable	0.1
SRK34S	192	20	0.1	Not biodegradable	0.1
SRK12D	140	10	0.07	biodegradable	0.1
SRK03S	184	10	0.05	biodegradable	<0.1
SRK03D	184	20	0.1	Not biodegradable	0.1
SRK21D	121	20	0.16	Not biodegradable	0.1
CAP01S	13	13	1	biodegradable	0.1
SRK15S	179	30	0.17	Not biodegradable	0.1
SRK15D	181	10	0.05	Not biodegradable	0.1

The percentage inhibition can be interpreted as the toxicity profile for the site. In general, all the results (Table 3-19) indicate that the groundwater located downgradient of source zones are fairly toxic, a factor that must be considered in risk assessments. While this is a rapid, on-site test for toxicity, it does not provide any information on the cause of toxicity. This is a limitation for sites with a large variety of contaminants that can contribute to the groundwater toxicity.

Table 3-19: Toxicity screening of groundwater

Borehole ID	% Inhibition	Location Descriptor
SRK02S	54.3	Downgradient of redundant waste site 2
SRK02D	49.2	Downgradient of redundant waste site 2
MLR01S	41.4	Located east of historical production and handling facilities
SRK34S	74	Downgradient of redundant waste site 1
SRK12D	27.3	North of southern effluent dams
SRK03S	31	Southern boundary of site
SRK03D	42.1	Southern boundary of site
SRK21D	65	Downgradient of historical production and handling facilities
CAP01S	19.4	Downgradient of southern effluent dams
SRK15S	71.2	Downgradient of redundant waste site 1
SRK15D	84.2	Downgradient of redundant waste site 1

3.3.6.3 Preliminary screening for PCE degradation using DNA-based techniques

Field measurements collected from the boreholes that were screened for biodegradation are provided in Table 3-20. Redox measurements indicate reducing conditions. Samples were taken during winter, hence the moderate groundwater temperatures recorded.

Table 3-20: Field physical measurements

Borehole ID	Temperature (°C)	pH	Conductivity (mS/cm)	ORP (MV)
MLR01S	18.3	7.59	6.72	4
SRK12D	15.5	7.27	1.20	31
SRK21D	18.3	7.12	9.43	12
SRK34S	19.4	7.37	2.62	20
SRK02S	18.4	6.51	13.8	-65
SRK02D	20.0	6.71	10.55	-29

Visible DNA was extracted from samples obtained from MLR01S, SRK34S and SRK02S (Figure 3-61a). All other samples were below detection limits. Subsequent addition of enzyme stabilisation additives allowed for further amplification of the DNA (shown in Figure 3-61b) shows visible DNA in all boreholes apart from SRK21D (located within the primary source zone). DNA concentration results and the purity of the genomic DNA extracts are provided in Table 3-21. The results indicate a correlation between DNA amplification and DNA concentration, with higher DNA extraction yields resulting in higher amplifications.

As this was only a screening method, no targeted PCE degrading bacteria were isolated from the samples. However, the presence of bacteria is evident in the samples, apart from the sample taken from SRK21D. The absence of bacteria from SRK21D is likely related to the high levels of contaminants in this sample, indicating that the technique might not be viable within source zones.

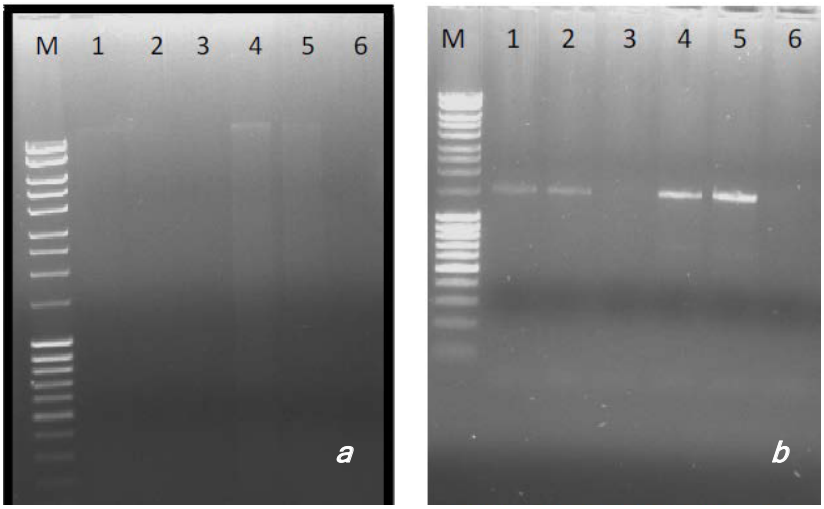

Figure 3-61: Genomic DNA extracted from selected borehole samples (a) pre-optimisation and (b) post-optimisation. Lane M, MassRulerTM DNA Ladder (Fermentas); lane 1, MLR01S, lane 2, SRK02D; lane 3, SRK12D; lane 4, SRK34S; lane 5, SRK02S, lane 6, SRK21D

Table 3-21: Summary of DNA concentration and purity of genomic DNA extracts

Borehole ID	Concentration (ng/µL)	A260/280
MLR01S	28.53	1.63
SRK12D	15.91	1.44
SRK21D	21.83	1.55
SRK34S	27.77	1.74
SRK02S	23.21	1.55
SRK02D	17.43	1.8

3.3.6.4 Compound specific isotope analytical results

CSIA ($\delta^{13}C$ and $\delta^{37}Cl$) was undertaken in 2008 and 2009 from existing boreholes at the site. The results obtained are summarised in Table 3-22. Samples were submitted from boreholes along downgradient transects of potential source zones (as was thought in 2008/2009) and included the historical production and handling facilities and the redundant waste sites.

SRK 21D, SRK 12 D and CAP01S are located on a transact with increasing distance from the primary source area. PCE and its daughter products were present in all boreholes in measurable concentrations. However, apart from TCE, the other daughter products (1,2-DCE and vinyl chloride) concentrations were too low to detect using CSIA. A further complication in interpreting the data is that there may have

been convergence of degradation pathways as parent products such as 1,1,2,2-TCA and PCE could have produced daughter products.

Figure 3-62 and Figure 3-63 show the plot of $\delta^{13}C$ versus the natural logarithm of the groundwater concentrations for PCE and TCE respectively measured during the same time period (2009). Also shown in the plot are the ranges for pure phase products, based on literature values provided in Section 2.1.2.2. SRK02S and SRK02 D display the same range in $\delta^{13}C$ as that expected for pure product PCE or TCE. This indicates very little transformation (biotic or abiotic) of the groundwater at this point. SRK02S/D is located immediately downgradient of the redundant hazardous waste site 2. The variation of the other samples from the expected ranges in $\delta^{13}C$ for pure phase product indicates transformation from the original source. The more positive $\delta^{13}C$ indicates enrichment of the samples compared to the source, indicating that degradation is occurring at the site. The variations of the samples in Figure 3-62 and Figure 3-63 from the Rayleigh correlation (shown as a straight line) indicate mixing with different contaminant sources. As different batches of pure product were manufactured at the site, this is not an unexpected result as different batches of pure product may have different isotopic signatures. Due to the small data set it is not possible to definitively state whether the field data show a Rayleigh correlation or not and hence whether Equation 2-8 can be applied.

The rapid decrease in chlorinated solvents concentrations from the source area, along the groundwater pathways to the southern intermittent stream (Figure 3-59) indicate that some biotic degradation may be a factor within source area (evidenced from the presence of daughter products that are known not to have been used or produced on site such as cis- and trans-1,2-DCE) while abiotic degradation becomes the significant contaminant reduction process within the dissolved phase plume.

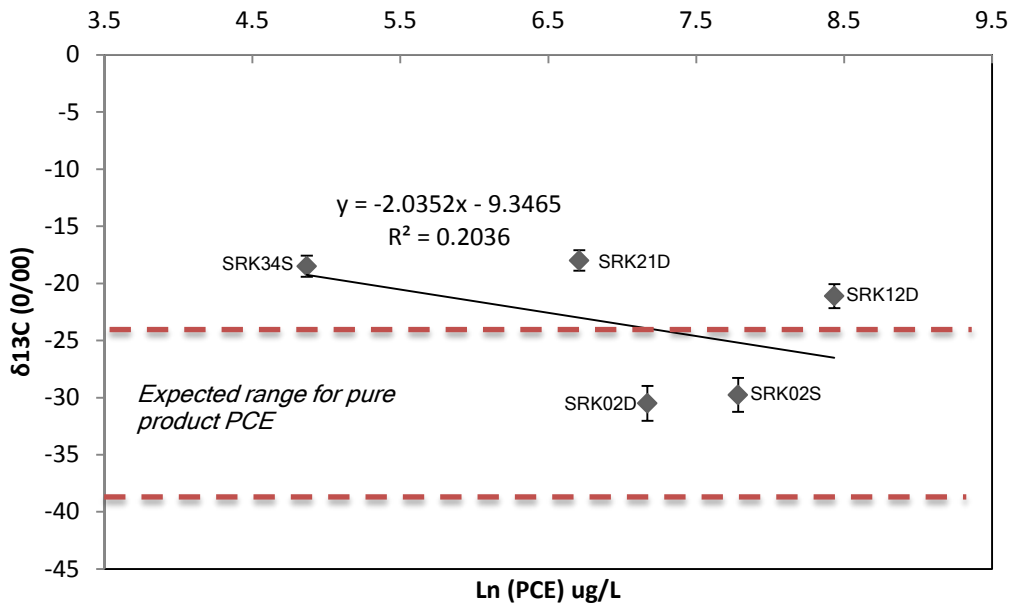

Figure 3-62: $\delta^{13}C$ vs natural logarithm of PCE concentration in boreholes

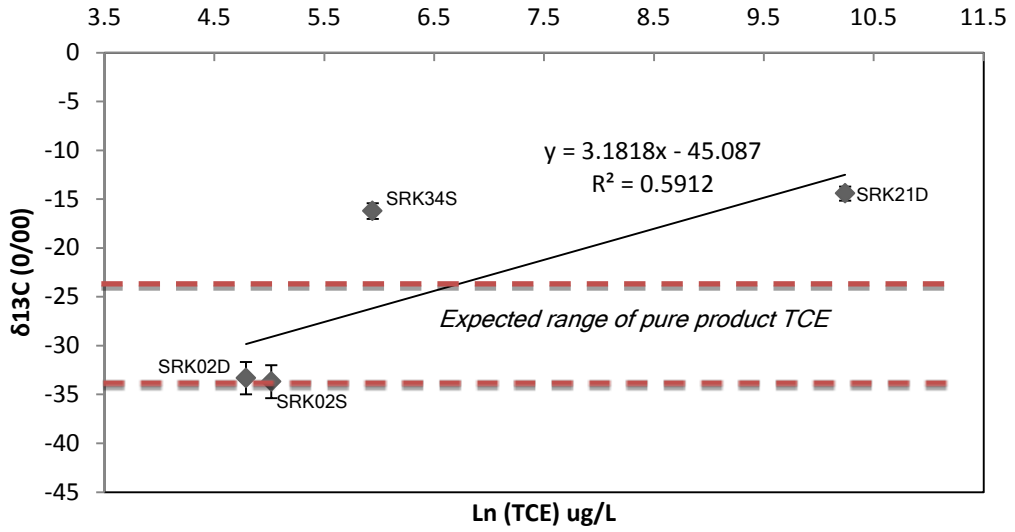

Figure 3-63: $\delta^{13}C$ vs natural logarithm of PCE concentration in boreholes

Table 3-22: Summary of compound specific isotope results

Borehole ID	δ13CVPDB (0/00)																δ37ClSMOC		
	1,1-DCE		cis-1,2-DCE		PCE		TCE		1,2-DCA		1,1,2-TCA		CHCl3		CCl4		PCE	TCE	cis-1,2-DCE
	Aug-08	Apr-09	Aug-08	Apr-09	Aug-08	Apr-09	Aug-08	Apr-09	Aug-08	Apr-09	Aug-08	Apr-09	Aug-08	Apr-09	Aug-08	Apr-09	Aug-08	Aug-08	Aug-08
SRK12D	BDL	BDL	BDL	BDL	-18.84	-21.11	BDL	BDL	BDL	BDL	BDL	BDL	-36.56	-25.52	-26.63	-32.54	-0.81	BDL	BDL
SRK21D	-22.44	-15.49	BDL	BDL	-19.02	-18	-20.17	-14.42	0.26	-5.31	-12.81	-8.56	-28.56	-14.52	-25.52	BDL	4.45	-0.41	10.91
SRK34S	BDL	BDL	BDL	-24.2	-17.74	-18.51	-21.23	-16.22	11.41	13.05	BDL	BDL	-18.67	-21.45	BDL	BDL	4.00	8.33	9.05
SRK02S	NA	BDL	NA	-29.49	NA	-29.77	NA	-33.7	NA	7.63	NA	BDL	NA	-30.55	NA	BDL	NA	NA	NA
SRK02D	NA	BDL	NA	-30.57	NA	-30.5	NA	-33.33	NA	8.47	NA	BDL	NA	-31.12	NA	BDL	NA	NA	NA
CAP01S	BDL	BDL	BDL	BDL	BDL	BDL	BDL	BDL	-5.92	8.88	BDL	BDL	BDL	BDL	BDL	BDL	BDL	BDL	BDL
SRK03D	BDL	BDL	BDL	BDL	BDL	BDL	BDL	BDL	-8.47	-7.15	BDL	BDL	BDL	BDL	BDL	BDL	BDL	BDL	BDL
MLR01S	BDL	BDL	BDL	BDL	-22.06	-27.73	BDL	BDL	BDL	BDL	BDL	-17.84	-52.25	BDL	-42.10	-40.72	BDL	BDL	BDL
SRK15S	NA	BDL	NA	BDL	NA	-26.7	NA	BDL	NA	BDL	NA	BDL	NA	BDL	NA	BDL	NA	NA	NA
SRK15D	NA	BDL	NA	BDL	NA	-28.5	NA	BDL	NA	BDL	NA	BDL	NA	BDL	NA	BDL	NA	NA	NA

3.4 Conceptual Site Model

The conceptual site models of the site are provided as simplified 2-dimensional interpretations of the DNAPL sources, the affected and influencing geological media, fate and transport mechanisms and potential exposure pathways. These are shown in Figure 3-64, which is the plan view conceptual site model; and Figure 3-65, which is the schematic cross sectional conceptual site model for the western perimeter of the site.

A mixture of chlorinated hydrocarbon DNAPLs are found at the Investigation Site in vapour, adsorbed, DNAPL and aqueous phases in the source zones and as vapour, adsorbed and aqueous phases in the dissolved plume. The distribution and concentrations of the chlorinated hydrocarbons at the site varies from one locality to the next and is dependent on the following:

1. DNAPL source
    - Location of release area
    - Volume of release
    - Nature of release
    - Physical properties of DNAPL(s)
2. Geological heterogeneities
    - Bulk density
    - Primary porosity
    - Permeability
    - Depth and extent of weathering
    - Joint/fracture intensity
    - Fracture orientation
    - Fracture interconnectivity
3. Hydrogeology
    - Fracture transmissivity
    - Groundwater flow direction
    - Hydraulic gradient
4. Biotic and abiotic degradation processes

This research has allowed an updated understanding of the release areas at the site. This is summarised in Table 3-23. Distinct vapour phase plumes are associated with the adsorbed DNAPL in the overburden. Smaller concentrations of vapour are

however found throughout the site indicating the partitioning of dissolved phase chlorinated hydrocarbon DNAPL in shallow groundwater into the unsaturated zone.

Table 3-23: Release areas and nature of release for the Investigation Site

Release Area	Nature of Release
Historical 1,2-DCA above ground storage tanks area	Regular release over a long time-frame
Historical production and handling facilities 2	Intermittent spills over a large area for a long time-frame
Redundant hazardous waste sites (1 and 2)	Once-off release of DNAPL (likely as a result of a drum leak or spills during off-loading) in a localised area

Sampling of the weathered profile indicated that the primary source zone in the weathered profile is located at the historical production and handling facilities (2) and sporadically around the redundant hazardous waste sites. Adsorbed and free phase DNAPL is found in the weathered profile.

Residual and free phase pooled DNAPL is found in the fractured bedrock in the following areas:

1. Below and continuously for a distance of approximately 850 m downgradient of the historical 1,2-DCA above ground storage tanks and 1,2-DCA production facilities. The signature of the DNAPL is predominantly 1,2-DCA and 1,1,2-TCA.
2. Below and continuously for a distance of approximately 250 m downgradient of the CCl_4 and PCE production facilities, with representative signatures.
3. At 2 localised positions associated with the redundant hazardous waste site 1.

The locations of residual DNAPL were identified using ribbon NAPL samplers and hydrophobic dyes on the cores. Pooled DNAPL was found primarily associated with stratigraphic traps associated with a decrease in porosity or above less permeable geological layers. Pooling of DNAPL occurs generally occurs at approximately 20 m bgl and 37 m bgl.

2-D surface resistivity anomalies in shallow and deep bedrock are mostly associated with the location of DNAPL source zones at the Investigation Site.

The dissolved phase chlorinated hydrocarbon plumes at the site were significantly less horizontally extensive than expected, given the extensive source zones. This is likely attributed to low transmissivity, limited interconnectivity of fractures and biotic and abiotic degradation.

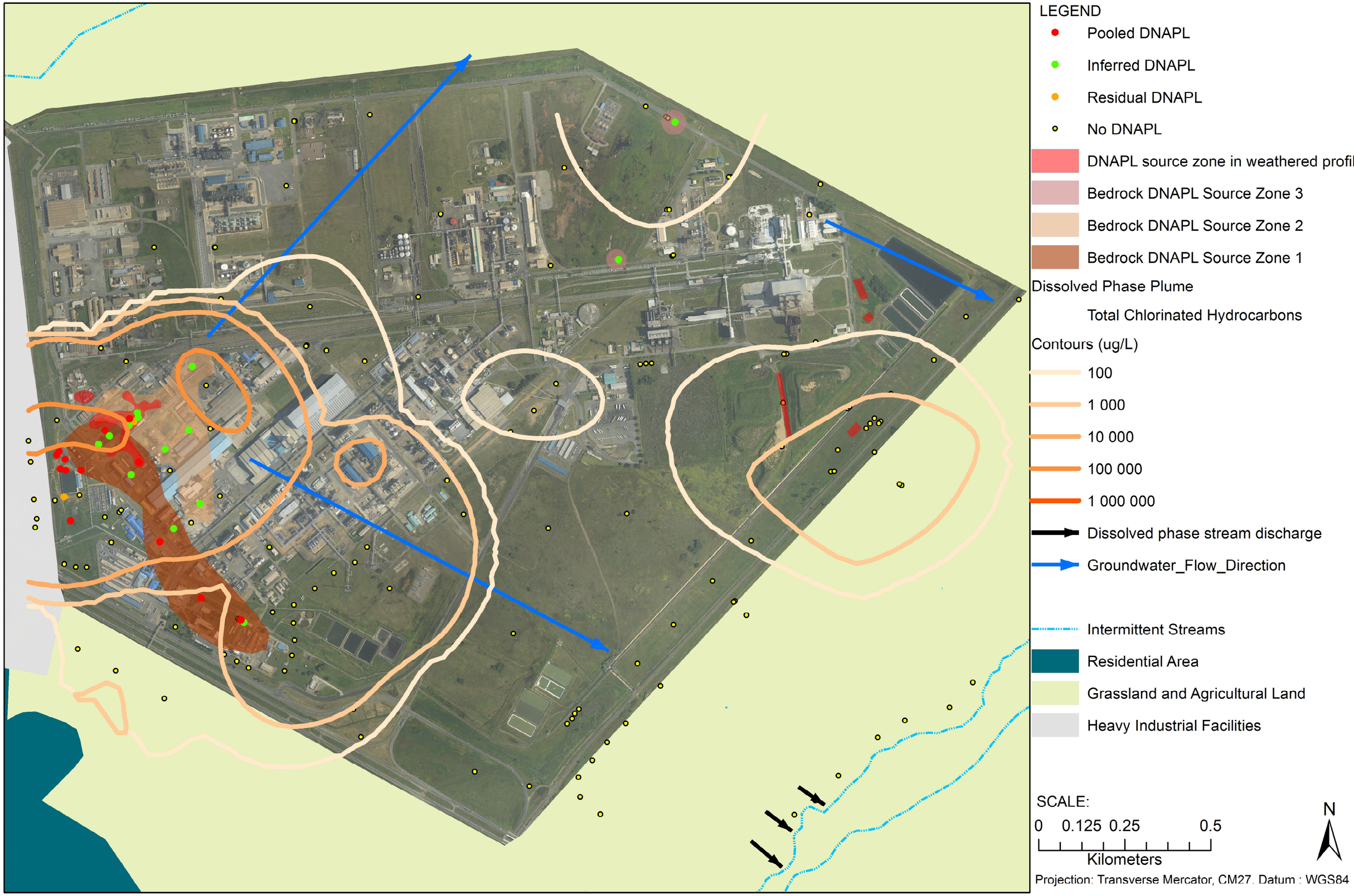

Figure 3-64: Plan view conceptual site model of the Investigation Site

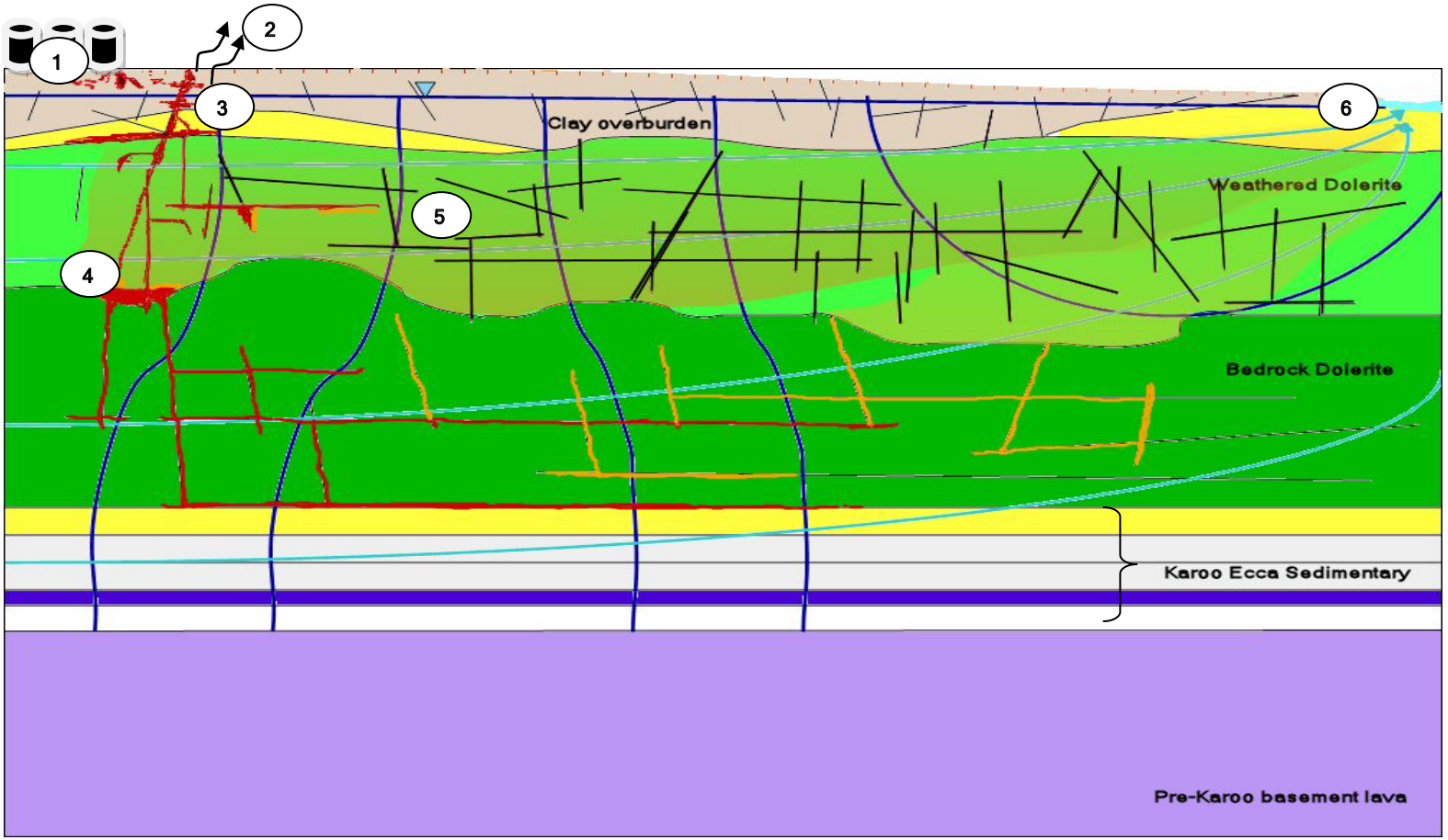

Figure 3-65: Schematic cross sectional view of the conceptual site model for the Investigation Site

1 Residual and adsorbed DNAPL in unsaturated zone

2 Vapour plume

3 Residual DNAPL in saturated zone

4 Pooled DNAPL

5 Dissolved phase plume

6 Dissolved phase discharge to stream

The chlorinated hydrocarbon DNAPL found at the site do not readily degrade. Additionally, microbial activity within source zones seems to no longer be viable. This is likely related to the high volume and toxicity of the source zones. However, the presence of daughter products of chlorinated ethenes and ethanes within source zones indicate that biotic degradation did take place initially. The predominantly reducing conditions as well as the presence of microbial activity in the dissolved plume indicate a potential for biodegradation of contaminants.

The permeability of the weathered profile is very low, with groundwater migration being controlled by the location, orientation and interconnectivity of joints and hydraulic gradients. In general, zones of deeper weathering are consistent with sub-vertical joint patterns and coincidental with synclinal and anticlinal flexure axes. The bedrock profile also has very low permeability. The flow of groundwater is controlled by the location, orientation and interconnectivity of joints/fractures and hydraulic gradients. Locally developed sub-vertical joint sets act as conduits for vertical groundwater (and DNAPL) transport through the low permeability dolerite sill to the more intensely jointed basal contact zone between the dolerite sill and the Karoo Ecca sandstone.

Based on the location and extent of the chlorinated hydrocarbon contaminated on the site, the following are identified as potential exposure pathways and receptors: direct dermal contact with shallow contaminated soils during construction, vapour intrusion into on-site buildings, and discharge into the intermittent stream south west of the site border. Human health and ecological risk assessments are beyond the scope of this study. A Tier 2 risk assessment is being undertaken by Consultants.

CHAPTER 4

4 DEFINING THE VALUE AND LEVEL OF SOURCE ZONE CHARACTERISATION REQUIRED IN A FRACTURED ROCK ENVIRONMENT

4.1 Source Zone Characterisation in a Complex Geo-contaminant Setting

DNAPL source zone characterisation is important to help define source zone remediation design. Site sub-surface heterogeneities make the detection of source zones (particularly adsorbed or residual DNAPL) difficult. Chapter 3 of this research explored a case study of an industrial site in South Africa where various approaches were used to delineate the DNAPL source zones in a complex geological setting. The site makes an interesting case study to explore the evolution of the value of efficient characterisation through different approaches over time of evolving legislative requirements and increasing knowledge of the risks and challenges posed by DNAPLs. Figure 4-1 is a schematic illustration of the effort made into understanding the site characteristics and risks associated with contaminants through reconnaissance and detailed assessments over time. The drilling of monitoring wells in the mid- to late- 1990's corresponds with the increased environmental awareness internationally of non-aqueous phase liquids as well as the promulgation of legislation related to the protection of natural resources and the duty of preventing and/or rectifying environmental damage.

A toolbox approach was adopted for characterisation of the site in the mid-2000's. This was followed by combination with the Triad approach in order to obtain better resolution data for the site. The outcome of studies at the site were to produce various numerical or conceptual models in order to assist with determining the risks associated with the contaminants at the site and to assist with further data gathering or remediation planning.

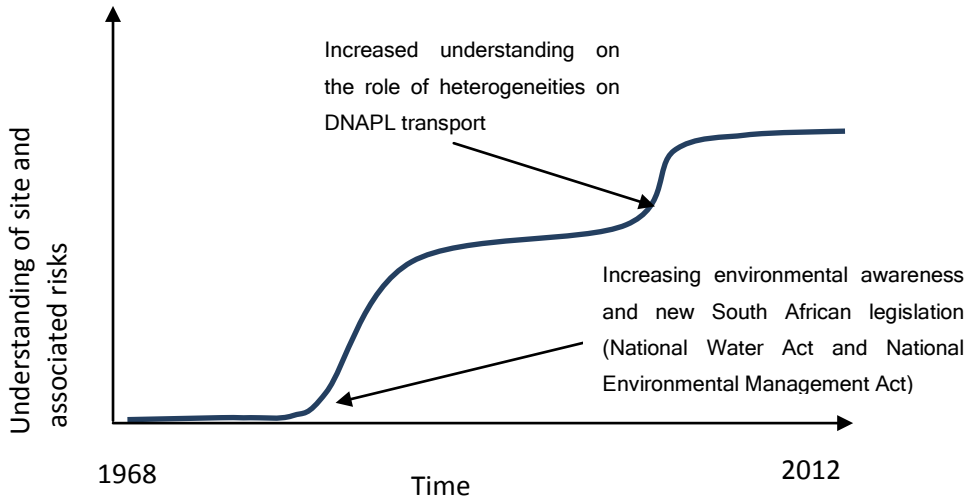

Figure 4-1: Schematic illustration of the extent of site assessments at the site over time

Traditional approaches can lead to either an under or over estimation of the source zones. Figure 4-2 is a schematic illustration of incorrect estimation of source zones based on a traditional approach. In the schematic, the borehole located in "actual source 1" is the only borehole that identifies a "true positive" source, while the extent of the "Actual Source 1" and the "Actual Source 2" go undetected. Real life geological setting are typically heterogeneous and anisotropic which further complicates the scenario of achieving cost optimisation of source zones through characterisation using traditional approaches.

The approaches used in this study for source zone characterisation are novel approaches that have been adapted to the South African scenario. In this case the use of rapid measurement tools and *in situ* bedrock characterisation tools has allowed for an improved understanding of site conditions. The decision on what remediation alternatives should be considered would be dependant on a site-specific risk assessment. This is being considered through other studies.

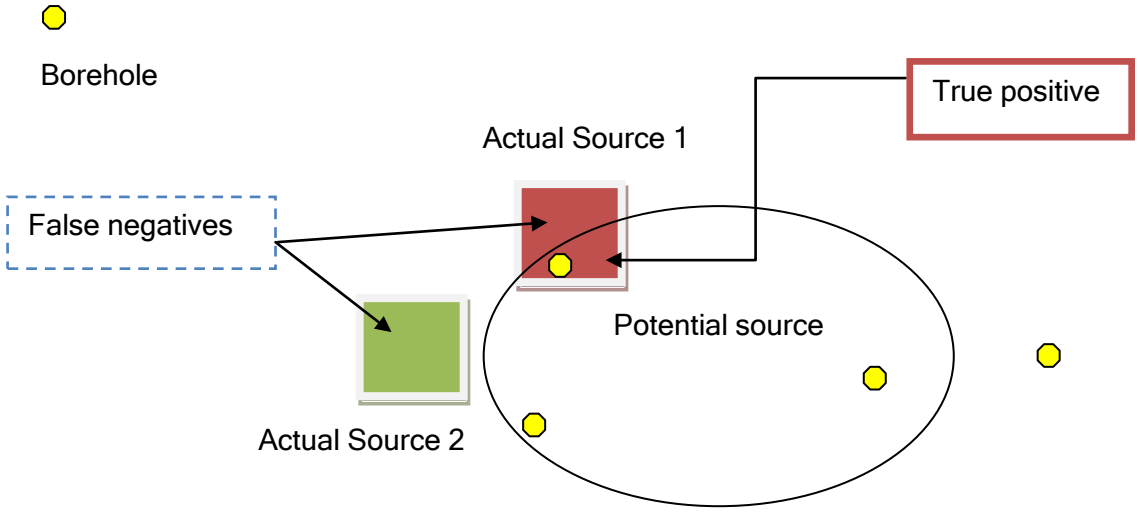

Figure 4-2: Schematic representation of incorrect estimation of source zones based on traditional site characterisation approach (modified from Ramsey *et al.*, 2002)

For the weathered zone investigation, the on-site laboratory equipment was imported from the USA at a cost of USD290 000/month (actual 2010 cost) or R2 552 000/month (using a R8.8 to a dollar exchange rate). A total of 1392 samples were collected and analysed over a 2 month period. The total cost for acquiring near real-time data that influenced decision making and allowed for delineation of the weathered source zone was hence approximately R5 million. This equates to a cost of approximately R3600/sample. If the same number of samples were collected using traditional approaches the cost of the analysis alone would be R1.7 million (assuming a cost per sample of R1200). This cost excludes the cost of mobilisation and demobilisation for every sample batch and the wait time for acquiring the analysis nor the time to analyse data periodically. Based on this comparison alone, the use of an on-site laboratory seems less cost-effective if one uses the quotient of efficiency of cost, where

$$\textbf{Efficiency}_{\textbf{cost}} = \frac{\textbf{quality of information}}{\textbf{cost of information}} \quad \textbf{Equation 4-1}$$

(modified from Miansney and McBratney, 2002).

In order to ensure that the quality of information obtained using an on-site laboratory was comparable to that which would have been obtained from an off-site laboratory strict QA/QC protocols were adhered to as described previously. If quality of information is assumed to be 1, efficiency of cost in this case then becomes a function of the reciprocal of the cost of information. A higher cost will hence produce a lower cost efficiency and *vice versa*. This calculation of efficiency does not take into consideration whether the data collected has a value or not. This is considered

further in the next chapter. Economies of scale however produce a very different scenario. Commercial laboratories analyse samples in batches as they are received from different clients. An on-site laboratory on the other hand is dedicated to the sampling program. An on-site laboratory can within a 2 month period analyse more samples than a commercial laboratory if allowed to run 16 hours a day[4]. Hence, if it is known (or planned) that sampling is likely to produce large sample sizes; use of an on-site laboratory can have a higher Efficiency of cost. Figure 4-3 is a plot of the cost of analysis for varying sample batch size using a commercial laboratory. At a critical mass of approximately 4000 samples the cost of analysis using a commercial off-site laboratory is equivalent to having a dedicated laboratory on-site for a two month period.

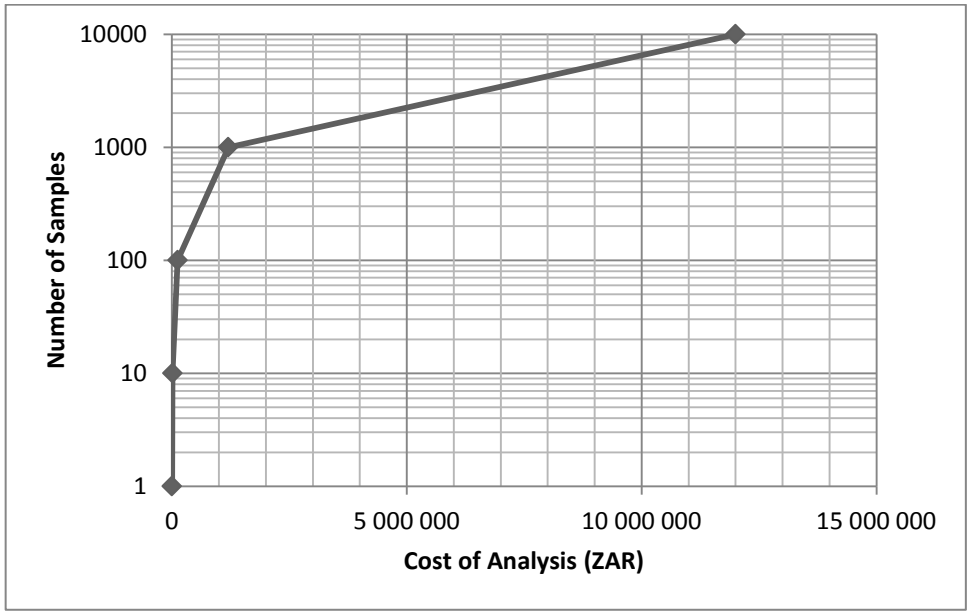

Figure 4-3: Plot of cost of analysis for batches of samples using an off-site commercial laboratory

The use of ribbon NAPL samplers in fractured rock at the Investigation Site allowed for qualitative, semi-quantitative as well as quantitative determinations of bedrock source zone characteristics. The information gathered from the use of the ribbon

[4] The on-site laboratory at the Investigation Site only operated during day shift hours (8 am-5pm) during a normal work week. Additionally, a limiting factor was the speed at which samples are supplied to the laboratory. Drilling also only took place during day shift/normal work week hours. This limitation can be overcome by having additional drill crews.

NAPL samplers included determination of the location of residual DNAPL, depth discrete fracture transmissivity calculations and semi-quantitative determination of depth discrete diffuse plume concentrations. In this case we have a single technology that can provide information that would traditionally require several other techniques. Efficiency of effort can be expressed as:

$$\mathbf{Efficiency_{effort}} = \frac{\mathbf{quality\ of\ information}}{\mathbf{effort\ to\ gather\ information}} \quad \text{Equation 4-2}$$

The installation of a ribbon NAPL sampler at the Investigation Site and the sampling took place on two separate days. The time taken to install the ribbon NAPL sampler was on average 3 hours and 23 minutes per borehole. Several other methodologies would have been employed (such as packer testing, single well tracer testing, installation and sampling of depth discrete piezometers) to gather the same information gathered through a single technology. Each of the alternative methodology would require a series of site mobilisation/demobilisation and site assessments of the drilled hole. A comparison of the tranmissivity measurements obtained through the use of the ribbon NAPL sampler vs that obtained by Packer testing at the Investigation Site indicates that higher sensitivities in terms of depth discrete fracture transmissivities are obtained through the use of the ribbon NAPL sampler vs Packer testing. This is however not always the case. Hence we can assume that the quality of information for the use of several technologies vs the ribbon NAPL sampler is the same. The Efficiency of effort therefore becomes the reciprocal of the effort to gather information. The ribbon NAPL sampler has a higher Efficiency of effort factor than using several other methodologies. As a result of less mobilisation the Efficiency of cost for the use of ribbon NAPL samplers are also higher than that of traditional approaches.

Table 4-1 provides a summary of the efficiency of cost and the efficiency for novel approaches used at the site compared to traditional approaches.

Table 4-1: Summary on the cost efficiency and the effort efficiency of novel approaches used at the Investigation Site

Methodology	$Efficiency_{cost}$	$Efficiency_{effort}$
High resolution soil sampling	Yes	Yes
On-site chemical analysis	Maybe	Yes
Ribbon NAPL sampling	Yes	Yes

4.2 Source Zone Characterisation Efficiency

While the gathering of further site information is useful in obtaining a clearer conceptual site model that can allow for the application of appropriate remediation technologies to reduce or mitigate risks at a site, a point is eventually reached when the knowledge obtained through the additional information does not justify the costs associated to obtain the additional information.

In the context of this study, the concept of the source zone characterisation efficiency is defined as the assessment of whether the methodology for assessing source zones in fractured rock environments are fit-for-purpose compared to the value that the method has in meeting an objective at minimum cost incurred. This is considered as an adaptation of the Level 2-type analysis in the Value of Information Analysis (VOIA framework proposed by Back, 2006) or data worth analysis (Freeze *et al.*, 1992) and is based on Bayesian decision cost-benefit analysis (Davis *et al.*, 1972; Korving and Clemens, 2002). Pre-posterior analysis is recommended by Baird (1989) and Freeze *et al.* (1992) prior to sample collection in order to determine its value.

Source zone characterisation efficiency can be estimated through analysing the value of information utilising the methodology outlined by Freeze *et al.* (1992). DNAPL source zones in fracture rock environments are typically heterogeneous and anisotropic. Efficiency can be a function of value of information using mathematical methods and/or the use of (subjective) intuition. The following steps are recommended which combines mathematical cost comparisons and intuitive methodologies.

Step 1: Undertake prior analysis

Let's assume a hypothetical scenario such as in Figure 4-4. A potential DNAPL source zone is identified at time t_0 through prior information analysis (reconnaissance site visits, interview of personnel, considering site history etc.). The potential DNAPL source zone is 100 m^2 (10m x 10 m) in this hypothetical case. The site is located on an unconsolidated sandstone unit. Fractured bedrock underlies the unconsolidated sandstone. This is underlain by compactly bedded unit of mudstone and siltstone. The water table level is at 5 m bgl. Release on site occurred 20 years ago over a 5 year period and has since stopped. Potential receptors are identified as the downgradient river and residents living downgradient of site

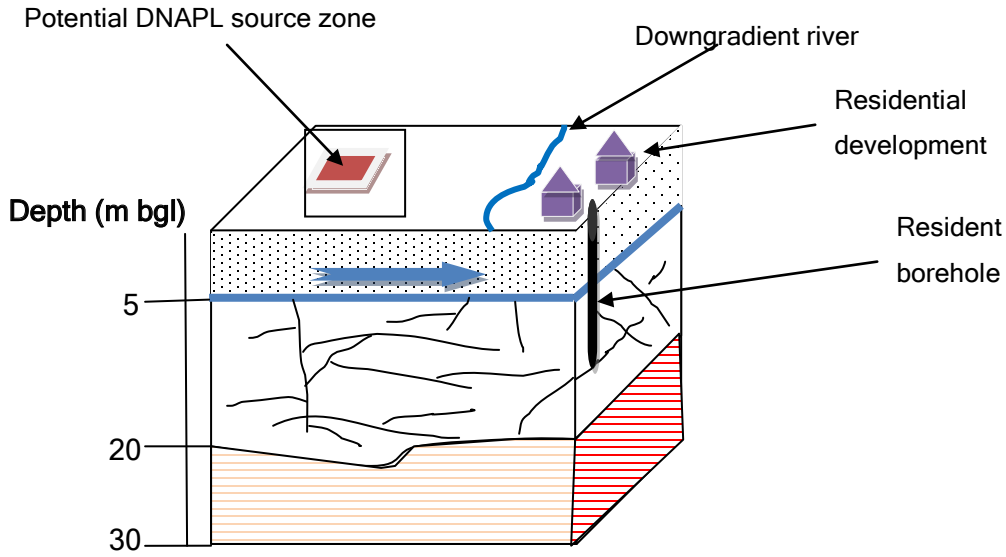

Figure 4-4: Hypothetical knowledge scenario at time t_0

Prior analysis is the analysis of available information available at time t_0. In this scenario very little information is available. A site owner is faced with the question as to whether the risk to potential receptors justifies the cost of further investigation. The probability that there is a risk to potential receptors can be designated as P(Risk), where P(Risk)at t_0 is a function of empirical indicators using the source-transportation pathways-potential receptors scenario. Hence, if P(Risk) is >0 (i.e. there is potential for harm to receptors), the cost of further investigation (C_{inv}) is justified.

Step 2: Undertake a pre-posterior analysis

Pre-posterior analysis considers the information that may be obtained through sampling at a particular point or interval. As various alternatives in sampling technologies are available in source zone characterisation, each alternative should be considered in terms of cost vs benefit. Another factor to consider is time-scale for completing an investigation.

For example, in the hypothetical scenario (Figure 4-4) the potential risks to receptors might not be considered imminent and the potential source zone may be further delineation through traditional approaches (i.e. batch sampling and analysis at an external laboratory over different time periods).

Pre-posterior analysis can be undertaken by following the data quality objective process (United States Environmental Protection Agency, 1994) combined with a cost-benefit analysis of each alternative.

Step 3: Posterior Analysis

Evaluate whether the information obtained through the data calculation has allowed for a decision. The question can be asked at this stage about whether there is sufficient information regarding the DNAPL source zone to evaluate appropriate remedial options to reduce risks to receptors.

Figure 4-5 is a proposed qualitative source zone efficiency estimation methodology that can be followed by site owners in evaluating how much more data collection is required. Should no data collection be warranted at that time, monitoring of the source zone should continue, with regular reviews of the situation to determine if the risk profile of the site has changed. This process is applicable to the South African context. A methodology for source zone characterisation in proposed in Figure 4-6, which integrates traditional and novel technologies. This methodology is based on the evaluations undertaken at the Investigation Site.

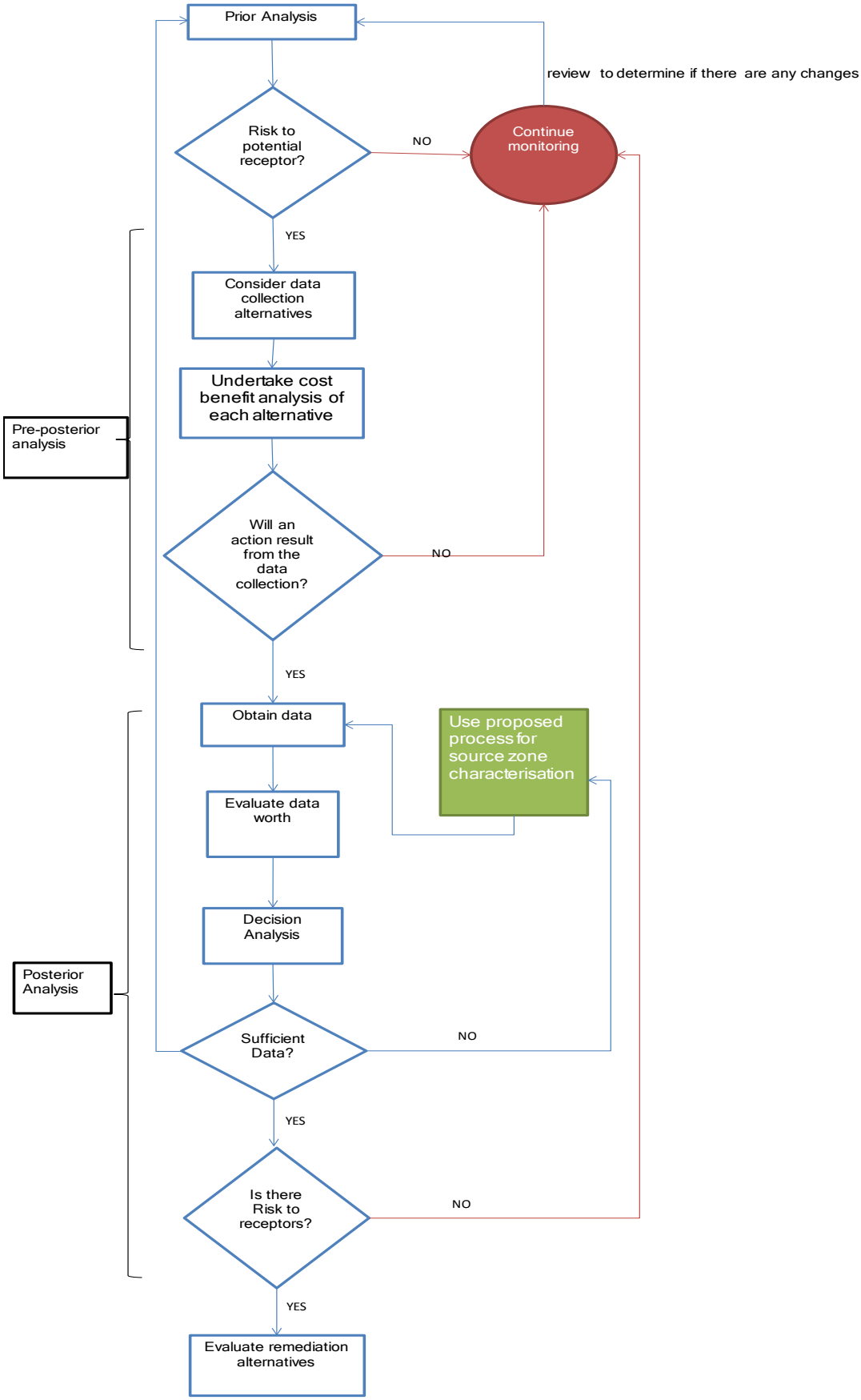

Figure 4-5: Proposed integrated appraoch to determine the level of source zone characterisation required

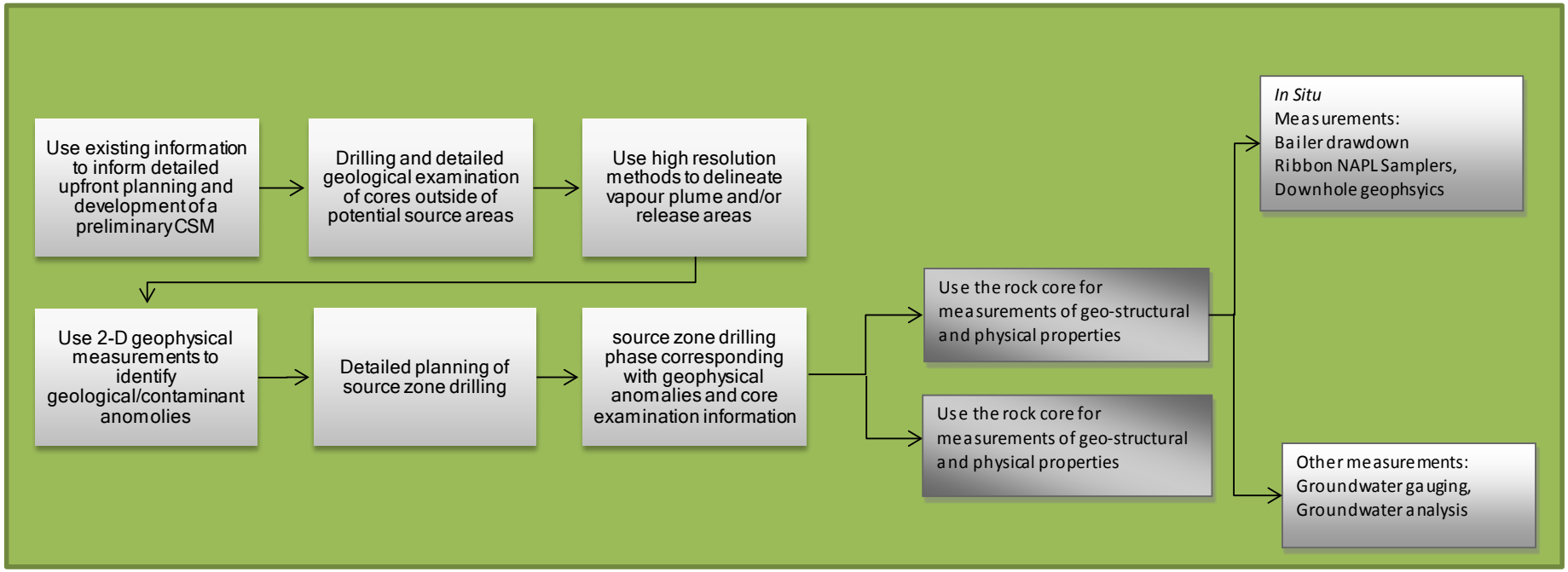

Figure 4-6: Proposed source zone characterisation methodology for the South African scenario

CHAPTER 5

5 CONCLUSIONS AND RECOMMENDATIONS

5.1 Novel Approaches to DNAPL Source Zone Characterisation in a Fractured Rock Environment

This research presents pioneering work in terms of source zone characterisation and the understanding on the architecture of chlorinated hydrocarbon DNAPLs in a fractured rock environment.

- This study is the largest known and most detailed mixed chlorinated hydrocarbon DNAPLs source zone characterisation in a fractured undertaken internationally.
- This is the first record of successfully locating and characterising in 3 dimensions the architecture of mixed chlorinated hydrocarbon DNAPLs in a fractured rock environment on a field scale.
- The success of locating and successfully characterising chlorinated hydrocarbon DNAPL sites has lagged in South Africa. This is largely due to the lack of available technologies. This study marks the first use of FLUTe^{TM} to characterise DNAPL in the South African fractured environment. The study also evaluates the cost efficiency and effort efficiency of this *in situ* technology and concludes that there is merit in importing this technology to South Africa due to its high success rate in locating residual DNAPL as well as in depth discrete fracture and dissolved phase plume characterisation.
- While previous South African authors (for e.g. Usher *et al.*, 2008) have proposed DNAPL site characterisation methodologies adapted to the South African scenario, the author in this research uses a systematic approach of combining traditional technologies together with emerging/novel technologies (such as high resolution sampling) to characterise chlorinated hydrocarbon DNAPL source zones. Various technologies are systematically evaluated in this study and the author can hence propose improved integrated approaches to undertake fractured environment source characterisation.

5.2 Source Zone Characteristics in a Fractured Rock Environment

The following conclusions are based on the evaluation of multiple lines of evidence to characterise mixed chlorinated hydrocarbon DNAPLs in a fractured rock environment:

- Properties that affect the architecture of DNAPL in fractured rock environments include:
    - The nature, location, size and extent of the release
    - Geological properties such as the depth of weathering, fracture intensity, fracture orientation and interconnectivity
    - Hydrogeological properties such as the fracture aperture transmissivity or permeability, vertical and horizontal hydraulic gradients and groundwater flow direction; and
    - Biotic and abiotic degradation processes
- Successful source characterisation in a fractured rock environment requires a systematic approach integrating traditional and novel approaches and utilising multiple lines of evidence.

5.3 Source Zone Architectures of the Investigation Site

The Investigation Site has had a long history of releases of chlorinated hydrocarbon DNAPLs. The following are concluded with respect to the architecture of source zones at the site:

- Release areas at the site can be inferred based on the soil-gas profile of the chlorinated hydrocarbon DNAPLs. Release areas are inferred at the historical production and handling facilities as well as the hazardous waste sites.
- Drip-releases of chlorinated hydrocarbon DNAPLs has led to variable 3-dimensional architectures in the weathered profile underlying the inferred release areas. The source zones in the weathered profile have an “onion” architecture with the highest concentrations located at the core of the contaminated mass. The most significant mass of chlorinated hydrocarbon DNAPLs at the Investigation Site is located at the historical production and handling facilities. Significantly less mass of chlorinated hydrocarbon DNAPLs is located at the redundant waste sites. This could be as a result of storage of the chemicals in drums prior to disposal on the redundant waste sites vs regular spills and leaks at the historical production facilities. While there has been vertical migration of chlorinated hydrocarbon DNAPLs in the weathered profile, there is very little evidence of lateral migration, largely attributed to the media properties.
- Continuous leaks of chlorinated hydrocarbon DNAPLs into the subsurface from the historical production and handling facilities has led to two long continuous DNAPL plumes (approximately 650 and 850 m in length) in the

fractured bedrock. The bedrock DNAPL plume emanating from the historical above-ground storage tanks is predominantly 1,2-DCA and VC while the plume emanating from the historical organics plant consists of PCE and CCl_4. The contiguous DNAPL plumes in the bedrock indicate movement along fractures.

- There are no significant biotic degradation reactions occurring in the DNAPL source zones. This can be attributed to the large volume of chlorinated hydrocarbon DNAPL present.

5.4 Recommendations for Future Work

- Sampling of boreholes along the source zone plumes and analysing for compound specific isotopes to determine the site-specific rate of biodegradation at the site. This will assist in the development of representative numerical models.
- Multiphase numerical models of the site.
- Simulating the effect of partial source removal on the dissolved phase plume.
- Evaluating the FLUTe^{TM} technologies in other DNAPL contaminated sites, with diverse geo-contaminant settings, in South Africa.
- Undertaking cost modelling to optimise sampling scales for high resolution investigations.

6 REFERENCES

Abe, Y.; Aravena, R.; Zopfi, J.; Shouakar-Stash, O.; Cox, E.; Roberts, J.D.; Hunkeler, D. (2009). Carbon and chlorine isotope fractionation during aerobic odixadion and reductive decholorinatiom of vinyl chloride and cis-1,2-dichloroethene. *Environmental Science and Technology, 43*(1), 101-107.

Adamson, A.W.; Gast, A.P. (1997). *Physical Chemistry of Surfaces* (6th ed.). New York: Wiley.

Adamson, D.T.; Parkin, G.F. (2001). Product distribution during transformation of multiple contaminants by a high-rate, tetrachlorethene-dechlorinating enrichment culture. *Biodegradation, 12*(5), 337-348.

Air Force Center for Engineering and the Environment. (2007, May). *AFCEE source zone initiative.* Retrieved May 10, 2009, from www.clu-in.org: http://www.clu-in.org/download/contaminantfocus/dnapl/Chemistry_and_Behavior/AFCEE-szi-2007a.pdf

Anderson, M.R. (1988). *The dissolution and transport of dense non-aqueous phase liquids in saturdated porous media.* PhD dissertation (unpublished), Oregon Graduate Center, Department of Environmental Science and Engineering, Beaverton.

Back, P.-E. (2006). *Value of information analysis for site investigations in remediation projects.* PhD Thesis (unpublished), Chalmers University of Technology, Göteborg.

Baird, B.F. (1989). *Managerial decisions under uncertainty: an introduction to the analysis of decision making.* New York: John Wiley and Sons.

Ballapragada, B.S.; Stensel, H.D.; Puhakka, J.A.; Ferguson, J.F. (1997). Effect of hydrogen on reductive dechlorination of chlorinated ethenes. *Environmental Science and Technology, 31*(6), 1728-1734.

Barnes, B. (2009, February). *Framework for the use of rapid measurement techniques (RMT) in the risk management of land contamination.* Bristol, United Kingdom: Environmental Agency. Retrieved November 18, 2012, from

Environmental Agency web site: http://publications.environment-agency.gov.uk/pdf/SCHO0209BPIA-e-e.pdf

Barranco, F.T.; Dawson, H.E. (1999). Influence of aqueous pH on the interfacial properties of coal tar. *Environmental Science and Technology, 33*(10), 1598-1603.

Barranco, F.T.; Dawson, H.E.; Christener, J.M.; Honeyman, B.D. (1997). Influence of aqueous pH and ionic strength on the wettability of quartz in the presence of dense non-aqueous-phase liquids. *Environmental Science and Technology, 31*(3), 676-681.

Bear, J. (1993). Modeling flow and contaminant transport in fractured rocks. In J. Bear, C. Tsang, & G. D. Marsily (Eds.), *Flow and Contaminant Transport in Fractured Rock* (p. 560). San Diego: Academic Press.

Belay, N.; Daniels, L. (1987). Production of ethane, ethylene and acetylene from halogenated hydrocarbons by methanogenic bacteria. *Applied Microbiology Biotechnology, 53*, 1604-1610.

Beneteau, K.M.; Aravena, R.; Frape, S.K. (1999). Isotopic chracterization of chlorinated solvents - laboratory and field results. *Organic Geochemistry, 30*, 739-753.

Bingham, E.C. (1916). An investigation of the laws of plastic flow. *U.S. Bureau of Standards Bulletin, 13*, 309-353.

Birkholzer, J.; Tsang, C. F. (1997). Solute channeling in unsaturated heterogeneous porous media. *Water Resources Research, 33*, 2221-2238.

Bottcher, J.; Strebel, O.; Voerkelius, S.; Schmidt, H.L. (1990). Using isotope fractionation of nitrate-nitrogen and nitrate-oxygen for evaluation of microbial denitrification in a sandy aquifer. *Journal of Hydrology, 114*, 419-424.

Boyles, W. (1997). *The science of chemical oxygen demand technical information.* Retrieved November 8, 2010, from Hach Company Web Site: http://www.hach.com/download-resources

Broholm, K.; Feenstra, S.; Cherry, J.A. (1999). Solvent release into a sandy aquifer. 1. Overview od source distribution and dissolution behavior. *Environmental Science and Technology, 33*(5), 681-690.

Burton, J.C.; Walker, J.L.; Jennings, T.V.; Aggarwal, P.K.; Hastings, B. (1993). Expedited site characterisation: a rapid, cost-effective process for remedial site characterisation. *Proceedings of the Superfund XIV Conference . II*, pp. 809-826. Greenbelt, MD: Hazardous Materials and Control Institute.

Carey, M.A.; Finnamore, J.R.; Morrey, M.J.; Marsland, P.A. (2000). *Guidance on the Assessment and Monitoring of Natural Attentuation of Contaminants in Groundwater.* National Groundwater and Contaminated Land Centre, UK Environment Agency.

Cary, J.W.; Simmons, C.S.; McBride, J.F. (1989). Predicting oil infiltration and redistribution in unsaturated soils. *Soil Science Society of America Journal, 53*(2), 335-342.

Chang, L.C.; Chen, C.H.; Shan, H.; Tsai, J. (2009). Effect of connectivity and wettability on the relative permeability of NAPLs. *Environmental Geology, 56*, 1437-1447.

Chapman, S.W.; Parker, B.L. (2005). Plume persistence due to aquitard back diffusion following dense nonaqueous phase liquid removal or isolation. *Water Resource Research, 41*(12), W12411.

Chatzis, I.; Morrow, N.R.; Lim, H.T. (1983). Magnitude and detailed structure of residual oil saturation. *Society of Petroleum Engineers Journal*, 311-326.

Chen, C.; Puhakka, J. A.; Ferguson, J. F. (1996). Transformation of 1,1,2,2-tetrachloroethane under methanogenic conditions. *Environmental Science and Technology, 30*, 542-547.

Cheremisinoff, P.N. (1990). Calculating and reporting toxic chemical releases for pollution control. New Jersey: SciTech Publishers.

Cho, H.J.; Fiacco, R.J.; Daly, M.H.; McTigue, J.W. (2004). Hydrochemical facies analysis of 1,1,1-trichloroethane and its degradation products in fractured bedrock. *USEPA/National Groundwater Association Fractured Rock Conference.* Portland.

Clark, I.D.; Fritz, P. (1997). *Environmental isotopes in Hydrogeology* (1st ed.). Boca Raton Florida: Lewis Publishers.

Cohen, R.M.; Mercer, J.W. (1993). *DNAPL site evaluation.* Florida: CRC Press Inc.

Cook, P.F. (Ed.). (1991). *Enzyme mechanism from isotope effects.* Boca Raton, Florida: CRC Press, Inc.

Cope, N.; Hughes, J. B. (2001). Biologically-enhanced removal of PCE from NAPL source zones. *Environmental Science and Technology, 35*(10), 2014-2021.

Davis, D. R.; Kisiel, C.C.; Duckstein, L. (1972). Bayesian decision theory applied to design in hydrology. *Water Resources Research, 8*(1), 33-41.

Dawson, H.; Illangasekasre, T.H. (1999). *Influence of geologic heterogeneity and chemical complexity on the transport and distribution of nonaqueous phase liquid waste .* USEPA Region 8: United States Environmental Protection Agency.

de Best, J.H.; Hunneman, P.; Doddema, H.J.; Janssen, D.B.; Harder, W. (1999). Transformation of carbon tetrachloride in an anaerobic packed-bed reactor without addition of another electron donor. *Biodegradation, 10*(4), 287-295.

de Best, J.H.; Salminen, E.; Doddema, H.J.; Janssen, D.B; Harder, W. (1997). Transformation of carbon tetrachloride under sulfate reducing conditions. *Biodegradation, 8*(6), 429-436.

Dennis, I.; Pretorius, J.; Steyl, G. (2010). Effect of fracture zone on DNAPL transport and dispersion: a numerical approach. *Environmental Earth Sciences, 61*(7), 1531-1540.

Diomampo, G.P.; Chen, C.Y.; Li, K.; Horne, R.N. (2002). Relative permeability through fractures. *Proceedings of the 27th Stanford Workshop on Geothermal Reservoir Engineering.* Stanford: Stanford University.

Doherty, R.E. (2000). A history of production and use of carbon tetrachloride, tetrachloroethylene, trichloroethylene, and 1,1,1-trichloroethane in the United States; Part 1, Historical background; carbon tetrachloride and tetrachloroethylene. *Journal of Environmental Forensics, 1*(2), 69-81.

Durnford, D.S.; McWhorter, D.B.; Miller, C.D.; Swanson, A.; Marinelli, F.; Trantham, H.L. (1997). *DNAPL and LNAPL distributions in soils: experimental and modeling studies.* Colorado State University, Chemical and Bioresources Engineering, Colorado.

Elsner, M.; Zwank, L.; Hunkeler, D.; Schwarzenbach, R. P. (2005). A new concept linking observable stable isotope fractionation to transformation pathways of organic pollutants. *Environmental Science and Technology, 39*, 6896-6916.

Ennis, E.; Reed, R.; Dolan, M; Semprini, L'; Istok, J.D.; Field, J.A. (2005). Reductive dechlorination of the vinyl chloride surrogate chlorofluoroethene in TCE contaminated groundwater. *Environmental Science and Technology, 39*, 6777-6785.

Feenstra, S.; Cherry, J. A.; Parker, B. L. (1996). Conceptual models for the behavior of dense non-aqueous phase liquids (DNAPLs) in the subsurface. In J. F. Pankow, & J. A. Cherry (Eds.), *Dense Chlorinated Solvents and Other DNAPLs in Groundwater* (pp. 53-88). Portland: Waterloo.

Fetter, C.W. (1999). *Contaminant Hydrogeology* (2nd ed.). New Jersey: Prentice Hall.

Fiacco, R.J.; Daly, M.H.; Drobinski, J.C. (2005). Application of the toolbox approach to characterize fractured bedrock sites. *Proceedings of the The Annual Conference on Soils, Sediments, Water and Energy.* Amherst, MA: Univesity of Massachusetts.

Field, J.A.; Istok, J.D.; Semprini, L.; Bennett, P.; Buscheck, T. (2005). Trichlorofluorethene: A reactive tracer for evaluating in situ trichloroethene remediation. *Ground Water Monitoring and Remediation, 25*, 1-10.

Fischer, A.; Herklotz, I.; Herrmann, S.; Thullner, M.; Weelink, S. A. B.; Stams, A. J. M.; Schlomann, M.; Richnow, H. H.; Vogt, C. (2008). Combined carbon and hydrogen isotope fractionation investigations for elucidating benzene biodegradation pathways. *Environmental Science and Technology, 42*, 4356-4363.

Freeze, R. A.; Bruce, J.; Massman, J.; Sperling, T.; Smith, L. (1992). Hydrogeological Decision Analysis: 4. The Concept of Data Worth and Its Use in the Development of Site Investigation Strategies. *Ground Water, 30*(4), 574-588.

Freeze, R.A.; Cherry, J.A. (1979). *Groundwater.* New Jersey: Prentice Hall, Inc.

Ge, S. M. (1997). A governing equation for fluid in rough fractures. *Water Resources Reseach, 33*, 53-61.

Gebrekristos, R.A. (2007). *Site characterisation methodologies for DNAPLs in fractured South African aquifers.* PhD thesis (unpublished), University of the Free State, Institute for Groundwater Studies, Bloemfontein.

Gebrekristos, R.A.; Pretorius, J.A.; Usher, B.H. (2008). *Manual for site sssessment at DNAPL contaminated sites in South Africa.* Pretoria: Water Research Commission.

Gooddy, D.C.; Bloomfield, J.P.; Harold, G.; Lehame, S.A. (2002). Towards a better understanding of tetrachloroethene entry pressure in the matrix of Permo-Triassic sandstones. *Journal of Contaminant Hydrology, 59*, 247-265.

Gossett, J. M. (1987). The measurement of Henry's Law constants for C1 and C2 chlorinated compounds. *Environmental Science and Technology. 21*, 202-208.

Griebler, C.; Safinowski, M.; Vieth, A.; Richnow, H.H.; Meckenstock, R.U. (2004). Combined application of stable carbon isotope analysis and specific

metabolites determination for assessing in situ degradation of aromatic hydrocarbons in a tar oil-contaminated aquifer. *Environmental Science and Technology, 38*, 617 – 631.

Griffin, T.W.; Watson, K.W.. (2002). A comparison of field techniques for confirming dense nonaqueous phase liquids. *Ground Water Monitoring and Remediation, 22*, 48-59.

Hageman, K.J.; Istok, J.D.; Buscheck, T.E.; Semprini, L. (2001). In situ anaerobic transformation of trichlorofluroroethene in trichloroethene-contaminated groundwater. *Environmental Science and Technology, 35*, 1729-1735.

Halogenated Solvents Industry Alliance. (2004). *Solvents Applications*. Retrieved May 8, 2009, from http://www.hsia.org/applications.htm

Harrison, B.; Sudicky, E.A.; Cherry, J.A. (1992). Numerical analysis of solute migration through fractured clayey deposits into underlying aquifers. *Water Resources Research, 28*, 515-526.

Harrold, G.; Gooddy, D.C.; Reid, S.; Lerner, D.N.; Leharne, S.A. (2003). Changes in interfacial tension of chlorinated solvents following flow through U.K. soils and shallow aquifer material. *Environmnetal Science and Technology, 37*(9), 1919-1925.

Hassanizadeh, S.M.; Celia, M.A.; Dahle, H.K. (2002). Dynamic Effect in the Capillary Pressure-Saturation Relationship and its Impacts on Unsaturated Flow. *Vadose Zone Journal, 1*, 38-57.

He, J.; Ritalahti, K. M.; Aiello, M. R.; Löffler, F.E. (2003). Complete detoxification of vinyl chloride by an anaerobic enrichment culture and identification of the reductively dechlorinating population as a Dehalococcoides Species. *Applied Environmental Microbiology, 69*, 996-1003.

Hiemenz, P.C.; Rajagopalan, R. (1997). *Principles of colloid and surface chemistry* (3rd ed.). New York: Marcel Dekker, Inc.

Horvath, A.L. (1982). *Halogenated Hydrocarbons: Solubility-Miscibility with Water.* New York, USA: Marcel Dekker.

Horvath, A.L.; Getzen, F.W.; Maczynska, Z. (1999). IUPAC-NIST solubility data series 67.Halogenated ethanes and ethenes with water. *Journal of Physical Chem Reference Data, 28*, 395-628.

Hughes, B.M.; Gillham, R.W.; Mendoza, C.A. (1990). Transport of trichloroethylene vapors in the unsaturated zone: a field experiment. *International Association of Hydrogeologist Conference on Subsurface Contamination by Immiscible Fluids.* Calgary.

Huling, S.G.; Weaver, J.W. (1991). *Ground Water Issue: Dense Nonaqueous Phase Liquids, EPA/540/4-91-002.* Washington, D.C.: United States Environmental Protection Agency Office of Solid Waste and Emergency Response.

Hulley, V. (2009, December). Application of GIS in contaminated site investigations and remediation planning: transition from data generation to decision-making. *PositionIT*, p. 4.

Hulley, V.; Smit, J.; Kotze, J. (2008). Case Study of Mixed-Contaminant Plume Characterization in a Fractured Rock Aquifer Environment. Monterey, California: Battelle.

Hunkeler, D; Aravena, R.; Butler, B. J. (1999). Monitoring microbial dechlorination of tetrachloroethene (PCE) in groundwater using compound-specific stable carbon isotope ratios: Microcosm and field studies. *Environmental Science and Technology, 33*, 2733-2738.

Hunkeler, D.; Andersen, N.; Aravena, R.; Bernasconi, S. M.; Butler, B.J. (2001). Hydrogen and carbon isotope fractionation during aerobic biodegradation of benzene. *Environmental Science and Technology, 35*, 3462-3467.

Hunkeler, D.; Aravena, R.; Cox, E. (2002). Carbon isotopes as a tool to evaluate the origin and fate of vinyl chloride: laboratory experiments and modelling of isotope evolution. *Environmental Science and Technology, 36*, 3378 – 3384.

Hunkeler, D.; Aravena, R.; Berry-Spark, K.; Cox, E. (2005). Assessment of degradation pathways in an aquifer with mixed chlorinated hydrocarbon contamination using stable isotope analysis. *Environmental Science and Technology, 39*(16), 5975-5981.

Hunkeler, D.; Meckenstock, R.U.; Sherwood Lollar, B.; Schmidt, T.C.; Wilson, J.T. (2008). *A Guide for Assessing Biodegradation and Source Identification of Organic Ground Water Contaminants using Compound Specific Isotope Analysis (CSIA).* Office of Research and Development. Ada, Oklahoma: United States Environmental Protection Agency.

Illangasekare, T.H.; Ramsey, J. L.; Jensen, K.H.; Butts, M. (1995). Experimental study of movement and distribution of dense organic contaminants in heterogeneous aquifers. *Journal of Contaminant Hydrology, 20*, 1-25.

International Atomic Energy Agency. (2002). Study of environmental change using isotope techniques. *Proceedings: Study of environmental change using isotope techniques* (p. 531). Vienna: International Atomic Energy Agency.

Interstate Technology and Regulatory Council. (2000, June). *Dense non-aqueous phase liquids (DNAPLs): review of emerging characterization and remediation technologies.* Retrieved May 5, 2009, from www.http://itrcweb.org/: www.itrcweb.org/Guidance/GetDocument?documentID=18

Interstate Technology and Regulatory Council. (2003, December). *Technical and regulatory guidance for the Triad Approach: a new paradigm for environmental project management.* Retrieved August 29, 2009, from http://www.itrcweb.org/GuidanceDocuments/SCM-1.pdf

Istok, J.D; Field, J.A.; Raes, E.; Millings, M.R.; Peacock, A.D. (2007). *Detecting and quantifying reductive dechlorination during monitored natural attenuation at the Savannah River CBRP site.* Washington: Savannah River Company.

Jackson, R.E.; Dwarakanath, V. (1999). Chlorinated degreasing solvents: physical-chemical properties affecting aquifer contamination and remediation. *Ground Water Monitoring and Remediation, 19*(4), 102-110.

Jeffers, P. M.; Ward, L. M.; Woytowitch, L. M.; Wolfe, N. L. (1989). Homogeneous hydrolysis rate constants for selected chlorinated methanes, ethanes, ethenes, and propane. *Environmental Science and Technology, 23*, 965-969.

Jellali, S.; Muntzer, P.; Razakarisoa, O.; Schäefer, G. (2001). Large scale experiment on transport of trichloroethylene in a controlled aquifer. *Transport in Porous Media*, 145-163.

Kerndorff, H.; Schleyer, R.; Milde, G.; Plumb, R.H. Jr. (1992). Geochemistry of groundwater pollutants at German waste disposal sites. In S. Lesage, & R. Jackson (Eds.), *Groundwater contamination and analysis at hazardous waste sites* (pp. 245-271). New York: Marcel Dekker Inc.

Kiersch, G.A. (1958). Geological causes for failure of Lone Pine Reservoir, Eastern Central Arizona. *Economic Geology, 55*, 854.

Klecka, G. M.; Carpenter, C. L.; Gonsior, S. J. (1998). Biological transformations of 1,2-dichloroethane in subsurface soils and groundwater. *Journal of Contaminant Hydrology, 34*, 139-154.

Kopinke, F.D.; Georgi, A.; Voskamp, M.; Richnow, H.H. (2005). Carbon isotope fractionation of organic contaminants due to retardation on humic substances: implications for natural attenuation studies in aquifers. *Environmental Science and Technology, 39*(16), 6052-6062.

Korving, H.; Clemens, F. (2002). Bayesian decision analysis as a tool for defining monitoring needs in the field of effects of CSOs on receiving waters. *Water Science and Technology, 45*(3), 175-184.

Kram, M.L.; Keller, A.A.; Rossabi, J.; Everett, L.G. (2001). DNAPL characterization methods and approaches, Part 1: Performance comparisons. *Ground Water Monitoring and Remediation, 21*, 19-123.

Kram, M.L.; Keller, A.A.; Rossabi, J.; Everett, L.G.. (2002). DNAPL Characterization Methods and Approaches, Part 2: Cost Comparisons. *Ground Water Monitoring and Remediation*, 46-61.

Kueper, B.H.; Davies, K.L (2009, September). *Assessment and delineation of DNAPL source zones at hazardous waste sites, EPA/600/R-09/119.* Retrieved February 17, 2010, from www.epa.gov/nrmrl/pubs/600r09119.htm

Kueper, B.H.; McWhorter, D.B. (1991). The behaviour of dense, nonaqueous phase liquids in fractured clay and rock. *Ground Water, 29*(5), 716-728.

Kueper, B.H.; Abbot, W.; Farguhar, G. (1989). Experimental observations of muliphase flow in heterogeneous porous media. *Journal of Contaminant Hydrology, 5*, 83-95.

Kueper, B.H.; Redman, D.; Star, R.B.; Reitsma, S.; Mah, M. (1993). A field experiment to study the behavior of tetrachloroethylene below the water table: spatial distribution of residual and pooled DNAPL. *Ground Water, 31*(5), 756-766.

Kueper, B.H.; Walthall, G.P.; Smith, J.W.N.; Leharne, S.A.; Lerner, D.N. (2003). *An illustated handbook of DNAPL transport and fate in the subsurface.* Bristol: Environmental Agency.

Lambe, W.T.; Whitman, R.V. (1969). *Soil mechanics.* John Wiley and Sons Inc.

Leighton, D.T.J.R.; Calo, J.M.. (1981). Distribution coefficients of chlorinated hydrocarbons in dilute air-water systems for groundwater contamination applications. *Journal of Chemical Engineering*, *26*, 382-385.

Lenhard, R.J.; Oostrom, M.; Dane, J.H. (2004). A constituitive model for air-NAPL-water flow in the vadose zone accounting for immobile, non-occluded (residual) NAPL in strongly water-wet porous media. *Journal of Contaminant Hydrology, 71*, 261-282.

Liang, X.; Dong, Y.; Kuder, T.; Krumholz, L.R.; Philp, P.; Butler, E.C. (2007). Distinguishing abiotic and biotic transformation of tetrachloroehtylene and trichloroethylene by stable carbon isotope fractionation. *Environmental Science and Technology, 41*(20), 7094-7100.

Liu, C.; Ball, W. P. (2002). Back diffusion of chlorinated solvent contaminants from a natural aquitard to a remediated aquifer under well-controlled field conditions: predictions and measurements. *Ground Water, 40*(2), 175-184.

MacDonald, J.A.; Kavanaugh, M.C. (1994). Restoring contaminated groundwater: an achievable goal? *Environmental Science and Technology, 28*(8), 362-368.

MacDougall, K.A.; Fenning, P.; Cooke, D.A.; Preston, H.; Brown, A.; Hazzard, J.; Smith, T. (2002). *Guidance on the selection of non-intrusive techniques for groundwater pollution studies, R&D Technical Report P2-178/TR/2.* Almondsbury, Bristol: Environmental Agency .

Mackay, D.; Bobra, A.; Shiu, W.Y.; Yalkowsky, S.H. (1980). Relationships between aqueous solubility and octanol-water partition coefficient. *Chemosphere, 9*, 701-711.

Mackay, D.; Shiu, W.Y.; Maijanen, A.; Feenstra, S. (1991). Dissolution of non-aqueous phase liquids in groundwater. *Journal of Contaminant Hydrology, 8*, 23-42.

Mackay, D.M.; Cherry, J.A. (1989, June). Groundwater Contamination: pump-and-treat remediation. *Environmental Science and Technology, 23*(6), 630-636.

Major, D.W.; McMaster, M.L.; Cox, E.E.; Edwards, E.A.; Dworatzek, S.M.; Hendrickson, E.R.; Starr, M.G.; Payne, J.A.; Buonanici, L.W. (2002). Field demonstration of successful bioaugmentation to achieve dechlorination of tetrachloroethene to ethene. *Environmental Science and Technology, 36*, 5106-5116.

Mancini, S.A.; Ulrich, A.C.; Lacrampe-Couloume, G.; Sleep, B.; Edwards, E.A.; Sherwood Lollar, B. (2003). Carbon and hydrogen isotopic fractionation during anaerobic biodegradation of benzene. *Applied Environmental Microbiolgy, 69*, 191-198.

Martinez, M. J.; Dykhuizen, R. C.; Eaton, R. R. (1992). The apparent conductivity for steady unsaturated flow in periodically fractured porous media. *Water Resources Research, 28*, 2879-2887.

McCarty, P.L. (1997). Biotic and abiotic transformations of chlorinated solvents in groundwater. *Proceedings of the symposium on natural attenuation of chlorinated organics in groundwater (EPA/540/R-97/504)* (p. 191). Washington, D.C.: United States Environmental Protection Agency Office of Research and Development.

Meckenstock, R.U.; Morasch, B.; Griebler, C.; Richnow, H.H. (2004). Stable isotope fractionation analysis as a tool to monitor biodegradation in contaminated aquifers. *Journal of Contaminant Hydrology, 75*, 215-255.

Melander, L.; Saunders, W.H. (1980). *Reaction rates of isotopic molecules* (1st ed.). New York: John Wiley and Sons.

Melber, C.; Kielhorn, J.; Mangelsdorf, I. (2004). *Coal tar creosote.* Geneva: World Health Organization.

Mercer, J.W.; Cohen, R.M. (1990). A review of immiscible fluids in the subsurface: Properies, models, characterisation and remediation. *Journal of Contaminant Hydrology, 6*, 107-163.

Meylan, W.M.; Howard, P.H.; Boethling, R.S. (1992). "Molecular topology/fragment contribution method for predicting soil sorption coefficients." *Environmental Science and Technology, 26,* 1560-1567.

Miansney, B; McBratney, A.B. (2002). The efficiency of various approaches to obtaining estimates of soil hydraulic properties. *Geoderma, 107*(1), 55-70. doi:10.1016/S0016-7061(01)00138-0

Middeldorp, P.J.M.; Luijten, M.L.G.C.; van de Pas, B.A.; van Eekert, M.H.A.; Kengen, S.W.M.; Schraa, G.; Stams, A.J.M. (1999). Anaerobic microbial reductive dehalogenation of chlorinated ethenes. *Bioremediation, 3*, 151-169.

Mohammad, O.I.; Kibbey, T.C.G. (2005). Dissolution-induced contact angle modification in dense nonaqueous phase liquid/water systems. *Environmental Science and Technology, 39*(6), 1698-1706.

Moran, M.J. (2006). *Occurence and implications of selected chlorinated solvents in ground water and source water in the United States and in the drinking water in 12 Northeast and Mid-Atlantic States, 1993-2002.* U.S. Geological Survey Scientific Investigations Report.

Murphy, J. R.; Thomson, N. R. (1993). Two-phase flow in variable aperture fracture. *Water Resources Research, 24*, 2033-2048.

National Research Council . (2000). *Natural attenuation for groundwater remediation.* Washington D.C.: National Academy Press.

National Research Council. (2004). *Contaminants in the subsurface: Source zone assessment and remediation.* Washington D.C.: National Academic Press.

Newell, C.J.; Aziz, C.E. (2004). Long-term sustainability of reductive dechlorination reactions at chlorianted solvents sites. *Biodegradation, 15*, 387-394.

O'Hara, S.K.; Parker, B.L.; Jorgensen, P.R.; Cherry, J.A. (2000). Trichloroethene DNAPL flow and mass distribution in naturally fractured clay: Evidence of aperture variability. *Water Resources Research, 36*(1), 135–147.

Oron, A. P.; Berkowitz, B. (1998). Flow in rock fractures: the local cubic law assumption reexamined. *Water Resources Research, 34*, 2811-2825.

Pagan, M.; Cooper, W. J.; Joens, J. A. (1998). Kinetic studies of the homogeneous abiotic reactions of several chlorinated aliphatic compounds in a aqueous solution. *Applied Geochemistry, 13*, 779-785.

Pankow, J.F.; Cherry, J.A. (1996). *Dense chlorinated solvents and other DNAPLs in groundwater.* Ontario: Waterloo Press.

Parker, B.L. (2007). Investigating contaminated sites on fractured rock using the DFN Approach. *U.S. EPA/NGWA Fractured Rock Conference: State of the Science and Measuring Success in Remediation.* Portland, Maine: U.S. EPA/NGWA.

Parker, B.L.; Cherry, J.A.; Chapman, S.W. (2004). Field study of TCE diffusion profiles below DNAPL to assess aquitard integrity. *Journal of Contaminant Hydrology, 74*, 197-230.

Parker, B.L.; Gillham, R.W.; Cherry, J.A. (1994). Diffusive disappearance of immiscible phase organic liquids in fractured geologic media. *Ground Water, 32*(5), 805-820.

Parker, B.L.; McWhorter, D.B.; Cherry, J.A. (1997). Diffusive loss of non-aqueous phase organic solvents from idealized fracture networks in geologic media. *Ground Water, 35*(6), 1077-1088.

Poulsen, M.M.; Kueper, B.H. (1992). A field experiment to study the behavior of tetrachloroethylene in unsaturated porous media. *Environmental Science and Technology, 26*(5), 889-895.

Powers, S.E.; Abriola, L.M.; Weber, W.J. Jnr. (1992). An experimental investigation of nonaqueous phase liquid dissolution in saturdated subsurface systems: steady state mass transfer rates. *Water Resources Research, 28*(10), 2691-2705.

Ramsey, M.H.; Taylor, P.D.; Lee, J. (2002). Optimized contaminated land investigation at minimum overall cost to achieve fitness-for-purpose. *Journal of Environmental Monitoring, 4*, 809-814.

Republic of South Africa. (1998, August 26). National Water Act (Act No 36 of 1998). *398*. Cape Town, Republic of South Africa: Republic of South Africa Government Gazette.

Rivett, M.O.; Lerner, D.N.; Lloyd, J.W. (1990). Chlorinated solvents in UK aquifers. *Water and Environment Journal, 4*(3), 242-250.

Robertson, B. K.; Alexander, M. (1996). Mitigating toxicity to permit bioremediation of constituents of nonaqueous-phase liquids. *Environmental Science and Technology, 30*, 2066-2070.

Sabljic, A.; Gusten, H.; Verhaar, H.; Hermens, J. (1995). QSAR modelling of soil sorption. Improvements and systematics of logKoc vs. logKow correlations. *Chemosphere, 31*, 4489–4514.

Sale, T.; Newell, C.; Stroo, H.; Hinchee, R.; Johnson, P. (2008). *Frequently asked questions regarding management of chlorinated solvents in soils and groundwater.* Environmental Security Technology Certification Program (ESTCP).

Sara, M. (2003). *Site assessment and remediation handbook.* Florida: CRC Press.

Schwarzenbach, R.P.; Gashwend, P.M.; Imboden, D.M. (1993). *Environmental organic chemistry.* New York: John Wiley and Sons Inc.

Schwille, F. (1988). *Dense chlorinated Solvents in porous and fractured media - model experiments.* (J. Pankow, Trans.) Florida: Lewis Publishers.

SERDP and ESTCP. (2001, August). *Expert panel workshop on research and development needs for cleanup of chlorinated solvent sites.* Retrieved March 3, 2008, from http://www.clu-in.org/products/tins/tinsone.cfm?num=29432415

SERDP and ESTCP. (2006, September). *Expert panel workshop on reducing the uncertainty of DNAPL source zone remediation.* Retrieved March 3, 2008, from http://www.serdp.org/Featured-Initiatives/Cleanup-Initiatives/DNAPL-Source-Zones

Shouakar-Stash, O.; Frape, S.K.; Drimmie, R.J. (2003). Stable hydrogen, carbon and chlorine isotope measurements of selected chlorinated organic solvents. *Journal of Contaminant Hydrology, 60*, 211-228.

Slater, G.F.; Dempster, H.D.; Sherwood Lollar, B.; Ahad, J. (1999). Headspace analysis: a new application for isotopic characterization of dissolved organic contaminants. *Environmental Science and Technology, 33*(1), 190-194.

Slater, G.F.; Dempster, H.D.; Sherwood Lollar, B.; Spivack, J.; Brennan, M.; Mackenzie, P. (1998). Isotope tracers of degradation of dissolved chlorinated solvents. *First International Battelle Conference on Remediation of*

Chlorinated and Recalcitrant Compounds. Monterey, California: Battelle Press.

Snow, D.T. (1968). Rock fracture spacings, openings, and porosities. *Journal of the Soil Mechanics and Foundations Division, 94*(1), 73-91.

Soesilo, J.A.; Wilson, S.R. (1997). *Site remediation - planning and management.* Florida: CRC Press.

Steele, A.; Lerner, D. N. (2001). Predictive modelling of NAPL injection tests in variable aperture spatially correlated fractures. *Journal of Contaminant Hydrology, 49*(3-4), 287-310.

Stiber, N.A.; Pantazidou, M.; Small, M.J. (1999). Expert system methodology for evaluating reductive dechlorination at TCE sites. *Environmental Science and Technology, 33*(17), 3012-3020.

Stroo, H.F.; Leeson, A.; Shepard, A.J.; Koenigsberg, S.S.; Casey, C.C. (2006). Monitored natural attenuation forum: environmental remediation applications of molecular biological tools. *Remediation Journal, 16*(2), 125-137.

Sturchio, N. C.; Clausen, J. C.; Heraty, L. J.; Huan, g L., Holt, B. D.; Abrajano, T. (1998). Stable chlorine isotope investigation of natural attenuation of trichloroethene in an aerobic aquifer. *Environmental Science and Technology, 32*, 3037-3042.

Sturchio, N.C.; Bohlke, J.K.; Beloso, A.D.; Streger, S.H.; Heraty, L.J.; Hatzinger, P.B. (2007). Oxygen and chlorine isotope fractionation during perchlorate biodegrtadation: laboratory results and implications for forensic and natural attenuation studies. *Environmental Science and Technology, 41*(18), 2796-2802.

Sudicky, E.A.; Gillham, R.W.; Frind, E.O. (1985). Experimental investigations of solute transport in stratified porous media 1) The non reactive case. *Water Resource Research, 21*(7), 1035-1041.

Taylor, A.E.; Dolan, M.E.; Bottomley, P.J.; Semprini, L. (2007). Utilization of fluoroethene as a surrogate for aerobic vinyl chloride transformation. *Environmental Science and Technology, 41*(18), 6378-6383.

Thomas, G.W. (1982). *Principles of hydrocarbon reservoir simulation.* Boston: International Human Resources Development Corporation.

Tsang, C.F.; Tsang, Y.W.; Hale, F.V. (1991). Tracer transport in fractures: analysis of field data based on a variable-aperture channel model. *Water Resources Research, 27*, 3095-3106.

United States Environmental Protection Agency. (1980). *Sources of toxic compounds in household wastewater, EPA 600/2-80-123.* Cincinnatti: Office of Research and Development. Retrieved from http://nepis.epa.gov

United States Environmental Protection Agency. (1990). *Handbook: Groundwater and Contamination Volume 1, EPA 625/6-90/016a.* Cincinnati: Center for Environmental Research Information.

United States Environmental Protection Agency. (1992, January). *Estimating potential for occurrence of DNAPL at Superfund Sites, 9355.4-07FS.* Office of Solid Waste and Emergency Response. Washington D.C.: Office of Solid Waste and Emergency Response. Retrieved April 18, 2008, from http://www.epa.gov/superfund/health/conmedia/gwdocs/pdfs/estdnapl.pdf

United States Environmental Protection Agency. (1993). *Evaluation of the likelihood of DNAPL presence at NPL Sites: national results, EPA 540R-93-073.* Office of Solid Waste and Emergency Response. Washington D.C.: Office of Solid Waste and Emergency Response.

United States Environmental Protection Agency. (1994). *Guidance for the data quality objectives process, EPA/600/R-96/055.* Washington D.C.: Office of Research and Development.

United States Environmental Protection Agency. (1998). *Technical protocol for evaluating natural attenuation of chlorinated solvents in ground water, EPA/600/R-98/128.* Washinton D.C.: Office of Research and Development.

United States Environmental Protection Agency. (1999, April). *Use of monitored natural attentuation at Superfund, RCRA corrective action and underground storage tank sites, Directive Number: 9200.4-17P.* Office of Solid Waste and Emergency Response (OSWER). Washington D.C.: Office of Solid Waste and Emergency Response. Retrieved October 5, 2009, from http://www.epa.gov/oust/directiv/d9200417.pdf

United States Environmental Protection Agency. (2001, July). *The state-of-the-practice of characterization and remediation of contaminated ground water at fractured rock sites, EPA542-R-01-010.* Washington D.C.: Office of Solid Waste and Emergency Response. Retrieved October 12, 2009, from www.epa.gov: http://epa.gov/tio/download/misc/fracrock_state.pdf

United States Environmental Protection Agency. (2003, December). *The DNAPL remediation challenge: Is there a case for source depletion?, EPA/600/R-03/143.* Cincinnati: National Risk Management Research Laboratory. Retrieved May 26, 2011, from www.epa.gov: http://nepis.epa.gov/Exe/ZyPDF.cgi?Dockey=300061GP.PDF

United States Environmental Protection Agency. (2004). *Site Characterization Technologies for DNAPL Investigations, EPA 542-R-04-017.* United States Environmental Protection Agency. Cincinnati: National Service Center for Environmental Publications.

United States Environmental Protection Agency. (2011). Estimation Programs Interface Suite™ for Microsoft® Windows, v 4.10. Washington, D.C.: United States Environmental Protection Agency.

Usher, B.H.; Pretorius, J.A.; Gebrekristos, R.A. (2008). *Guidelines for the acceptance of monitored natural attentuation processes in South Africa.* Pretoria: Water Research Commission.

Usher, B.H.; Pretorius, J.A.; Dennis, I.; Jovanovic, N.; Clarke, S.; Cave, L.; Titus, R. (2004). *Identification and prioritisation of groundwater contaminants in South Africa's urban catchments, Report Number: 1326/1/04.* Pretoria: Water research Commission.

van Wamerdam, E.M.; Frape, S.K.; Aravena, R.; Drimmie, R.J.; Flatt, H.; Cherry, J.A. (1995). Stable chlorine and carbon isotope measurement of selected chlorianted organic solvents. *Applied Geochemistry, 10*, 547-552.

Vogel, T.M.; McCarty, P.L. (1987). Abiotic and biotic transformations of 1,1,1-trichloroethane under methanogenic conditions. *Environmental Science and Technology, 21*, 1208-1213.

Vogel, T.M.; Criddle, C.S.; McCarty, P.L.. (1987). Transformations of halogenated aliphatic compounds. *Environmental Science and Technology, 21*(8), 722-736.

Wang, J.S.Y.; Narashiman, T.N. (1985). Hydrologic mechanisms governing fluid flow in partially saturated, fractured, porous medium. *Water Resources Research, 21*, 1861-1874.

Wang, Y.; Huang, Y. (2003). Hydrogen isotopic fractionation of petroleum hydrocarbons during vaporization: implications for assessing artificial and natural remediation of petroleum contamination. *Applied Geochmistry, 18*(10), 1641-1651.

Wiedemeier, T.H.; Rifai, H.S.; Newell, C.J.; Wilson, J.T. (1999). *Natural attenuation of fuel hydrocarbons and chlorinated solvents.* New York: John Wiley and Sons.

Wilson, J.L.; Conrad, S. H.; Mason, W.R.; Peplinski, W.; Hafgan, E. (1990). *Laboratory investigations of residual liquid organics from spills, leaks, and the disposal of hazardous wastes in groundwater.* Oklahoma: United Stated Environmental Protection Agency.

Woodford, A.C.; Chevallier, L. (2002). *Hydrogeology of the Main Karoo Basin: current knowledge and future reserach needs.* Pretoria: Water Research Commission.

Yang, Y.; McCarty, P.L. (2000). Biologically enhanced dissolution of tetrachloroethene DNAPL. *Environmental Science and Technology, 34*(14), 2979-2984.

Yang, Y.; McCarty, P.L. (2002). Comparison between donor sustrates for biologically enhanced tetrachloroethene DNAPL dissolution. *Environmental Science and Technology, 36*, 3400-3404.

Zhang, Z.F.; Smith, J.E. (2002). Visualization of DNAPL fingering processes and mechanisms in water-saturated porous media. *Transport in Porous Media, 48*, 41-59.

Zogorski, J.S.; Carter, J.M.; Ivahnenko, T.; Lapham, W.W.; Moran, M.J.; Rowe, B.L.; Squillace, P.J.; Toccalino, P.L. (2006). *The quality of our Nation's waters—Volatile organic compounds in the Nation's ground water and drinking-water supply wells.* United States Geological Survey.

ABSTRACT

The remediation of sites contaminated by dense non-aqueous phase liquids (DNAPLs) continues to present a significant environmental challenge globally. Contributing to this challenge is the difficulty in locating source zones due to local heterogeneities in the sub-surface. Heterogeneities are significant in fracture rock environments, such as those found in South Africa, which together with the fluid properties determine the fate and transport of DNAPLs.

This research is based on evaluating the effectiveness of combining traditional and novel source zone characterisation methodologies in order to delineate chlorinated hydrocarbon DNAPLs in a fractured rock environment. The research documents and evaluates the characterisation process followed in the application of various methodologies to an Investigation Site in South Africa. A site-specific conceptual site model is presented indicating the delineation of the multiple chlorinated hydrocarbon DNAPL source zones at the site. Additionally, a DNAPL source characterisation approach is proposed for application in fractured rock environments. This approach allows for the convergence of traditional approaches (such as drilling within a fixed grid) with more novel approaches (such as high resolution sampling and analysis).

The pioneering use of ribbon NAPL samplers (FLUTe^{TM} activated carbon technology membranes) in South Africa is documented in this research. *In situ* source zone characterisation using this technology in a fractured rock environment is shown to be successful in determining depth discrete fracture transmissivities and residual DNAPL zones that would have gone unobserved through methods such as direct observation and testing rock cores with hydrophobic dyes. The efficiency of this technology renders it ideal for future continued use in South Africa.

OPSOMMING

Die remediëring van terreine wat besoedel is met digte vloeistowwe in 'n nie-akwatiese fase (DNAPL's), bied steeds wêreldwyd 'n wesentlike omgewingsuitdaging. Die problematiese bepaling van bronsones weens die lokale heterogeniteite ondergronds dra verder by tot hierdie uitdaging. Heterogeniteite is betekenisvol in breukrotsomgewings soos wat in Suid-Afrika aangetref word, wat tesame met die vloeistofeienskappe, die lot en vervoer van DNAPL's bepaal.

Hierdie navorsing is gegrond op die evaluering van die doeltreffendheid van tradisionele en ongewone bronsone-karakteriseringsmetodologieë in kombinasie om chloorkoolwaterstof-DNAPL's in 'n breukrotsomgewing te delinieer. Die navorsing dokumenteer die karakteriseringsproses wat in die toepassing van verskeie metodologieë met betrekking tot 'n Ondersoekterrein in Suid-Afrika gevolg is. 'n Terreinspesifieke konseptuele terreinmodel word aangebied wat die deliniasie van die veelvuldige chloorwaterstof-DNAPL-bronsones op die terrein toon. Daarbenewens word 'n DNAPL-bronkarakteriseringsbenadering voorgestel wat in breukrotsomgewings toegepas kan word. Hierdie benadering maak daarvoor voorsiening dat tradisionele benaderings (soos om in 'n vaste rooster te boor) en ongewone benaderings (soos hoëresolusie-monsterneming en analisering) samelopend gevolg kan word.

Die baanbrekerswerk in die gebruik van NAPL-lintmonsters (FLUTe^{TM}-geaktiveerde koolstoftegnologiemembrane) in Suid-Afrika word in hierdie navorsing gedokumenteer. Waar hierdie tegnologie in 'n breukrotsomgewing vir *in situ* bronsone-karakterisering gebruik is, was dit suksesvol in die bepaling van dieptediskrete breuktransmissiwiteite en residuele DNAPL-sones wat nie deur metodes soos direkte observasie en die toets van rotskerne met hidrofobiese kleurstowwe waargeneem sou word nie. Die doeltreffendheid van hierdie tegnologie maak dit ideaal vir voortgesette toekomstige gebruik in Suid-Afrika.

KEY WORDS

Dense non-aqueous phase liquid (DNAPL)

Fractured rock

Source characterisation

Chlorinated hydrocarbons

Site characterisation

Fracture network characteristics

High resolution characterisation

Source zones

Conceptual site model

Characterisation efficiency